THE EFFECT OF THE ADDITION OF FLY ASH ON THE HYDRATION OF CEMENT

by

Yick Hsuan Halse

A thesis submitted for the degree of Doctor of Philosophy in the University of London, and for the Diploma of Imperial College

Department of Metallurgy & Materials Science
Royal School of Mines
Imperial College of Science & Technology
University of London

March 1985

ABSTRACT

The effect on the hydration of cements of a 30% replacement by fly ash has been studied by a combination of techniques including calorimetry, thermogravimetry (accompanied by DTA and DTG), X-ray diffractometry and electron microscopy.

The development of microstructure has been studied during the hydration of the neat and fly ash cements. The progress of the reaction has been monitored using calorimetry and X-ray diffraction. By relating these results, the effect of the fly ash on the hydration of major cement components can be deduced.

In fly ash cement pastes a noticeable change in the amount of calcium hydroxide and the strength occurs after 7 days hydration at 20 °C. The pozzolanic reaction is accelerated as C_3S content in the cement is increased. The decrease in calcium hydroxide content followed dissolution of the fly ash surface, and the reaction augments the compressive strength.

The increase of the hydration temperature has advanced and enhanced hydration of all the cement components and has a particularly strong effect on the pozzolanic reaction.

ACKNOWLEDGEMENT

I am grateful to Professor P L Pratt for his supervision and constructive criticisms. My thanks are also due to Mr W A Gutteridge for advice and assistance in analysing materials, Mr J A Dalziel for discussions and the provision of fly ash samples, Dr C J Gillham who wrote some data analysis programs, Dr K L Scrivener for her comments on this thesis, the Department of Mineral Resources Engineering for allowing the use of their facilities, the SERC and Marine Technology Directorate of SERC for financial support, and to Catherine Young for typing this thesis.

I would especially like to thank my husband, who read through the manuscript, and my parents Mr and Mrs Hsuan for their encouragement and support.

CONTENTS

LIST OF TABLES

LIST OF FIGURES

LIST OF PLATES

GLOSSARY

The cement compounds are usually expressed by shortened notation which describes each oxide composition by one letter :

$C = CaO$	$S = SiO_2$	$A = Al_2O_3$	$F = Fe_2O_3$
$\bar{S} = SO_3$	$H = H_2O$	$N = Na_2O$	$K = K_2O$

For examples : Tricalcium silicate $3Ca.SiO_2 = C_3S$ and calcium hydroxide $Ca(OH)_2 = CH$

Ferrite phase	continuous solid solution series between C_2F-C_2A. The general formula is $C_2(F_{1-p})A_p$, $0<p<0.7$ and commonly $p=0.5$ ie.C_4AF.
Aluminate phase	tricalcium aluminate C_3A.
Insterstitial phase	collective term for aluminate and ferrite phases.
Clinker	the product of burning the mineral in a kiln.
AFm phase	aluminate-ferrite-monosubstituent eg. C_4AH_{13} or tetracalcium aluminate monosulphate($C_4A\bar{S}H_{12}$).
AFt phase	aluminate-ferrite-trisubstitued,most typical one is ettringite($C_6A\bar{S}_3H_{32}$)
C-S-H gel	calcium silicate hydrate, mainly in amorphous gel form with a variable composition between CaO and SiO_2.
PFA	pulverized fuel ash and also is known as fly ash.
Cement paste	a mixture of cement powder and water.
Blended cement	cement mixed with other substant which may be fly ash, silica fume or furnace slag.
W/C ratio	ratio of mass of water to mass of cement in cement paste

W/S ratio	ratio of amss of water to mass of solid in a paste mixture.
C/S ratio	ratio of molar of CaO/SiO_2
BEI	back scattered electron image.
STEM	scanning transmission electron microscopy.
SEM	scanning electron microscope/microscopy.
TEM	transmission electron microscope/microscopy.

CHAPTER 1

INTRODUCTION

The fly ash collected from power stations is usually dumped as waste. The cost of disposal is not negligible and production is likely to increase with time. Therefore it is very important to find uses for this material.

Fly ash frequently exhibits pozzolanic properties, so it has been used as a constituent of concrete which is the most extensively used material in the construction industry. Although the foremost advantage of the fly ash lies in the economy resulting from reduction of cement, good quality fly ash can improve the long term strength, workability and durability of the concrete.

The effect of fly ash on cement has been studied for a long time, especially in the development of mechanical properties. In order to understand better the role of fly ash in the properties of the concrete, a full study of the effect of the pozzolanic reaction and of the cement hydration by the fly ash is necessary.

Raising the curing temperature during hydration is known to accelerate the cement hydration and improves the early age strength. In the fly ash cement, an additional contribution to the strength from the pozzolanic reaction is also temperature dependence and this becomes increasingly significant as the curing temperature is raised.

In the present work, the pozzolanic activity, hydration reaction, strength and microstructure for different cements, with one type of fly ash are compared. All the pastes are mixed at realistic water to solid ratios around 0.45. In addition, one of the ordinary Portland cements and a cement/fly ash blend have been investigated at a curing temperature of 40 °C, and limited study has been made of the properties of the fly ash.

The various techniques which have been applied in the present work are described in Chapter 2.

Chapter 3 gives the chemical and physical analyses of the materials which have been used.

Some characteristics of the fly ash which has been used and a brief review of the formation of the fly ash are described in Chapter 4.

Chapter 5 describes various experiments to investigate the pozzolanic reaction, hydration of neat and blended cements, and the compression strength of both the pastes, while similar experiments which have been carried out at 40 °C are the subject of Chapter 6.

Chapter 7 relates all the results and discusses the hydration of cement and the influence of the fly ash, the pozzolanic reaction, and the high temperature effect on both of them.

Chapter 8 summarises the conclusions of the present work and outlines the areas for further work.

CHAPTER 2

TECHNIQUES FOR STUDYING THE HYDRATION OF CEMENT AND FLY ASH CEMENT

2.1 CALORIMETRY

The heat evolution during the hydration of cements under isothermal conditions was measured by a conduction calorimeter manufactured by Wexham Instruments Ltd. The calorimetry cell is based on the design by Forrester [1970] and the construction is shown in Fig.2.1.1. The output of the calorimeter is the e.m.f. difference between two sets of sensors. Both sets are fixed to the heat sink, which is maintained at constant temperature. One sensor supports the sample holder, the other supports a thermal compensation ring. Therefore water bath fluctuations are largely eliminated. The output of the data is recorded onto a microcomputer [Appendix I].

An unfortunate feature of the calorimetry study is that the heat output is summed over all the reactions occurring at any particular time. Therefore, individual reactions cannot always be clearly resolved, so that peak heights and positions may only be known approximately. Another problem arises if the cement paste is mixed outside the calorimeter. The large heat output just after the addition of water (often referred to as peak 1) cannot then be accurately obtained. The first peak of heat evolution can be measured by adding the water inside the calorimeter, but this technique will lead to a poor resolution of the small peaks, such as peaks 3 or 4.

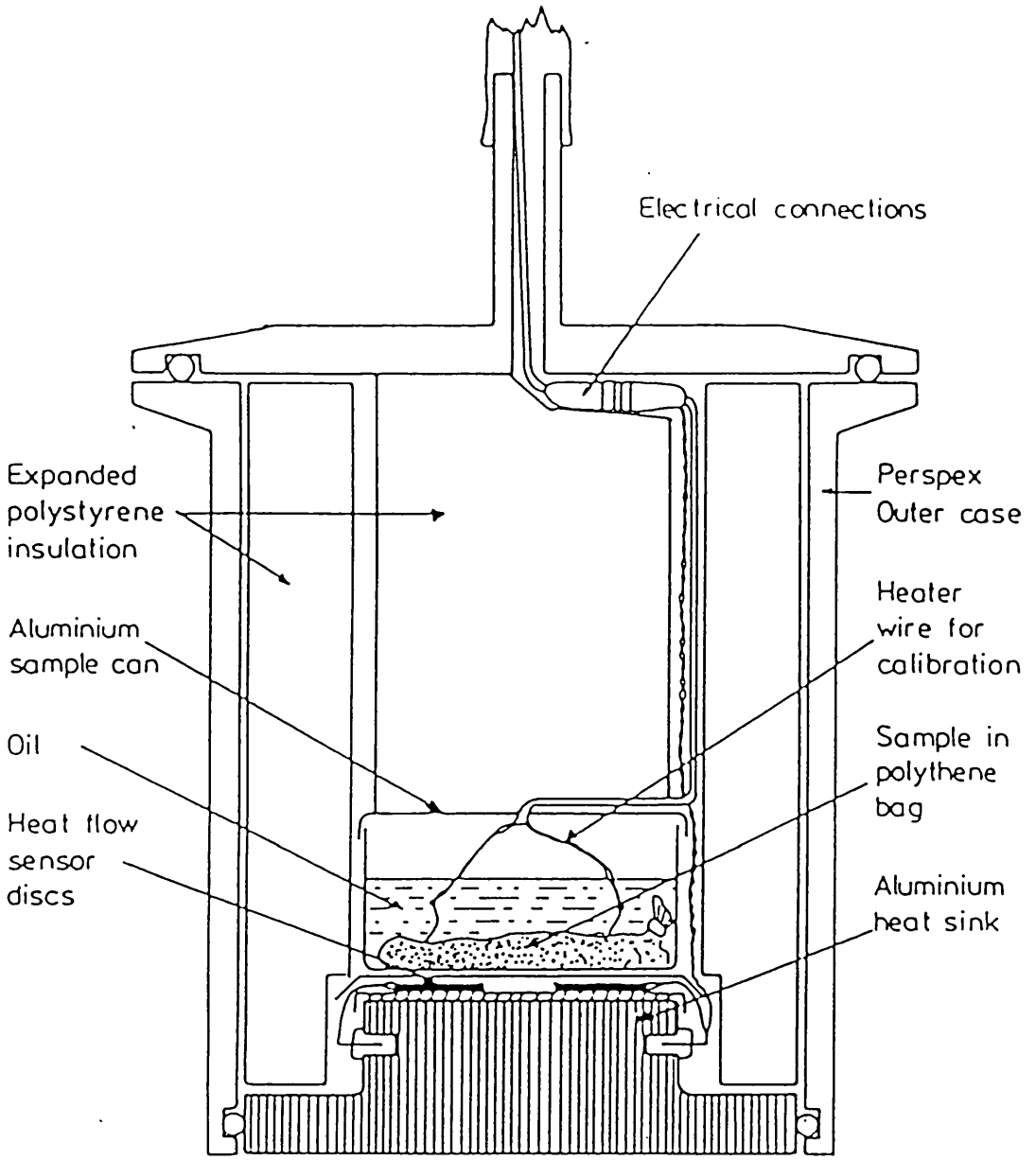

FIG. 2.1.1 DIAGRAM OF CALORIMETER (FROM FORRESTER, 1970)

Experimental procedure

The cement paste or blended cement paste, which have the same w/s ratio, are mixed in a beaker for 3 minutes by stirring with a metal spatula. Equal weights of paste are weighed out in a polythene bag and immediately put into the sample cells in the calorimeter, the heat output data being recorded by computer.

2.2 PARTICLE SIZE ANALYSIS

The particle size distribution of any powder form material (e.g. p.f.a., cement or clinker) can be measured by using a Malvern 3600 particle size analyser [Appendix II]. Particle sizes in the range of 1.2 to 118 microns can be analysed with a 63 mm focus lens. Particles smaller than 1 micron, such as silica fume, cannot be analysed with this apparatus. In the experiment the powder is required to disperse into a solvent when the particles can be disaggregated by using a magnetic stirrer. The choice of the solvent is vital and sometimes a wetting agent is required to help the separation of the particles. For analysing cement powders, methanol seems to be a suitable solvent,and for the fly ash a mixture of water with 5% of sodium tripolyphosphate (5% concentration) is used.

2.3 DRYING TECHNIQUES

Freeze drying

The hydrating sample is put into a mixture of solid CO_2 and methanol which reaches a temperature of -80 °C. All the unbonded water will change to ice in a very short time, stopping the hydration. The cold sample is placed in the cold chamber (-30 °C) of the freeze dryer in which the ice sublimates to vapour condensing in a secondary chamber

at backing pump pressure. The sample stays in the freeze dryer for about 1 week, and during this period the temperature of the cold chamber is gradually increased to room temperature.

Solvent replacement

The unbonded water in the sample is replaced by a solvent, which can be acetone, methanol or propan-1-ol, so that the hydration is stopped. When all the water is replaced by the solvent, the weight of the sample becomes constant. The sample is then left in a vacuum desiccator to allow the solvent to dry out.

The freeze drying technique has the advantage of stopping the hydration in a shorter time than that by the solvent replacement technique, which generally requires from a few hours to 2 weeks to reach a steady level [Parrott, 1984], e.g. a 1-day sample sized 25 x 8 x 3 mm required 6 hours. Another advantage of freeze drying is that very young samples (<12 hours) can be maintained in their cast shape so that it may be easier to perform further experiments. Using the other technique, the samples would fall apart when mixed with the solvent.

2.4 MICROSCOPY

Light microscopy

This technique is useful for examining the fly ash particles because of their diverse optical properties. The crystal phases in p.f.a. can be identified by their morphology, colour and contrasting appearance under cross polarized light. Haematite has an iron red colour; quartz is optically anisotropic,whereas magnetite is optically isotropic and highly reflective due to the iron content.

The specimen is prepared using resin (Araldite) to bind the fly ash powder, and then polished on cloths impregnated with successively finer grades of diamond paste.

Scanning electron microscopy (SEM)

The fracture surface of hydrated cement paste is coated with gold, to provide a conducting surface, and examined in a JEOL JSM 35 electron microscope using the secondary electron mode. Low energy secondary electrons are generated by the incident beam fairly near the surface of the specimen, and are collected by a biased detector. The intensity of the secondary electrons emitted from the surface is increased as the angle between the incident and the local normal is increased [$I \alpha \frac{1}{\cos \theta}$], thus a shadowless image is produced.

The polished surface of the cement paste is coated with carbon and is observed in the SEM using the back scattered electron mode. The variation of contrast on the image depends entirely on the average atomic number of the scanned area - areas of high atomic number appearing brightest. The molecular formula of each phase present in the sample can be used to calculate a mean atomic number so that their relative brightness can be estimated. Thus the areas and positions of the various phases can be deduced; confirmation can be provided by analysis of the image using an X-ray energy disperser [Scrivener, 1984].

Transmission electron microscopy (TEM)

Javelas et.al. [1975] and Dalgleish et.al. [1980, 1981] have studied the microstructure of cement in electron transparent section. Since cement is a very brittle material the sample needs to be impregnated with resin to support the delicate microstructure. The thin section is first polished down to an almost semi-transparent stage on a

diamond wheel and finally the electron transparent foil is prepared in an ion-beam mill. The thin foil samples were examined in a JEOL 1200X Temscan electron microscope operating at 100 kV. Chemical analysis of the phases is also possible using EDXA.

2.5 X-RAY DIFFRACTOMETRY ANALYSIS

Quantitative X-ray analysis

The abundance of the phases in the unhydrated cement can be deduced using quantitative X-ray powder diffraction analysis (QXDA) which has been developed by Gutteridge [1984] [Appendix III]. The method was also applied to the hydrated cement to investigate the hydration of each phase, such as the onset and the rate of hydration, the rate of formation of hydrates (e.g. CH) and the transformation of the aluminate phase. Gutteridge has extended the work to study the change in glass content upon hydration with an OPC/p.f.a. blend. The amount of glass in the p.f.a. can be equated with the difference from 100% of the total percentage of crystalline phase.

The samples were prepared and loaded in the same way as previously discussed in Appendix III. The X-ray data were collected by step counting for 20 seconds at intervals of 0.05 degrees 2-theta over the peak area in a Philips PW1710 diffractometer. The intensity of the peak can be calculated by a microcomputer built into the machine. There are three alternative ways of performing this calculation:

1) If the peak is not influenced by another the background at either side is measured, then the mean value of the two backgrounds is subtracted. The resulting net intensity can be visualised by the area above the connecting line of the two backgrounds.

2) If the peak is partially overlapped by another peak, only one side of the background is measured and can be the low or high background. This value is subtracted and the net intensity is the area above a horizontal line through this background point.

3) No background subtraction - when the background can be neglected relative to the peak intensity, or the same background is used for several peaks.

Qualitative X-ray analysis

Qualitative X-ray analysis is used to investigate the existence of hydration products, such as ettringite. The samples were prepared by hand-grinding in an agate mortar to avoid violent grinding which can destroy the structure of ettringite by reducing the number of water molecules. The samples were examined using a Philips PW 1710 diffractometer with monochromatised upper K-alpha radiation operating at 40 kV, and either 30 mA or 40 mA. The geometry of the diffractometer and its slit system are kept constant. The intensity data were collected by continuing to scan in the time constant, 2.

2.6 THERMAL ANALYSIS

Differential thermal analysis (DTA)

DTA measures the temperature difference between the test sample and an inert reference material at a constant rate of heating. As a reaction takes place in the test sample, a thermal change will occur whereas the thermal level in the reference material remains constant. Clearly exothermic and endothermic reactions will respectively raise and lower the temperature of the sample relative to that of the reference material. When the reaction is proceeding a peak will be produced in the DTA curve [Fig.2.6.1] [Mackenzie, 1964], the area of which is proportional to the heat evolved.

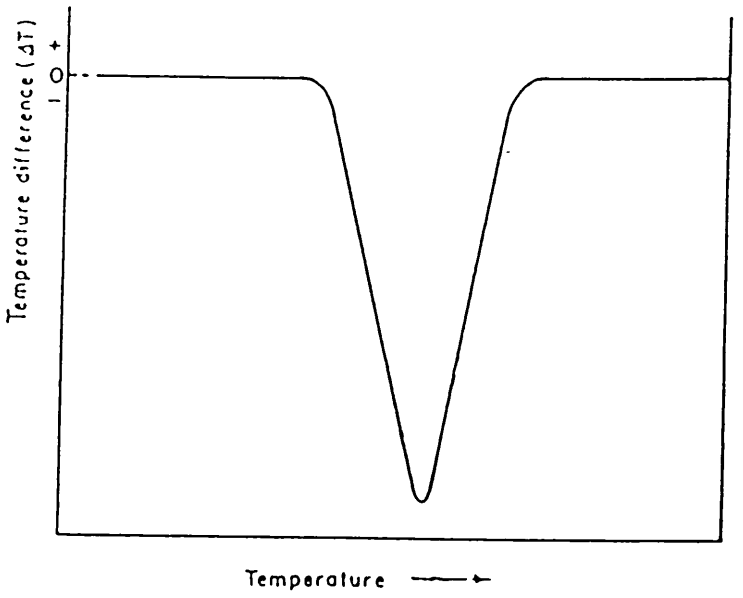

FIG. 2.6.1 FORMALIZED DIFFERENTIAL THERMAL CURVE (FROM MACKENZIE, 1964)

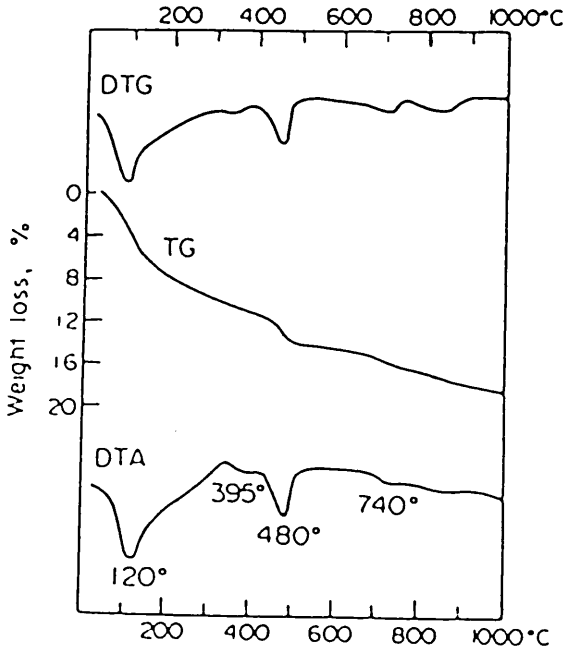

FIG. 2.6.2 COMPARISON OF DTA, TG, DTG OF HYDRATED FOR 28 DAYS (FROM BEN-DOR, 1983)

Thermogravimetry (TG) and differential thermogravimetry (DTG)

Thermogravimetry measures the changing weight of the test sample during a constant heating rate. At certain temperatures some of the phases will be dehydrated causing a rapid weight loss corresponding to the amount of bonded water. By knowing the stoichiometry of the dehydration reaction the percentage of these phases in the sample can be deduced. After differentiation of the TG curve (DTG) each dehydration reaction produces a peak. As can be seen in Fig.2.6.2 [Ben-Dor, 1983], the reactions are brought out much more clearly in the DTG curve than in the TG curve. It is seen that the DTG and DTA curves are almost identical indicating that all the reactions taking place in the heating range are dehydration reactions.

Experimental procedure

The thermal analyses, including DTA, TG and DTG, were carried out by using a Stanton Red-Croft model 780. This can give simultaneous TG records and DTA curves and calculates the DTG at the end of the experiment. The analyses were performed between 30 °C and 850 °C in a nitrogen atmosphere with a heating rate of 10 °C/min, and a gas flow rate of 50 ml/min. To ensure that the atmosphere is CO_2- and moisture-free, the nitrogen gas was passed through soda-lime, silica gel and a molecular sieve type 13X (i.e. sodium alumino-silicate). The sample weights used were about 40 mg.

2.7 COMPRESSION TEST

Specimen preparation

a) The cement paste with w/s = 0.45 was cast in a 5 x 11 x 2 inch rectangular prism with a metal plate in the middle to separate the mould into two 5 x 5 x 2 inch sections. The samples were placed

with the 5 inch side vertical for 24 hours, then de-moulded and cured in water at room temperature. At the appropriate time the sample was cut into four 2 inch cubes for the test.

b) The cement paste was cast in a 3.6 x 7.3 x 0.5 inch prism mould which was rotated along its longest axis for 24 hours. The sample was then de-moulded and cured in saturated lime water at room temperature. At the appropriate time the samples were cut into 0.5 inch cubes for testing.

c) The cement paste was cast in a 3.6 x 7.3 x 0.5 inch prism mould which was rotated in an oven at 40 °C for 8 hours. The samples were then de-moulded and cured in saturated lime water at 40 °C. At the appropriate time the samples were cut into 0.5 inch cubes for compression testing.

Testing procedure

The compression tests of the 2 inch cube samples were carried out on a ± 250 KN Servo-hydraulic testing machine, with a loading rate of 0.005 mm/sec. The 0.5 inch samples were tested on an Instron testing machine with a loading rate of 0.5 mm/min.

2.8 EXTRACTION OF CEMENT PHASES

"SAM" extraction

The silica phases and all the hydration products of the cement can be dissolved in a "SAM" solvent, a mixture of salicylic acid and methanol, in the proportion of 7 g of acid to 40 ml of methanol. To dissolve 1 gramme of cement, 100 ml of "SAM" solvent is required with a stirring time of 1 hour, followed by filtering and washing by methanol. Finally the residue is dried at 60 °C. In the hydrated

samples, the silica gel hydrates are more difficult to dissolve, a second wash being required to ensure dissolution.

"KOSH" extraction

The interstitial phases can be dissolved in a "KOSH" solvent which is a mixture of K(OH), sugar and water in the ratio of 1:1:10. To dissolve 1 gramme of cement, 50 ml of the solvent, which is heated up to about 95 °C, is required. The optimum mixing time is about 1 minute; if this period is prolonged filtration becomes more difficult.

There are many other techniques for extracting phases from anhydrated or hydrated cement as stated by Klemm and Skalny [1977]. The two methods described above are relatively more effective and cause less damage to the residual phases.

Extraction of fly ash from a blended cement

The hydrated blended cement is ground into a fine powder in an agate mortar for 40 minutes using cyclohexane as a grinding aid. The powder samples are first washed in "SAM" solvent to dissolve the unhydrated silica phases and most of the C-S-H gel. The residue is then washed in "KOSH" to dissolve the interstitial phases. Finally, to ensure that all the C-S-H gel is dissolved, a second treatment of "SAM" is necessary, leaving a residue of fly ash.

2.9 EXTRACTION OF THE GLASSY PHASE FROM THE FLY ASH

To reveal the crystal phases of the fly ash, the glassy phase needs to be removed by washing in HF acid. 1 gramme of fly ash is first disagglomerated by washing in 10 g of water for 1 hour, and then mixed into 50 ml of 2% HF for 1 hour. Most of the glass phase will be etched away.

CHAPTER 3

MATERIALS

3.1 DATA ON CEMENTS USED IN THE PRESENT WORK

In total five commercial cements were studied in the present work: three British ordinary Portland cements (OPC); one British white cement, and one Danish white cement.

Blue Circle OPC (BT) and Blue Circle white cement (BW) were supplied by Blue Circle Industries, Technical Research Division, D44 by the Cement and Concrete Association, Westbury OPC by UKAEA Winfrith, and the AW (white cement) by Aalborg Portland Cement, Denmark. The chemical analysis and Bogue composition were provided with the cements.

The chemical compositions of the cements are given in Table 3.1.1. The phase composition was determined by QXRA carried out with the assistance of Mr W A Gutteridge at the Cement and Concrete Association. The Bogue and QXRA phase compositions are given in Table 3.1.2. The particle size distribution of the cements was measured by Malvern laser particle size analyser 3600 and is plotted in Fig.3.1.1.

3.2 DATA ON THE FLY ASHES USED IN PRESENT WORK

Three kinds of fly ash supplied, together with the chemical analyses, by Cement and Concrete Association, were studied. The chemical composition of the fly ashes, named according to the power station where they are produced, is shown in Table 3.2.1. The quantity of crystalline phase was measured by Mr W A Gutteridge as shown in Table 3.2.2.

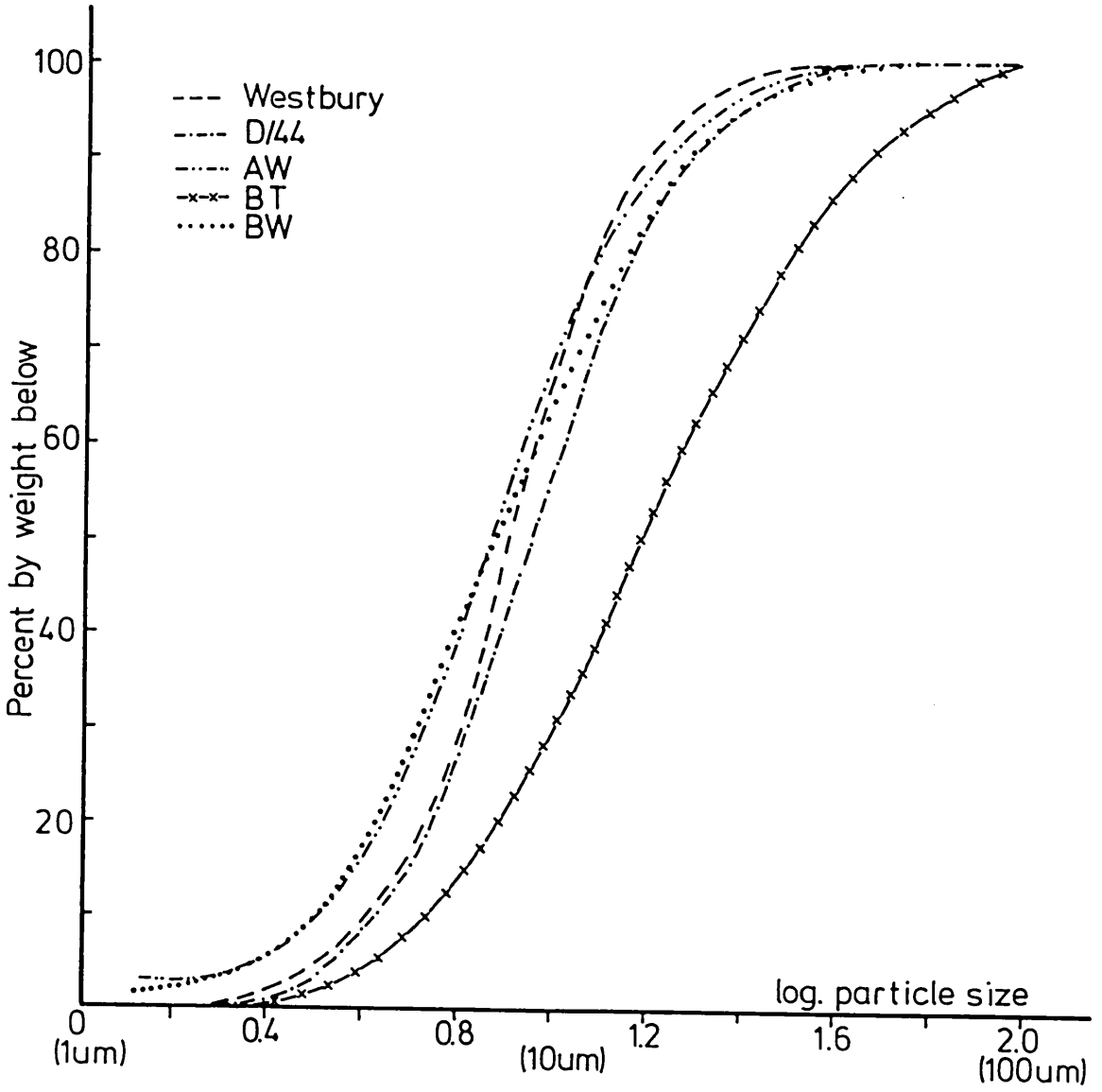

FIG. 3.1.1 PARTICLE SIZE DISTRIBUTIONS OF THE CEMENTS.

The particle size distribution of the fly ashes, measured using the Malvern 3600 (Section 2.2), is plotted in Fig.3.2.1 and shows that Fiddlers Ferry is the finest followed by Bold and Drax.

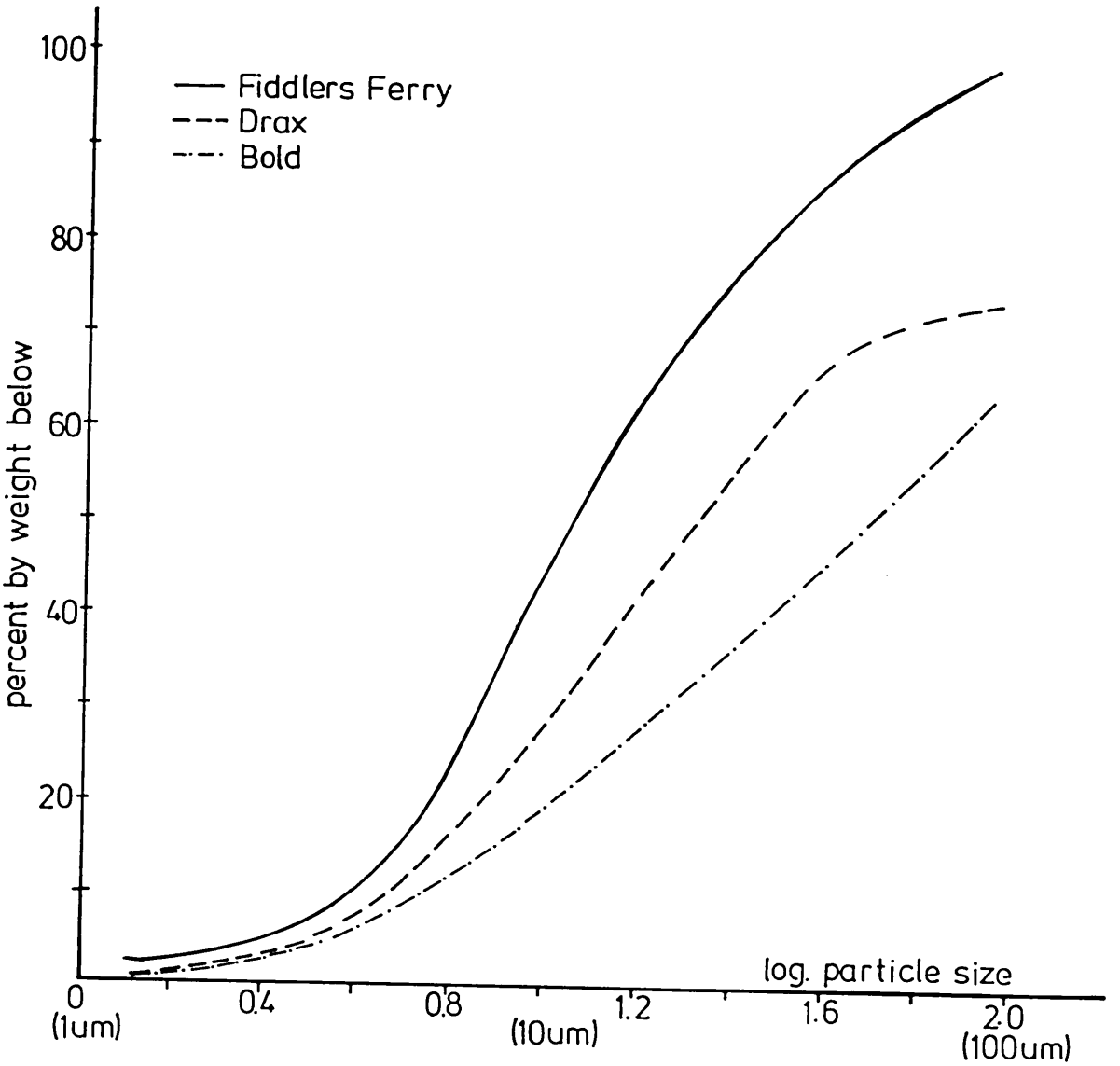

FIG. 3.2.1 PARTICLE SIZE DISTRIBUTIONS OF THE FLY ASES.

TABLE 3.1.1 CHEMICAL COMPOSITIONS OF THE CEMENTS (WT %)

Cement	BT	BW	AW	Westbury	D/44
SiO_2	20.3	22.5	24.01	19.9	21.5
Al_2O_3	5.2	4.5	1.79	6.7	4.8
Fe_2O_3	3.1	0.27	0.36	3.2	2.0
CaO	64.7	67.5	69.26	64.7	64.6
Na_2O	0.19	0.14	0.15	0.34	0.2
K_2O	0.34	0.12	0.04	0.54	0.7
MgO	1.1	0.4	0.52	1.2	1.9
SO_3	2.8	2.3	1.64	2.5	2.7
P_2O_5	0.2	0.09	N/A	N/A	0.1
TiO_2	0.27	0.02	N/A	0.3	2.27
Mn_2O_3	0.11	0.03	N/A	N/A	0.06
Free lime	0.7	2.1	2.46	0.9	1.1

TABLE 3.1.2 PHASE COMPOSITION (WT %) OF THE CEMENTS BY BOGUE AND QXRA

Phase	BT	BW	AW	Westbury	D/44
C_3S					
Bogue	59	58	8.23	53.3	54
QXRA	67	70	84	68	69
C_2S					
Bogue	13.7	20.8	6.8	16.9	20
QXRA	15	23	10	8	22
C_3A					
Bogue	8.5	11.5	4.13	13.9	7
QXRA	5	5.5	2	14	5.5
C_4AF					
Bogue	9.4	0.9	1.10	6.6	6
QXRA	6	0	0	3.5	3
Calcium sulphate					
Bogue	4.6	3.9	2.9	5.0	4.5
QXRA[1]	H,A	G,H	G,H	A	H

Note:

[1] Qualitative X-ray analysis on the form of calcium sulphate

Cement	H = hemihydrate	A = anhydrite	G = gypsum
BT	2.5	2.0	-
BW	1	-	1
AW	1.5	-	1
Westbury	-	4.5	-
D/44	2.0	-	-

TABLE 3.2.1 CHEMICAL COMPOSITION OF THE FLY ASHES (WT %)

Fly ashes	Bold	Drax	Fiddlers Ferry
SiO_2	44.6	51.3	44.6
Al_2O_3	27.2	25.8	25
Fe_2O_3	13.76	10.29	11.8
CaO	1.99	1.24	3.39
Na_2O	0.69	0.93	0.38
K_2O	3.72	3.69	3.47
MgO	1.21	1.54	1.67
P_2O_5	0.2	0.26	0.34
SO_3	0.7	0.14	0.62
LOI	3.48	3.68	3.16

TABLE 3.2.2 CRYSTAL PHASE COMPOSITION IN FLY ASHES OBTAINED BY QXRD (WT %)

Fly ash	Mullite	Quartz	Magnetite	Haematite	'Glassy' material by difference from 100%
Bold	13	3	14	2	68
Drax	8	6	10	1	75
Fiddlers Ferry	8.8	3.8	7.4	0.5	79.5

CHAPTER 4

CHARACTERISATION OF FLY ASH (P.F.A.)

Fly ash is the portion of incombustible material in a coal fired boiler that is carried through the combustion chamber and heat exchange ducts. It is captured by mechanical collection or electrostatic precipitation as a fine particulate residue from combustion gases before they are discharged to the atmosphere.

4.1 REVIEW OF PREVIOUS WORK

4.1.A *THE FORMATION OF FLY ASH*

The coal from which fly ash is derived is ground to fine powder and then injected into the boiler furnace. Temperature increases rapidly as particles are swept into the burning zone. The organic material in the coal burns quickly and the residual particles, inorganic minerals, fuse to a viscous liquid before undergoing vitrification and partial recrystallisation. The length of time the coal stays in the burning zone is very short. Raask [1969] observed that during the fusion process the particles lose their irregular shape, becoming spheres as a result of the action of surface tension, with the exception of the large quartz particles whose sharp edges are only rounded off. At the same time, a sequence of chemical reactions occurs, including dehydration and evolution of CO_2, SO_2 and SO_3 gases, during the combustion.

4.1.B *MINERALS PRESENT IN FLY ASH*

To understand what takes place in the inorganic part of the ash on burning, it is useful to consider the actual mineral

components present in coal. Table 4.1.1 gives the common mineral components in coal ash. As the coal ashes pass through the burning zone they undergo a sequence of physical and chemical changes. Table 4.1.2 [Raask, 1980] lists the principal changes in the minerals of coal on burning.

TABLE 4.1.1 COMMON MINERAL CONSTITUENTS OF COAL

MINERAL	TYPE	COMPOSITION
Muscovite	Mica	$K_2O.3Al_2O_3.6SiO_2.3H_2O$
Biotite	Mica	$K(Mg,Fe)_3.(AlSi_3O_{10}).(OH)_2$
Kaolin	Clay	$Al_2O_3.2SiO_2.H_2O$
Quartz	Silica	SiO_2
Pyrites	Sulphide	FeS_2
Calcite	Carbonate	$CaCO_3$
Halite	Chloride	NaCl
Sylvite	Chloride	KCl

TABLE 4.1.2 THE PHYSICAL AND CHEMICAL CHANGES OF MINERALS DURING COMBUSTION

MINERAL	PHYSICAL CHANGES IN THE FLAME	PRODUCTS
Mica	Fusion and vitrification	Glassy spheres
Clay	Fusion, partial vitrification and recrystallisation	Glassy spheres, mullite and quartz
Quartz	Partial fusion and vitrification	Amorphous silica spheres and unfused particles of α-quartz
Pyrites	Decomposition and oxidation	Magnetite, haematite and SO_2
Carbonates	Decomposition and sulphation	Sulphates and CO_2
Chlorides	Volatilization and sulphation	Sulphates and HCl

It can be seen that the typical crystalline materials present in fly ash are quartz (SiO_2), mullite ($2SiO_2 . 3Al_2O_3$), magnetite (Fe_3O_4) and haematite (α-Fe_2O_3), although the glass phase is the most common phase. Simons and Jeffery [1960] have examined British fly ash by QXRD and the resulting range of the crystalline phases is shown in Table 4.1.3.

TABLE 4.1.3 MINERALOGICAL COMPOSITION OF P.F.A.

CRYSTALLINE MATERIAL	RANGE % BY WEIGHT
Quartz	1 - 6.5%
Mullite	9 - 35%
Magnetite and haematite	5% or less

We now proceed to discuss each crystalline phase in turn:-

Quartz (SiO_2)

The crystalline quartz phase present in fly ash is α-quartz, a low temperature phase which appears to be present in the original ash [Diamond, 1981]. This indicates that the time the coal ash spends in the boiler flame is too short to convert the α-quartz to a high temperature phase such as tridymite and cristobalite. The amount of crystalline quartz is decreased after combustion; this is because the smaller particles are converted to a glassy phase in the flame [Raask, 1980].

Mullite ($3Al_2O_3.2SiO_2$)

Mullite is formed by a high temperature (>1400 °C) change of kaolin [Raask, 1980; Watt, 1969] as shown in the formula (1)

$$3[2SiO_2.Al_2O_3.H_2O] \rightarrow 3Al_2O_3.2SiO_2 + 4SiO_2 + 3H_2O\uparrow \quad .....(1)$$

The SiO_2 liberated in the formation of mullite appears as a cristobalite phase if equilibrium is reached [Watt, 1969]. However in practice the time of combustion is too short for the cristobalite phase to form so the SiO_2 will exist as a glassy phase in the fly ash. In fact the mullite, which appears as microscopic needles, is always embedded in a glassy matrix.

Haematite (α-Fe_2O_3) and magnetite (Fe_3O_4)

Haematite and magnetite are formed by the decomposition and oxidation of pyrites (FeS_2) [Raask, 1980; Thorpe et.al., 1984] as shown in formulae (2), (3) and (4).

$$FeS_2 \rightarrow FeS + \tfrac{1}{2}S_2 \qquad \ldots\ldots(2)$$

$$FeS + \tfrac{5}{3}O_2 \rightarrow \tfrac{1}{3}Fe_3O_4 + SO_2\uparrow \qquad \ldots\ldots(3)$$

$$2Fe_3O_4 + \tfrac{1}{2}O_2 \rightarrow 3Fe_2O_3 \qquad \ldots\ldots(4)$$

Thorpe et. al. [1984] discussed the oxidation of FeS_2 and noted that the mixture of sulphates and oxides formed depends on the oxygen partial pressure in addition to the temperature and particle size.

During the combustion process there will be some interaction between the oxides. Kiss et. al. [1972] observed that magnetite occurs as dendritic spinels, occasionally together with alumino-iron oxide spinel (hercynite).

Besides these major crystalline phases, there are other minor crystal phases present such as:-

Alkali sulphate

The sulphur, which is decomposed from the pyrite (formula 2), is emitted as sulphites and oxidized to sulphates in the gas stream. The sulphates rapidly combine with alkali or calcium and condense

onto the surfaces of the fly ash [Diamond, 1981]. Raask [1982] proved that the alkali and calcium sulphates dissolve rapidly in water.

Lime (CaO)

Lime is formed by the decomposition of calcite mineral which decomposes to CO_2 and CaO at ∿900 °C.

4.1.C *THE MORPHOLOGY OF FLY ASH*

The majority of fly ash particles are of spherical shape because of the action of surface tension during fusion [Raask, 1969, 1982]. A few irregular particles are of quartz or unburned coal. Most of the fly ashes consist of fine, dense spheres, but there are cases of relatively large particles having voids in the interior, which have been classified into two types, cenospheres and plerospheres:-

Cenospheres [Raask, 1968, 1970; Lauf, 1981]

Cenospheres are completely hollow particles with the thickness of the shell being about 10% of the radius. Raask [1968] determined the composition of the gas in the cenospheres by gas chromatography and found it to be mainly carbon dioxide and nitrogen, and he also pointed out that the cenospheres contain more silica and less calcium oxide than the denser particles.

Plerospheres [Diamond, 1981]

Plerospheres are hollow shells which contain minute spheres. The small particles may be dense or hollow. However their formation is still not very clear.

4.1.D *CHEMICAL COMPOSITION OF FLY ASH*

The oxide composition of fly ashes varies considerably, especially for silica, iron oxide and CaO, due to the different minerals present in the various types of coal. For example, bituminous and anthracite coals usually produce low calcium ash which contains low calcium oxide but high silica and iron oxide; lignitic and sub-bituminous coals produce high calcium oxide ash. Generally the fly ash produced in Britain is a low calcium ash. Table 4.1.4 shows a typical range of chemical compositions of British ashes.

TABLE 4.1.4 CHEMICAL COMPOSITION RANGES IN BRITISH ASHES

OXIDE	WEIGHT % RANGE
SiO_2	40 - 52
Al_2O_3	23 - 29
Fe_2O_3	8 - 14
CaO	1 - 8
MgO	1.6 - 3.0
Na_2O	0.2 - 2
K_2O	1.5 - 4.0
SO_3	0.6 - 2.5

4.1.E *CHEMICAL REACTION BETWEEN FLY ASH AND CEMENT*

Fly ash has been recognised as an artificial pozzolana which is defined as "a siliceous or siliceous and aluminous material which in itself possesses little or no cementitious value but which will combine with lime at ordinary temperature in the presence of water to form compounds possessing cementitious properties". The pozzolanic activity of the fly ash is believed to be due to the dominance of the glassy phase [Kokubu, 1968]. Partially replacing

the cement by fly ash in concrete mixes can increase the long term strength, as the pozzolanic reaction converts the CH phase and larger pores into less dense C-S-H and smaller pores [Mehta, 1983]; also there are other benefits such as improvement in the workability, decrease in heat evolution, increased sulphate resistance and reduction of cost. The reactivity of the reaction may depend on the fineness of the ash, and on the SiO_2 and Al_2O_3 content.

4.2 PRESENT WORK

4.2.A *MICROSTRUCTURE OF FLY ASH*

The internal and external structure of the fly ash has been examined under various types of microscope. Polished sections of fly ash, which had been dispersed in resin, were examined under the reflected light microscope and the BEI mode of the SEM; and the surfaces of fly ash were observed using secondary electrons in the SEM.

Plate 4.2.1 shows a scanning electron micrograph of fly ash particles dispersed on double-sided sellotape. The wide range of particle sizes can be seen. All the surfaces are covered by many submicro-structures [Plate 4.2.2], which are dominated by sulphate particles [Raask and Goetz, 1981] but also contain some fine gypsum crystals. Occasionally, some fly ashes have the crystal phase exposed on the surface when there is no layer of glassy phase forming on these ash surfaces. However, a disadvantage of this technique is that the internal structure cannot be revealed.

Plate 4.2.3 shows a back scattered image of the fly ash. The internal structure can be observed more clearly than in an optical micrograph [Plate 4.2.5] because of better resolution at higher

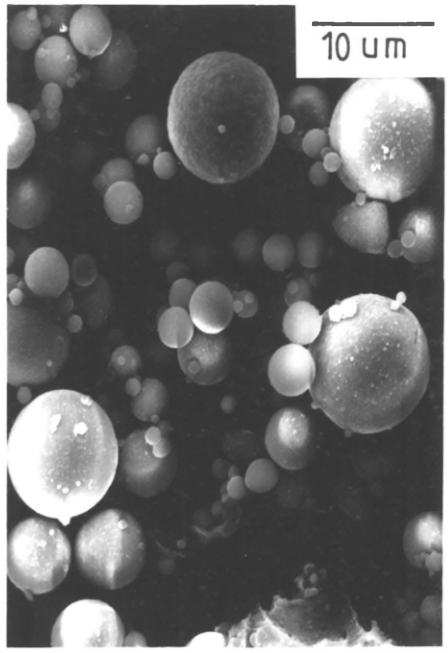

PLATE 4.2.1

Fly ash (Fiddlers Ferry) in the SEM

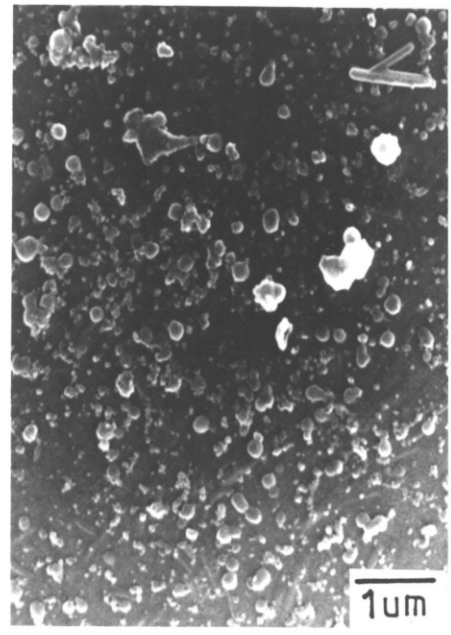

PLATE 4.2.2

Fly ash surface microstructure (Fiddlers Ferry)

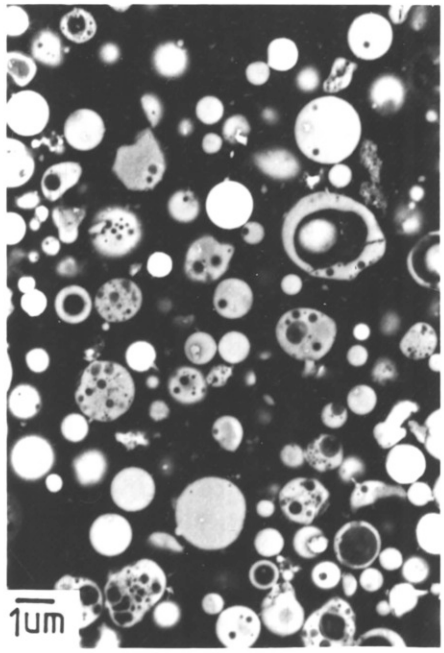

PLATE 4.2.3

BEI of fly ash dispersed in resin

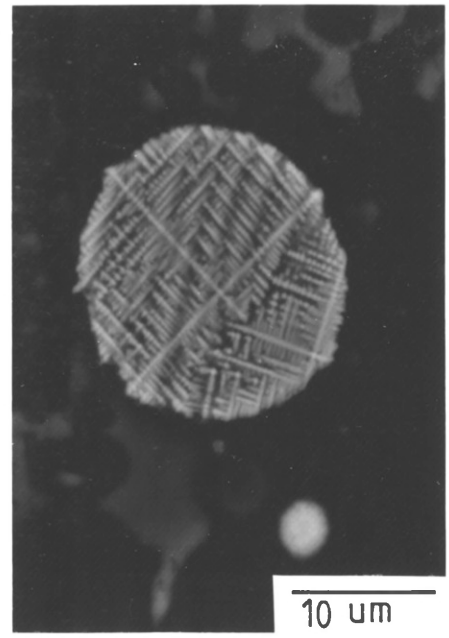

PLATE 4.2.4

BEI of a magnetite particle

magnification. Many of the spheres have internal pores which may be mistaken for solid spheres in the optical micrograph. Those spheres which contain a high concentration of iron can be recognised by their brighter appearance resulting from the higher average atomic number. Sometimes the internal microstructure of the iron spheres can be seen as shown in Plate 4.2.4 and, from the dendritic structure, they can be identified as magnetite spheres. A minor disadvantage of this technique is that not all phases present in the particles can be recognised immediately as in optical microscopy.

Plate 4.2.5 shows an optical micrograph of the fly ash in which a surprising diversity of microstructure can be seen. Some types of particle can be identified by their optical properties. In general the particles can be divided into several categories:-

1) Solid spheres (S) - Solid spheres appear as grey circular particles surrounded by a dark ring. There are many of these, with a large variation in size. It is difficult to judge whether the particles are purely glass phase or accompanied by crystals since the major crystal phase, mullite, and the glass phase have very similar optical properties.

2) Cenospheres (C_o) - Cenospheres are shown up as grey colour rings.

3) Plerospheres (P) - Plerospheres can be identified easily on the polished surface as a large circles surrounding many small discs. The wall of the plerosphere may sometimes contain small bubbles.

4) Haematite - The haematite phase does not show up in the black and white micrograph but can be recognised easily by their red iron colour, especially under the polarised light. They have been seen together with other phases frequently, but can also form whole particles.

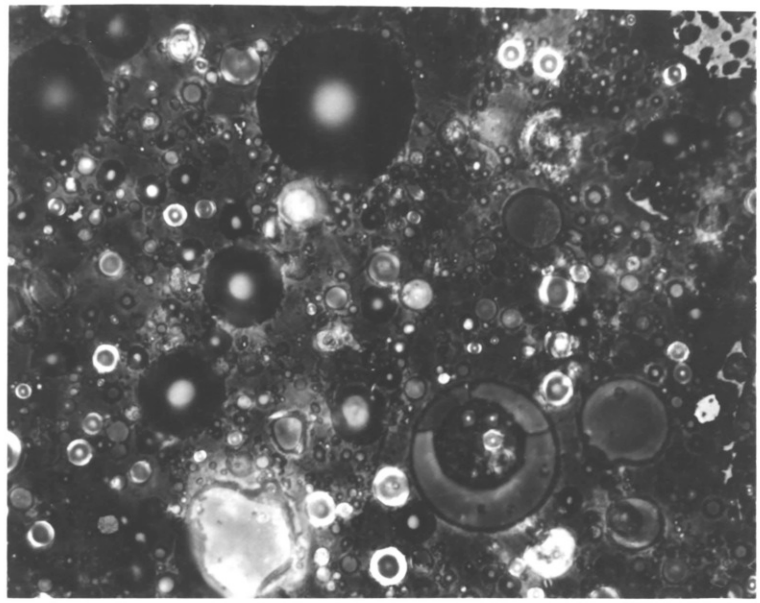

PLATE 4.2.5(a

Optical micro graph of fly ash dispersed in resin, showing the diversity in the types of particle
Mag. = x333

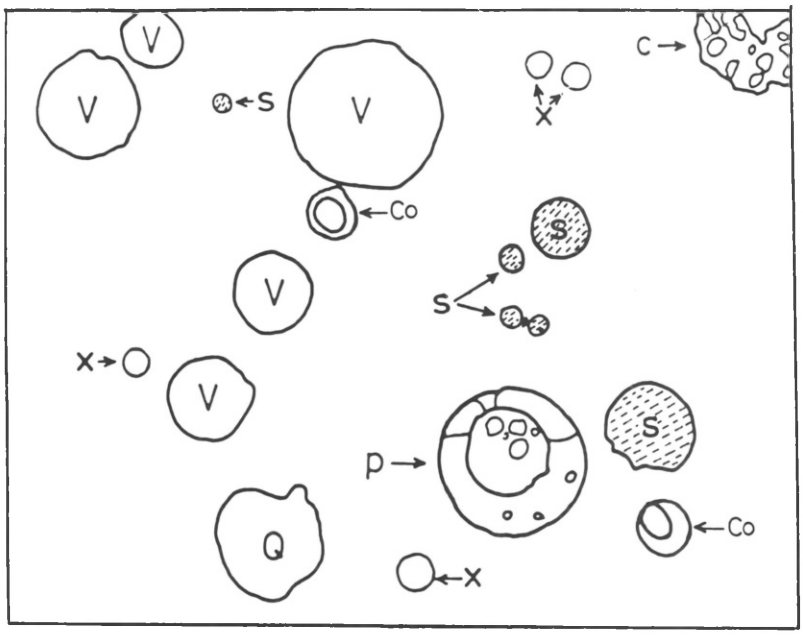

V=voids S=solid spheres X=unknown
Q=quartz Co=cenospheres
C=coal P=plerospheres

PLATE 4.2.5(b

Diagrammatic representatic of the variou types of particles

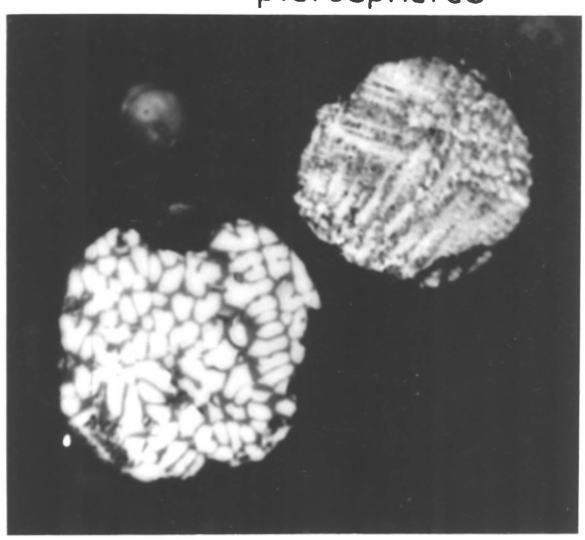

PLATE 4.2.6

Optical micrograph of two high iron content fly ashes
Mag. = x833

5) Magnetite spheres - Magnetite spheres are shown in Plate 4.2.6. These are mostly solid spheres and are highly reflective and optically isotropic. They are also easily recognised by their dendritic structure, e.g. the R.H.S. sphere in the picture is a magnetite particle. However, there is another phase, spinel, having Fe_3O_4 composition but with a different crystal structure; this is defined by Lauf [1982] as a "ferrophase". In the picture, the left hand side of the larger sphere may consist of this phase since it has a morphology different from the dendritic structure of the other section.

6) Quartz (Q) - Quartz usually has an irregular shape and, being optically anisotropic, can be distinguished under cross polarised light. In reflected light it appears as light grey particles.

7) Unburned coal (C) - Unburned coal appears as large irregular particles containing a skeleton of sintered ash.

8) Voids (V) - Voids show as an area of black ring surrounding a white circle. They are probably formed by a fly ash being pulled out during the polishing. On the other hand, Lauf [1982] suggested that they are cenospheres.

9) Unknown (X) - Those appearing as bright surrounding a dark disc with a bright spot in the centre. Occasionally small circular particles can be seen inside the ring. The bright central spot indicates that these might be voids. However, the cause of the bright ring is not yet understood.

4.2.B *ETCHED FLY ASH*

Estimation of glass phase in fly ash

The glass phase in the fly ash is etched away by HF acid, hence the amount of glass phase may be estimated by weighing the ash before and after treatment [Section 2.9]. Six fly ashes have been etched by HF acid and their glass contents are compared with those obtained by QXRD [Table 4.2.1]. The two sets of results are almost identical. However, if the etched fly ashes are re-examined by QXRD, it is found that a small amount of glassy phase is still present and that the amount of silica and mullite is reduced slightly. This indicates that the acid is etching some of the crystalline phase as well as leading to a false estimate of the amount of glassy phase in the fly ash.

Microstructure of etched fly ash

The microstructure of the crystalline phase can be revealed clearly after the acid treatment on the fly ash. With the assistance of the energy dispersive X-ray analyses (EDXA) in the SEM, the elements in the crystal can be detected. This may help to identify the phases present.

Plate 4.2.7 shows that the majority of the spheres consist of crystals which are identified by their long needle shape. The mullite needles are orientated in various directions and infill the whole sphere. They may be surrounded by a layer of spinel material [Plate 4.2.8] which has a high concentration of Fe and Al. Both spheres in Plates 4.2.9 and 4.2.10 contain high concentrations of Fe, and traces of Si and Al which are higher in the latter Plate. The sphere in Plate 4.2.9 has a dendritic microstructure, hence it is probably magnetite, and that in Plate 4.2.10 may be a "ferrosphere" which contains some submicro-structures on its grains which may correspond to spinel consisting of iron oxide, alumina and silica.

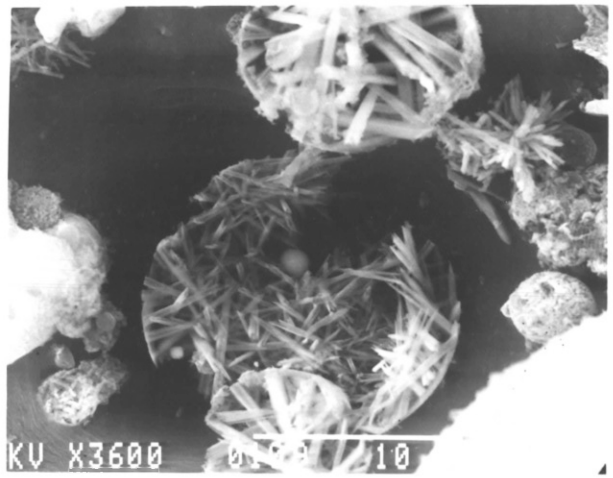

PLATE 4.2.7

Etched fly ash (Fiddlers Ferry), showing most of the fly ash consistent with mullite crystal

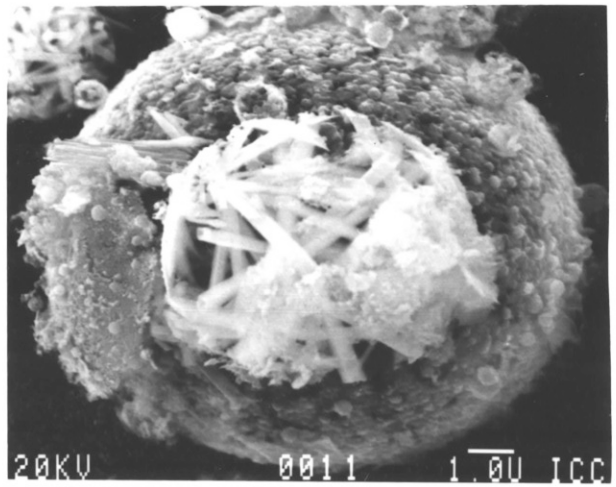

PLATE 4.2.8

An etched fly ash consisting of two phases, a mullite centre surrounded by a layer of spinel

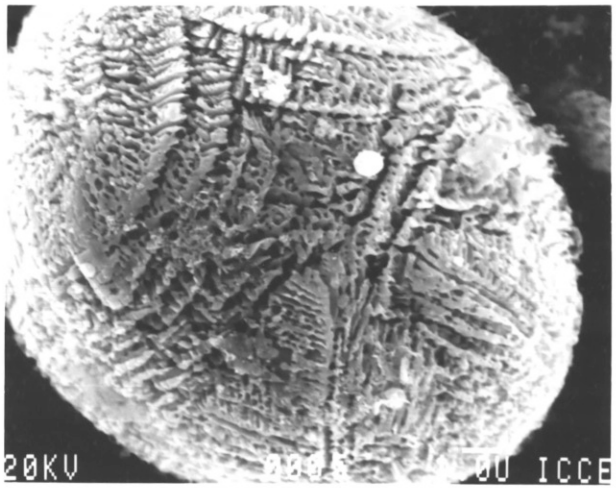

PLATE 4.2.9

An etched magnetite particle

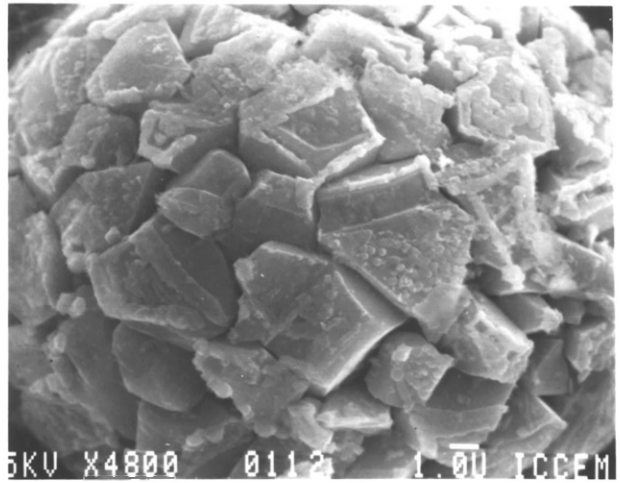

PLATE 4.2.10

An etched "ferro-sphere"

4.2.C *THE EFFECT OF THE POZZOLANIC REACTION ON THE FLY ASH SURFACE*

Once the pozzolanic reaction takes place between the cement hydrate, CH, and the glassy phase in the fly ash, the crystal phase structure of the fly ash will start to appear and become more prominent as the reaction progresses. The continuing dissolution of glass phase can be observed in Plate 4.2.11 which also shows the two most common types of microstructure on the reacted ash surface.

Plates 4.2.11 (a), (b) and (c) show the appearance of long needle crystals of mullite which may appear at any orientation, as can be seen in Plate 4.2.7. Therefore the small square crystals on the surface may be the cross-sections of the mullite needles. The mullite crystals are partially embedded in a finer crystalline matrix [Plate 4.2.11 (c)] which may dissolve in HF acid much faster than mullite, hence they have not been seen in etched ash.

Plates 4.2.11 (d), (e) and (f) show another type of surface microstructure. This contains many circular patterns, with diameters approximately 10 μm, which consist of a highly soluble material around a small crystal; they are embedded in a very fine crystal matrix. Sometimes these particles will be accompanied by a few mullite crystals [Plate 4.2.11 (f)]. However, this type of microstructure has not been seen in the etched fly ash implying that the phase present in these fly ashes is soluble in HF acid. A possibility is that the structure described above as a crystal matrix in both sets of fly ashes is actually glassy phase which is gradually etched away by CH.

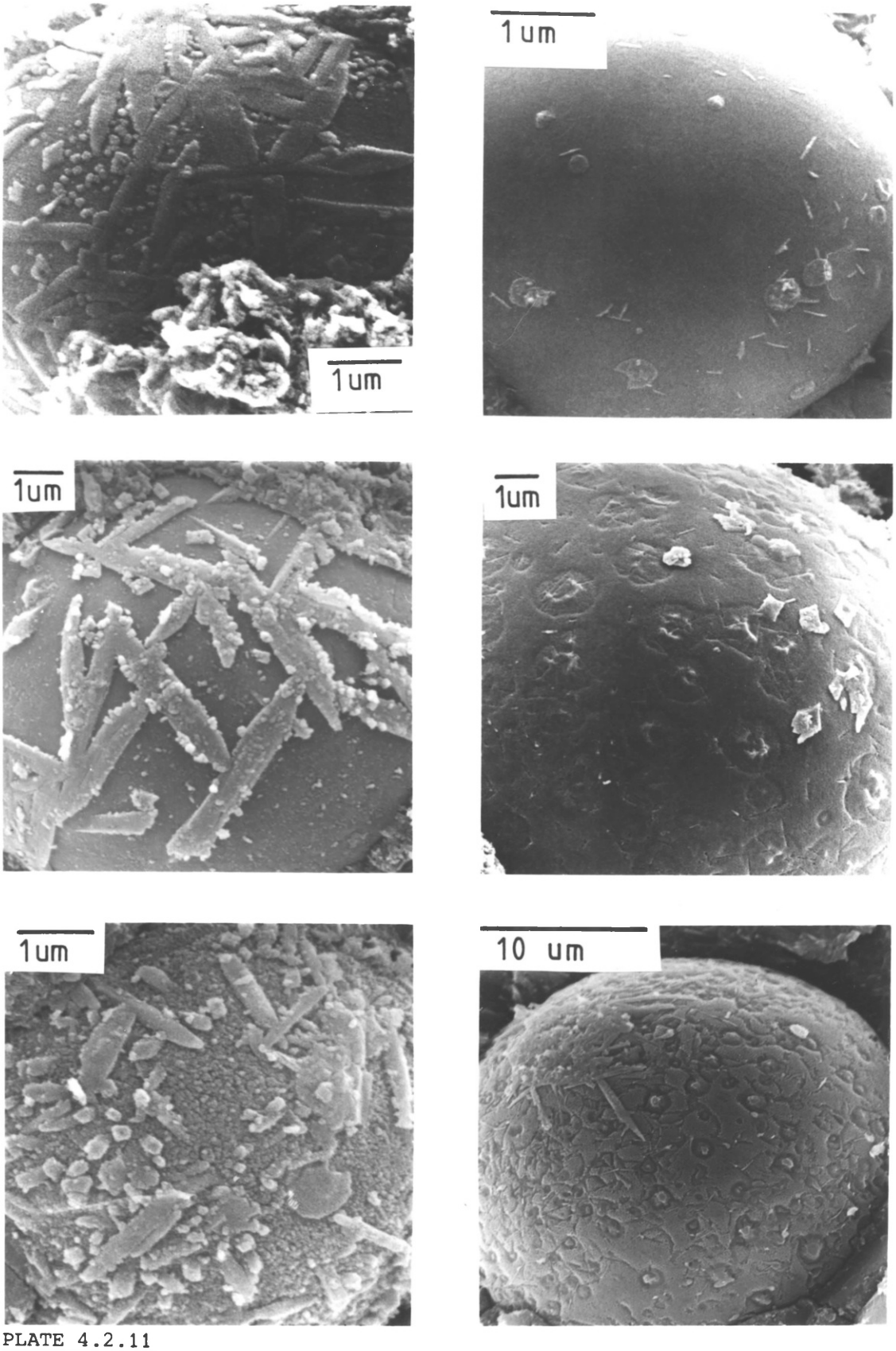

PLATE 4.2.11

Crystalline phases revealed by dissolution of the glassy phase of Fiddlers Ferry fly ashes after

(a) 14 days
(b) 28 days
(c) 90 days
(d) 14 days
(e) 28 days
(f) 90 days

CHAPTER 5

HYDRATION OF CEMENT AND FLY ASH CEMENT

5.1 REVIEW OF PREVIOUS WORK

5.1.A *MANUFACTURE OF PORTLAND CEMENT*

[Pollitt, 1964; Lea, 1970; Neville, 1981; Bye, 1983]

The essential ingredients of Portland cement are lime, silica, alumina and iron oxide. All of these occur in nature as calcareous materials (e.g. chalk, limestone), or argillaceous materials (e.g. clay, shale, kaolin), and marls, a mixture of both.

The process of cement manufacture consists of grinding the raw materials to obtain a homogeneous mixture, burning the mix in a kiln to produce clinker and finally the grinding of the clinker together with calcium sulphate. There are two processes known as "wet" and "dry". An advantage of the "wet" process is that there is greater control of the raw mix; however, a large amount of energy is consumed in evaporating the water.

The heat treatment in the rotary kiln, which is a long cylinder rotating on its axis and inclined so that the materials fed in at the upper end travel slowly to the lower, can be divided into five sections:-

1) Drying zone - the slurry is dried in the upper part of the kiln at temperatures up to 100 °C and the water driven off as steam.
2) Preheating zone - the temperature in this area reaches 350 °C - 650 °C and the decomposition of clay materials occurs.
3) Calcining zone - any combustion of organic matter and decarbonation of the calcium carbonate takes place at a temperature of 1000 °C.

4) Clinkering zone - the temperature in the kiln increases to 1300 °C - 1500 °C according to the composition and fineness of the material and is maintained at this temperature sufficiently long for the materials to coalesce into small balls or lumps of clinker which consist mainly of crystals of C_2S and C_3S, together with liquid containing $CaO.Al_2O_3.Fl_2O_3$ and MgO, but relatively low in SiO_2.

5) Cooling zone - at the end of the kiln the clinker passes into a cooler region in which the melt solidifies with the crystallisation of C_3A and C_4AF.

Finally the clinker is ground with gypsum which prevents the "flash setting" of the cement.

5.1.B *HYDRATION OF CEMENT CONSTITUENT PHASES AND THE EFFECT OF ADDING FLY ASH*

The cement-water interaction is very complicated so it is often useful to study first the simplest single mineral-water systems. The clinker components in Portland cement are:- tricalcium silicates ($3CaOSiO_2$, C_3S), tricalcium aluminate ($3CaOAl_2O_3$, C_3A), dicalcium silicate ($2CaOSiO_2$, C_2S), and alumino-ferrite phase ($4CaOAl_2O_3Fe_2O_3$, C_4AF). The hydration of each of these phases is affected differently by the fly ash. The hydration of each cement component has been studied in many review papers [Copeland and Kantro, 1968; Skalny and Young, 1980, and Pratt, 1982], and the effect of fly ash on their hydration has been reviewed by Takemoto and Uchikawa [1980] and Pratt [1982]. The brief summary presented here is not intended to concentrate on the hydration of the pure phases, but rather on the effects of adding other species such as gypsum, CH, etc, and to compare these to that of fly ash.

5.1.B.1 *Hydration of tricalcium silicate*

Crystal structure and polymorphic forms

The major phase in most modern Portland cement clinkers is a form of C_3S which occurs in several polymorphic forms, the stability of which is temperature dependent. Seven polymorphs have been discovered [Regourd and Guinier, 1974; Maki and Chromy, 1978], a rhombohedral crystal forms at high temperature (>1070 °C), while three monoclinic and three triclinic structures exist in the range 980 - 1070 °C and below 980 °C respectively. All these polymorphs have an almost trigonal crystal structure (a = 7, c = 25 Å), made up of independent SiO_4 tetrahedra on trigonal axes, linked by calcium ions which are octahedrally coordinated; the structure contains three holes per formula weight [Jeffery, 1952].

In commercial cement, some impurities, such as Mg, Al, Fe, K, Na etc are present in the C_3S (alite). These foreign ions can be incorporated into the C_3S crystal lattice to stabilise the high temperature polymorphic forms at room temperature [Jeffery, 1952]; indeed most alite in cement is found to be in monoclinic form [Regourd, 1979; Maki and Chromy, 1978], but triclinic and rhombohedral forms have been found in a few cements [Berger et.al., 1966; Regourd and Grinier, 1974].

Hydration of C_3S

C_3S is the major cementitious component of most Portland cements and its hydration is often used as a model for hydration of cement. A typical curve of the rate of heat evolution of C_3S against time is shown in Fig. 5.1.1, and can be divided into four stages [Kondo and Ueda, 1968; Jennings et.al., 1981].

(I) Pre-induction period - an initial fast reaction giving off a burst of heat lasting for a few minutes

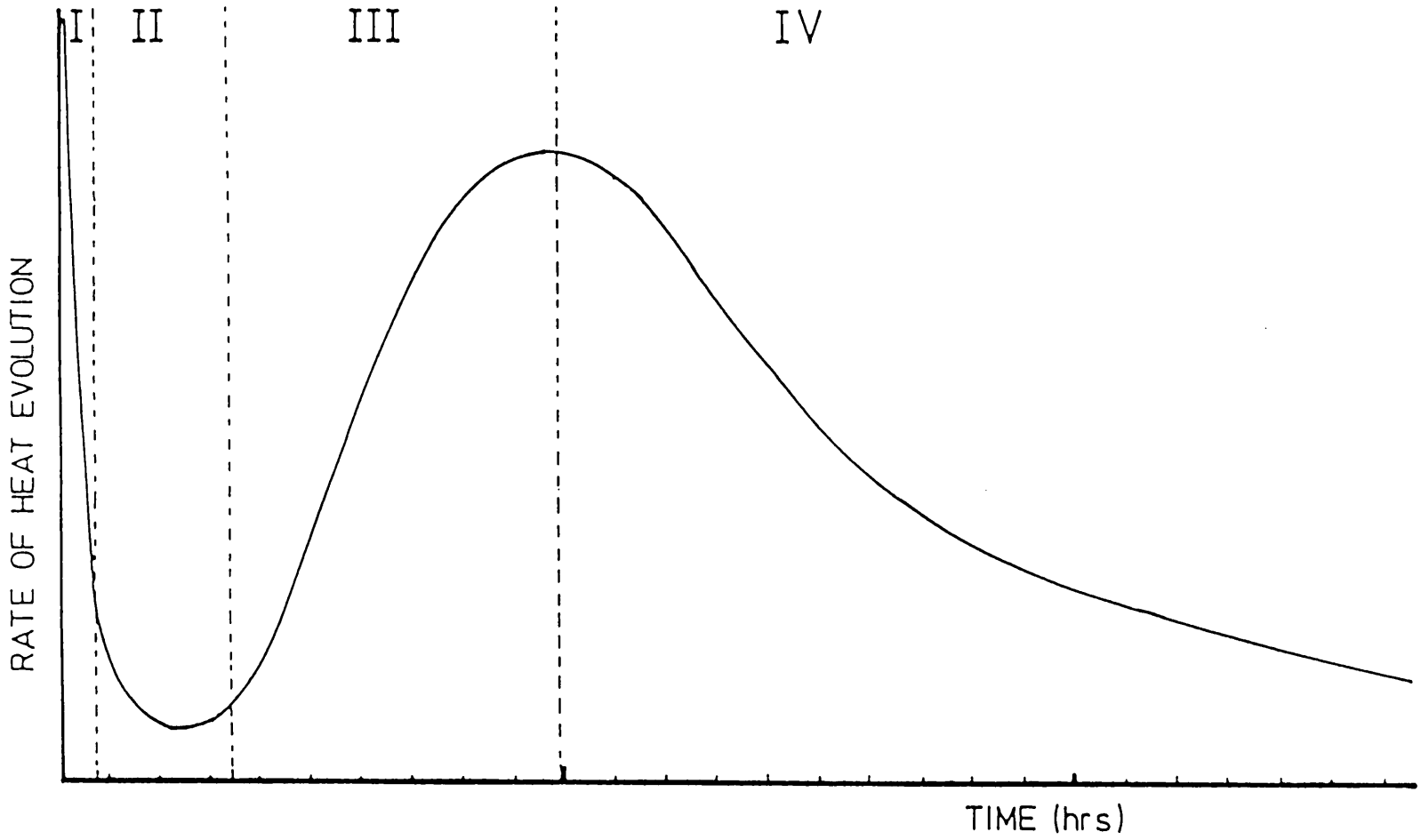

FIG. 5.1.1 SCHEMATIC REPRESENTATION OF THE DIFFERENT STAGES OF HYDRATION FOR C_3S

(II) Induction period - lasting for a few hours, during which the rate of heat output is very small

(III) Acceleration period - a period of increasing quantities of heat are given off

(IV) Deceleration period - the rate of heat evolution decreases, finally reaching a constant low value

Mechanism of hydration

There are many different theories of the hydration of C_3S, especially in the induction period (stage II). Various proposals have been put forward to explain the onset and end of this period.

a) Young, Skalny and co-workers (Skalny and Young, 1980; Young, 1972; Taylor et.al., 1976; and Taylor, 1979) suggested that initial hydrolysis with water causes Ca^{2+} leaching into solution. However, these ions are attracted to, and remain close to, the resulting negatively charged silicate region, forming an electrical double layer which then inhibits further dissolution hydrolysis. The concentration of Ca^{2+} in solution still slowly builds up, until it becomes supersaturated with respect to CH. Calcium hydroxide nuclei are then formed and rapid precipitation of CH begins. This disrupts the electrical double layer by reducing the Ca^{2+} concentration on one side and enhances the further dissolution and reaction of C_3S. This theory is supported by the maximum concentration of Ca^{2+} being at the end of the induction period, [Young et.al., 1977], and a positive zeta-potential being obtained on the surfaces of the C_3S particles [Tadros et.al., 1976(a), and Suzuki et.al., 1981].

b) Fierens and Verhaegen [1976] and others have proposed that the induction period is caused by delayed growth of C-S-H. Following the rapid chemisorption of water onto the C_3S particles, Ca^{2+} ions

are leached from the surface. Simultaneously, the hydration product C-S-H nucleates on the action sites. The induction period ends when the nuclei reach their critical size and start growing.

c) A protective hydrate theory has been developed by de Jong et.al. [1967], Stein [1977] and others. A layer of high C/S (3 = 1) silicate hydrate is formed in the first few minutes of hydration, and acts as a barrier layer. During the induction period, this phase transforms into a second hydrate with C/S ratio 0.8 - 1.5 which is more permeable.

d) A membrane/osmosis model has been developed by Double [1983] and Birchall et.al. [1978]. A membrane of CH and silicate indicates the induction period during which water passes through the membrane to continue the attack on the anhydrous grain. The membrane is ruptured by the osmotic pressure.

Although the first hypothesis has more direct evidence in its favour, it is in conflict with the results of Odler and Dörr [1979], and Kondo and Ueda [1968]. Kondo found that the induction period is extended if the C_3S is hydrated in liquid saturated with respect to CaO. Odler added CH crystals into the initial mix, as seeds, and found a negligible effect on the duration of the induction period. However, if C-S-H and CH are both added, a shortening effect is found. Similar results have also been found by Brown [1984], and these support the second and third hypotheses which have much in common [Taylor et.al., 1984]. Taylor et.al. [1984] pointed out that all the hypotheses are similar in that any nuclei of CH that are formed before the end of the induction period are poisoned by silicate and do not grow until a highly supersaturated solution is formed.

The rate of hydration during the acceleratory period is mainly controlled by chemical processes, such as the dissolution of C_3S and the nucleation and growth of products, but may also be affected by the diffusion rate of ions away from the C_3S surface through the thin C-S-H layer. The growth of C-S-H is confined to the surface because of the difficulties in transporting silica. The CH initially grows near the surface due to the higher concentration of ions, but some also forms in the pores and grows more quickly because of the greater space available [Kondo and Ueda, 1968].

In stage IV, the rate of hydration is controlled by the diffusion rate of ions through the low permeability C-S-H gel, but the reduction in C_3S surface area may also be relevant.

Effect of polymorphism and impurities on the C_3S hydration

The rate of C_3S hydration is influenced by the properties of the hydrating mixture, such as the various polymorphic forms are present and the presence of other substances (e.g. inorganic salts).

The variation in hydraulic activity, due to the presence of foreign ions which are used to stabilise the various polymorphs at room temperature, may be caused by the differences in crystal lattice, composition or lattice defects [Ono et al., 1965; Regourd and Grunier, 1974]. Yamaguchi et al. [1966] found a similar result in the MgO stabilised alites, but they and others [Masoto et al., 1973 and Sterula and Petrovic, 1981] conclude that the chemical effect of the impurities was greater than that due to the polymorphism. However, Harada et al. [1978] obtained a different effect, the order of reactivities at early stages of hydration being rhombohedral,

triclinic, and finally monoclinic. The differences diminished with age, and after 3 months they become negligible.

In commercial cement, gypsum is always present to delay the rapid hydration of C_3A. Gypsum also accelerates the alite hydration, as has been deduced from heat liberation data [Copeland and Kantro, 1969] and DTA data [Raccanelli, 1964]. The latter found that the acceleration is affected by both the calcium and alkali sulphates, but not by the concentration of sulphate ions. Kawada and Nemoto [1967] conclude that this acceleration is caused by the supersolubility with respect to $Ca(OH)_2$ rising in the presence of gypsum.

It is generally believed that inorganic salts (e.g. $CaCl_2$) have an accelerating effect on the hydration of C_3S [Kantro, 1975]. Young and co-workers [1977; 1978] found that the addition of $CaCl_2$ causes CH supersaturation to occur rapidly, thereby reducing the duration of the induction period. On the other hand, some inorganic salts (generally those that yield precipitates) do retard the hydration [Taylor et al., 1984].

Many organic substances have a retarding effect on C_3S hydration by inhibiting the precipitation of CH or C-S-H [Thomas and Birchall, 1983].

Morphology and microstructure of the hydrates

The hydration of C_3S produces a calcium hydroxide (CH) and calcium silicate hydrate (C-S-H) gel whose composition depends on the ages. CH first forms in the water space in small hexagonal plates which grow into large blocks with cleavage steps.

C-S-H gel appears to have several morphologies [Diamond, 1976; Jennings et.al., 1981]. The variation is attributed to: hydration time, space available, C/S ratio and mechanism of formation (through solution or topochemical). The classification for C-S-H in cement paste introduced by Diamond [1976] is based on observation of the hardened paste fracture surface. This work has been modified and extended by Jennings et.al. [1981], who also used transmission methods to observe the hydrating C_3S paste. The results are summarised in Table 5.1.1.

Hydration of C_3S with fly ash

The addition of fly ash is widely believed to have an accelerating effect on the C_3S hydration, but to prolong the induction period. This is possibly caused by the provision of more precipitation sites for the hydrates [Kawada and Nemoto, 1968] or the change in ionic concentration of the liquid phase [Stein and Stevels, 1964], or both.

The retardation of the main C_3S peak in the presence of fly ash was noted by Ogawa et al. [1980], and by Jawed and Skalny [1981] who, invoking hypothesis A (5.1.B.1), suggested that this is caused by the delay of the nucleation of $Ca(OH)_2$. This delay may be due to the chemisorption of some Ca^{2+} ions in the fly ash particles, and the presence of soluble silicate and, particularly, aluminate species known to have a poisoning effect on the CH nucleation and crystallisation. Although the mechanism of retardation of the C_3S hydration by aluminate ions is not fully understood, de Jong et al. [1968(a) and (b)] proposed that Al incorporated into the "first hydrate" retards its conversion to "second hydrate"; alternatively Cottin and Vibert [1976] suggested that the retardation is due to

TABLE 5.1.1 MICROSTRUCTURAL TYPES OBSERVED FOR CALCIUM SILICATE HYDRATE

Classification 1[1]	Classification 2[2]	Period Formed	Morphology and Habits
Type E		First few hours; Stages I and II	Thin flakes or foils which, when dried, become cigar-shaped tubes 0.25 μm long, radiating from C_3S grains at all angles
Type 0		Between 4-24 hr; Stages III and IV	Amorphous gel ∿ 0.5 μm thick surrounding C_3S grains; behaves as wet plastic material for first several days; changes into other morphologies depending on space available
Type 1	Type I	Forms from Type 0 during first few days	Slightly tapered needles 0.75-1.0 μm long, radiating perpendicularly from C_3S grains, with aspect ratio of ∿10; formed from type 0 in open areas > 1μm; encouraged by drying and/or age
Type 1'		Can be formed from Type 0 during first few days	Tapered fibres 0.25-0.5 μm long, often branching; formed from Type 0 by pulling apart particles; seen only on young fracture surfaces
	Type II	Formed in first few days	Reticular network (interlocking or honeycomb structure), always occurs in cement, but rarely in C_3S, unless hydrated in the presence of impurities or admixtures
Type 3	Type III	Forms from Type 0 after several days	Partly crumpled foils which are interlocked; formed as Type 0 ages and/or dries in regions where original interparticle spacing is < 1 μm
Type 4	Type IV	After first 24 hrs	Dense gelatinous inner product

[1] from Jennings et al. [1981]

[2] from Diamond [1976]

the formation of an impermeable film of hexagonal calcium aluminate hydrate on the C_3S particles surfaces. Jawed and Skalny [1981] performed a further experiment to confirm the prolonging effect of aluminate ions released from fly ash by adding sodium aluminate to C_3S [Fig. 5.1.2]. On the other hand, the addition of silicate ions into the C_3S hydration system has not confirmed the poisoning effect of silicate as shown in Fig. 5.1.2; indeed the C_3S hydration peak is apparently advanced. This phenomenon has also been observed on mixing amorphous silica into the C_3S + water system [Stein and Stevals, 1984] where it is claimed that the advancement is caused by silica lowering $[Ca^{2+}]$ and $[OH^-]$ in the solution, (hypothesis c, 5.1.B.1) accelerating the conversion from the retarding film ("first hydrate") to a more permeable layer ("second hydrate"). Hence it appears that the prolongation of the induction period on addition of fly ash is due to the presence of aluminate ions.

Once the renewed C_3S hydration begins, the rate of reaction is much faster in the blended cement as shown by the calorimetry output [Ogawa et al., 1980] and the X-ray analysis of the reacted C_3S [Mohan and Taylor, 1981]. This acceleration is believed to be caused by the fly ash surface providing extra precipitation sites for the C-S-H gel, so quickening the dissolution of C_3S.

Mohan and Taylor [1981] found that the amount of CH produced from the hydration, expressed in g per g C_3S, is higher in the presence of fly ash at one day, confirming that more C_3S has reacted at that time. On the other hand, the rate of formation decreases faster in the blend, leading to its being overtaken by that of the

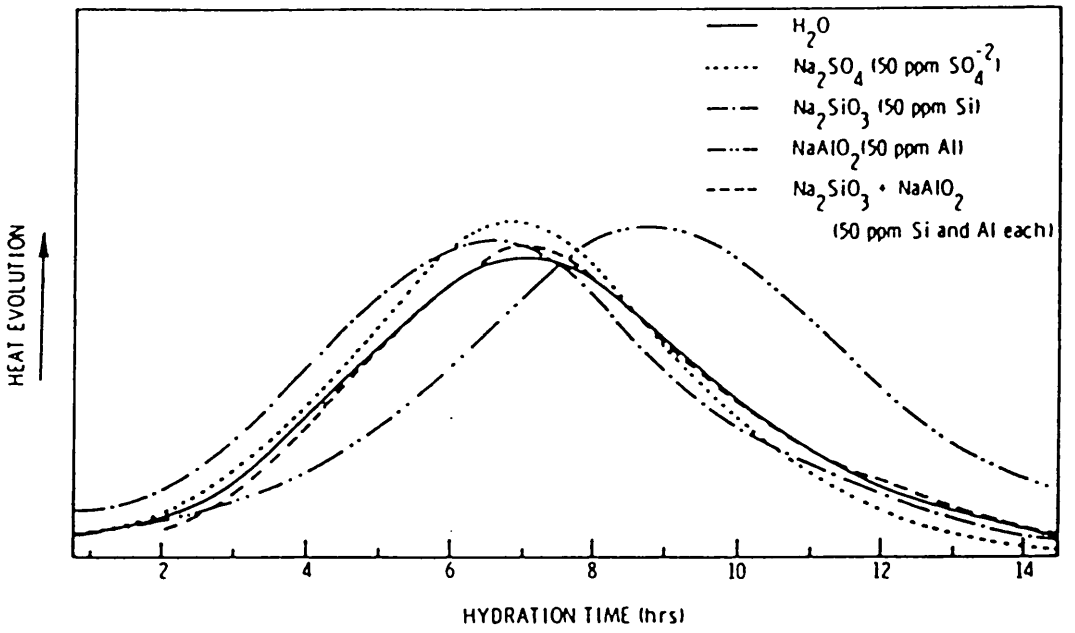

FIG. 5.1.2 HEAT EVOLUTION PROFILES FOR C_3S HYDRATED IN WATER AND SODIUM SULFATE, SILICATE AND ALUMINATE SOLUTIONS

(Jawed and Skalny, 1981)

neat cement at 3 days hydration. This decrease is caused by the pozzolanic reaction between the CH and the fly ash which has started to react at least by one day. A similar result has been found by Ogawa et al. [1980], but with a more slowly decreasing rate, caused by the use of a less reactive fly ash, so that the overtaking occurs at about 14 days.

Using analytical electron microscopy in fine ground samples, Mohan and Taylor [1981] found that fly ash lowered the mean C/S ratio in C-S-H particles from 1.51 to 1.43 from 1 day onwards. However, their method cannot determine the variation of C/S ratio in the different types of C-S-H produced by the C_3S hydration or pozzolanic reaction. Ogawa et al. [1980] used EDXA (energy dispersive X-ray analysis) to obtain C/S ratios on the flat hardened paste at 3 and 90 days. They found that in the C_3S-pozzolana system, C/S ratio in the area near C_3S particles is substantially the same as that of C_3S itself, 2.0. However, the ratio decreases stepwise from C_3S grains towards pozzolana, and the time taken to obtain a given X-ray count increases indicating that the C-S-H has a low specific gravity or porous structure. The stepwise decrease in C/S ratio is due to the zonal structure of C-S-H and each zone having its own chemical composition.

Ogawa et al. [1980] have proposed a mechanism for the reaction of pozzolana in the system pozzolana-C_3S. The dissolution of K^+ and Na^+ from the pozzolana causes the formation of a Ca-Si-Al amorphous film which is ruptured by osmotic pressure. SiO_4^{4-} and AlO_2^- inside the film diffuse out to meet with Ca^{2+} forming C-S-H and Ca-Al hydrates. The hydrates do not precipitate inside the film because of the high concentration of alkalies. Therefore vacant space always

exists between the film and the pozzolana grain. When alkalies are not present, hydrates fill in the clearance area and no space is observed between pozzolana grains and hydrates.

5.1.B.2 *Hydration of dicalcium silicate*

Dicalcium silicate (C_2S) is one of the most important components of Portland cement clinker, especially in low heat cement which contains up to 50% of C_2S. The hydration of C_2S and C_3S can be discussed in terms of similar mechanisms; however, the reaction of the former proceeds much more slowly. Hence, C_3S gives the dominant contribution to the strength of the paste at early ages, but as hydration proceeds C_2S plays an increasingly important role.

Crystal structure and polymorphic forms

There are several polymorphic forms of C_2S but only one, γ-C_2S, is stable at room temperature. The others, α, α'_H, α'_L, α'_M and β, are only stable at high temperature in the pure state, although they can be stabilised at room temperature by the addition of impurities [Ghosh, 1983; Midgley, 1974]. Each of these polymorphs has a well defined crystal structure made up of independent SiO_4 tetrahedra connected by calcium atoms [Lea, 1970].

In Portland cement, C_2S exists in an impure form, known as belite, consisting mainly of β-C_2S although the α and α' polymorphs may also be found, depending on which minor elements are present and the exact cooling rate of clinkers. This dominance of the β-form, which gives the greatest strength (see below), is ensured by rapid cooling from the high temperature of clinker formation at which it

naturally stable [Midgley, 1964]. On the other hand, slow cooling produces γ-C_2S, which leads to a weaker structure (see below). The α-α' and α'-β transformations often produce twinning structures resulting in strain accumulations [Glasser, 1979].

Hydration of C_2S

The γ-form of C_2S is known to be the least reactive polymorph at room temperature. Bensted [1978] found the γ-C_2S, containing Fe_2O_3, hydrates only to the extent of 20-25% after 5 years. Nurse [1952] has shown that α' gives very poor strength, α is non-hydraulic, and that β hydrates at a rate dependent on the stabilizer. However, Yamaguchi et al. [1963] have reported that the α-form gives much more strength than the others, and Ono et al. [1968] also showed that doped α' and α forms react with water. However, the sequence of reactivity between $\alpha.\alpha'$ and β is still uncertain [Bensted, 1983; Boikova, 1980; Ono et al., 1980; Gutt and Osborne, 1970] because the reactivity of α and α' is sensitive to their thermal history, and to the type and level of stabilizing oxides [Skalny and Young, 1980].

β-C_2S can be stabilized by various oxides and the resulting hydraulic activity has been studied by Nurse [1952], Pritts and Daughtery [1976], and by Copeland and Kantro [1968] who found that laboratory prepared β-C_2S does not demonstrate the reactivity of belite in ordinary Portland cement.

Hydration of β-C_2S

The hydration of β-C_2S produces a similar type of C-S-H to that of C_3S, containing much less CH and yielding a more porous hydrated paste than does C_3S with the same W/S ratio [Berger et al., 1979).

The hydration pattern of β-C_2S is very similar to that of C_3S, except that the induction period is generally longer in the former. Tong and Young [1977] have shown that during hydration of β-C_2S the release of the ionic species is slow leading to a low degree of supersaturation with respect to CH. This may be due to the dense packing of the crystal structure [Brunauer and Kantro, 1964].

The β-C_2S hydration is very sensitive to changes in the temperature. At room temperature the induction period extends for 80-100 hours, but at 50 °C it lasts only about 8 hours [Pratt, 1982]. However, after 70% hydration ($\sim$50 days) the amount reacted becomes greater at the lower temperature, indicating a negative temperature dependence [Brunauer and Kantro, 1964]. β-C_2S hydration is accelerated by $CaCl_2$, as is that of C_3S, but to a lesser degree. Copeland and Kantro [1969] showed that belite in various kinds of cement reacts differently, the belite in white cement appearing less reactive, probably due to the absence of iron. Odler and Schüppstuhl [1981] have shown that C_3S significantly accelerates the hydration of β-C_2S, and they have attributed this to the C-S-H from the C_3S acting as nuclei for the hydration of β-C_2S.

Microstructure of hydrates of β-C_2S

Most workers have reported that the C-S-H produced from β-C_2S and C_3S has very similar composition and morphology [Bensted and Varma, 1974; Kurczyk and Schwiete, 1960; Williamson, 1972], although Tong and Young [1977] have found differences in microstructural details. The CH crystals are larger in β-C_2S than in C_3S [Young and Tong, 1977] because of formation in a solution having a low degree of supersaturation.

Recently, Scrivener [1984] also examined the hydration of belite using HVEM (wet state) and found that the C-S-H product appears similar to that formed in alite. She saw a foil-like product at one day which transforms on ageing or drying to a fibrillar or needle-like structure. Rujii and Kondo [1979] reported that a thin layer of well developed 'crystals' of C-S-H forms beneath the fibrillar products at later ages. This is also reported by Funk [1960].

Hydration of C_2S with fly ash

There have been no reports in the literature, it is believed, concerning the effects of fly ash addition on the hydration of C_2S. However, it seems reasonable to suppose that there may be some similarity between the changes in the C_3S reaction. The onset of pozzolanic reaction in the fly ash/C_2S system should occur at a later time due to the slower formation of CH.

5.1.B.3 *Hydration of tricalcium aluminate*

Tricalcium aluminate (C_3A) usually comprises ∿5-15% of Portland cement. It reacts with water very rapidly. When lime is present, a hydrate C_4AH_{13} is formed and is stabilized at room temperature by the high lime environment. This is the principal cause of flash setting in Portland cement.

Crystal structure and solid solution of C_3A

Pure C_3A has a cubic lattice structure with no polymorphic modifications. There are eight holes per formula unit in the structure [Mondal and Jeffery, 1971; Nishi and Takeuchi, 1975] so that ions can be incorporated. In the presence of impurities (Na_2O,

K_2O, MgO, Fe_2O_3 and CaO), five polymorphic forms have been discovered, two cubic, two orthorhombic and one monoclinic [Regourd, 1979(b); Herath Banda, 1978; Han , 1981]. In commercial clinker, cubic and orthorhombic C_3A can be found, but not the monoclinic form [Regourd, 1979(c)].

Fe, Mg, Si, Ti, Na and K can all enter into solid solution up to a proportion of 2 - 10 wt % [Regourd and Grunier, 1974; Tarte, 1968; Lea, 1970].

Hydration of C_3A

a) $C_3A + H_2O$ system

Breval [1976] found that in C_3A hydration there is only one stable product, cubic C_4AH_6. It can exist as single crystals, formed by nucleation in the liquid as the hydration takes place, at temperatures above 40 °C. At ambient temperature, a gel is formed in the first few minutes of hydration, followed by the formation of metastable hexagonal hydrates, $C_2AH_8.C_4AH_{13}$ (or C_3AH_{19}), via the transformation of the gel phase and a secondary precipitation process, which later converts to cubic C_4AH_6 at a rate depending on temperature, W/S ratio and grain size.

$$2C_3A + 21H \rightarrow C_2AH_8 + C_4AH_{13}$$
$$\rightarrow 2C_3AH_6 + 9H \quad \ldots\ldots\ldots (1)$$

or

$$2C_3A + 27H \rightarrow C_2AH_8 + C_4AH_{19}$$
$$\rightarrow 2C_3AH_6 + 15H \quad \ldots\ldots\ldots (2)$$

There is some uncertainty over which of these reactions takes place during hydration of C_3A, or indeed whether both occur.

In the saturated lime environment, the hydrate C_2AH_8 is not stable, and only C_4AH_{13} is formed,

$$C_3A + CH + 12H \rightarrow C_4AH_{13} \quad \ldots\ldots\ldots (3)$$

leading to flash setting in the cement [Bensted, 1983]. The addition of gypsum can be used to prevent this process (see below).

Tadros et al. [1980] and Marinho and Glasser [1983] have found that there is more calcium than aluminium ions in the solution after a short time of dissolving C_3A in H_2O and Na solid solution respectively, suggesting that an Al-rich layer is formed near the surface of C_3A. Tadros et al. [1976(b)] proposed that the induction period represents the process responsible for the removal of this gel layer. However, Spiercings and Stein [1976] have suggested that the gel may be responsible for the later retardation of C_3A hydration because the induction period is quite short.

b) <u>C_3A + gypsum and H_2O system</u>

To prevent the flash setting of cement, gypsum ($CaSO_4.2H_2O$. $C\bar{S}H_2$) can be added. This prevents the formation of C_4AH_x by forming ettringite hydrate.

$$C_3A + 3C\bar{S}H_2 + 26H \rightarrow C_6A\bar{S}_3H_{32}$$
(ettringite)

Ettringite is a stable hydrate only while there is an ample supply of sulphate available. If the concentration of sulphate is reduced, the ettringite reacts with C_3A to form monosulphate.

$$2C_3A + C_6A\bar{S}_3H_{32} + 4H \rightarrow 3C_4A\bar{S}H_{12}$$
(monosulphate)

A typical heat output during the hydration of C_3A with gypsum is shown in Fig.5.1.3. The first peak is primarily due to the formation of ettringite and is followed by a region of continuously decreasing heat evolution. After some time, a second peak rises which is believed to correspond to the formation of monosulphate, which occurs once the gypsum has been completely consumed [Stein, 1963; Schwietz et al., 1966]. Hence, the time at which the second peak appears depends on the amount of gypsum and its form (e.g. hemihydrate or anhydrite); it can also be affected by the concentration of calcium hydroxide in the solution. Collepardi et al. [1978, 1979(a)] have examined the retardation effect of gypsum on the C_3A hydration, both with and without lime. Some of their results are displayed in Fig.5.1.4 and show an increased amount of gypsum (>5% and >40%) which can reduce the initial reaction rate (peak 1) and delay the appearance of the second peak which is split into two. The presence of lime emphasises both of these effects. It was suggested that the double second peak is due to the difficulty in homogeneously mixing samples at the low w/s ratio. There have been many proposed explanations for these effects of gypsum on the C_3A hydration.

i) Formation of a hydrolysed double layer [Tadros et al., 1976 and 1977; Feldman and Ramachandran, 1966].

ii) Formation of an amorphous hydration product (gel) [Corstanji et al., 1973 and 1974); Holten and Stein, 1977; Stein, 1980].

iii) Formation of ettringite around the C_3A grains [Schweite et al., 1966; Collepardi et al., 1978 and 1979a].

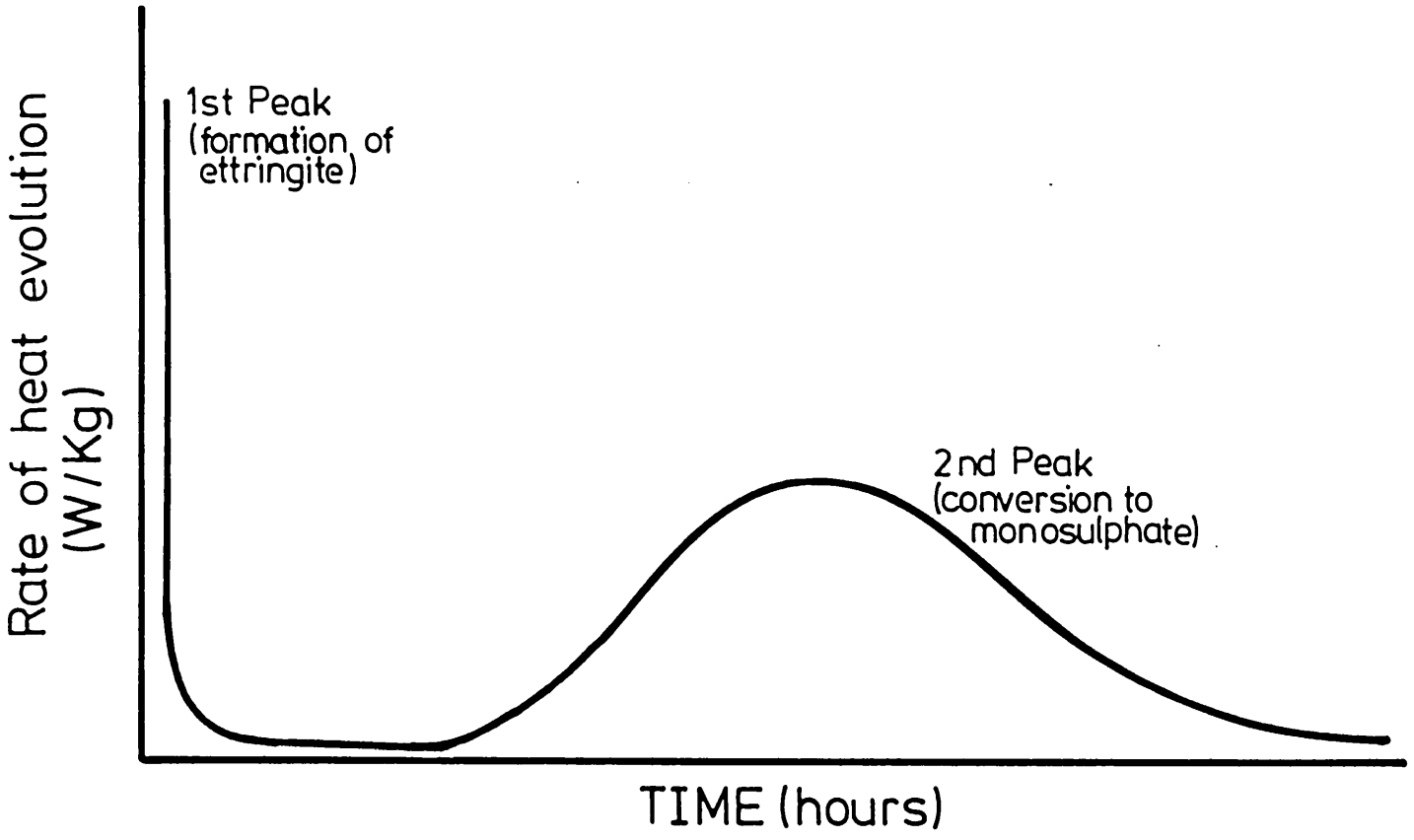

FIG. 5.1.3 RATE OF HEAT EVOLUTION DURING THE HYDRATION OF TRICALCIUM ALUMINATE WITH GYPSUM.

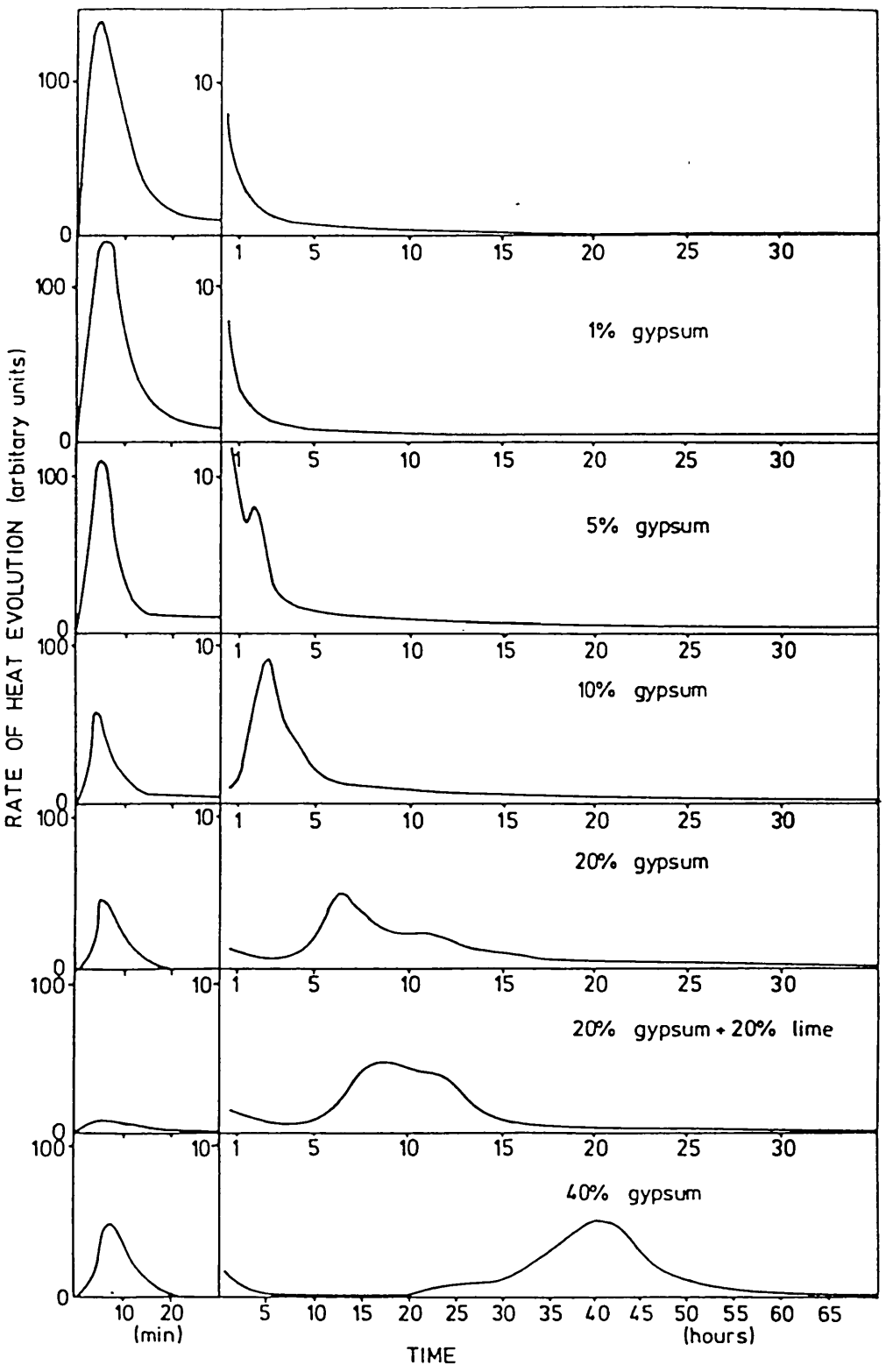

FIG. 5.1.4 INFLUENCE OF GYPSUM, AND GYPSUM + LIME ON THE RATE OF HEAT EVOLUTION DURING THE HYDRATION OF C_3A.
(from Collepardi et al 1978;1979 a)

The first theory suggests that the retardation is caused by decreasing the number of active sites by the chemisorption of Ca^{2+} and SO_4^{2-} on an aluminate-rich surface layer formed by the incongruent dissolution of C_3A. However, Collepardi et al., [1979a] find evidence against this hypothesis in that there is no retardation of the reaction of C_3A on adding Na_2SO_4; it was found that the retardation occurs only when gypsum is present. This leads them to conclude that ettringite is responsible for the reduction of the reaction rate. They also explained that, in the presence of lime, the ettringite forms in small, colloidal crystals which are able to fit better on the irregular C_3A surface, leading to even more retardation.

Corstanji et al. [1973 and 1974] proposed that the retardation is due to the precipitation of amorphous AH_3 on the C_3A surface, beneath the "insulating layer" formed by the hexagonal hydrates, C_4AH_x. The "insulating layer" itself does not severely retard the C_3A hydration since water molecules and ions can pass through. On the other hand, Gupta et al.[1973] have proposed that the retardation is caused by thin crystals of C_4AH_x forming an impervious coating around the C_3A grains.

Holten and Stein [1977] also find that an amorphous layer of AH_3 is formed, retarding the hydration, and that the formation of AH_3 is caused by the depletion of $(SO_4)^{2-}$ due to the formation of ettringite. Stein [1980] suggested that the amorphous layer is formed by preferential extraction of Ca^{2+} from the C_3A and its replacement by H^+.

Recently, Birchall et al. [1980] applied the membrane/osmosis model to explain the action of gypsum in C_3A hydration. The initial ettringite forms an amorphous and gelatinous solid which is adapted to become a membrane. When the pressure is sufficient to rupture this membrane, the reaction products inside it are expelled to form tubules of $C\bar{A}\bar{S}H$.

Scrivener [1984] has observed an amorphous layer around C_3A grains during hydration with gypsum, and suggests that this is re-precipitated after formation in solution. She also observed that ettringite rods appear at the edge of an amorphous layer, and in solution some distance from the surface of the C_3A grains, indicating that they form through a solution mechanism. These observations seem to indicate that the amorphous layer, which is commonly believed to consist only of AH_3, also contains ettringite rods, forming a complex product layer. The rate of hydration of C_3A depends on the diffusion of ions through this layer.

Effect of admixtures

It is known that the reactivity of C_3A decreases as the Na_2O content in the solid solution increases [Boikova et al., 1977; Regourd, 1979(b)]. This has been attributed to the formation of a less reactive structure as Na^+ ions fill the holes in the lattice. On the other hand, Spierings and Stein [1976] suggested that the retardation effect is caused by changes in the solution following the release of Na ions. There are few reports on the effect of alkalies in the system C_3A + gypsum, and they appear to contradict each other on the effect of the solubility of aluminium [Jones, 1944(a) and (b); Shin and Glasser, 1983].

The addition of finely divided quartz increases the rate of reaction of C_3A, possibly by providing precipitation sites for ettringite, so retarding the formation of barriers around the C_3A grains [Holten and Stein, 1977], although this explanation ignores any possible reactions between quartz and the solution.

Combined hydration of C_3S and C_3A

Stein and co-workers [and Corstanji et al., 1973 and 1974; de Jong et al., 1968(a) and (b)] studied the combined reaction of C_3S and C_3A in water and found that the hydration of C_3S is retarded by C_3A. This is attributed to the incorporation of aluminium ions into the first "barrier layer" hydrate, increasing its stability, and the changes of CH concentration in the solution. In contrast, small amounts of C_3S, which are analogous to amorphous silica, advance the hydration of C_3A by accelerating the transformation of C_4AH_x to C_3AH_6; however, for $C_3S/C_3A > 3/5$, the transformation is retarded.

On replacing the CH in the mixture by C_3S, Seligmann and Greening [1964] found that the formation of ettringite is accelerated but the hydration of the latter (formation of monosulphate and tetra-calcium aluminate hydrate) is retarded; formation of poorly crystallised products also takes place. In addition, no C_4AH_{13} was found in the hydration products, which may be related to the ability of the calcium silicate gel to absorb alumina.

Scrivener [1984] has studied the hydration of a $C_3A : C_3S : C\bar{S}\frac{1}{2}H$ mixture in the SEM, and finds that there is a layer of hydrated shell around the particles which is not observed in the individual hydrated pastes. The C_3A dissolves beneath the shell forming a separated, hydrated shell.

Hydration of C_3A with fly ash

In the sulphate-free C_3A hydration system, the addition of fly ash retards the onset of hydration as well as slowing the reaction [Plowman and Cabrera, 1980; 1981; 1982] as shown in Fig.5.1.5. These effects have been attributed to the sulphate released from the surface of the fly ash during the first few minutes, forming secondary gypsum; the first may also be caused by sulphate ions being adsorbed onto the C_3A surface, reducing the active dissolution sites. Following the initial hydration, a layer of hexagonal hydrates forms around the C_3A grains, reducing the hydrate rate. These hydrates are stabilised by the incorporation of sulphate and by the reduction of the available water in their vicinity due to the formation of ettringite. Hence the conversion from hexagonal hydrates to cubic hydrates (C_3AH_6) is delayed, further reducing the C_3A hydration rate. Recently Cabrera et al. [1981] have shown that kiln-produced C_3A (extract from cement clinker) reacts faster than synthetic C_3A because of smaller particle size and more angular shapes. Hence care must be taken when comparing the hydration of these two types of C_3A.

Collepardi et al. [1978] have also observed a decrease of C_3A hydration rate in the presence of pozzolana, but suggest that it is due to the adsorption of pozzolana onto the C_3A surface. This effect is rather small when the rate of hydration of C_3A is retarded by $CaSO_4.2H_2O$ and/or $Ca(OH)_2$.

The addition of fly ash accelerates the rate of the initial hydration of C_3A, given the presence of gypsum [Uchikawa and Uchida, 1980]. This is caused by the fly ash surface acting as

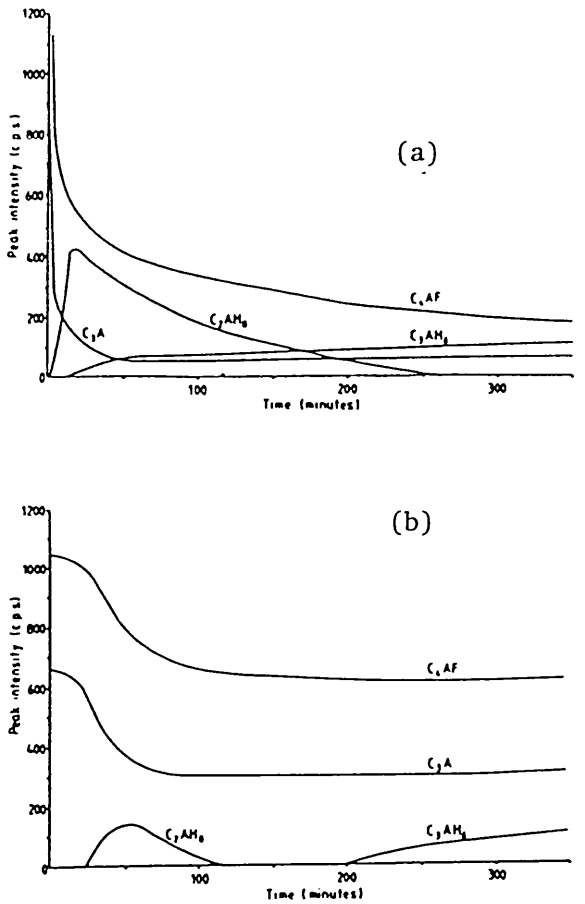

FIG. 5.1.5 RATE OF HYDRATION OF A MIXTURE OF
(a) C_3A + C_4AF
(b) C_3A + C_4AF + 30% PFA
(from Plowman and Cabrera, 1980)

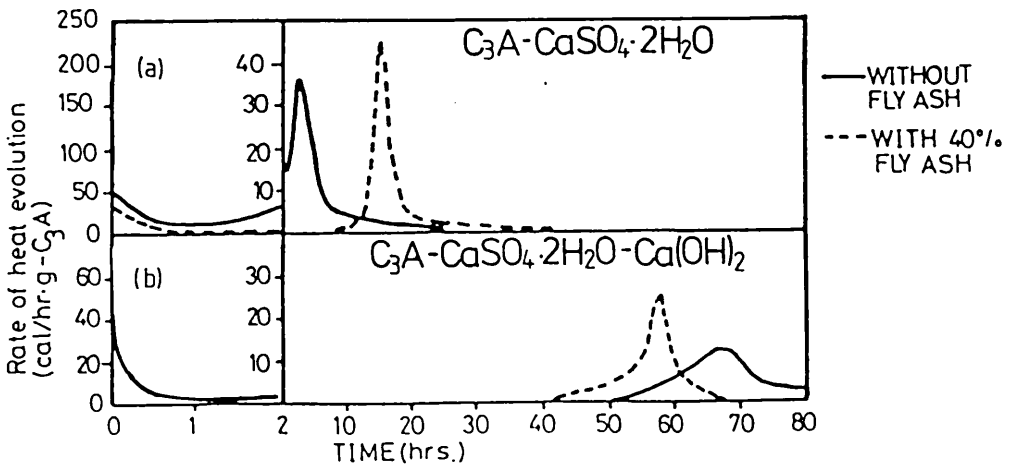

FIG. 5.1.6 HEAT EVOLUTION CURVE IN THE HYDRATION IN THE SYSTEM CONTAINING C_3A (from Uchikawa and Uchida, 1980)

precipitation sites for ettringite, so that less forms on the C_3A surface, increasing its dissolution. As more ettringite forms, the consumption of calcium sulphate is accelerated as is the formation of monosulphate, as shown by the increased height of peak 2 in their calorimetry result; however, the onset of this peak is delayed by 12 hours [Fig.5.1.6(a)]. This last observation is rather unexpected, as a similar mechanism occurs in the system containing finely ground quartz studied by Holten and Stein [1977] which displays and advanced onset of conversion. However, the fly ash might actually retard the conversion because of the corresponding extra calcium sulphate:- Collepardi et al. [1979(a)] have observed that an increased addition of gypsum retards the formation of monosulphate. Uchikawa and Uchida [1980] reported that, in the presence of CH (pozzolana-C_3A-$CaSO_4.2H_2O$-CH), the formation of ettringite and its conversion to monosulphate are retarded [Fig. [Fig.5.1.6(b)]. In addition, we notice that the second peak in Fig.5.1.6(b), corresponding to the formation of monosulphate, appears later in the fly ash mixed paste. All this indicates that there is still much uncertainty concerning the effects of fly ash on the hydration of C_3A with gypsum, especially regarding the formation of monosulphate.

Uchikawa and Uchida [1980] found that C_3AH_6 appears at fairly early ages, and consider this to be caused by the high concentration of alkalies, dissolved from the alkali rich fly ash, decreasing the stability of the hexagonal Ca-Al hydrate [Spierings and Stein, 1976]. They also observed that C-S-H appears after 3 days and that the fly ash starts to react after one day [Fig.5.1.7], suggesting that the pozzolanic reaction takes place between one and three days; this is

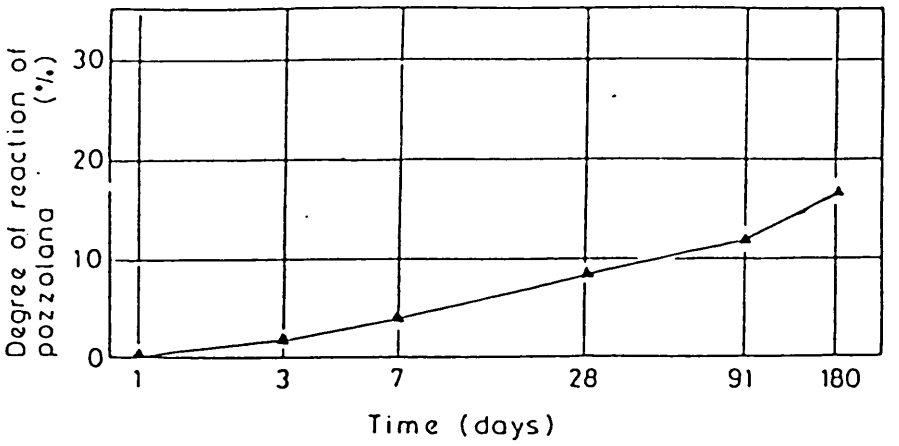

FIG. 5.1.7 DEGREE OF REACTION OF POZZOLANA IN THE PASTE (POZZOLANA-C_3A-$CaSO_4 \cdot 2H_2O$-$Ca(OH)_2$)
(from Uchikawa and Uchida, 1980)

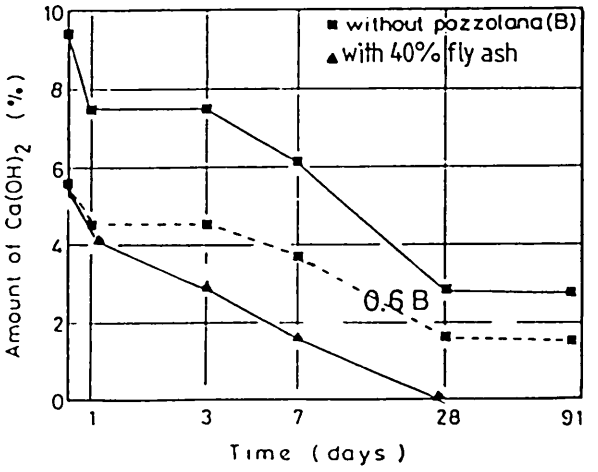

FIG. 5.1.8 AMOUNT OF $Ca(OH)_2$ IN THE PASTE (POZZOLANA-C_3A-$CaSO_4 \cdot 2H_2O$-$Ca(OH)_2$)
(from Uchikawa and Uchida, 1980)

consistent with the appearance of pozzolanic reaction products observed by Plowman and Cabrera [1980]. The $Ca(OH)_2$ decreases very rapidly and is completely consumed at 28 days [Fig.5.1.8] by which time all the C_3A has also been completely hydrated so that no more $Ca(OH)_2$ can be produced. These two results seem to imply that the pozzolanic reaction has stopped by 28 days. However, the fly ash still continues to react. A possible explanation is that some amorphous CH, which cannot be detected by X-rays, is present in the system.

Uchikawa and Uchida [1980] have proposed a mechanism for the reaction of pozzolana in the hydrating C_3A system which is very similar to that in the hydrating C_3S system suggested by Ogawa et al. [1980]. The Ca^{2+} released from the hydration of the C_3A grains is adsorbed onto the negatively charged pozzolana providing a mechanism for the precipitation of ettringite. Under the protonic attack of water, Na^+ and K^+ begin to dissolve from the pozzolana resulting in a Si and Al rich amorphous layer. This layer gradually swells and is eventually broken by the osmotic pressure. The SiO_4^{4-} and AlO_2^- bursts out forming ettringite, Ca-Al hydrate, and small C-S-H foils which form only on the surface of amorphous film. These hydrates do not form inside the film because of the high concentration of alkalies. When the alkalies have completely diffused out, the film disintegrates allowing Ca^{2+} to move inside forming hydrates which fill the clearance.

5.1.B.4 *Hydration of calcium aluminoferrite (ferrite phase)*

Structure and solid solution

The ferrite phase is actually a solid solution within the C_2A-C_2F system. The limiting composition at the iron-rich end is C_2F, and at the alumina-rich end only just reaches beyond C_6A_2F, [Midgley, 1964]. C_4AF and C_6A_2F are common compositions found in cement; C_4AF is commonly used to refer to the ferrite phase because this is its average composition.

The crystal structure of C_2F has been determined by Bertraut et al. [1959] and consists of alternating layers of FeO_6 octahedra and FeO_6 tetrahedra, with Ca Atoms in holes between. In the other ferrites, the Al atoms are able to replace both the octahedrally and tetrahedrally co-ordinated Fe [Jeffery, 1960].

Mg, Si, Ti, Mn and Cr can all be incorporated into the lattice of the ferrite phase. Their oxides substitute for up to about 10% (molar) of the $(Al, Fe)_2O_3$.

Hydration of the ferrite phase (C_4AF)

It is generally accepted that hydration of the ferrite phase is very similar to that of C_3A, but proceeds at a slower rate. The reactivity increases with increasing A/F ratio. In the absence of gypsum, hexagonal and cubic hydrates, which are iron(III) substituted C_4AH_{13} and C_3AH_6 respectively, are formed. When gypsum is present an iron(III) substituted ettringite (referred to as AFt) and monosulphate (referred to as AFm) are formed.

Jawed et al. [1976] and Collepardi et al. [1979(b)] have studied the hydration of C_4AF in the presence of lime and gypsum using

calorimetry, and compared it with that of C_3A. However, their results do not seem to be totally consistent. Jawed et al. [1976] found that C_4AF hydrates slightly slower than C_3A, and that the presence of lime accelerates the C_4AF hydration. On the other hand, Collepardi et al. [1979(b)] observed that the hydration of C_4AF is much slower than that of C_3A and is retarded by the addition of lime. The only significant difference between these two sets of experiments is that the w/s ratio is much higher in the former. Nevertheless, they agreed that the hydration of C_4AF is significantly retarded by gypsum, and is further enhanced by CH, especially the early hydration. Fukuhara et al. [1981] also observed such effects. They showed that the retardation becomes greater as the amount of gypsum is increased [Fig.5.1.9], and that an increase in the lime can retard the appearance of the second peak [Fig.5.1.10] which corresponds to the formation of AFm, presumably because the solubility of AFt is very low in the presence of lime.

At high gypsum contents, Ramachandran and Beaudoin [1976] observed conversion of AFt to AFm before all the gypsum had been exhausted. This may have been caused by local depletions due to the screening action of AFt.

Combined hydration of C_4AF and C_3A

Since their hydration is so similar, C_3A and C_4AF must compete for sulphate ions. Jawed et al. [1976] found that small quantities of C_3A accelerated the rate of hydration of a C_4AF + gypsum paste. This is due to the SO_4^{2-} ions preferentially being taken up by C_3A, leaving a low sulphate solution which is then less effective in retarding the hydration of C_4AF.

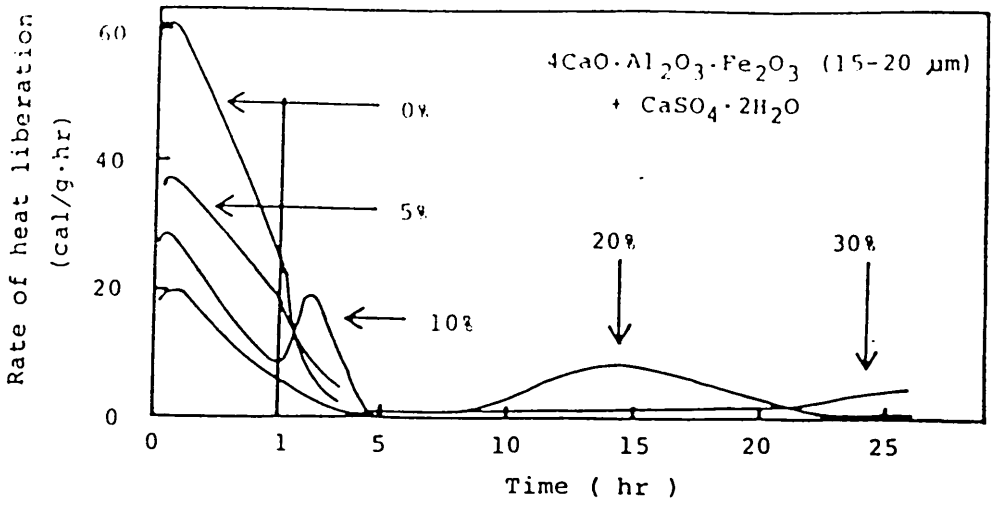

FIG. 5.1.9 EFFECT OF THE AMOUNT OF $CaSO_4 \cdot 2H_2O$ ON THE RATE OF HEAT LIBERATION OF $4CaO.Al_2O_3 \cdot Fe_2O_3$ HYDRATION
(from Fukuhara et al, 1981)

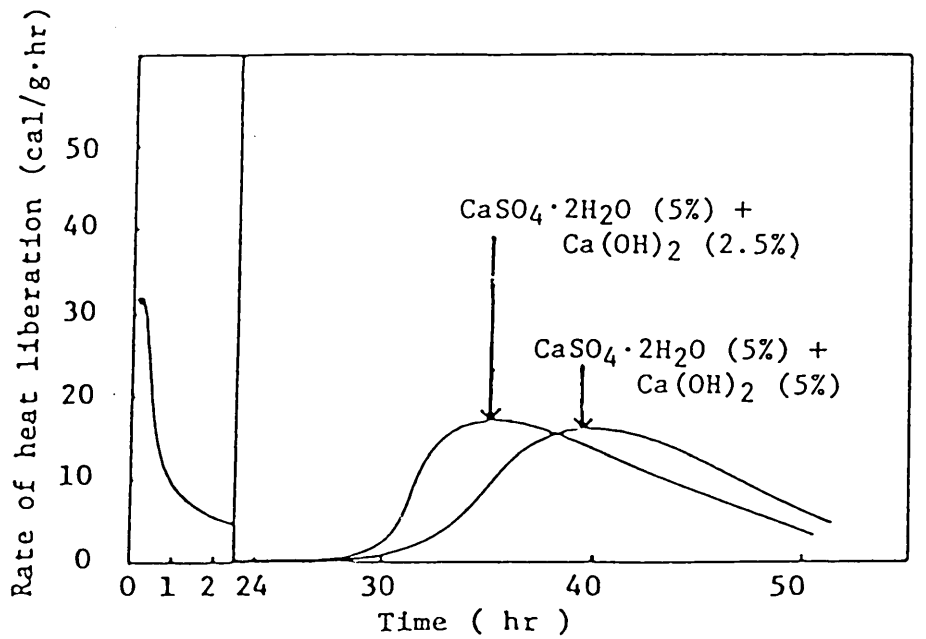

FIG. 5.1.10 EFFECT OF $CaSO_4 \cdot 2H_2O$ AND $Ca(OH)_2$ ON THE HYDRATION OF $4CaO.Al_2O_3 \cdot Fe_2O_3$
(from Fukuhara et al, 1981)

Because the hydration of C_3A initially proceeds faster than that of C_4AF, the majority of the ettringite formed during the very early hydration (∿ first 5 hours) originates from C_3A. In the monosulphate phase, there is a considerable amount of iron(III) substitution because much ferrite has hydrated at later ages when the gypsum is depleted.

Hydration of C_4AF with fly ash

Plowman and Cabrera [1980] showed that the addition of fly ash affects the hydration of C_4AF in an analogous manner to that of C_3A [Fig.5.1.5 (a) and (b)], retarding the initial hydration by the formation of AFt. Although there is no published evidence that this correspondence also holds in the presence of gypsum, where the C_3A hydration is accelerated [Uchikawa and Uchida, 1980], this is expected to be the case.

5.1.C *HYDRATION OF PORTLAND CEMENT*

The preceding discussion is mainly concerned with the hydration of the phases found in Portland cement. In order to provide a framework for discussion of the hydration of Portland cement itself, it can be seen that the hydration of each compound takes place independently of the others. However, this assumption is not completely valid, since the hydration of each phase can be affected by their mutual interaction between them and the presence of impurities; another factor may be the distribution of the phases as Scrivener [1984] has observed that most cement grains contain more than one phase.

Heat evolution during hydration

Fig.5.1.11 shows a typical heat evolution curve for Portland cement. After the large initial heat output, peak 1, there are two or three other peaks depending on the particular type of cement.

The first peak represents a combination of exothermal wetting, hydrolysis and formation of the early products (the amorphous gel layer or dense first hydrate), leading to the induction period. There have been may proposals for the hydration mechanism during this period, and these have been reviewed by Skalny and Young [1980].

The second peak, at the end of the induction period, is generally accepted to be due to the hydration of alite. There is much controversy over which reactions are responsible for the third peak, although the most probable are the hydration of C_3A or the transformation of ettringite to monosulphate.

Lerch [1946] found that the amount of sulphate present in the paste can affect the position and height of peak 3 [Fig.5.1.12]. At very low sulphate content (14.3% C_3A and 1.25% SO_3), the corresponding reaction even occurs before the second peak but is delayed as the amount of SO_3 increases. It is also shown that the peaks become lower with each progressive increase in SO_3 content. He measured the volume change to show that, before the appearance of peak 3, the systems have an already reduced sulphate content implying that the peak corresponds to the formation of monosulphate rather than ettringite. In addition the present observations are very similar to those concerning the monosulphate peak in the C_3A + gypsum hydration system [Collepardi et al., 1978 and 1979(a)] [Section 5.1.B.3]. The appearance of this third peak is affected

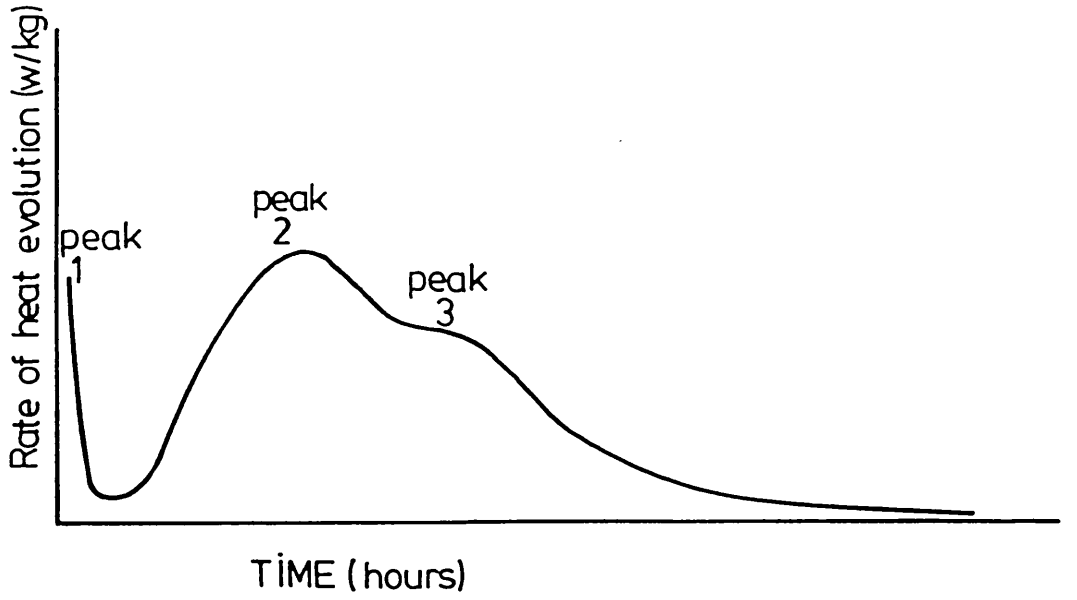

FIG. 5.1.11 RATE OF HEAT EVOLUTION DURING THE HYDRATION OF PORTLAND CEMENT

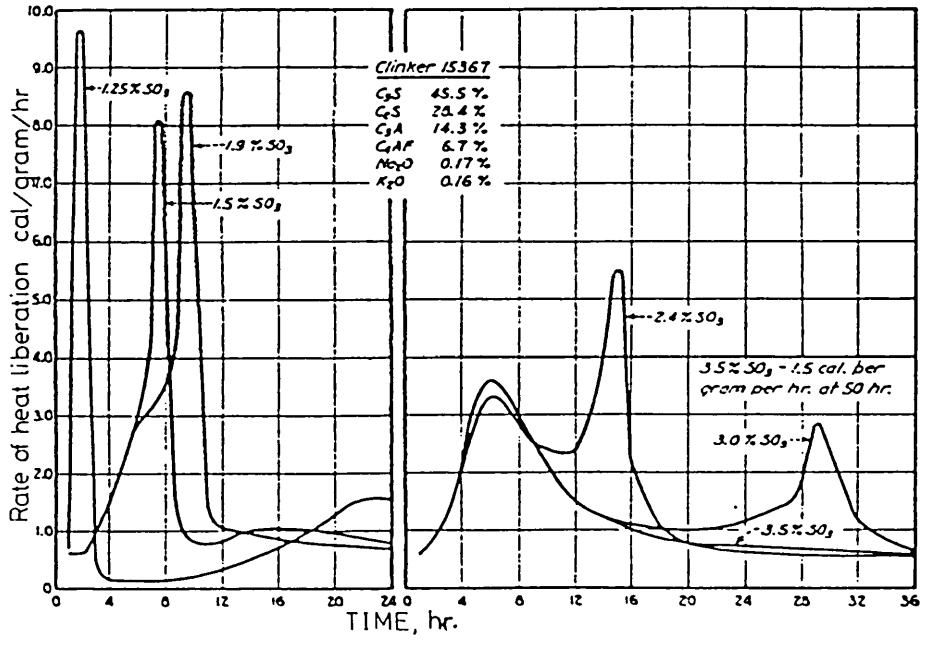

FIG. 5.1.12 RATE OF HYDRATION OF CEMENTS WITH SO_3 VARIED
(from Lerch, 1946)

by the alkali and C_3A content, and the fineness of the cement. With 1.25% SO_3, the second peak, corresponding to C_3S hydration, appears much later at 24 hours (rather than 6 hours). This is probably caused by the early formation of monosulphate which reduces the available water for C_3S hydration, and increases the aluminate concentration in the solution by increasing the solubility of C_3A.

The calorimetry curves of the cements investigated by Stein [1961] have a peak at about 50 hours hydration, which changes with the C_3A content in a similar way to the third peak in Lerch's curves. The shoulder on the second peak, it is suggested, corresponds to an acceleration of the C_3S hydration caused by an increase in the permeability of C-S-H layer, or alternatively to the advanced hydration of β-C_2S:- additional C_3S intensifies the second peak and accelerates the shoulder. Scrivener [1984] also observed such a shoulder peak in most of her examined cements and found it to coincide with the appearance of long AFt rods in the microstructure of the cement, consistent with the observations of Pratt and co-workers [Dalgleish et al., 1982(a) and (b); Pratt and Ghose, 1983]. This indicates that the peak is associated with a reaction of C_3A which causes the secondary growth of AFt. Scrivener also showed that the intensity of this should peak is sensitive to the mixing time (and the shearing force); the longer the mixing time, the higher the peak. Forrester [1980] has shown that the speed and duration of high shear mixing can also affect the intensity and position of the peaks in the calorimetry curve.

Abdul-Moula and Odler [1980] have suggested that the third peak in their calorimetry curves represents the formation of monosulphate, but this is not supported by their X-ray and DTA results. The time at which most ettringite is present coincides with peak 3, and monosulphate is only detected after 3 days hydration.

Generally, monosulphate has been initially detected from between 1 to 7 days, by XRD, DTA and volume distribution [Mather, 1976; Lachowski et al., 1980; Jons and Osbaeck, 1982].

Recently, Ghose and Pratt [1981] observed a fourth peak in the hydration of the fly ash blended cement between 25 and 40 hours. Scrivener [1984] also found a weak fourth peak in some cements, occurring at the same time as the appearance of monosulphate. In white cement, she found a strong fourth peak coinciding with the appearance of large, thin hexagonal plates. However, it is not known whether the two are connected.

Development of microstructure

First stage

The first stage extends up to the end of the induction period. Double [1978] has observed (in the wet call) a gelatinous layer forming on cement grains after 20 minutes contact with water, and Groves [1981] has seen a gel layer as early as 5 minutes in the thinned clinker hydration. However, gelatinous hydrates have not been observed on the fracture surface, presumably because drying causes the gel layer to fall back onto the surface of the grains. This gelatinous material is thought to form a membrane which, being impervious to Al and Si ions, causes the induction period. On the other hand, Dalgleish et al. [1982(a)] has found evidence of etch-pitting in some areas of the fracture surface.

After 1 hour's hydration small amounts of AFt rods have been observed on some cement grains. These form in solution and fall back onto the surface on the particles during drying [Dalgleish et al., 1982(a) and (b); Scrivener, 1984]. The amount of AFt formed during the early hydration depends on how much aluminate dissolves into the solution before the membrane completely surrounds the grains.

In the cement pastes which contain a high amount of gypsum and/or hemihydrate, large rod crystals can be found. These are either gypsum which has recrystallised during drying [Dalgleish, 1982(b)], or secondary gypsum formed from solution supersaturated with respect to gypsum following the dissolution of hemihydrate [Scrivener, 1984].

Second stage

This stage begins at the end of the induction period and extends up to 3 days hydration. The membrane ruptures under osmotic pressure, terminating the induction period [Double et al., 1978; Double, 1983], then C-S-H, formed in very fine needles, and CH crystals start to appear, rapidly increasing in size and number. The shell around the grains is thicker and the cohesion between the grains becomes stronger. After 12 hours, the inter-shell bonding becomes sufficiently strong to cause some shells to rupture during fracture [Dalgleish, 1982(a) and (b)]. The particles with broken shells have been named "Hadley grains" [Barnes et al., 1978; 1979]. After 18 hours, most of the Hadley grains show a particle/shell separation. Dalgleish et al. [1982(a)] suggested that this is caused by contraction of C-S-H during drying. On the other hand,

Scrivener [1984] has observed this separated shell morphology in the environmental cell, proving that it is not a result of the drying. Pratt and Ghose [1983] reported that the gap between the core and the shell is produced by dissolution of C_3A at early ages.

Long fibres have been observed after 16 hours hydration. Their morphology is similar to that of AFt, and they comprise Al, Si, S, K and Ca [Dalgleish, 1982(a) and (b); Jennings and Pratt, 1979(a)].

After one day, AFm hexagonal platelets can be observed inside the separated shells, where the concentration of sulphate is low [Scrivener, 1984].

Third stage

This stage extends around 3 days. After 3-4 days, most of the space is filled by hydrates, commonly large blocks of CH. The C-S-H structure loses its identity, becoming more dense and homogeneous, and develops strength and rigidity. AFt fibres can still be seen in some isolated porosity areas, even as late as eight months [Dalgleish, 1982(b)].

Hydration of cement with fly ash

The effect of the addition of fly ash on the hydration of Portland cement might be expected to follow from that of the separate components, although the individual hydration reactions and their reaction kinetics may change in different ways when they occur simultaneously. Takemoto and Uchikawa [1980] have studied the effect of 40% replacement fly ash on the early hydration using heat evolution curves. They found that the C_3S peak is significantly retarded, as also occurs in the pure C_3S case. Killoh [1980] has made a more detailed study using the same technique, but varying

the fly ash percentage. Again it was found that the C_3S peak is retarded and that the degree of retardation increases with the amount of fly ash [Fig.5.1.13]. This retardation may be attributed to the aluminate ions released from the fly ash, increasing the stability of the membrane [Jennings and Pratt, 1978(a)]. Takemoto and Uchikawa [1980] found that alite hydration is accelerated by fly ash as early as one day; presumably the surfaces of the fly ash particles provide extra precipitation sites for the C-S-H hydrates as in the C_3S case [Section 5.1.B.4].

The third peak, corresponding to the secondary growth of AFt rods is likely to be affected more strongly by the soluble components of fly ash. Killoh [1980] has found that peak 3 is retarded by the addition of fly ash and that the degree of this retardation increases with the amount of fly ash. This effect has also been observed by Ghose and Pratt [1981]. However, the cause is still uncertain since the mechanism of this reaction is not yet understood.

The pozzolanic reaction has been studied by comparing the amount of $Ca(OH)_2$ revealed by X-ray diffraction from the same cement, with and without fly ash, although present analysis does not allow for the enhanced hydration of alite in the presence of fly ash. The total amount of CH starts to decrease after 7 days [Takemoto and Uchikawa, 1980]. Similar results have been found by Halse et al. [1984] using thermogravimetric analysis.

Ghose and Pratt [1981] have observed the development of the micro-structure. Early products appear on the cement and fly ash particle surfaces at the end of the induction period. The amount of C-S-H increases with hydration time and gradually develops the cohesion

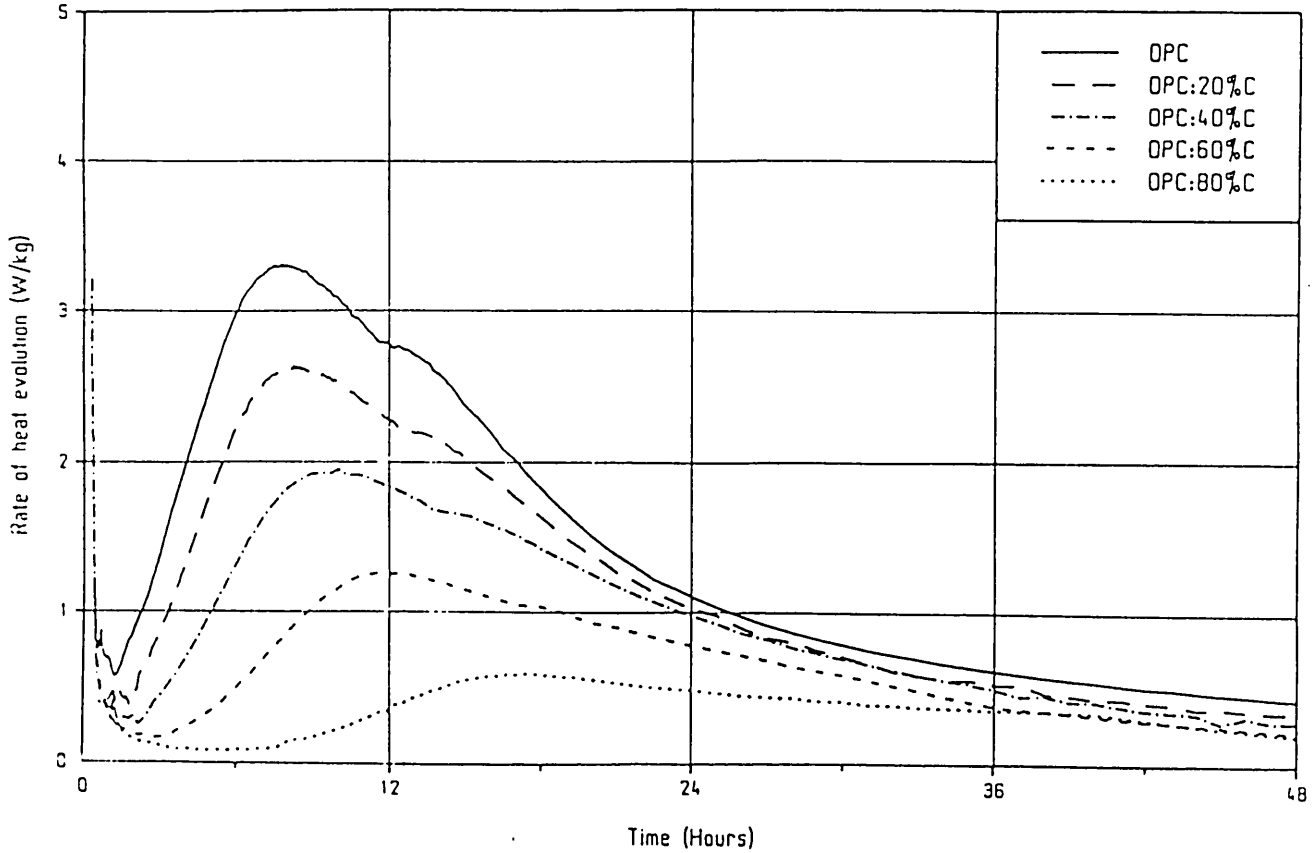

FIG. 5.1.13 HEAT EVOLUTION RATE (PER K_g BLEND) AGAINST TIME FOR BLENDS OF PFA (C) 20°C W/S 0.5
(from Killoh , 1980)

between the particles. After 18 hours, Hadley grains are revealed by the fracture of their shells. Long fibrous AFt rods appear after 1 day's hydration and the hydrates coating the fly ash surface start to become detached, revealing the etched grain. After a few months, much of the glassy phase of the spheres has been eaten away, leaving the crystalline phases.

Rayment [1982] found that the silicate hydrate around the alite grains in the fly ash cement has a lower C/S ratio than that in the neat cement. The effect is caused by extra Si present.

The hydration of high-lime fly ash

High-lime fly ash contains more than 30% of CaO, a high percentage of sulphate, and relatively low amounts of SiO_2 and Al_2O_3. Crystalline components identified include C_3A, free lime, anhydrite, quartz, mullite and haematite, although glass is the major component. Diamond [1980] showed that a pozzolanic reaction can take place in the high lime fly ash and water mixture because there is enough CaO to form CH.

Grutzeck et al. [1980] have studied the hydration mechanisms of high-lime fly ash in Portland cement at 38 °C, and these are illustrated in Fig.5.1.14. The pozzolanic reaction begins at the surface of the glass rim, forming a thin interfacial zone between the glass and the cement paste and leading to a clear fracture between the glass surface of the fly ash and the cement matrix. After 7 days, more reaction takes place, progressing inwards, and leaving a rim of radiating C-S-H fibres. This C-S-H structure is very open so that there is free movement of fluids to and from the glass sphere surface. Depending on the diameter of the sphere, complete reaction takes place within 90 days.

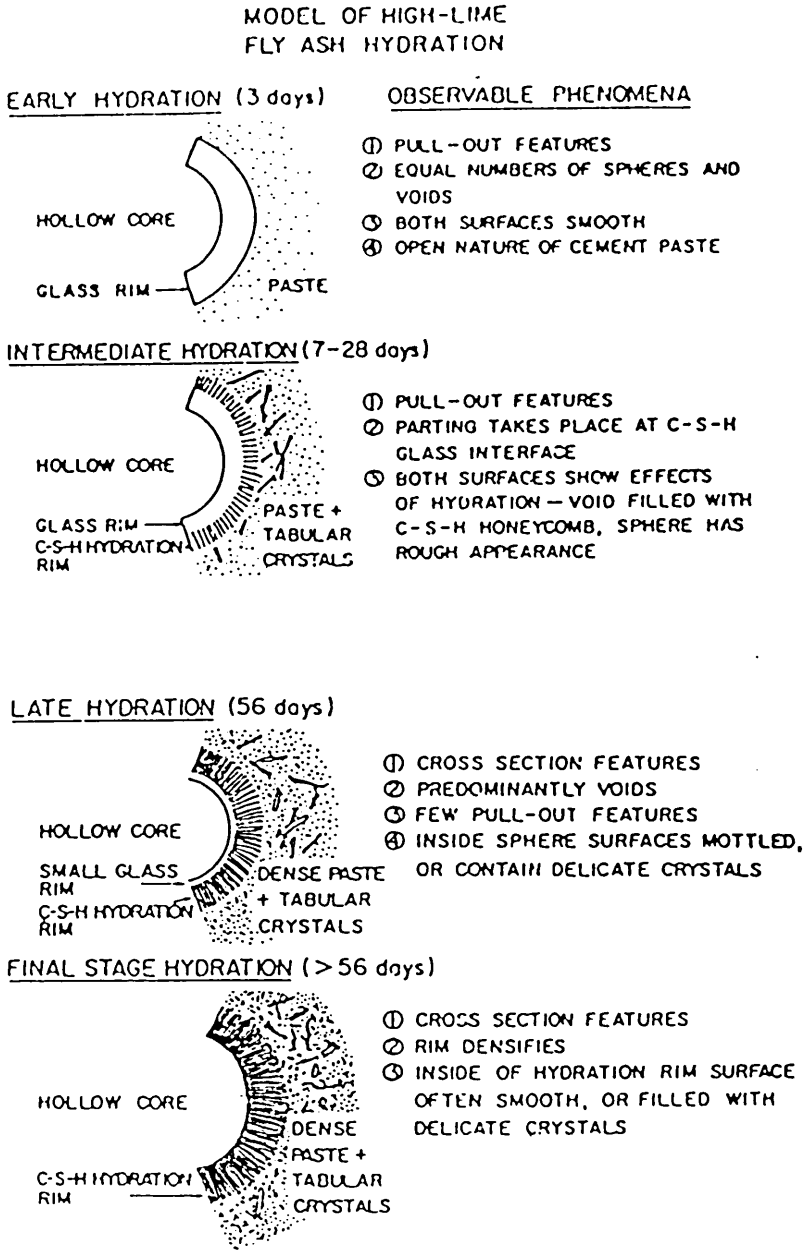

FIG. 5.1.14 MODEL OF HIGH-LIME/PFA HYDRATION.
(from Grutzeck et al, 1980)

5.1.D *STRENGTH OF CEMENT PASTE*

Strength may be defined as a measure of the resistance against failure and collapse under an external load. The early age strength values are very important for the setting of the hydrated products. The setting time of a cement paste (initial set) corresponds closely to the end of the induction period, when normal setting behaviour is observed, indicating that the setting is controlled primarily by the hydration of C_3S [Young, 1981]. Dalgleish [1982(b)] reported that the initial setting is caused by the formation of C-S-H and that the final setting is associated with C-S-H forming over the particles. However, Locher et al. [1976] suggested that normal setting occurs upon the recrystallization of ettringite. Nevertheless, it is generally believed that the early strength development is determined by the rate of C_3S hydration.

Of the four major components of Portland cement, the silicates have the greatest compressive strength [Fig.5.1.15]; the low strength of C_3A and C_4AF is probably due to the large expansion in the microstructure accompanying the ettringite formation and the disruption of microstructure during the conversion of ettringite to monosulphate. This indicates that the strength of Portland cement is mainly contributed by the silicate phases, a conclusion which has now been confirmed [Sprung, 1980; Chatterjee, 1979].

It is interesting to find what gypsum content maximises the strength of a given cement. Too much gypsum results in the formation of excessive amounts of ettringite after the paste has hardened, causing unrestrained expansion and disruption of the paste microstructure. However, too little gypsum allows AFm to form before

peak 2, resulting in a longer induction period as shown in Fig.5.1.13 [Section 5.1.C].

The influence of fly ash on the strength of cement paste

Fly ash cement generally shows improved workability, cohesiveness and ultimate strength and durability. This is partly because of the spherical shape of the ash particles, and their wide range of size enables pores in the cement to be filled.

The replacement of a portion of Portland cement by fly ash on a one for one basis (either by volume or by weight) results in lower compression and flexural strength up to a few months of curing, the exact time depending on the quantity of the fly ash. This is due to the smaller amount of active material present [Kovacs, 1975]. The strength of the fly ash cement gradually develops, eventually exceeding that of the corresponding neat cement. This is attributed to the formation of secondary hydrates (C-S-H), through the pozzolanic reaction, which fill the pores producing a more dense structure. Manmohan and Mehta [1981] showed that the addition of fly ash is instrumental in causing pore refinement. Another factor in causing the increased strength is the reduction in the amount of CH, which is often considered as a "weak link" in the microstructure.

Although the addition of fly ash into cement can improve long term strength, and is certainly economical, large amounts of fly ash will reduce the strength at all ages. The optimum amount of replacement is around 30 to 40%.

There are numerous reports which state that the effect of fly ash differs with the type of cement. Davies [1949] reported that fly ash is more effective with normal and moderate heat Portland cement than with low heat Portland cement, probably because the former have a large C_3S content. Recently Dalziel [1982] found that, replacing 30% of the cement by fly ash, the strongest OPC benefited most. More importantly, his results also show that the effect on the strength varies significantly with the type of fly ash used, and cannot be predicted simply by the pozzolanicity of the fly ash.

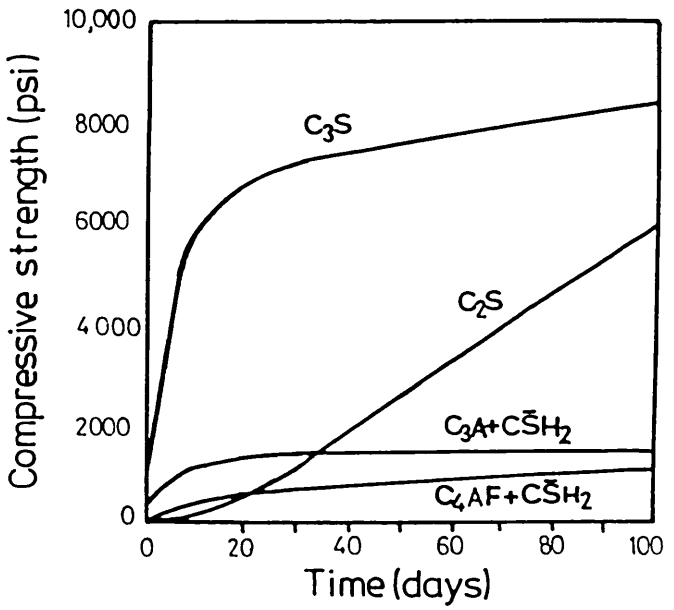

FIG. 5.1.15 COMPRESSIVE STRENGTH DEVELOPMENT IN PASTES OF PURE CEMENT COMPOUNDS (from Young, 1981)

5.2 PRESENT WORK

Experimental approach

a) Two blended cement pastes were formed by replacing 30% of BT cement by Drax or Bold fly ash and mixing in w/s ratio of 0.5 (i.e. w/c = 0.71); the neat cement was mixed with w/c = 0.5. The pastes were cast into polystyrene cylinder moulds, sealed and cured at room temperature. The hydration was stopped by the freeze-dry technique.

b) The other four blended cement pastes were formed by replacing 30% of AW, BW, D/44 and Westbury cements by Fiddlers Ferry fly ash and mixing with w/s ratio of 0.45 (i.e. w/c = 0.64). The corresponding neat cement pastes were also mixed with w/s = 0.45. The pastes were cast into polystyrene syringes producing an air tight system. The syringes were rotated along their axes for 24 hours before being opened; the samples were cured in a humid atmosphere at room temperature. The hydration was stopped by using the freeze-dry technique.

5.2.A *THE HEAT OF HYDRATION OF CEMENTS AND FLY ASH CEMENTS*

The rate of heat evolution during the hydration of the five neat cements and six fly ash blended cements studied is shown in Figs 5.2.1-3. The BT cement [Fig.5.2.1(a)] used in the present experiments had been kept for 2 years. A calorimetry curve of the fresh cement was obtained by Ghose [1981], and this showed a higher heat output during peaks 2 and 3 but no peak 4. This suggests that the cement had been pre-hydrated during the 2 year storage. The D/44 cement used in the mixtures cast in syringes had been stored for about 1 year, but the compression samples were a mixture of fresh and old cement whose calorimetry curves are shown in Figs 5.2.2(a) and (b) respectively.

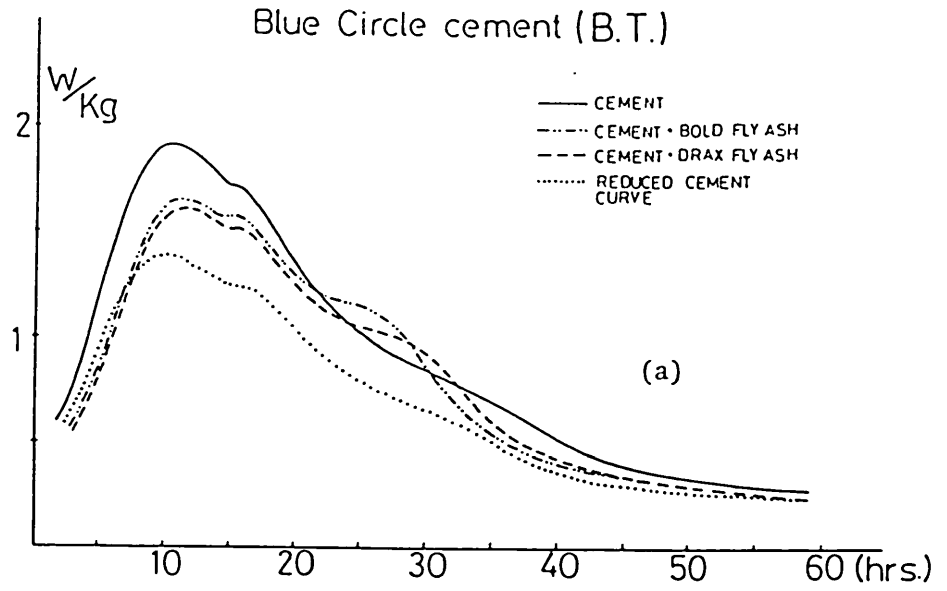

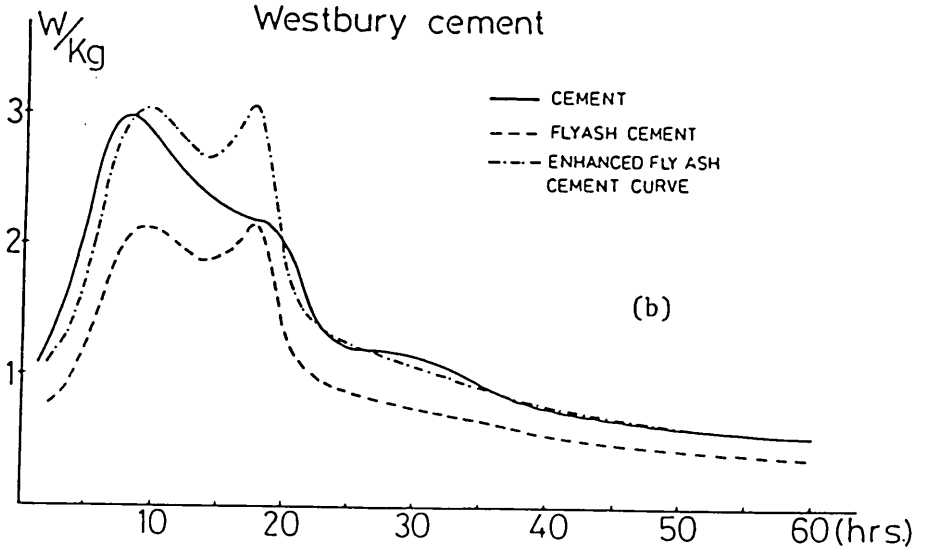

FIG. 5.2.1 Rate of heat evolution for
(a) BT and BT+Bold or Drax fly ash
(b) Westbury and Westbury+Fiddlers Ferry fly ash

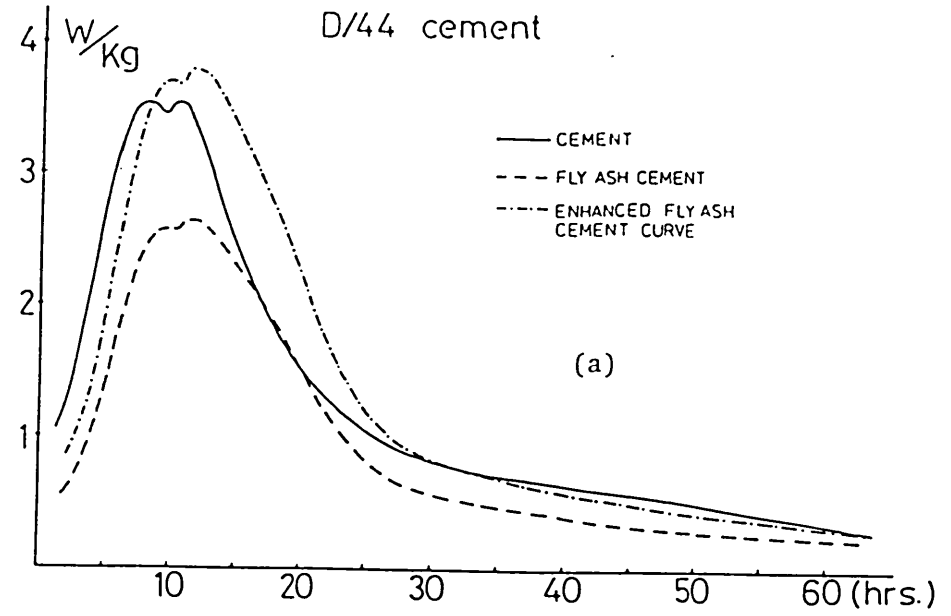

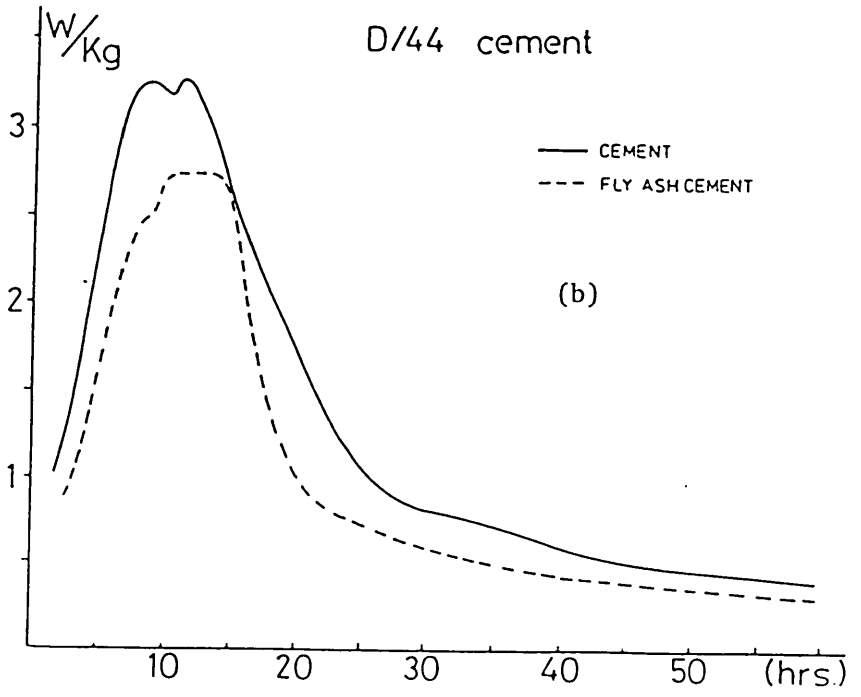

FIG. 5.2.2 Rate of heat evolution for D/44 and D/44+Fiddlers Ferry fly ash
(a) fresh cement (b) old cement

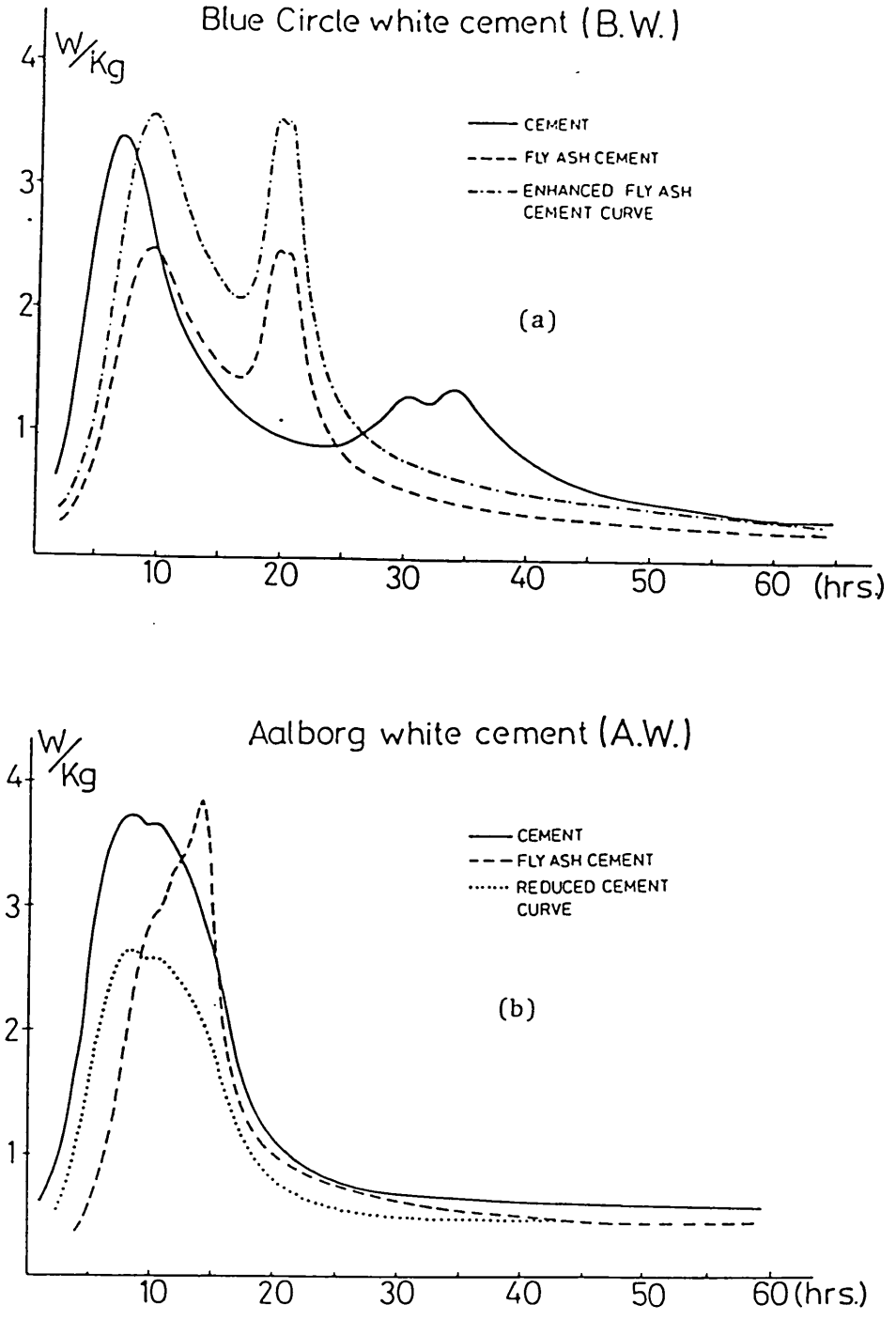

FIG. 5.2.3 Rate of heat evolution for
(a) BW and BW+Fiddlers Ferry fly ash
(b) AW and AW+Fiddlers Ferry fly ash

Using the technique described in Section 2.1, the heat output within the first ½ hour of hydration, peak 1, is not obtained. The curve starts at the onset of peak 2 following a rapid increase of heat evolution (accelerating period) which is believed to be caused by the rapid growth of CH and C-S-H from the hydration of C_3S. The maximum of peak 2 occurs between 7 and 8 hours in most of the neat cements except BT where it appears slightly later, at 10 hours.

The area under the individual peaks cannot be reliably estimated hence, in particular, it is difficult to use peak 2 to find a quantitative relation between C_3S content and heat output in the various cements; the height of the peak is related, but not directly proportional, to the C_3S content of the cements as shown in Table 5.2.1.

TABLE 5.2.1 HEIGHT OF PEAK 2 AND C_3S %

Cement	C_3S %	Height of peak 2 (w/kg)
BT	67	(1) 2.3 or 1.9 ± 0.1*
Westbury	68	3.0 ± 0.14
D/44	69	(2) 3.5 ± 0.1 or 3.2 ± 0.1
BW	70	3.4 ± 0.14
AW	84	3.8 ± 0.12

Notes:-

(1) The value is measured from the curve obtained by Ghose [1981].

(2) The value is measured from the curve in Fig.5.2.2(a).

* The errors are probably caused by slight variation in the mixing process.

There is also a third peak, which is believed to correspond to the renewed hydration of C_3A [Dalgleish et.al., 1982(a) and (b), and Pratt and Ghose, 1983]. The position and height of this peak vary tremendously from cement to cement. For instance, BW (5.5% of C_3A) has a very late and small third peak (at 30 hours) whereas the peak in AW (2% C_3A) is very close and of similar height to the second peak (at 11 hours), as in D/44 cement (5.5%). This variation is determined by the relative concentrations of gypsum and C_3A, the form of the gypsum present in the anhydrous cement [Theisen, 1983], and may also be affected by the concentration of calcium ions in the solution [Scrivener, 1984].

In some of the cements, a fourth peak can be observed which is relatively weaker and broader, except in BW for which it has the same heat output as the third peak. In AW a fourth peak has not been clearly observed, but there is a broad shoulder following peak 3. In both the fresh D/44 and BT cement mixtures [Fig.5.2.2(a)], no fourth peak can be found, but one does appear in the old cement mixtures, [Fig.5.2.1(a) and Fig.5.2.2(b)], at 35 hours, indicating that the pre-hydration of the cements has accelerated the corresponding reaction. However, there is still some uncertainty over which reaction is in fact responsible for this peak although Scrivener [1984] has found that it coincides with the appearance of a monosulphate phase on the fracture surface.

To study the effects of addition of fly ash on the cement hydration, the blended cement calorimetry curve should be enhanced to compensate for the difference in cement weights, or equivalently the neat cement curve can be reduced. There are several differences between the hydration of the neat and of the blended cements:-

(a) The addition of fly ash has a retarding action on the initiation of peak 2 (i.e. lengthening the induction period) indicating that the onset of C_3S hydration is delayed. This is believed to to due to the delay in the nucleation of CH crystals and the decrease in C_3S solubility [Jawed and Skalny, 1981]. The peak height is also enhanced by the fly ash, the enhancement varying from paste to paste being much smaller in Westbury cement. Thus the fly ash accelerates the hydration of C_3S, probably by providing extra precipitation sites for the resulting hydrates [Takemoto and Uchikawa, 1980].

(b) The effect of fly ash on peaks 3 and 4 varies tremendously between the cements.

(i) BT blended cement - the position of peak 3 is not significantly affected but the height is enhanced by both fly ashes. The fourth peak is advanced and enhanced, and is affected more strongly by Bold fly ash.

(ii) Westbury blended cement - the position of peak 3 is the same as that in the neat cement, but the height is enhanced enormously by the addition of fly ash. No fourth peak appears in the curve, but it may possibly be that the fourth peak is advanced and has merged with the third peak.

(iii) D/44 blended cements - in the fresh blended cement, peak 3 is slightly retarded, but the peak height is enhanced. There is a weak but broad shoulder following peak 3 which may indicate a fourth peak.

In the old blended cement, "peak 3" is very broad and may correspond to the combination of the real peak 3 with an advanced peak 4. Hence it is difficult to judge the position of peak 3, nevertheless it seems as though it is enhanced by the fly ash.

(iv) BW blended cement - both peaks 3 and 4 are advanced and enhanced greatly into two close taller and narrower peaks compared with those in the neat cement. This is the only cement for which peak 3 is advanced by the addition of Fiddlers Ferry fly ash.

(v) AW blended cement - peak 2 is followed by a small shoulder and then a tall peak. It is difficult to decide which of these corresponds to the same reaction as peak 3 in the neat cement. Nevertheless, these two peaks are well above the neat cement curve, and are retarded by the fly ash, contrary to the effect in BW.

All this shows that the renewed hydration of C_3A is enhanced by the fly ash which provides precipitation sites for ettringite [Uchikawa and Uchida, 1980], but the onset of the renewed hydration varies in each mixture.

5.2.B *THE RATE OF REACTION OF FLY ASH*

In the fly ash cement the amount of the unreacted fly ash can be determined by dissolving all the cement constituents and hydrates in "SAM" and "KOSH" [Section 2.8].

The AW blended cement samples have been washed in these two solvents and the percentage of the fly ash reacted is plotted against the ageing time in Fig.5.2.4. It shows that the fly ash has started to dissolve as early as a half day's hydration and that this process continues so that at 90 days ∿20% of fly ash has reacted. The

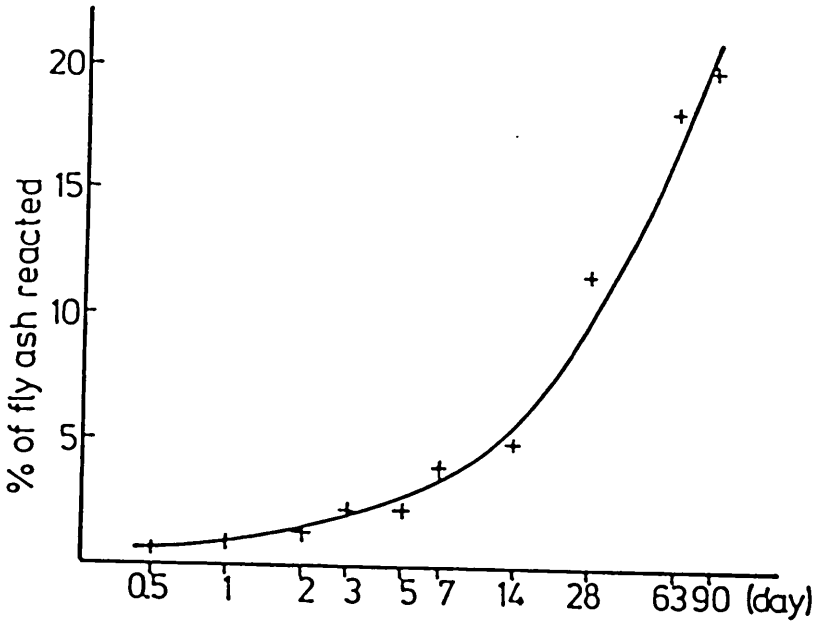

FIG. 5.2.4 Amounts of fly ash reacted.

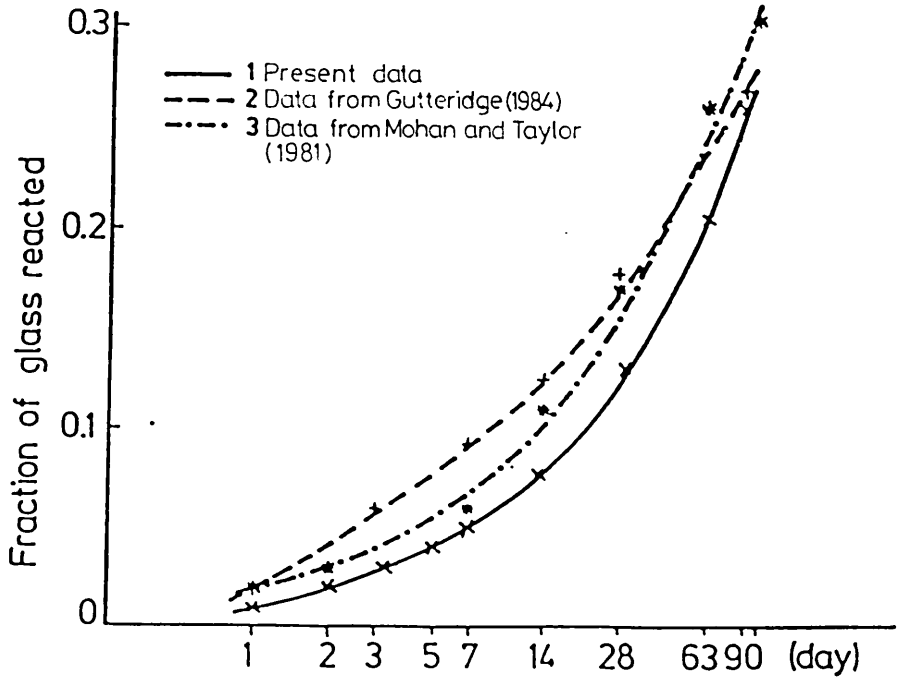

FIG. 5.2.5 Fraction of 'glass' in a fly ash which has reacted during hydration.

fraction of the glass reacted with lime is shown in Fig.5.2.5 together with two other results obtained by Gutteridge [1984], and Mohan and Taylor [1981] (using Eggborough fly ash). The present results, and those of Mohan, are obtained from the corresponding fly ash curves in the assumptions that only the glass phase reacts and that this was initially 80% of the Eggborough fly ash, as for Fiddlers Ferry fly ash [Section 3], whereas those of Gutteridge are measured directly by X-ray analysis. The curves are very similar, but Eggborough fly ash reacts faster at the early hydration, probably because it is in a C_3S/p.f.a. system. All the curves show that the amount of glass dissolution increases gradually with time and has already started by 1 day's hydration. The early reaction of the glass is believed to be with KOH and NaOH formed from the dissolution of alkalis mainly from the fly ash [Diamond; 1982], and later with the CH as a pozzolanic reaction.

5.2.C *THE RATE OF FORMATION AND CONSUMPTION OF CALCIUM HYDROXIDE IN THE NEAT AND BLENDED CEMENT*

The amount of water associated with CH can be measured by thermogravimetry (TG) [Section 2.7] so that the amount of CH can be deduced [Appendix IV]. The weight of CH per weight of cement ignited residue at 800 °C is plotted against hydration time for four sets of neat and blended cements in Fig.5.2.8-9.

The decrease in the rate of CH formation with age in both the neat the blended cements indicates that the C_3S hydration proceeds progressively more slowly. This is probably influenced by the decrease in the rate of diffusion of ions through the hydrate layer around the larger cement particles, which increases in density and thickness with time.

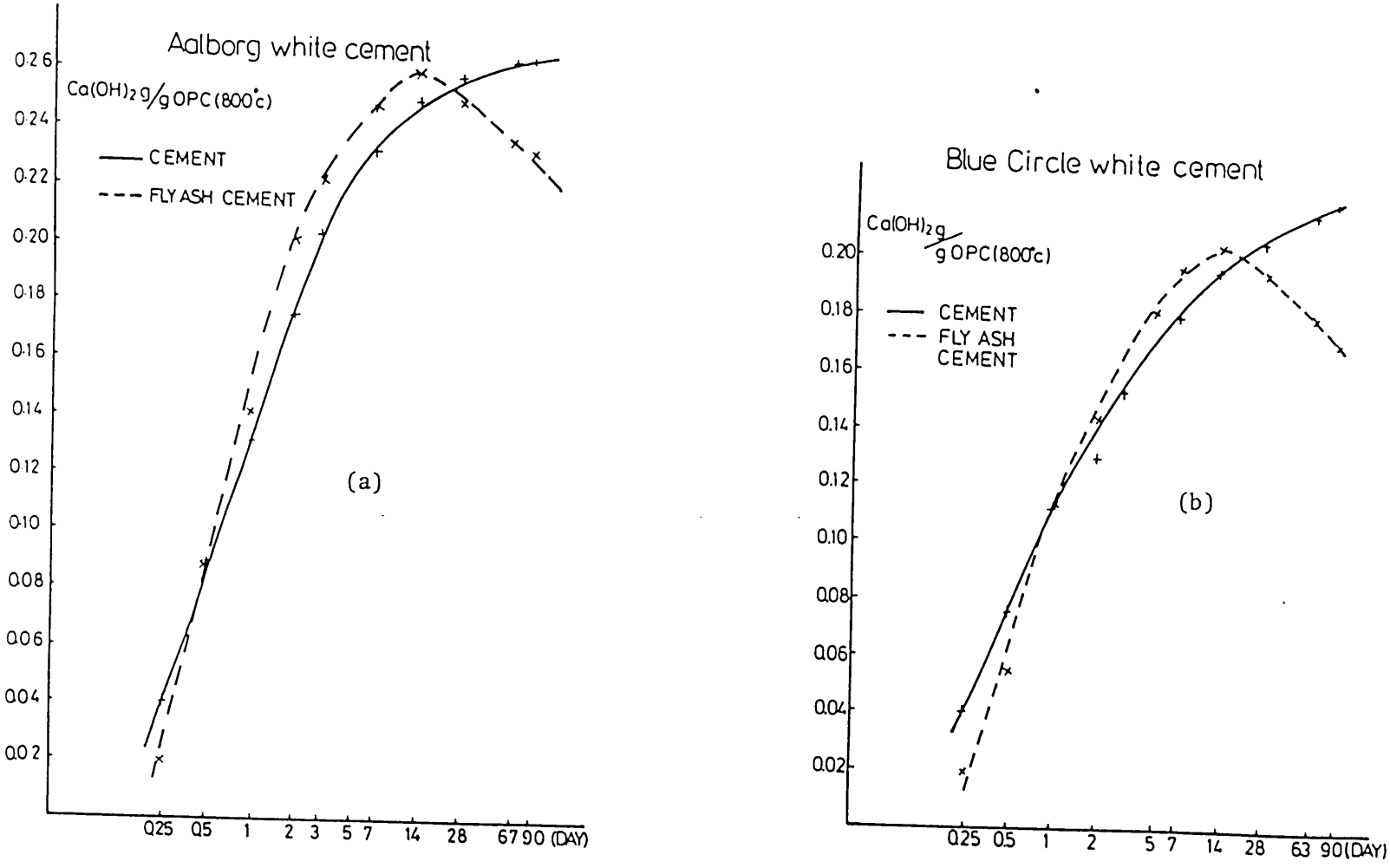

FIG. 5.2.8 Calcium hydroxide content in (a) AW and AW+Fiddlers Ferry fly ash
(b) BW and BW+Fiddlers Ferry fly ash

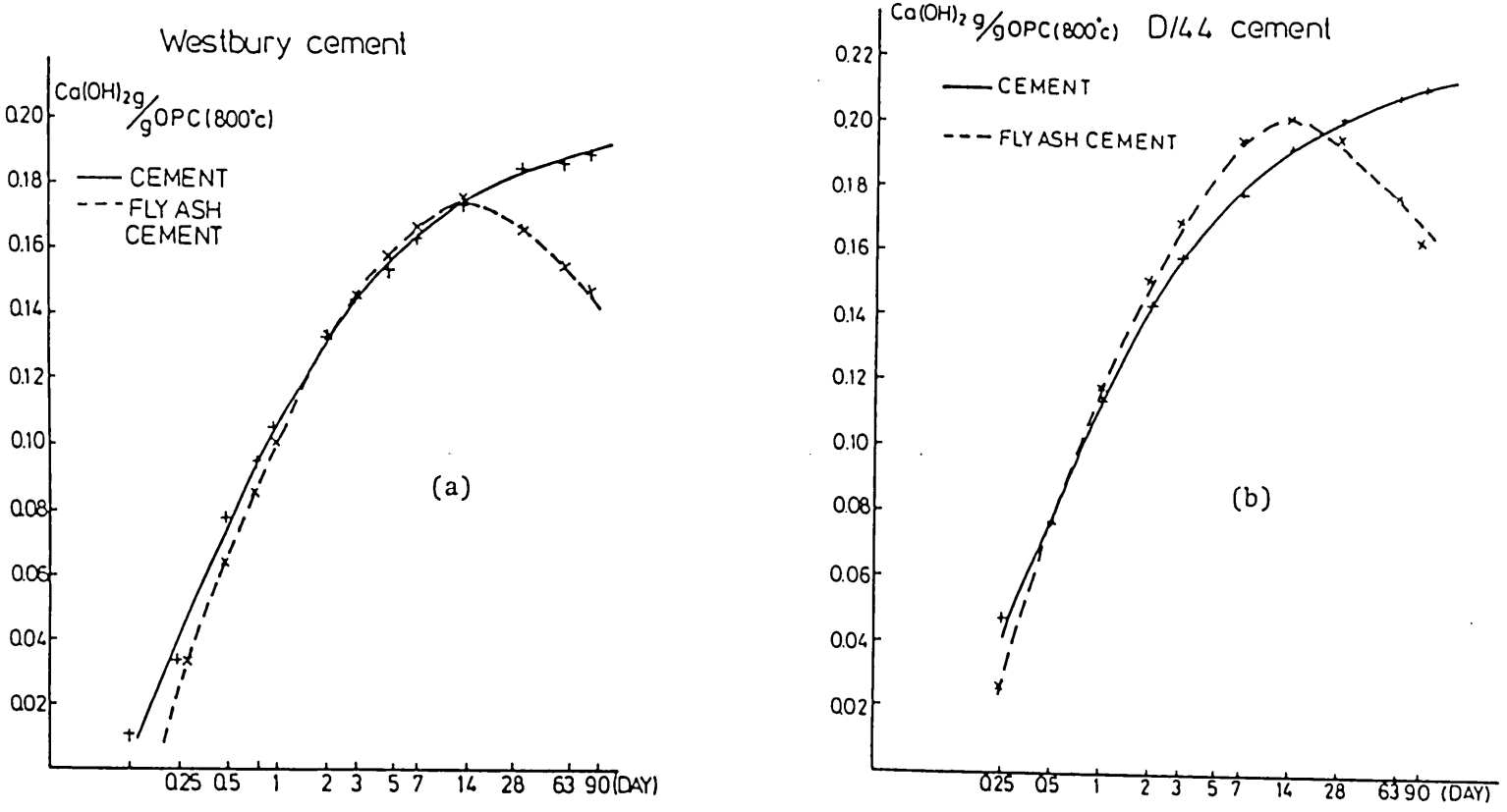

FIG. 5.2.9 Calcium hydroxide content in (a) Westbury and Westbury+Fiddlers Ferry fly ash
(b) D/44 and D/44+Fiddlers Ferry fly ash

The formation of CH in the fly ash cement is slower than that in the neat cement at early ageing time because the onset of C_3S hydration is retarded as shown by the calorimetry curves. However, it is typically enhanced by one day. There is one exception - Westbury blended cement [Fig.5.2.9(a)] - in which the amount of CH stays lower until after 3 days, when the enhancement is still smaller than for the others, consistent with the change in peak 2 in the calorimetry curves [Section 5.2.A]. The general result indicates that the C_3S hydration, once started, is accelerated by the addition of fly ash. This is believed to be due to the hydrates, C-S-H, precipitated on the ash surface, reducing the density of the hydrate layer in the cement grains and allowing ions to be exchanged between the solution and cement grains faster than in the neat cement at the same age.

The rates of formation of CH in various cements are plotted together in Fig.5.2.10. Some correlation can be found between the curves and the composition of the cements [Table 3.1.2]. AW produces a longer amount of CH than the others as it contains about 17% extra C_3S, and has only 2% C_3A and no C_4AF, both of which are believed to retard the C_3S hydration by releasing the Al ions into solution so reducing the solubility of silica [Jennings, 1983]. The hydration of these phases also takes up a large amount of the water in the paste leading to depletion near C_3S surfaces and hence reduces the hydration of C_3S at later ages [Jons and Osbaeck, 1980]. D/44 and BW, which contain roughly the same amount of C_3S and C_3A, produce CH at a very similar rate before 7 days; the rate then decreases faster in D/44, probably caused by the 3% of C_4AF in this cement, BW having none. Although Westbury cement also has a similar amount of C_3S to that in D/44 and BW, the CH formation rate decreases faster giving 10% less CH at 90 days hydration. This is probably due to the higher C_3A content, 14% and 5% respectively.

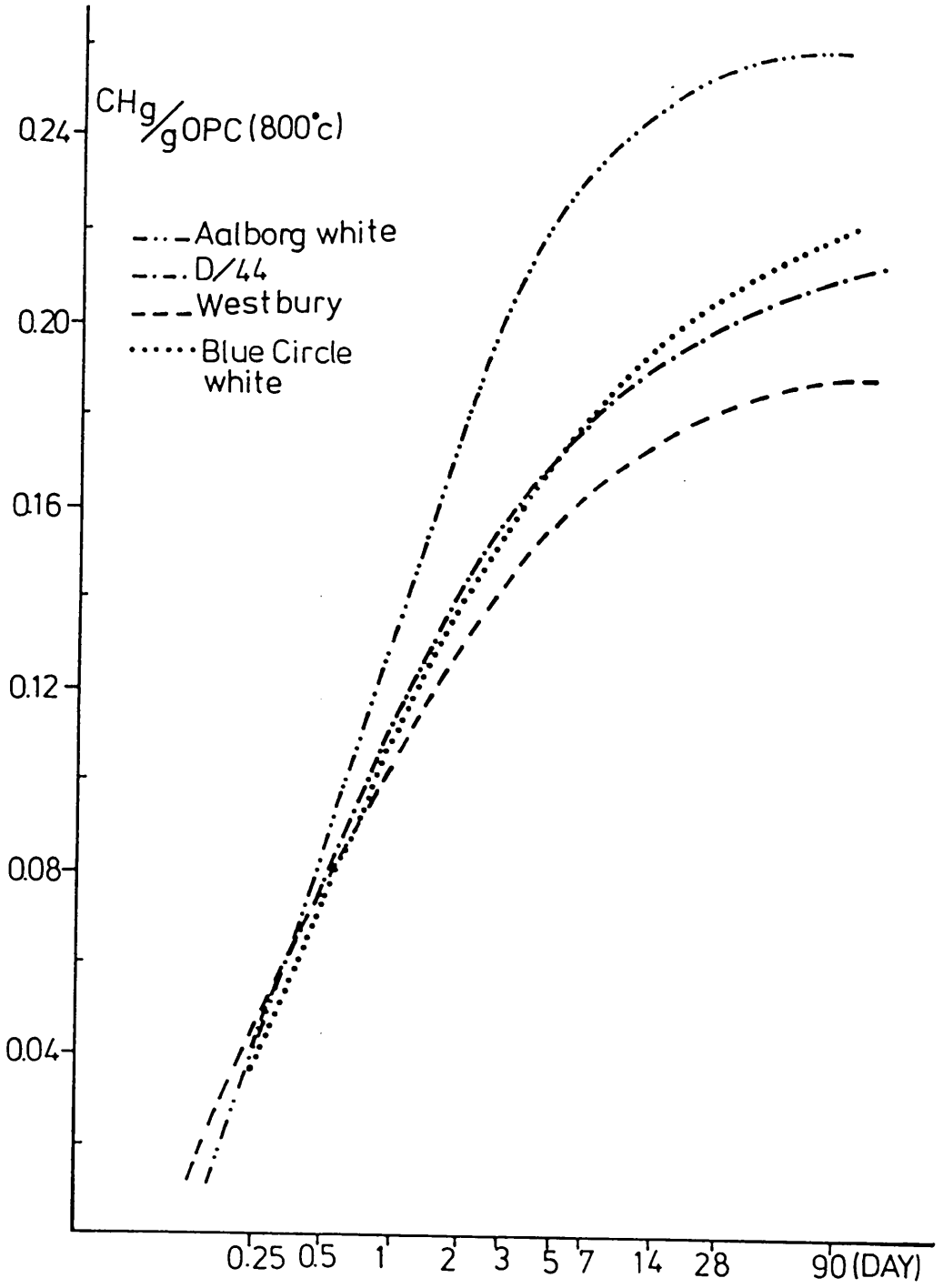

FIG. 5.2.10 Rate of formation of CH in various of cements.

At 14 days hydration, the CH content in the fly ash cement reaches its maximum indicating that the amount of CH consumed by the glass phase through the pozzolanic reaction starts to exceed that produced by the hydration of the silicate phases.

To investigate the effect of curing conditions on cement hydration and pozzolanic reaction the D/44 neat and blended cements discussed above [Fig.5.2.7(a)] were compared with those cured in sealed moulds at room temperature without rotation. The amount of CH in each of the four samples is plotted against time in Fig.5.2.11(a) and (b) and several differences can be observed:-

1) The dry cured cements produce more CH before 3 days hydration. This implies that the hydration of C_3S is being retarded by the rotation during the early age in the humid cured pastes. This may be caused by later start to CH formation in the latter following a longer induction period.
   In the still condition, supersaturation with respect to CH in the solution around the cement grains can be reached faster than in the moving condition. In the latter case, the slight movement of the solution could even up the concentration of calcium ions through the whole system, diluting the concentration of the solution near the particles. The local supersaturation in the first case leads to earlier CH nucleation and growth.
   On the other hand, the experimental errors can emphasise the differences, such as variation of CH distribution in the sample, the error in carrying out extrapolation and measurements (usually in the range ± 0.005), and the serious bleeding in the still

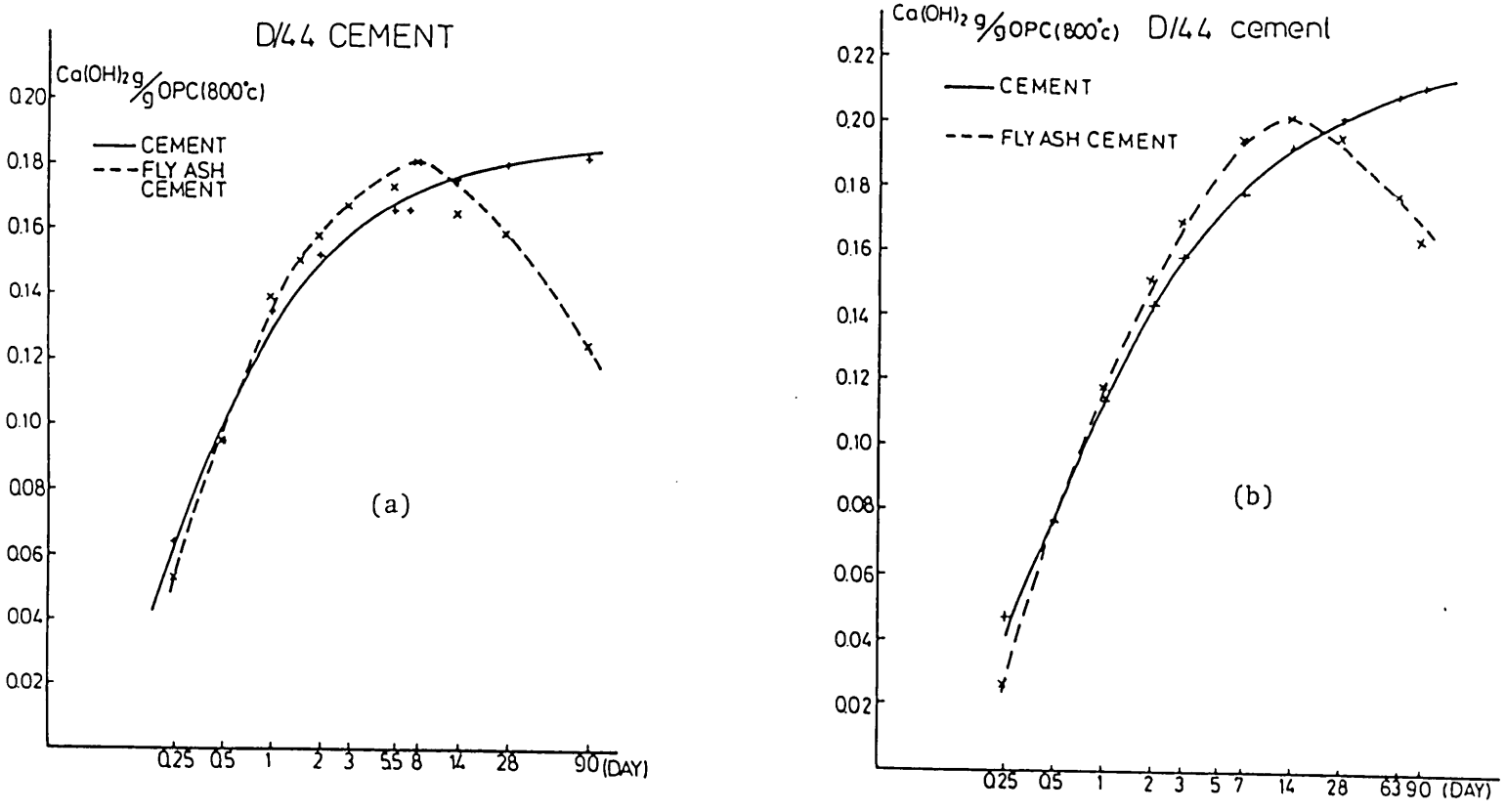

FIG. 5.2.11 Calcium hydroxide content in (a) dry curing pastes
(b) wet curing pastes

condition leading to slightly lower w/s ratio at the very early time, and can affect the formation of CH.

2) The rate of formation of CH is similar in both neat cements from about 6 to 24 hours; later the rate decreases faster in the dry cured cement, becoming negligible after 14 days. This may be due to less water being available to the dry cured cement, leading to a decrease in the hydration of C_3S. Eventually the hydration may stop as all the water has been consumed.

3) The rate of formation of CH is almost the same before 2 days in both blended cements as shown by the similarity of the gradients. The CH concentration in the dry cured samples reaches its maximum value before that in the wet cured pastes. This is presumably caused by less CH being produced at later ages in the former, as indicated by the neat cements. If this is indeed the correct explanation it seems reasonable to suggest that the pozzolanic reaction proceeds at a similar rate in both sets of samples.

5.2.D *THE DEVELOPMENT OF COMPRESSION STRENGTH*

The compression strength is one of the most important mechanical properties of cement. The development of strength in D/44 neat and blended cement was studied using 0.5 inch cube specimens [Section 2.7]. Fig.5.2.12 shows the compression strength development with ageing time of both the cements. The strength of the fly ash cement is consistently below that of the neat cement up to 90 days, which should be expected as there is 30% less cement and the w/c ratio is higher in the fly ash cement. The strength of the neat cement paste initially increases approximately linearly with the logarithm of the time, but slows down after 14 days hydration, whereas

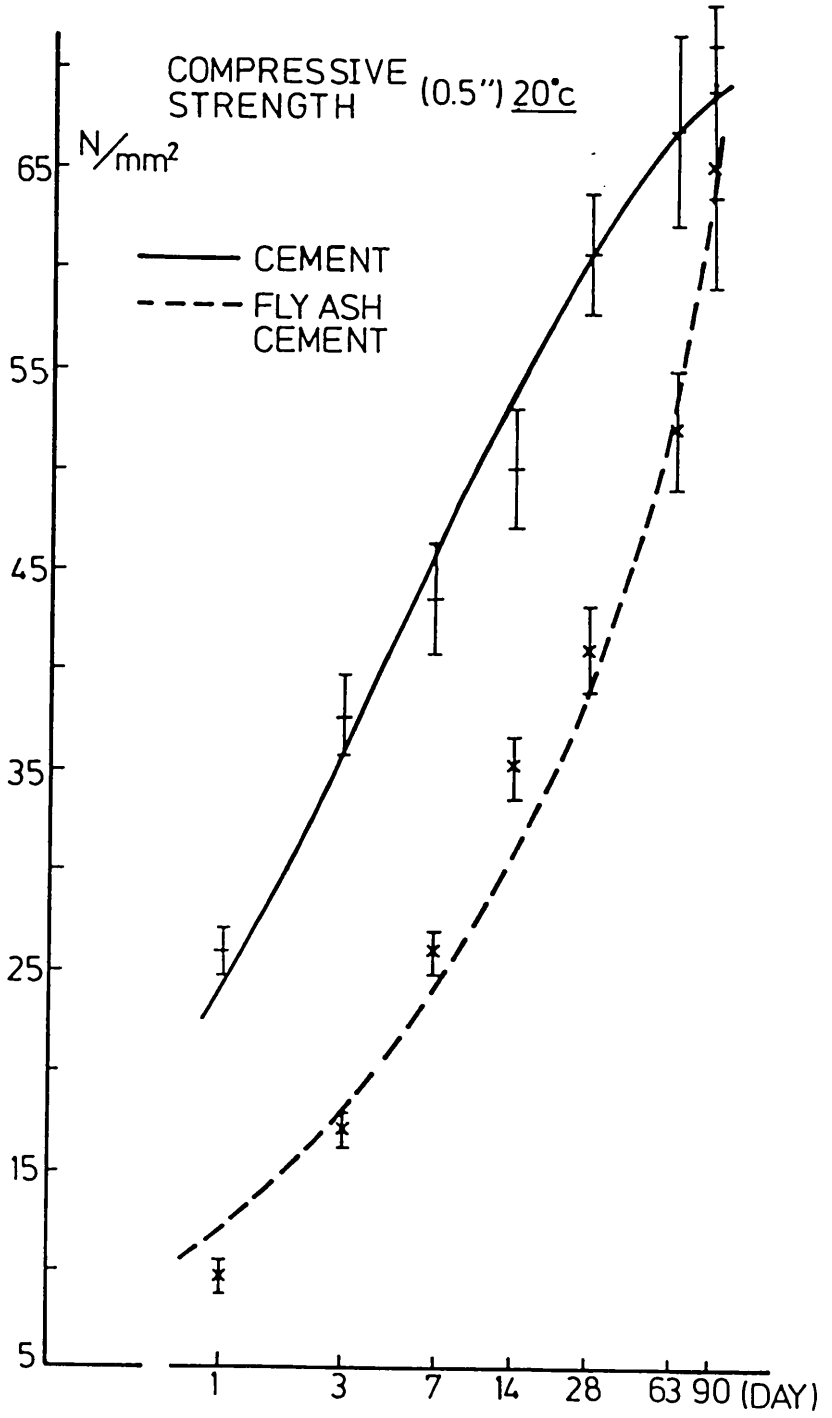

FIG. 5.2.12 Development of strength in cement and fly ash cement.

that in the blended cement continues to increase and almost certainly will become higher than that of the neat cement by 180 days due to the contribution of the pozzolanic reaction.

The strength development of the same cements has also been measured in 2 inch cube samples [Section 2.7], and the results are plotted against the hydration time in Fig.5.2.13. The increase in specimen size seems to affect the strength of neat cement by lowering the rate of increase by a significant amount. On the other hand, there is only a minor effect on the strength of fly ash cement and that is only apparent at early ages. The strength of the blended cement is lower than that of the neat cement until 90 days, when they are almost the same value.

The smaller samples exhibit a lower strength at early ages probably because these have been rotated during the first 24 hours of hydration. As explained above [Section 5.2.C], the rotation can reduce the amount of CH produced from the silicate phases indicating that less C-S-H is also formed. The C-S-H phase gives the dominant contribution to the strength of the cement.

The ratio of strength in the blended and neat cement is plotted against ages in Fig.5.2.14 and shows that the contribution of the fly ash to the strength of the blend starts after 7 days, consistent with the results found by Gutteridge [1984] and Mehta [1983]. The large samples have a higher ratio because of the relatively lower strength in the neat cement paste. The time at which the fly ash starts to affect the strength, by producing more C-S-H or aluminate hydrates through the pozzolanic reaction, is earlier than that corresponding to the maximum concentration of CH (14 days) found by TG [Section 5.2.C], implying that this phase has already

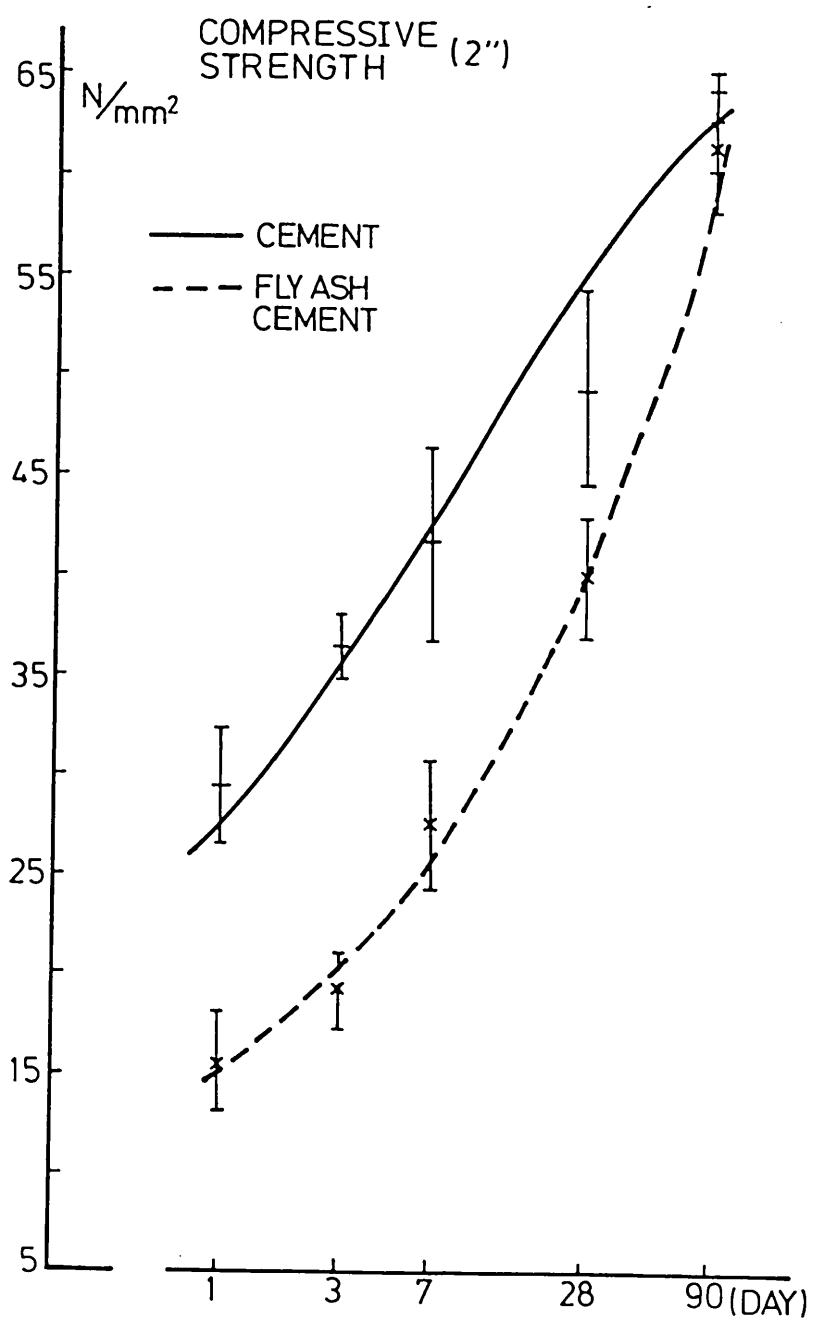

FIG. 5.2.13 Development of strength in cement and fly ash cement

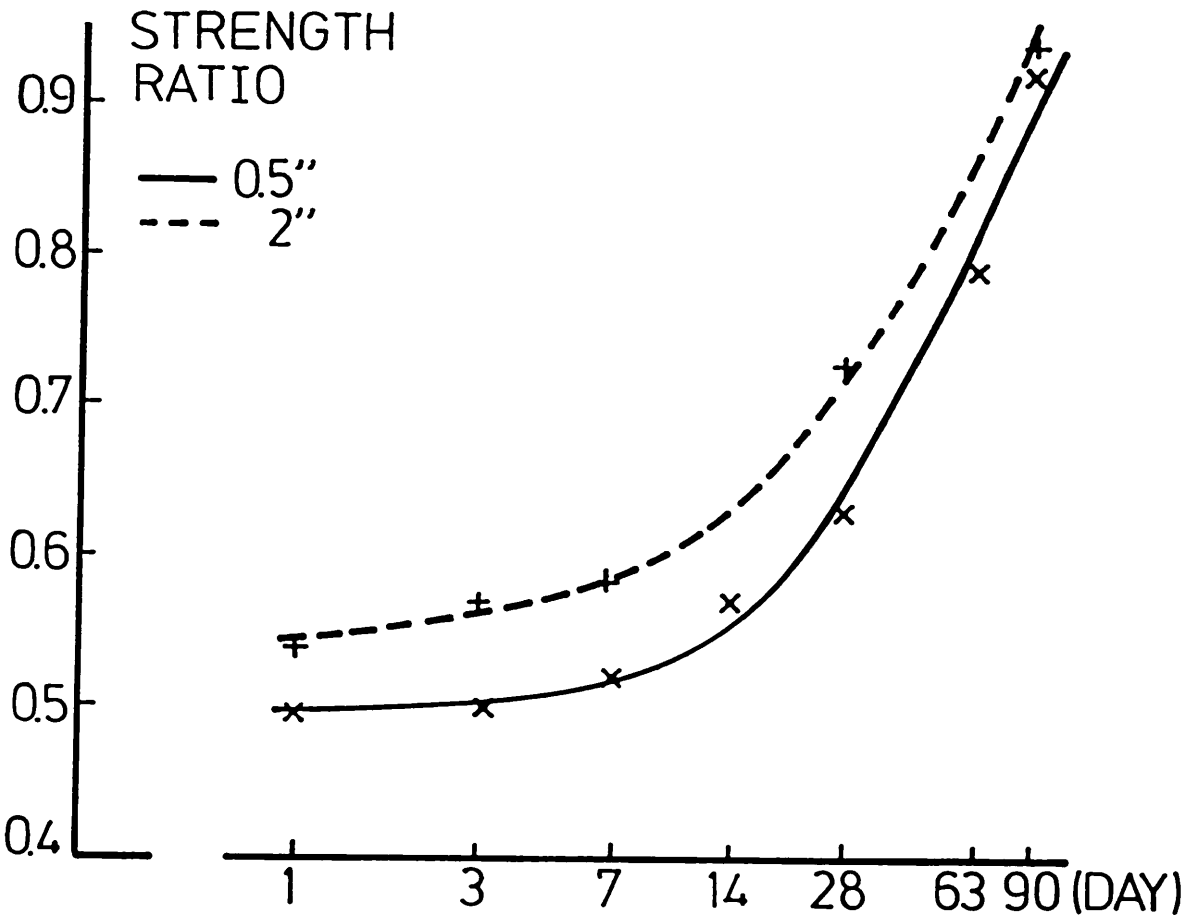

FIG. 5.2.14 Ratio of strength of the fly ash cement paste to the strength of the neat cement paste as a function of age.

started to be consumed, and also suggesting that the reaction may start at 3 to 7 days as the glass phase in the fly ash is already dissolving [Section 5.2.B].

5.2.E *CALCIUM ALUMINATE HYDRATES*

X-ray analysis

A quantitative X-ray analysis was used to investigate the possible existence of calcium aluminate hydrates [Section 2.5], such as AFt (ettringite) and AFm (monosulphate, C_2AH_8, C_4A_{19} or C_4AH_{13}), at various ages. The X-ray results of the four sets of neat and blended cements studied are shown in Fig.5.2.15-22. The analyses of AW hydrated samples were performed in a different diffractometer using a lower sensitivity (1×10^3) with $\frac{1}{2}°$ slit, with the exception of the wet sample analysis which was performed using 2×10^2 sensitivity with $\frac{1}{4}°$ slit as for the others.

Gypsum, whose strongest diffraction line is at 11.7°, 2θ (7.56 Å), is still present up to 6 hours and 12 hours hydration in AW and BW mixtures respectively [Fig.5.2.15-18]. Hemihydrates in these samples rapidly dissolves on mixing with water to form a solution of calcium sulphate supersaturated with respect to gypsum. Part of the solution reacts with C_3A to form AFt rods and part of it is reprecipitated to form secondary gypsum [Scrivener, 1984]. The gypsum present in BW mixtures, at least until 12 hours, may be partly responsible for the delay of peak 3 in the calorimetry curves [Fig.5.2.3(a) and (b)].

A peak at about 14.9°, 2θ (5.9 Å) is present up to a four day hydration in all the examined samples. This can be caused by two possible calcium sulphate phases, hemihydrate or soluble anhydrite, which have almost identical diffraction patterns, the only difference being in the relative intensity [Mather 1976].

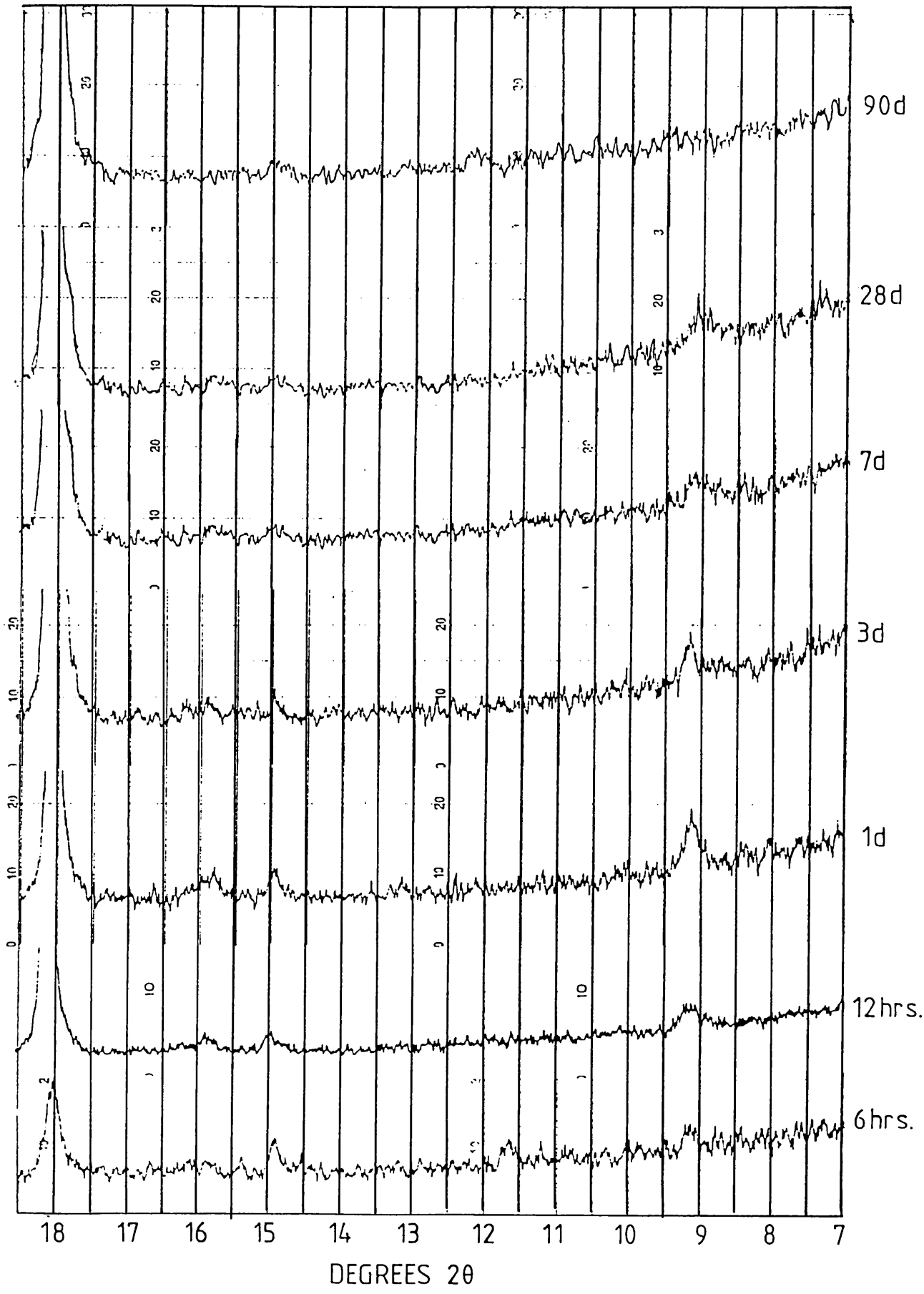

FIG. 5.2.15 XRD traces for AW neat cement paste at various ages.

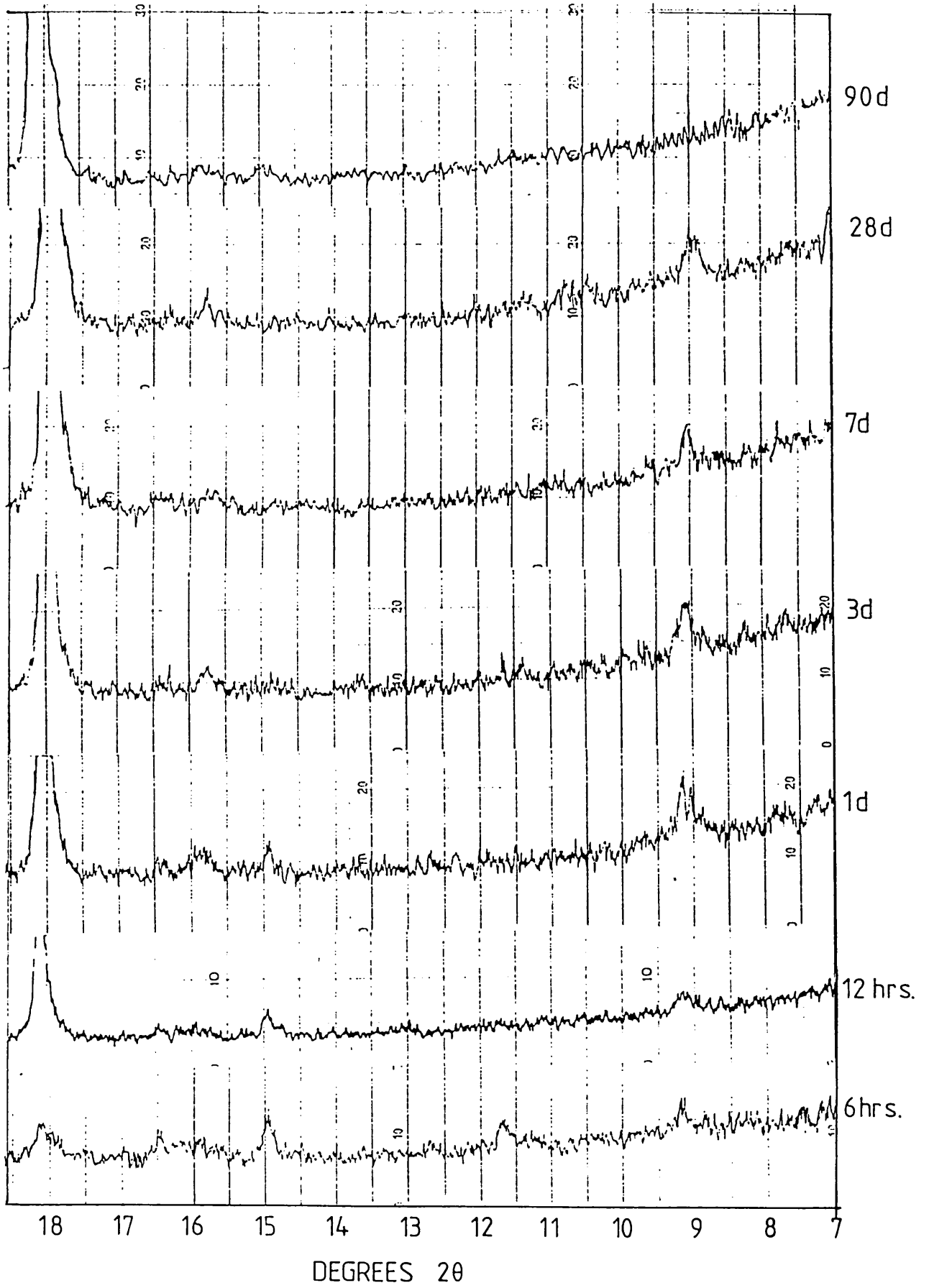

FIG. 5.2.16 XRD traces for AW blended cement paste at various ages.

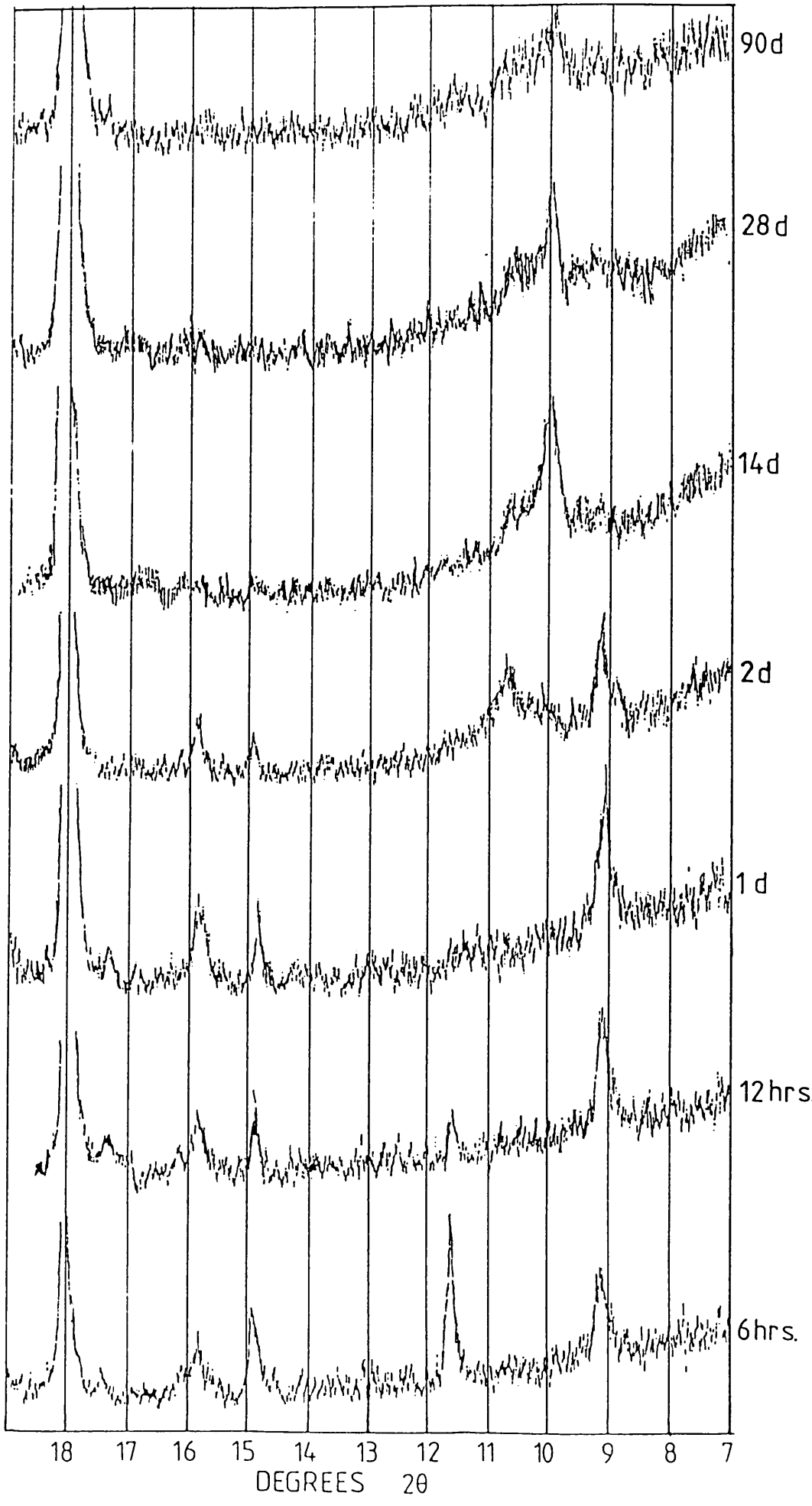

FIG. 5.2.17 XRD traces for BW neat cement paste at various ages.

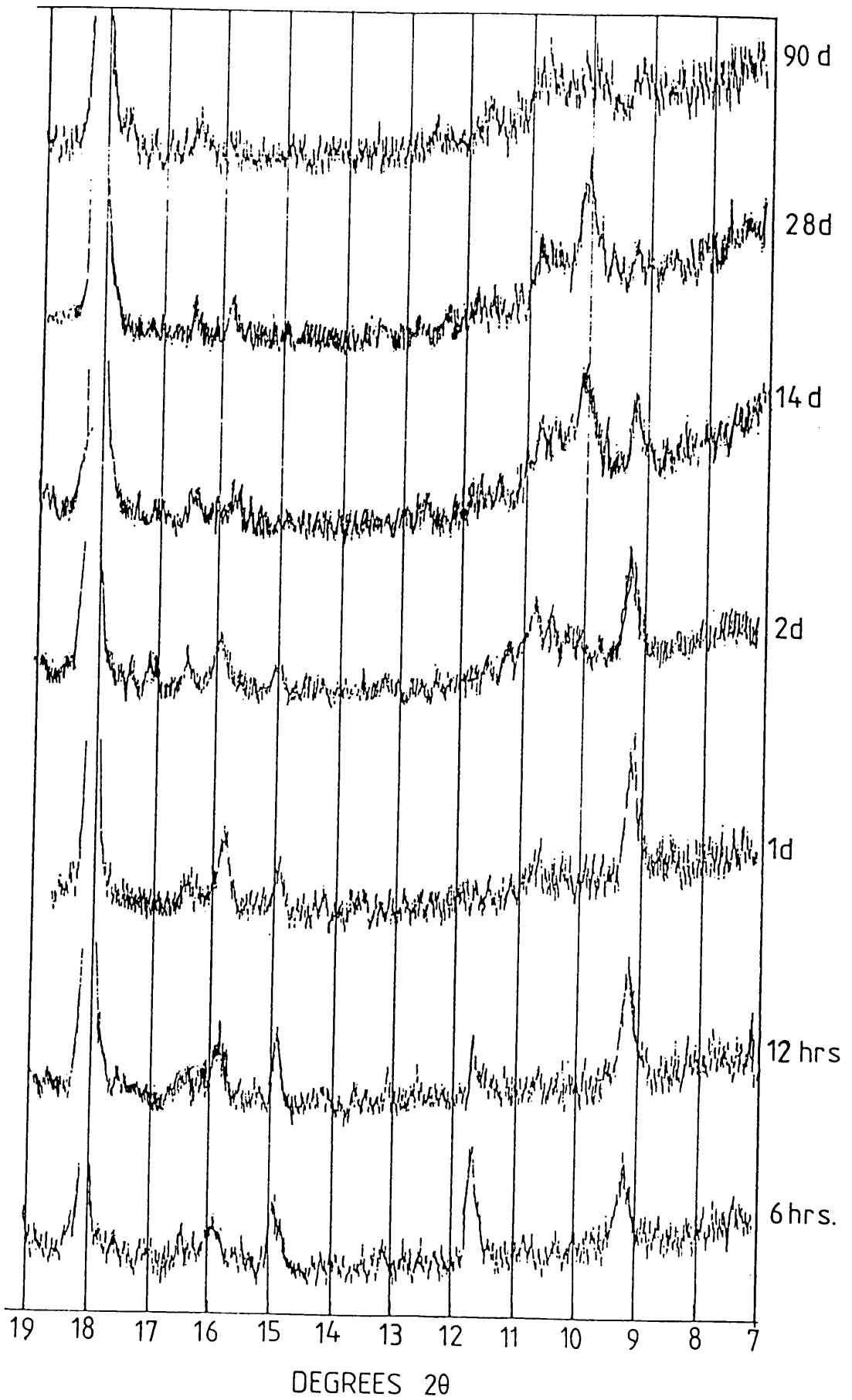

FIG. 5.2.18 XRD traces for BW blended cement paste at various ages.

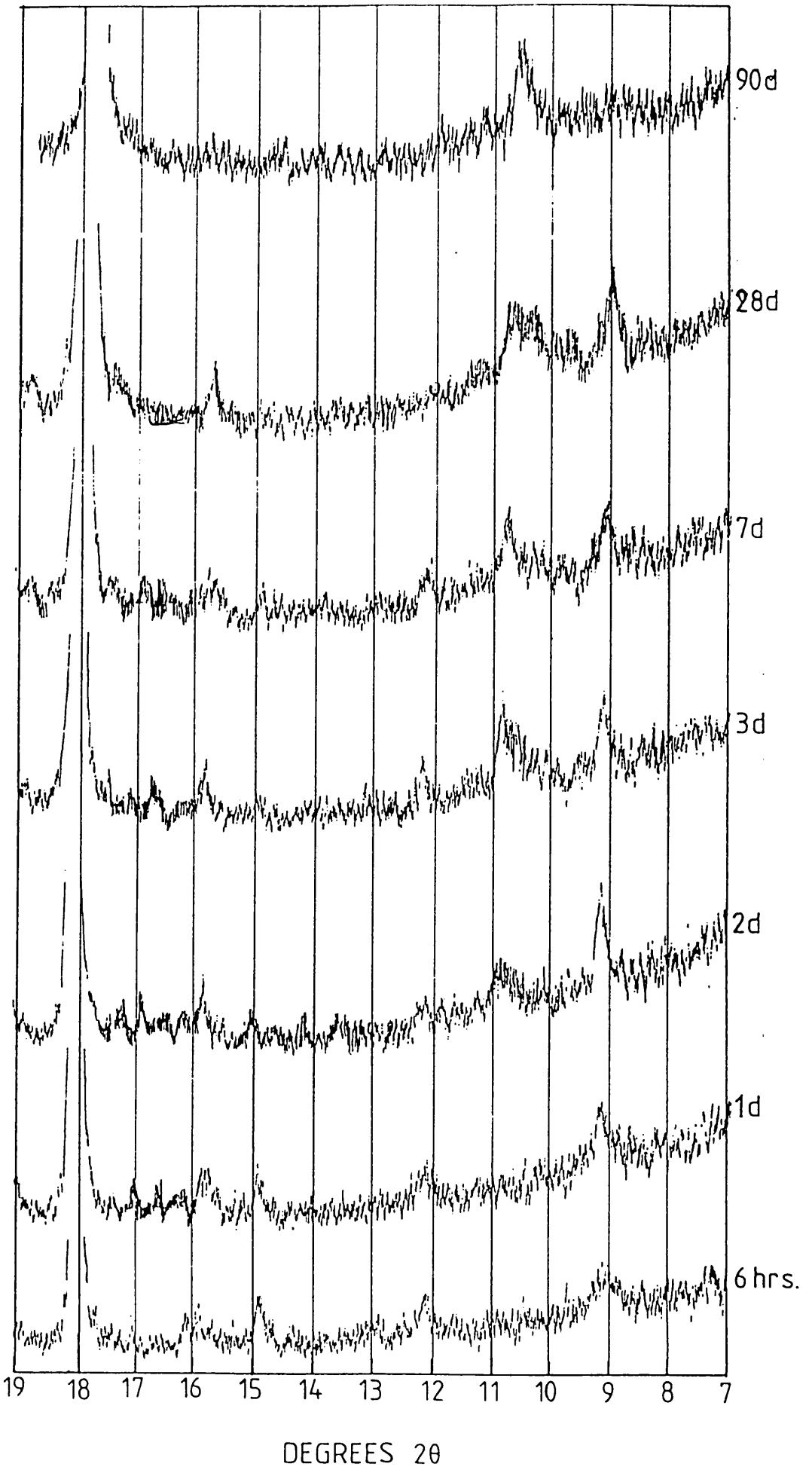

FIG. 5.2.19 XRD traces for D/44 neat cement paste at various ages.

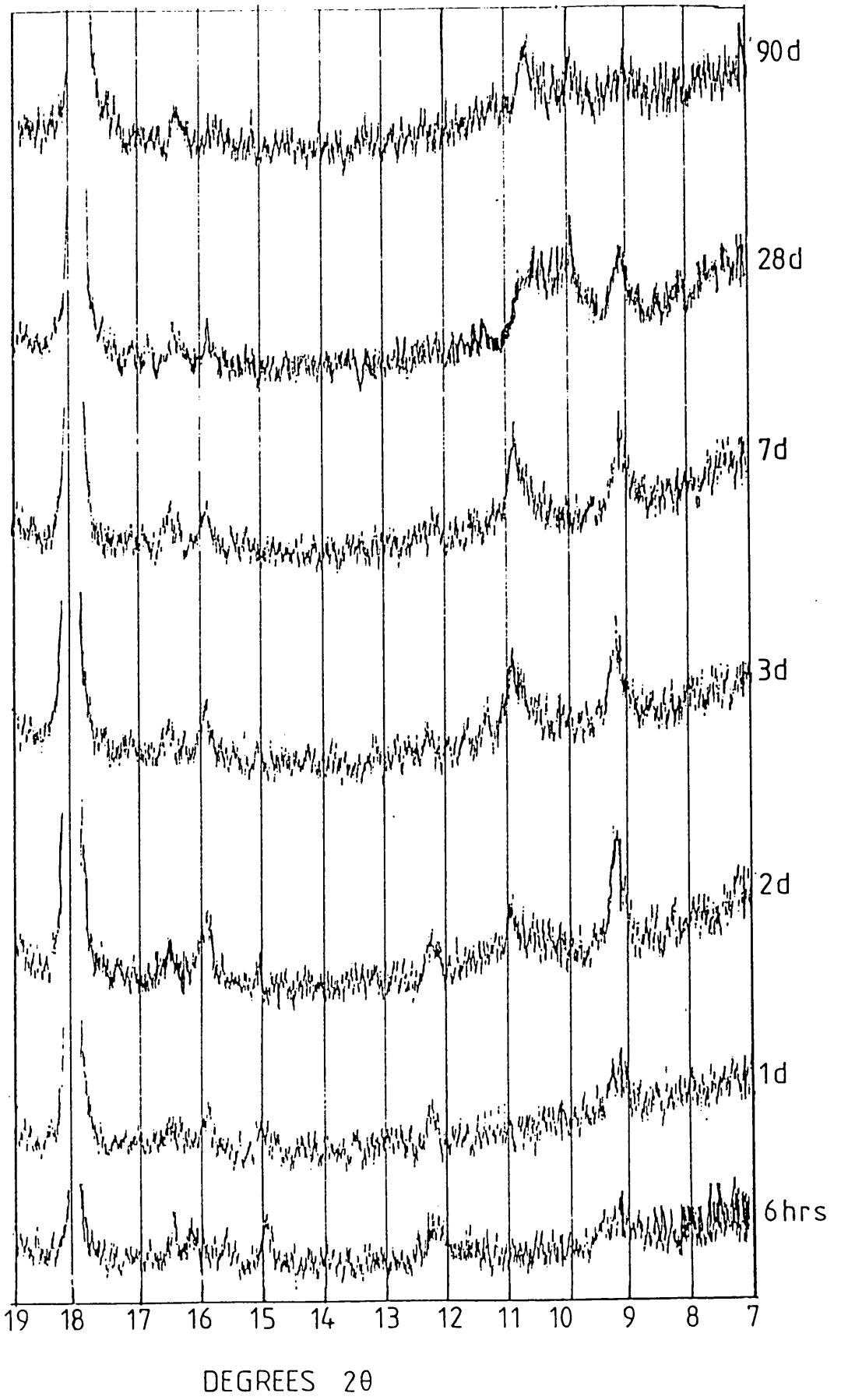

FIG. 5.2.20 XRD traces for D/44 blended cement paste at various ages.

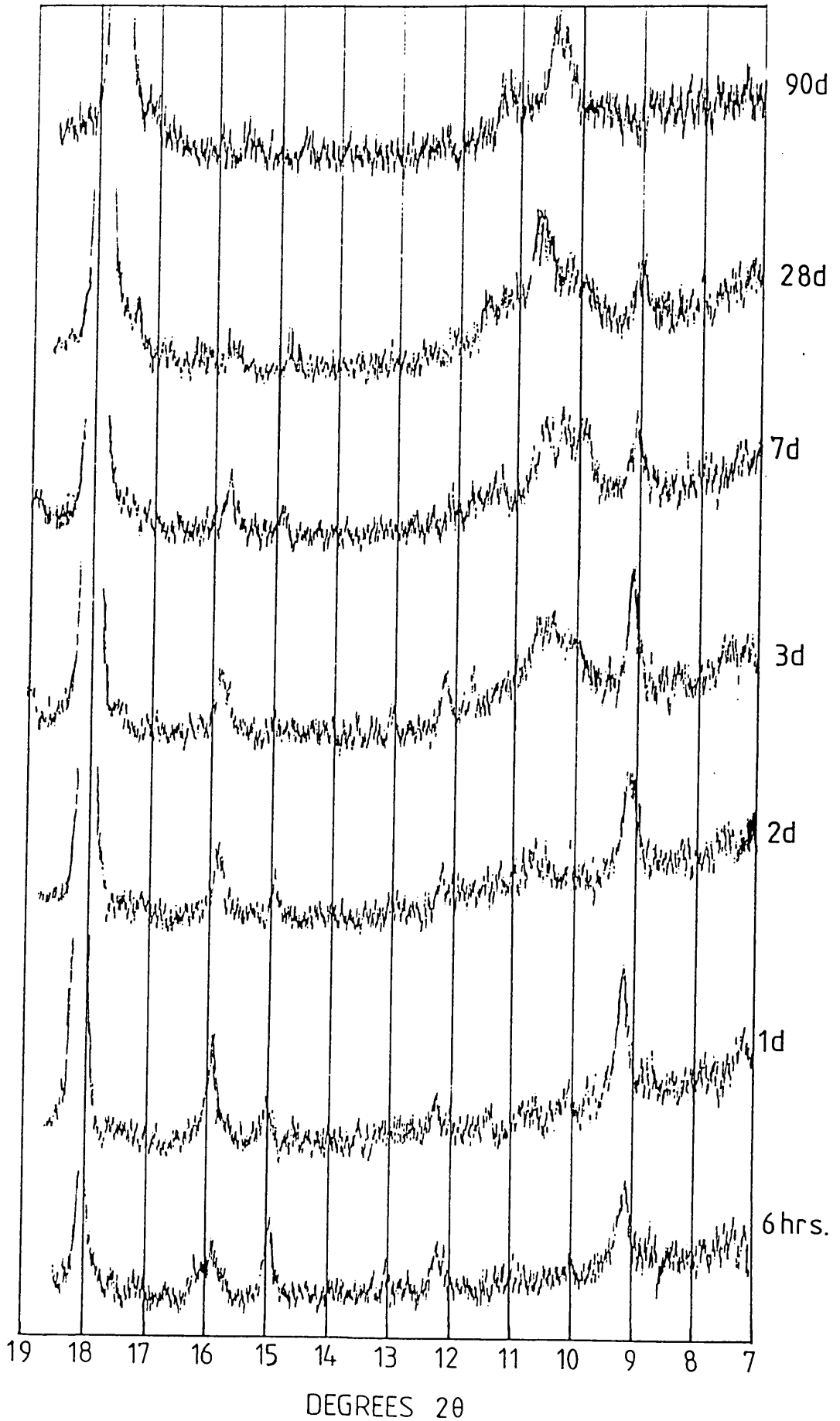

FIG. 5.2.21 XRD traces for Westbury neat cement paste at various ages.

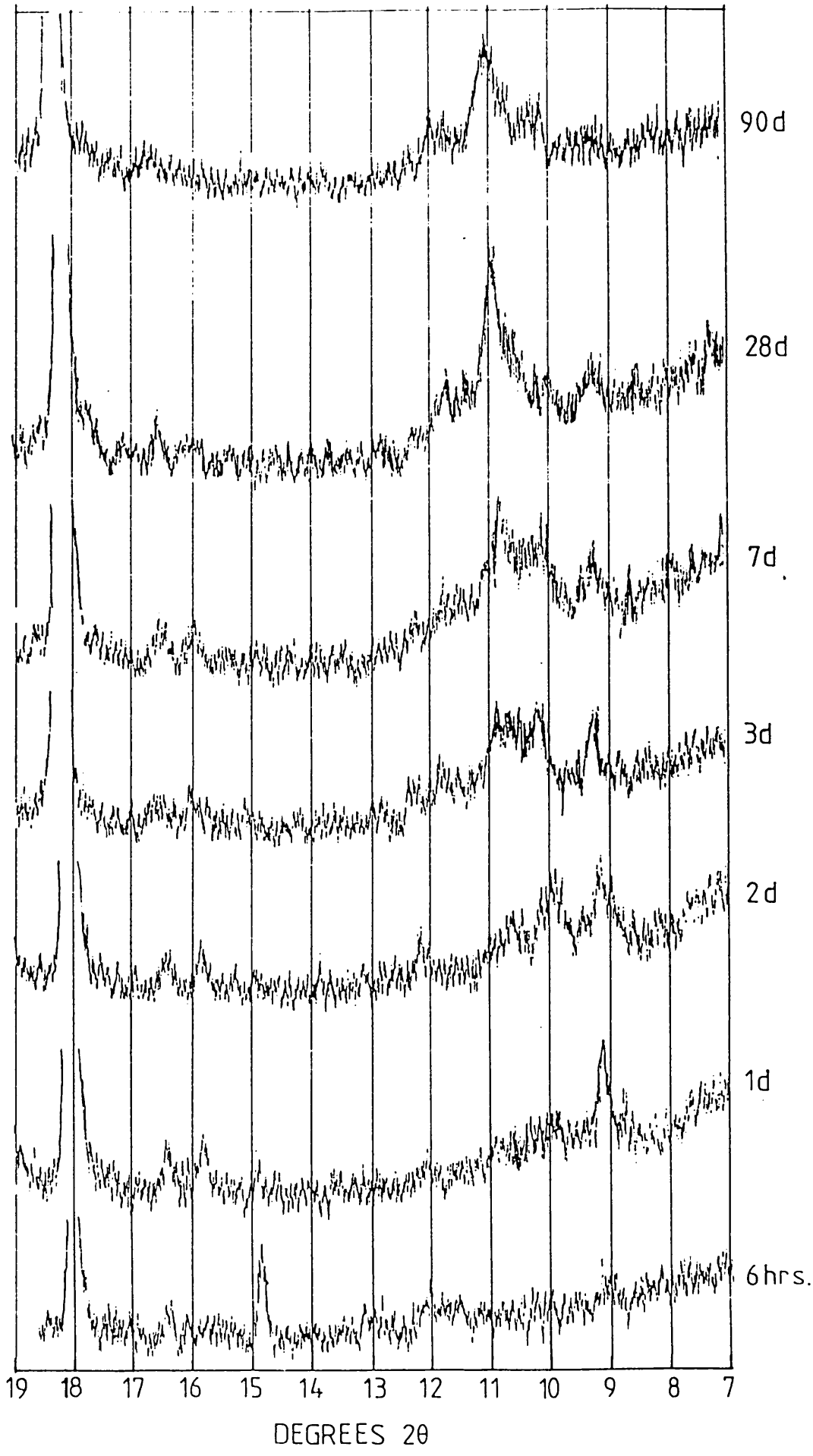

FIG. 5.2.22 XRD traces for Westbury blended cement paste at various ages.

It is very unlikely that the original hemihydrate phase still exists after 6 hours hydration as explained above. On the other hand, the Ca^{2+} and SO_3^{2-} ions in the solution may recrystallise during drying to form either soluble anhydrite, or to reform hemihydrate by combining with water.

D/44 contains only the hemihydrate form of calcium sulphate, and starts to form gypsum within 20 minutes of mixing. The gypsum has been dissolved by 6 hours hydration [Fig. 5.2.19-20] and the peak at 5.9 Å corresponds to recrystallised calcium sulphate phase. Anhydrite is the sulphate form in Westbury cement, which has a relatively slower rate of dissolution than the other sulphates, hemihydrate and gypsum. Therefore the calcium sulphate in the solution cannot reach super-saturation with respect to gypsum but forms recrystallised sulphate during drying. The anhydrite (not shown in the diffraction patterns) has been dissolved between 12 and 24 hours.

1. D/44, Westbury, BW pastes:

   AFt (ettringite) phase, which has a strongest reflection at 9.73 Å, is the only calcium aluminate hydrate appearing before 1 day,* except in BW blended cement where AFm phases have been formed in the 1 day old sample. In other cements, except the AW mixtures, AFm phases have formed between 1 and 2 days hydration indicating that the sulphate content in the systems is dwindling. The AFm phases present in the samples have various diffraction peaks between d-spacing 8.9 Å and 8.2 Å, the major ones beings at 8.9 Å, 8.4 Å and 8.2 Å.

---

* The ettringite peak in the 6 hours old Westbury blended cement does not show up strongly because some of the ettringite phase has been destroyed by removal of water molecules during drying or storage (discussed below).

The peak at 8.9 Å corresponds to the monosulphate phase, ($C_3A.CaSO_4.12H_2O$). However, the basal reflection can be changed by the number of water molecules binding with the compound. If $C_3A.CaSO_4.12H_2O$ forms during the hydration, drying the sample at 20 °C and a partial water vapour pressure of 0.2 mm Hg reduces the water content to about $10H_2O$ and shifts the basal reflection from 8.9 to 8.2 Å. Hence various modifications can be produced on drying under various conditions, and are illustrated in Fig.5.2.23 [Copeland and Kantro, 1964].

The 8.2 Å peak could also reflect two other possible AFm phases which are α-C_4AH_{13} and $C_4A.\bar{C}_{0.5}H_{12}$. However, the existance of α-C_4AH_{13} is still in dispute. Seligmann and Gruning [1964] have shown that α-C_4AH_{13} is really a quarter carbonate ($C_4A\bar{C}_{0.5}H_{12}$) which is formed in solution saturated with alumina and lime precipitate solids, in a carbon dioxide atmosphere.

Besides these two major AFm phases there are some incomplete solid solution series formed from the monosulphate dissolved in calcium aluminate hydrates (e.g. C_4AH_{13}, C_4AH_{19}), which may give a diffraction peak at 8.4 Å.

In the Westbury mixed samples [Fig.5.2.21-22], a peak at 11.6°, 2θ (7.6 Å) which corresponds to the tetracalcium aluminate carbonate ($C_4A\bar{C}H_{12}$) [Taylor, 1964] can be seen from 2 days onwards. This indicates that these cement pastes contain a higher percentage of carbonate which may come from the 1% of dolomite in the cement.

After the AFm phases have appeared, the size of the ettringite peaks is gradually reduced, but at a very slow rate. The ettringite peak still can be seen in most of the 28 days old samples, the exception being the BW pastes in which ettringite has not been found from

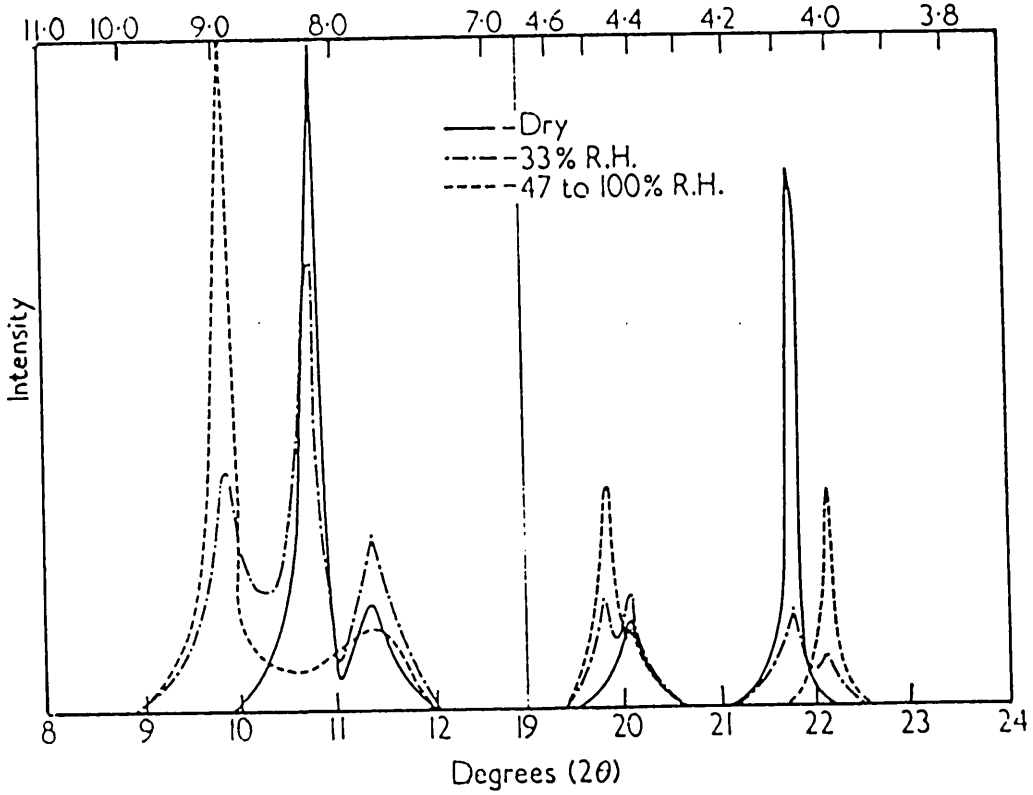

FIG. 5.2.23 Shifts of basal reflections of calcium aluminate monosulphate hydrate with changes in humidity. (from Copeland and Kantro, 1964)

14 days in the neat cement and 28 days in the blended cement, where a relatively stronger 8.9 Å monosulphate peak has been detected. However, the ettringite peak reappears in the 90 days BW blended cement when the AFm peaks are diminished. In most of the other 90 days cement pastes, except D/44 blended cement, no ettringite has been found. On the other hand, two sets of 6 months old wet powder samples, obtained by grinding the hydrating BW and D/44 pastes, were examined by X-ray analysis. The results [Fig.5.2.24] show that strong ettringite and monosulphate peaks are present in all of them, and small amounts of AFm solid solution (8.4 Å) are found in both BW samples.

The results obtained from the wet samples suggest that the ettringite phase in some of the younger dried samples was destroyed by removal of the bonded water molecules, as also concluded by Copeland and Kantro [1964], and Skoblinskaya and co-workers [1975(a),(b)]. This problem is more likely to occur in the older samples which contain less free water. It was also found that the ettringite peak reappears by re-wetting the sample under 100% relative humidity. The 28 days old BW dry powder samples were re-wetted for 6 hours and an ettringite peak was detected [Fig.5.2.25(a)]. However, the length of the wetting time can strongly affect the size of the reformed peak. After 1 week wetting time, the size of the ettringite peak is doubled and most of the AFm phase was carbonated to form $C_3A.CaCO_3.11H_2O$ at 7.57 Å [Fig.5.2.25(c)].

Since the wet samples show only one strong 8.9 Å monosulphate peak, the various peaks at 8.9 Å and 8.2 Å in the dry samples may just be caused by monosulphate in various states of dehydration.

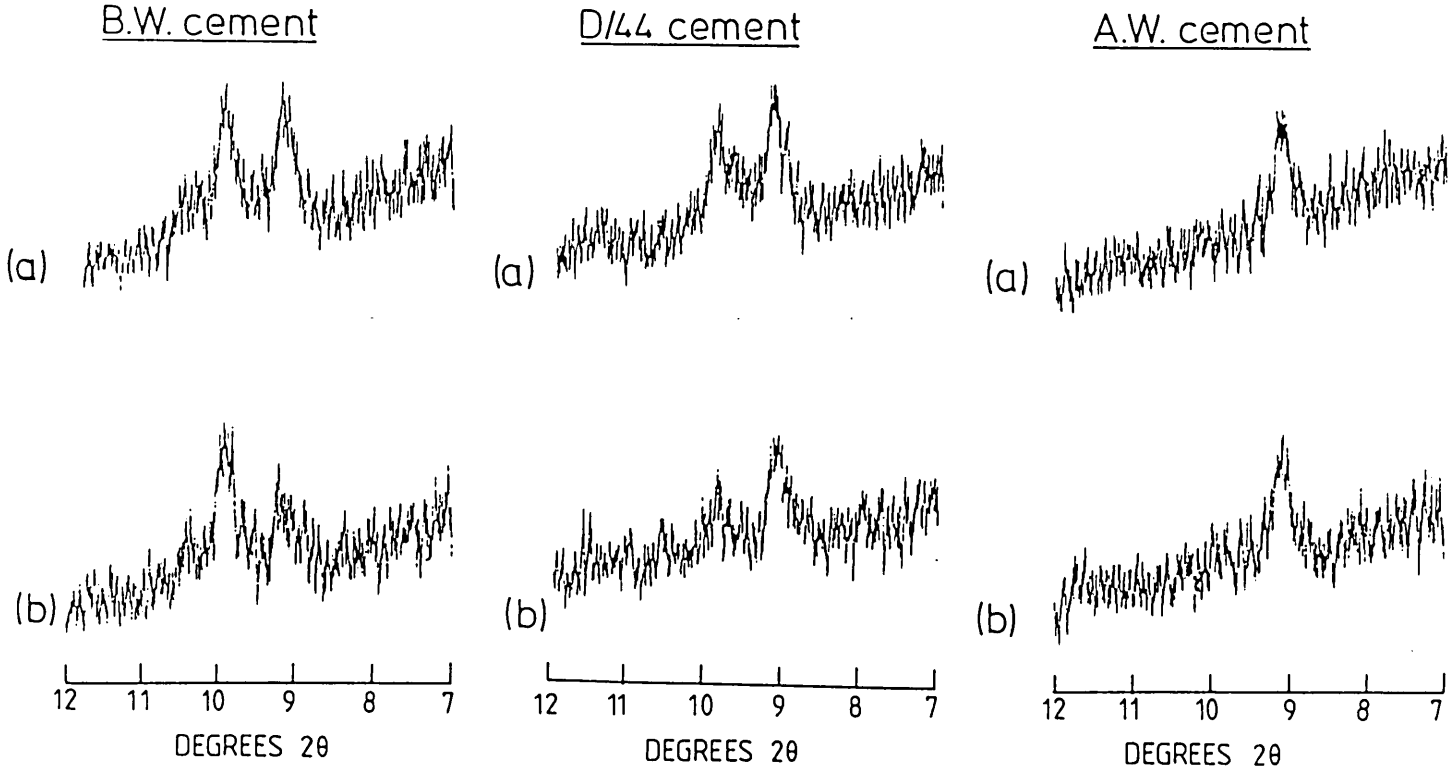

FIG. 5.2.24 XRD traces of hydrating undried samples at the age of 6 months.
(a) neat cement pastes (b) blended cement pastes

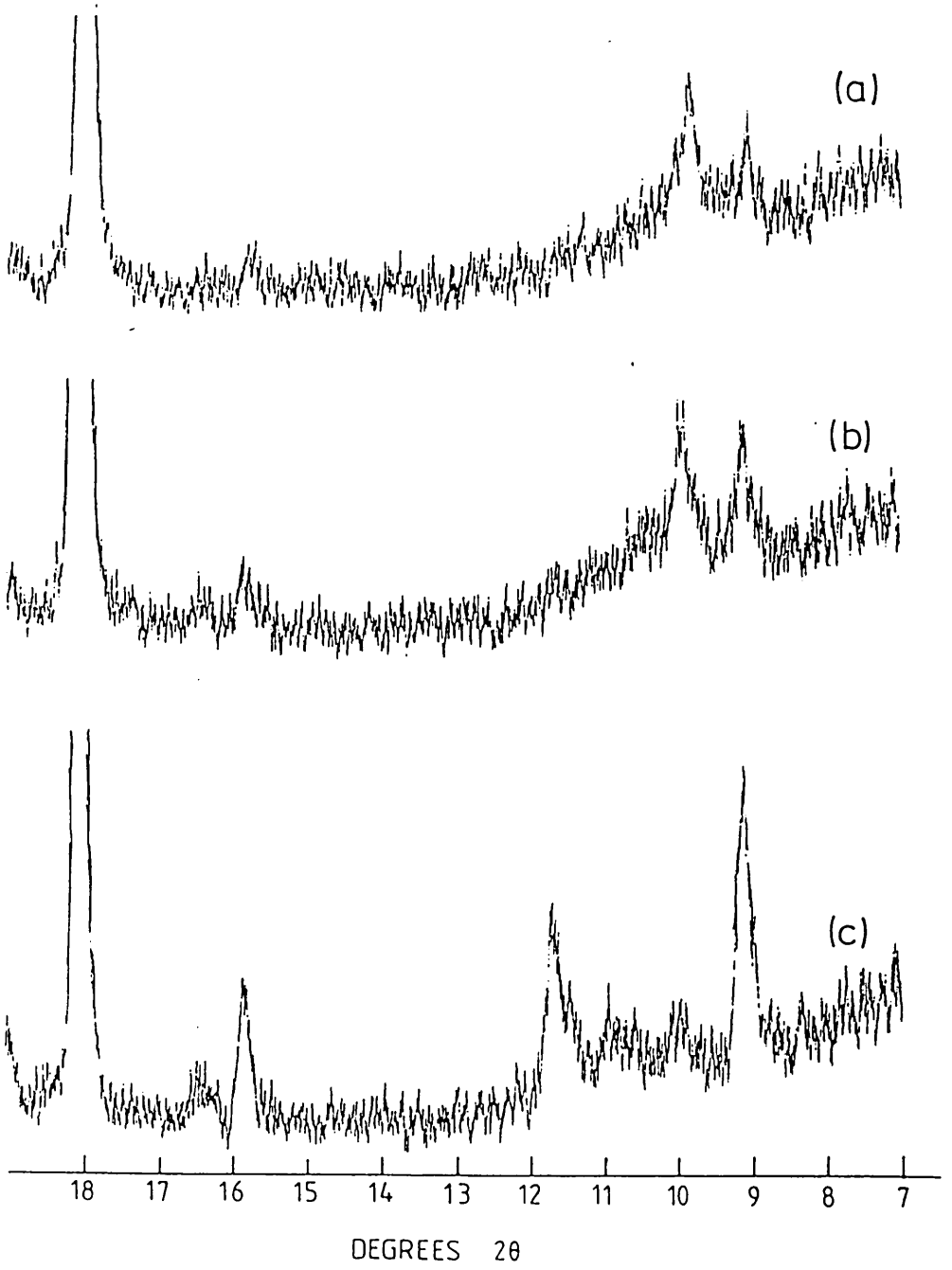

FIG. 5.2.25 XRD traces of re-wetted cement powder at the length of (a) 6 hrs. (b) 2 days (c) 1 week.

2. AW mixtures [Fig.5.2.15-16]:-

AW neat and blended cements are unusual as ettringite is the only hydrate formed from the calcium aluminate phase in most of the samples examined, even when there is no calcium sulphate present, i.e. no soluble anhydrite has been detected. This is probably due to the small amount of C_3A (2%) in the cement which has completely hydrated before all the $CaSO_4$ has been used up so that there is no C_3A to react with the AFt to form AFm. The wet 6 months old samples were also analysed [Fig.5.2.24] and show that an ettringite peak appears in both mixtures. Therefore the ettringite phase was destroyed by drying of the 90 days samples.

Hence an important point when using X-rays to analyse AFt or AFm phases is that the wet powder samples will provide much more accurate results.

Differential thermal analyses

The hydrates in the sample could in principle be identified by their individual decomposition temperatures in the thermal analyses [Section 2.6]. However, this investigation is limited by the over-lapping of peaks, especially between 100 and 200 °C. Fig.5.2.26-27 show four sets of DTA results between temperatures of 25 °C and 300 °C where the decomposition of calcium aluminate hydrates and C-S-H takes place.

For the white cement samples [Fig. 5.2.26(a) and (b)] at early hydration times, a peak at 136 °C has appeared and has also been observed in the unhydrated BW cement suggesting that it is associated with decomposition of gypsum; the disappearance of this peak at later times coincides with that of gypsum as shown in the X-ray diffraction patterns

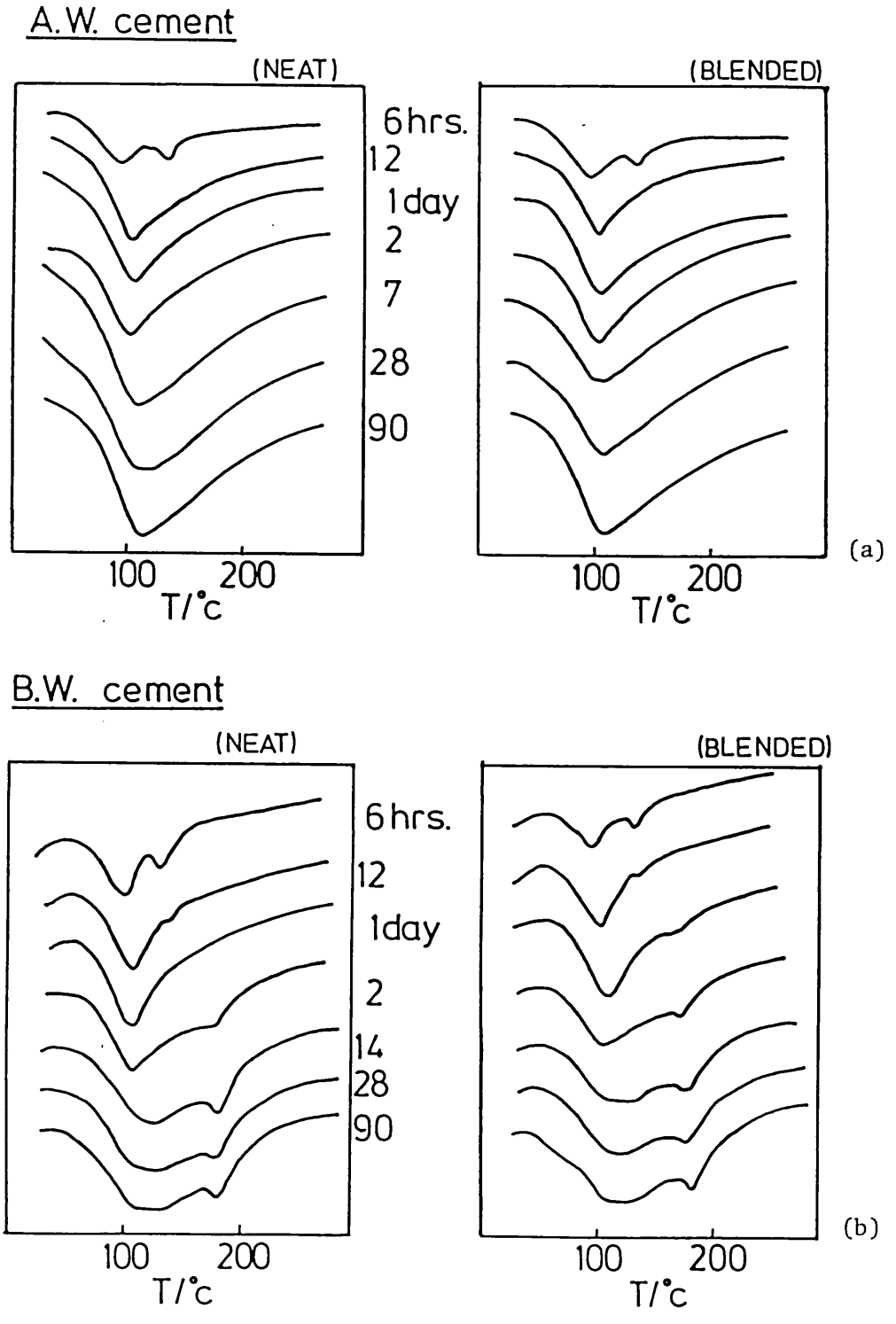

FIG. 5.2.26 DTA cures of the white cement pastes.

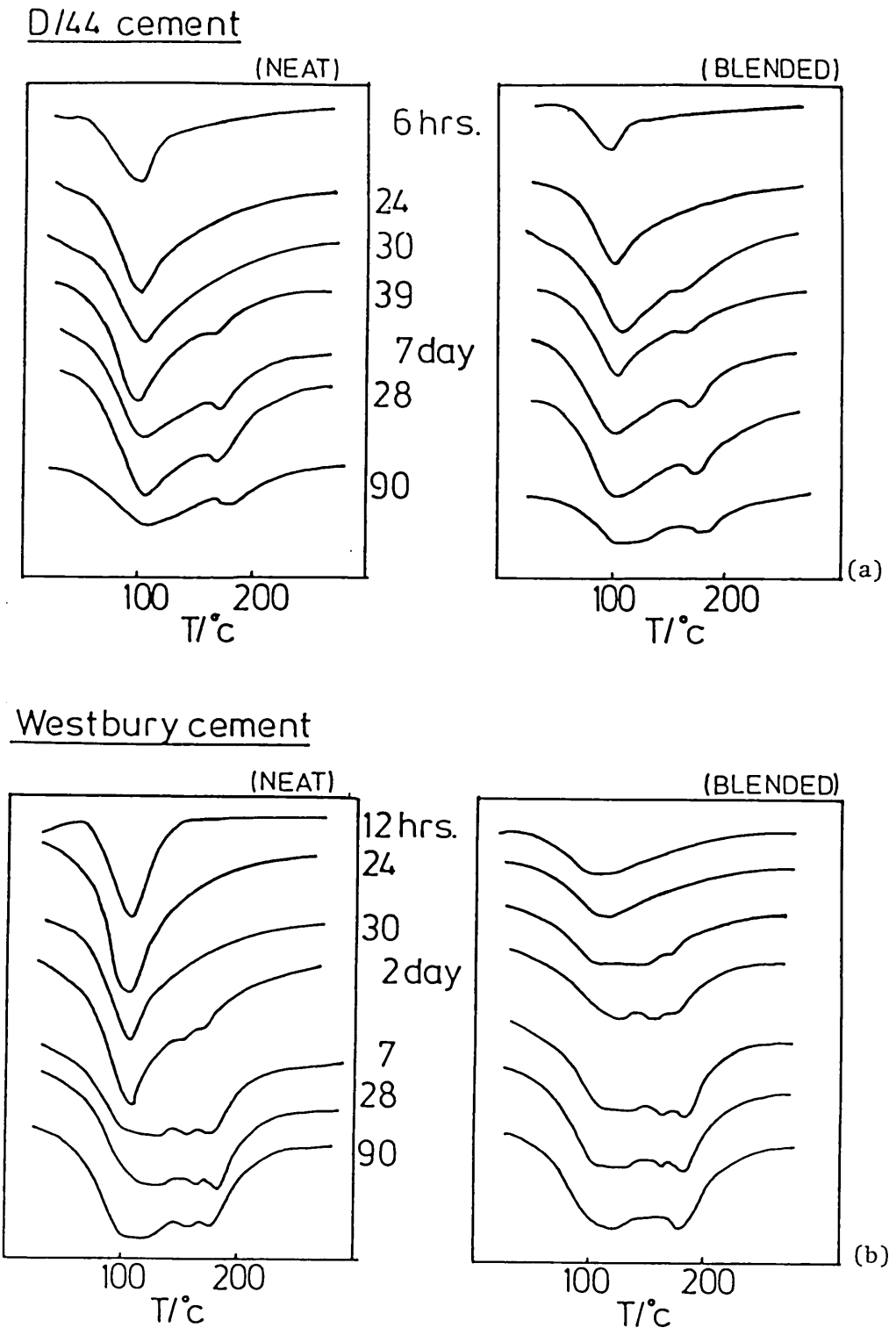

FIG. 5.2.27 DTA cures of the ordinary portland cement pastes

[Section 5.2.D). This temperature is found to be similar to the result of Odler and Abdul-Maula [1984] but is inconsistent with Bye [1983]. The variation may be caused by differences in sample preparation (size and packing) and the exact composition of the phase.

A peak at about 100 °C, present in all the samples examined, corresponds to the decomposition of C-S-H and ettringite, the closeness of whose peaks prohibits an estimation of the relative amount of each phase. In Westbury cement this peak is shallower in the blended mixture up to 2 days because ettringite phase is destroyed during the grinding or storage as proved by subsequent X-ray analyses of these samples. The position of this peak in most 6 hour old samples is at slightly lower temperature, presumably because the products have a poorly developed crystal structure.

A peak at about 170 °C, corresponding to the dehydration of the AFm phase, appears between 1 - 2 days hydration in most of the hydrated cements, except for the AW mixtures in which AFm has not been formed. The times are consistent with those found in the X-ray diffraction. The DTA analysis was performed more frequently, so that the time when the AFm appears can be narrowed down to a smaller range, as shown in Table 5.2.2:-

TABLE 5.2.2 THE TIME RANGE OF AFm APPEARANCE FROM DTA

	Time range	
Cement	Neat cement	Blended cement
BW	1 - 2 (day)	12 hr - 1 day
AW	-	-
Westbury	30 - 36 (hr)	24 - 30 (hr)
D/44	30 - 39 (hr)	24 - 30 (hr)

This result shows that the addition of fly ash has advanced the formation of AFm by adsorption of sulphate ions leading to depletion of those in solution.

The time AFm appears in the neat cements, and BW blended cements, coincides with that of peak 4 in the calorimetry curves [Fig.5.2.1(b), 5.2.2(b) and 5.2.3(a)]. However, for the other blended cements, the time does not coincide with any of the noticeable peaks indicating that the reaction, if it does indeed correspond to peak 4, is slower in these pastes.

The variation in the position of the AFm peak (170-180 °C) does not seem to be directly correlated to the shift in the corresponding X-ray peak [Fig.5.2.17-22], and may instead by caused by irregularities in the grinding procedure.

In Westbury samples [Fig. 5.2.27(b)] there is an endothermic reaction at 159 °C which is probably due to the decomposition of tetra-calcium aluminate carbonate 12-hydrate, as this phase corresponds to a peak at 7.6 Å in the X-ray diffraction pattern which similarly only appears for these mixtures.

5.2.F *THE HYDRATION OF THE FERRITE PHASE (C_4AF)*

A possible candidate for the exothermic reaction which causes peak 4 in some of the cement pastes is the hydration of C_4AF. To test this, samples corresponding to hydration times before and after peak 4 were examined by QXRD to measure the amount of the C_4AF phase then present [Section 2.5].

BT and two different BT blended cements were examined at the Cement and Concrete Association, by Mr Gutteridge. The results are shown in Tables 5.2.3(a) and 5.2.4(a) and (b).

Westbury neat and blended cement hydrated samples were examined using a Philips PW1710 diffractometer at Imperial College. This cement contains only 3.5% of C_4AF and so will give only a small diffraction peak in the X-ray pattern making the measurement inaccurate. To overcome this problem, the ground hydrated cement powders were washed in "SAM" solvent to extract the interstitial phases [Section 2.8], enhancing the C_4AF peaks in the X-ray diffraction pattern and also diminishing the C_3S and CH peaks which overlap with that of C_4AF ($\sim$34 °, 2θ). The "SAM" residue powder was mixed with TiO_2 which acts as an internal standard. The area under the peaks at 27.443 °, 2θ [3.25 Å] and 34.09 °, 2θ [2.63 Å] corresponding to TiO_2 and C_4AF respectively, was measured by the diffractometer.

Alexander and Klug [1948] have shown that the ratio of mass of a crystalline phase Mi to the mass of a standard Ms is related to the intensities of characteristic reflections of the crystalline phase and the standard by the ratio:-

$$\frac{Mi}{Ms} = k \frac{Ii}{Is}$$

where the intensities of the characteristic reflections may be represented by the areas under the peaks, and k is a constant which is assumed to be unchanged in examining the same crystalline structure.

k Was chosen so as to reproduce the percentage of C_4AF (3.5%) measured by Gutteridge [Section 3] in the Westbury anhydrated cement; by knowing Ii, Is, k and Ms, the Mi, which is the mass of C_4AF, can be deduced [Appendix V]. The amount of C_4AF per weight of cement in the hydrated neat and blended cements at the ageing times near peak 4 are listed in Table 5.2.3(b) and 5.2.4(c) respectively.

The neat BT cement displays only a minor variation in the amount of C_4AF, but there is a significant decrease in its corresponding fly ash cements, which is fairly even with Drax fly ash, and largely before 22 hours with Bold. Both Westbury neat and blended cements show a continuous decrease in the amount of C_4AF and the rate of decrease is faster in the latter paste. All this suggests that there is no sudden reduction in the C_4AF content around the hydration times corresponding to peak 4, which cannot then be associated with the hydration of C_4AF. However, it has been shown that the hydration of C_4AF is accelerated by the addition of fly ash.

TABLE 5.2.3 THE AMOUNT OF C_4AF IN NEAT CEMENT AT VAROUS AGES

(a) BT (b) Westbury

(a)

Hydration time (hr)	C_4AF in % of weight of cement
0	6
30	6.37
50	6.20

(b)

Hydration time (hr)	C_4AF in % of weight of cement
0	3.50
18	2.40
24	2.54
48	2.39
72	2.13

TABLE 5.2.4 THE AMOUNT OF C_4AF IN FLY ASH CEMENT AT VAROUS AGES

(a) BT/Drax (b) BT/Bold (c) Westbury/Fiddlers Ferry

(a)

Hydration time (hr)	C_4AF in % of weight of cement
0	6
20	4.33
48	2.47

(b)

Hydration time (hr)	C_4AF in % of weight of cement
0	6
22	3.8
40	3.5

(c)

Hydration time (hr)	C_4AF in % of weight of cement
0	3.5
7	2.79
12	2.35
24	2.14
48	1.87

5.2.G *MICROSTRUCTURE DEVELOPMENT OF THE HYDRATES IN ORDINARY PORTLAND CEMENT AND FLY ASH CEMENT*

Microstructure in the first hour of hydration

The first hour of hydration produces a large heat output, appearing as peak 1 in the calorimetry curve. A common feature of fracture samples at this time is that the surfaces of the particles are covered by many short hexagonal rods of AFt [Plate 5.2.1] which are formed by the rapid hydration of C_3A in the presence of gypsum. Scrivener [1984] has observed a hydrating sample in the environmental cell showing that these AFt rods form in the solution surrounding the cement grains. During drying, the AFt rods will fall back onto the particles with random orientation.

The density of the AFt rods on the particle surface varies from region to region as shown in plates 5.2.2 and 5.2.3. This may be caused by the inhomogeneous mixing of gypsum crystals and the non-uniformly dispersed C_3A phase in the cement. It is difficulty to estimate the variation between different cements and fly ash cements at this early age because it is less than that between different regions in any one cement.

In the cements containing hemihydrate, large amounts of secondary gypsum crystals have been observed in the first half hour's hydration [Plate 5.2.4]. The secondary gypsum is formed by the rapid dissolution of hemihydrate leading to a supersaturated sulphate solution and so to reprecipitation in gypsum form [Scrivener, 1984]. The amount of secondary gypsum is reduced significantly in 1 hour samples because of the consumption of sulphate ions by the rapid reaction with C_3A. In Westbury neat and blended cement, no secondary gypsum crystals are observed as the cement contains only anhydrite which has a much slower dissolution rate than the hemihydrate and gypsum. Hence the relatively rapid reaction of the resulting gypsum during the hydration of C_3A to form AFt prohibits supersaturation.

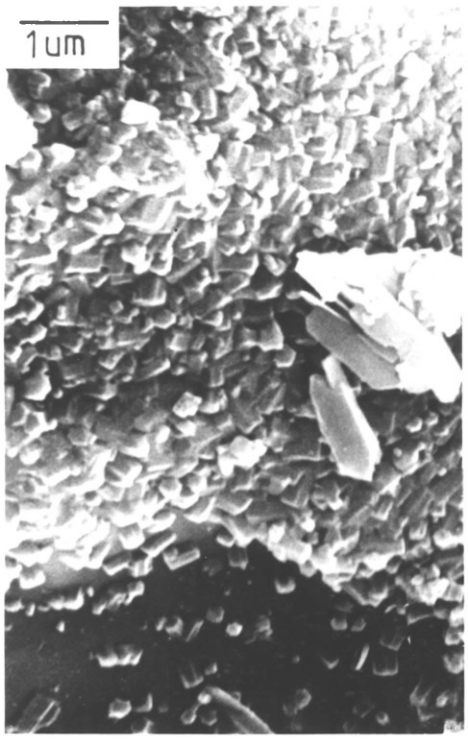

PLATE 5.2.1

Dried fracture surface of cement (D/44) hydrated for 1 hour

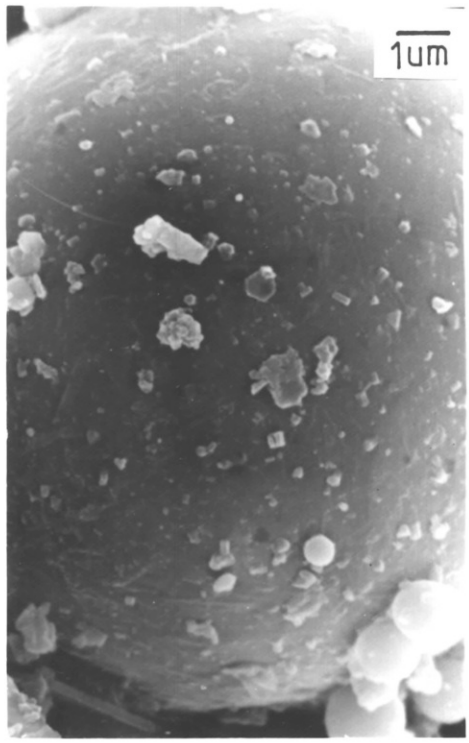

PLATE 5.2.2

A fly ash surface in BT/Drax blended cement after ½ hour hydration

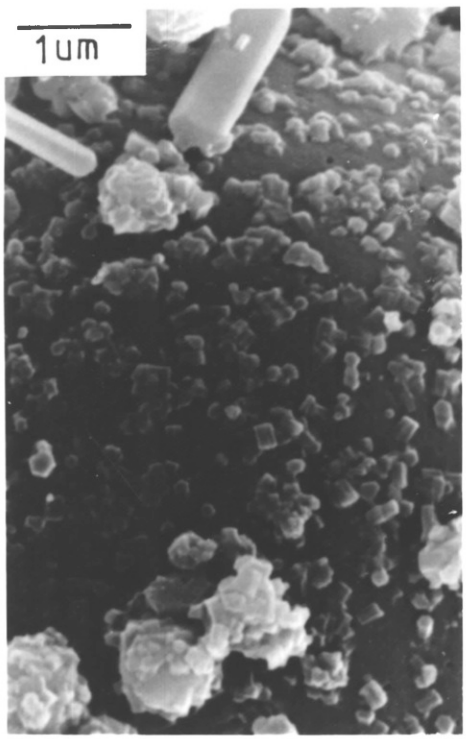

PLATE 5.2.3

A Fly ash heavily covered by AFt rods in 1 hour hydration BT/Drax blended cement

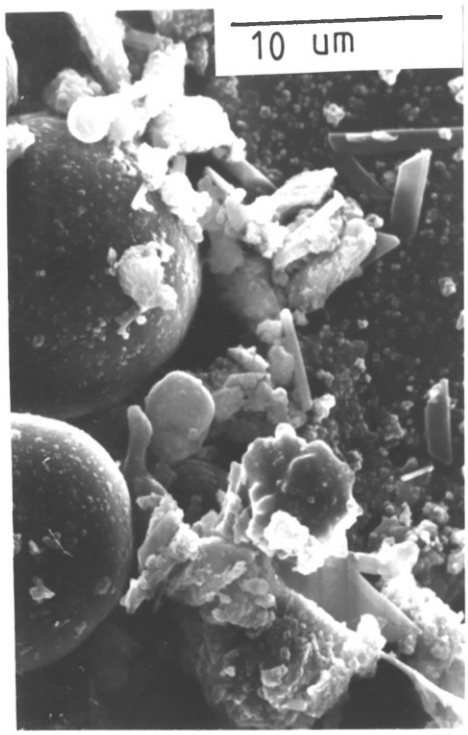

PLATE 5.2.4

Fracture surface of BT/Bold blended cement hydrated for ½ hour, showing large number of secondary gypsum crystals

At this early time, the hydration of C_3S is very slow as shown by the absence of small needles of C-S-H on the surface of the particles; some crumpled foils of C-S-H have been observed, e.g. on the fly ash surface shown in plate 5.2.2.

Microstructure development between 3 and 48 hours hydration

At 3 hours hydration [Plate 5.2.5], the onset of peak 2 in the calorimetry curve for the neat and blended cements has started, and fine needles of C-S-H have been seen on the particle surfaces. The amount of C-S-H on the particles also varies from region to region and is greater on the particles which are less covered by AFt rods. There is no significant difference between the various types of cement except in the BT blended cements which still contain some large secondary gypsum crystals up to 4 hours hydration. This may be due to the extraction of gypsum from the anhydrite.

After 6 hours hydration, a difference in the microstructure of the neat and blended fly ash cements is the appearance of the C-S-H. The C-S-H in the blended cement particles is smaller and less plentiful than that on the neat cement particles [Plate 5.2.6-7]. Since the onset of the C_3S hydration is retarded by the fly ash as shown in calorimetry curves [section 5.2.A], less product forms.

The number and size of C-S-H is increased during the acceleratory period of peak 2, so that the AFt rods formed at early age are gradually covered [Plate 5.2.8]. The C-S-H appears in the fibrillar morphology (Diamond type I) [Diamond, 1976], and completely covers the surfaces of the particles by 12 hours in both cements. Sometimes, groups of small hydrates, C-S-H and AFt, form on the particle surface (e.g. right hand side of plate 5.2.8); these may be caused by the hydration of small cement grains which originally agglomerated on the surface of the particles.

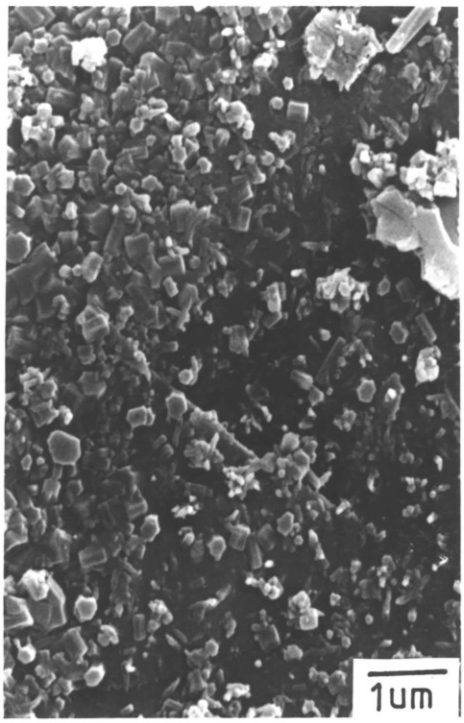

PLATE 5.2.5

Cement grain surface (Westbury blended cement) after 3 hours hydration

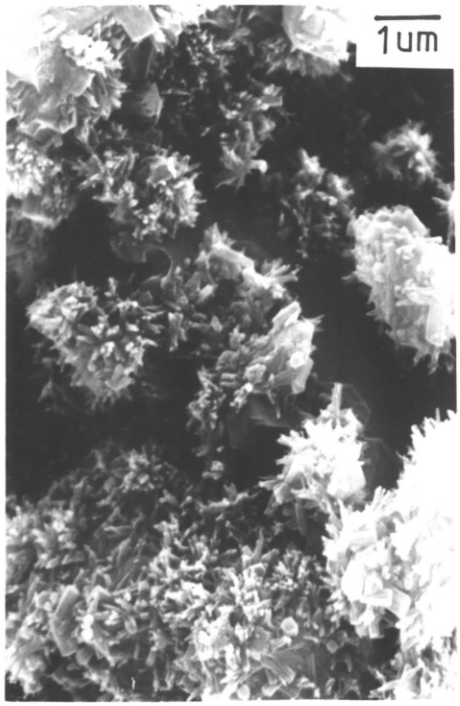

PLATE 5.2.6

Fracture surface of neat cemen (Westbury) hydrated for 6 hour

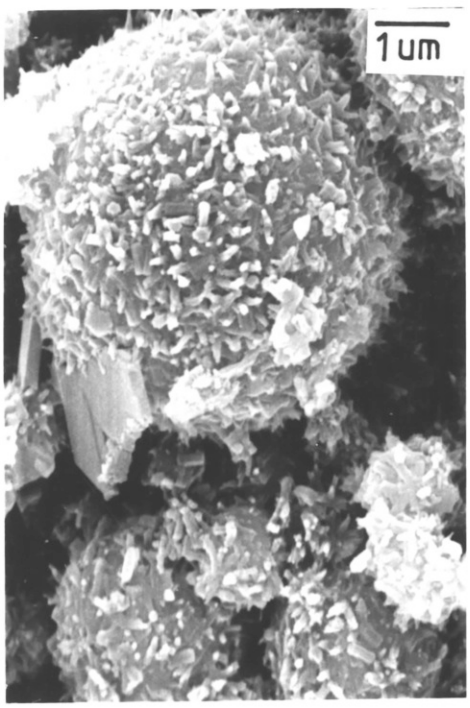

PLATE 5.2.7

Fracture surface of fly ash cement (Westbury blended cement) hydrated for 6 hours

PLATE 5.2.8

Fly ash surface in Westbury blended cement after 12 hours hydration

After about 12 hours [Plate 5.2.9], the secondary growth of AFt rods occurs in all of the neat and blended cements and is probably due to the decrease of sulphate and CH in the solution. The time of the secondary growth, and the growth rate, varies from cement to cement since there is a difference in their solution environments. In Westbury cement mixtures, long AFt rods can be seen at 18 hours hydration [Plate 5.2.9(a) and (b)], corresponding to the maximum of peak 3, and the growth occurs at the acceleratory period of peak 3. In D/44 pastes, the growth takes place between 12 and 18 hours at the deceleratory period of peak 3 [Plate 5.2.9(c) and (d)], for BT blended cements, between 14 and 20 hours, corresponding to peak 3 [Plate 5.2.9(e)], and the growth rate in this period is very small, only short AFt rods emerging through the C-S-H hydrate layer. The length of the rods increases with age and by 30 hours [Plate 5.2.9(f)] large numbers of long AFt rods have been observed. This growth also has been seen in others up to 2 days as expected from the continuing decrease of the concentration of sulphate and CH in the solution.

There are more AFt rods in the Westbury cement pastes than in the others, probably due to the higher content of C_3A. The AFt rods in the Westbury blended cement are shorter and thicker than those in the neat cement, but there is no noticeable difference between the two D/44 pastes.

After 12 hours, bonding between the hydrates surrounding different grains in the neat cement is strong enough to rupture the hydrate shells during fracture as shown by the appearance of Hadley grains [Barnes et. al., 1978][Plate 5.2.9(c)]. However, the strength development is slightly slower in the blended cement where Hadley grains appear after 15 hours, since less hydrate has been produced per gram of solid. In the ion-thinned section [Plate 5.2.10] the inner core of the anhydrous

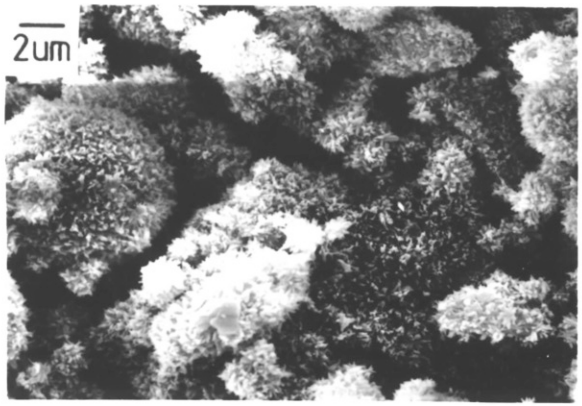

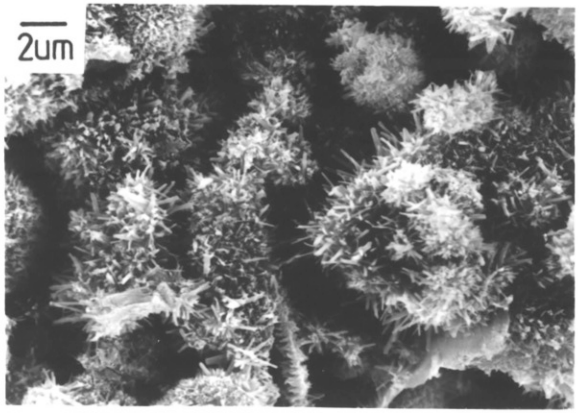

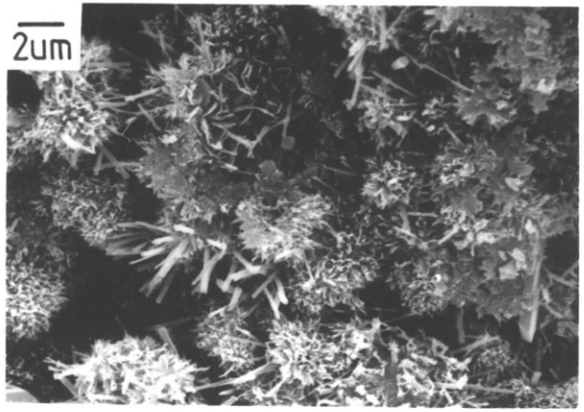

PLATE 5.2.9

The regrowth of AFt rods in OPCs

(a) 12 hr Westbury blended cement
(b) 18 hr Westbury blended cement
(c) 12 hr D/44 neat cement
(d) 18 hr D/44 neat cement
(e) 14 hr BT/Drax blended cement
(f) 30 hr BT/Drax blended cement

grain is attached to the shell at two places and the density of the hydrates in the shell is not uniform. The water in the solution may go through the less dense region to react with the core leading to an increase in the thickness and density of the shell. In the 1 day hydrated samples, various kinds of Hadley grains can be seen on the fracture surface. Some of these are only hollow shells as the original grains have been completely hydrated, while others contain a hydrating core [Plate 5.2.11-13]. Plate 5.2.11 shows a Hadley grain 20 μm across with remnants of a core. There is a large space between the shell, which consists of long AFt rods and type I C-S-H, and the core, which is believed to be due to the early dissolution of C_3A from the latter [Pratt and Ghose, 1983]. In addition a few AFm platelets can be seen on the inner surface of the shell (lower right hand corner). Most of the small cement grains (less than 5 μm) are completely reacted leaving behind a hollow shell as shown in Plate 5.2.12 but, occasionally leaving a belite particle which reacts slower than the other cement phases. It is very common to see small AFm platelets in the inner wall of the shells indicating that the sulphate concentration is low in those regions. Actually these platelets have only been found inside the hollow shell, consistent with the observation of Scrivener [1984] who suggested that the shell isolates the inside environment from the solution and that the sulphate trapped inside the shell is rapidly consumed to form AFt which then reacts with C_3A or C_4AF to produce AFm. Plate 5.2.13 shows a complex hydrated grain whose shell wall thickness is difficult to estimate as it merges into the surrounding matrix. On the inner wall, some AFm platelets can be seen, and the shell is occupied by a skeleton structure of crystals which are believed to be C_4AF [Scrivener, 1984] with two spherical belite particles. These two phases were probably originally embedded within the C_3S.

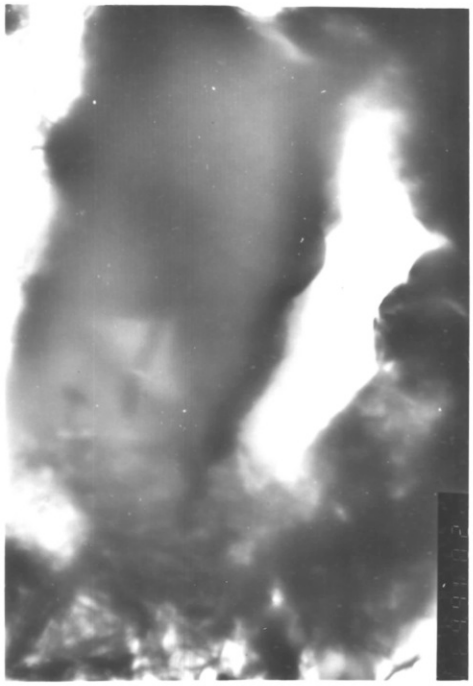

PLATE 5.2.10

Ion-thinned 48 hours D/44 blended cement paste. STEM Mag. = x20k

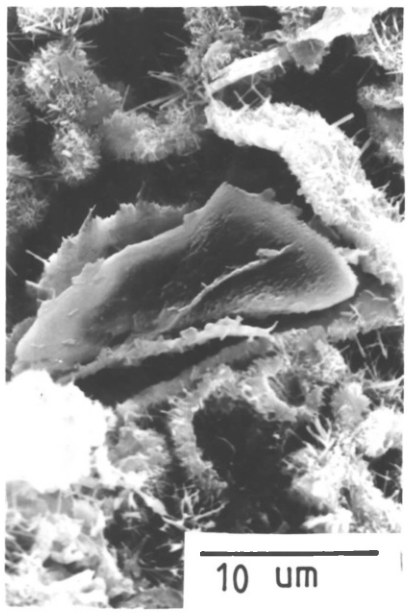

PLATE 5.2.11

Hadley grain in 1 day old BT/Drax blended cement

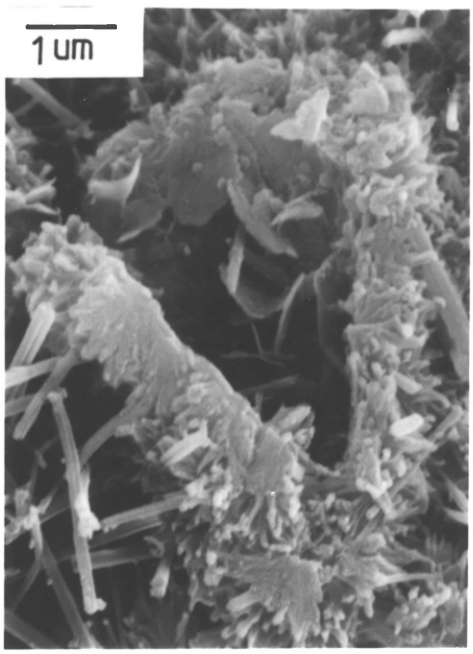

PLATE 5.2.12

Hollow shell in 1 day hydrated D/44 cement

PLATE 5.2.13

Hadley grain in 1 day hydrated D/44 cement

There is a dramatic change in Westbury blended cement after 1 day hydration, when many large hexagonal plates are formed [Plate 5.2.14]. Although these plates are also seen in the other cements, except BT cement mixtures, they are only found in very small amounts. The exact composition of these plates is not very clear, but their appearance coincides with the time when the AFm peak occurs in DTA and X-ray results, indicating that they probably consist of an AFm phase. However, the formation of this phase does not seem to be correlated to any of the peaks in the calorimetry curve.

After 1 day, most of the C-S-H appears in a "honeycomb morphology" especially in D44 [Berger et.al., 1979] or "Diamond type II" [Plate 5.2.15]. This structure can be clearly observed in the ion thinned sample [Plate 5.2.16] which shows that the outer edge of the C-S-H layer has a fibrillar morphology, whereas the inner C-S-H gel displays a honeycomb morphology which grows outwards linking the fibres together. This gives better binding between the hydrates on the grain surface and also acts as a bridge to bind the grains together [Williamson, 1972].

The CH hexagonal plates, formed in the early stages, gradually become more massive, lose their hexagonal outline, and grow into large blocks which fracture on parallel planes with smooth featureless surfaces [Plate 5.2.17].

Microstructure development after 2 days hydration

After 2 days hydration, small AFm platelets can be seen more frequently, because of the increase in the number of broken hollow shells. They are often found together with many small spheres of submicron size [Plate 5.2.18]. Occasionally, these spheres appear on their own. The composition of these spheres is not known, but they

PLATE 5.2.14

Fracture surface of 2 days old Westbury blended cement

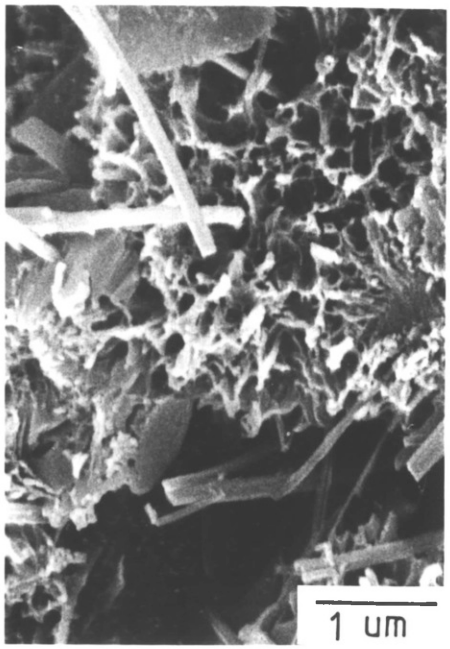

PLATE 5.2.15

Type II C-S-H morphology

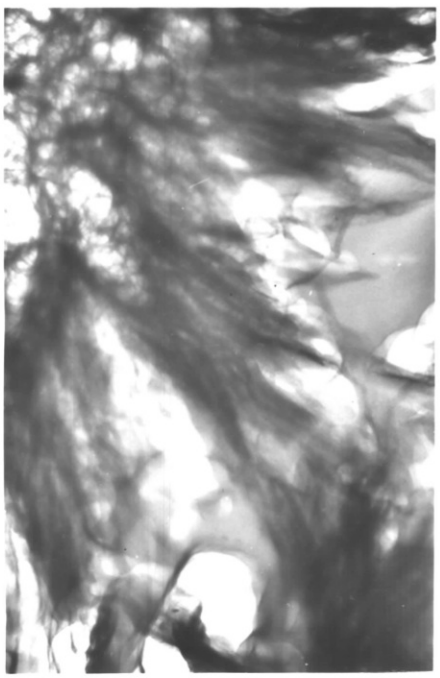

PLATE 5.2.16

Ion-thinned 48 hours D/44 cement paste. STEM
Mag. = x66k

PLATE 5.2.17

CH crystal in 2 days old cement paste (D/44)

often present together with the AFm platelets inside the hollow shells. Some kind of AFm solid solution or carbonated AFm phase is indicated.

On the other hand, the number of AFt rods gradually decreases with age after 2 days hydration, except in Westbury blended cement where the decrease starts when the hexagonal plates are formed (∿30 hours) suggesting that there is a transformation process between these two phases. In the other systems only a few large hexagonal plates have been formed so that most of the AFt has probably been buried by other hydrates becoming difficult to observe. AFt rods are still present even up to 90 days hydration in all of the samples examined, but only in the porous area [Plate 5.2.19].

In the month old samples, only a few Hadley grains, which still contain a hydrating core, can be seen. Plate 5.2.20 shows a heavily hydrated grain surrounded by a rim of hydrate about 1.5 μm thick. The inside wall of the shell and the surface of the core is fully covered by AFm crystals implying that the core consists mainly of interstitial phase, consistent with the observation of a thin shell wall. There are still many AFt rods around the Hadley grains, implying that there is no interstitial phase to react with AFt to form AFm and so suggesting that the shell wall has isolated the inside environment from the bulk. Plate 5.2.21 shows another type of Hadley grain which consists of a thick shell (10 μm) and a small, thoroughly disintegrated core which is probably a belite particle judging by its spherical shape. The original cement grain may have contained a high concentration of C_3S producing a dense "inner" product and so thickening the shell wall. This "inner" product shrinks faster than the "outer" fibrous hydrates during drying, leaving a gap between them along which the fracture is likely to take place. Hence some of the

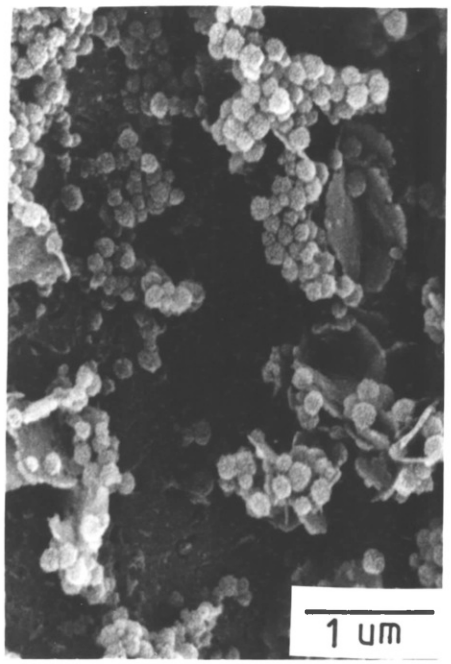

PLATE 5.2.18

AFm phase after 3 days hydration

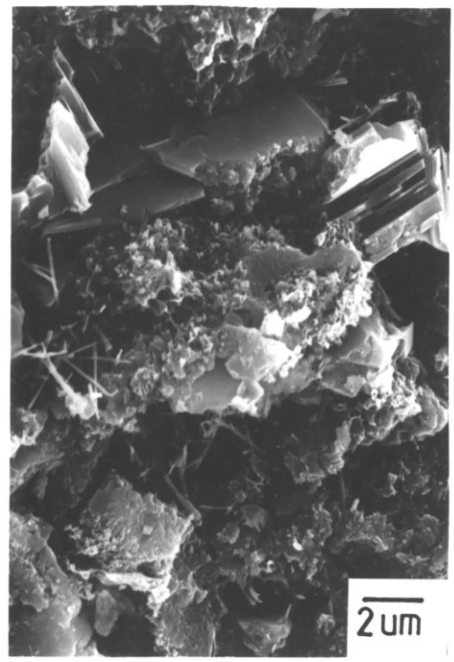

PLATE 5.2.19

Fracture surface of cement paste (Westbury) after 90 days hydration

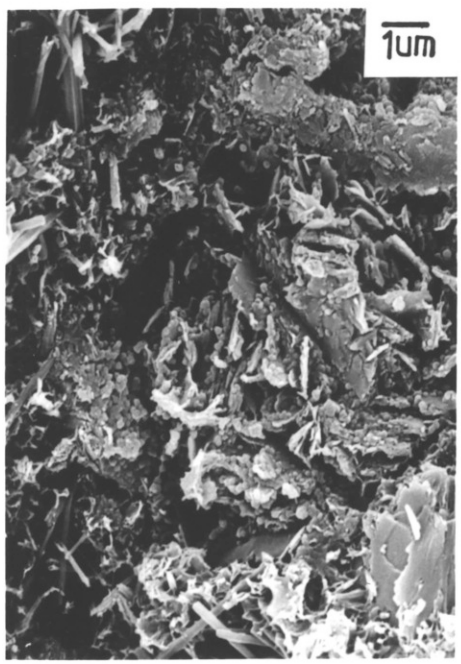

PLATE 5.2.20

Hadley grain in 1 month old D/44 cement

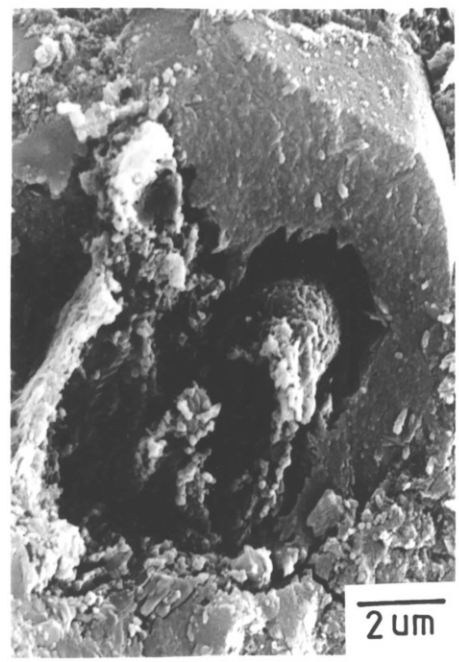

PLATE 5.2.21

Hadley grain in 2 months old D/44 cement

Hadley grians, which are surrounded by a thick hydrate wall, appear to take up the morphology of the original particle [Pratt and Ghose, 1983].

With increasing hydration times, the structure is made more compact following the growth of hydates, especially C-S-H and CH [Plate 5.2.22]. The inner product of C-S-H grows inwards to form a thick shell wall around some of the cement grains. The water space is mainly filled with large blocks of CH and the earlier fibrous hydrates (type I or II C-S-H and AFt) which interlock each other, and with some large plates of AFm. In the fly ash cement, the amount of fly ash in the 90 days sample is less than at 7 days, as some of the particles have been consumed by the pozzolanic reaction. However, the decrease in CH, another effect caused by the pozzolanic reaction, is not easily noticed on the fracture surface, but is more easily studied on the back scattered image (BEI).

Plate 5.2.23 shows the back scattered images of polished neat and blended cement paste after 7 and 90 days hydration. The CH can be identified as light grey regions. The anhydrous cement grains, and fly ash with a high concentration of iron, appear as white; if the contrast and brightness are suitably adjusted, the various phases present in the anhydrous grains can be observed.

After 7 days hydartion, most of the anhydrous cement grains are surrounded by a thin non-uniform layer of hydrate, which increases in thickness with hydration time; at 90 days, some grains have been completely replaced by the hydrates (e.g. the grain indicated in Plate 5.2.23(c)). The difference in the amount of CH between the two 7 day cement pastes and the two blended cements is very difficult to judge quantitatively, but there is a noticeable increase in the neat cements and much more CH in the neat cement than in the blended cement

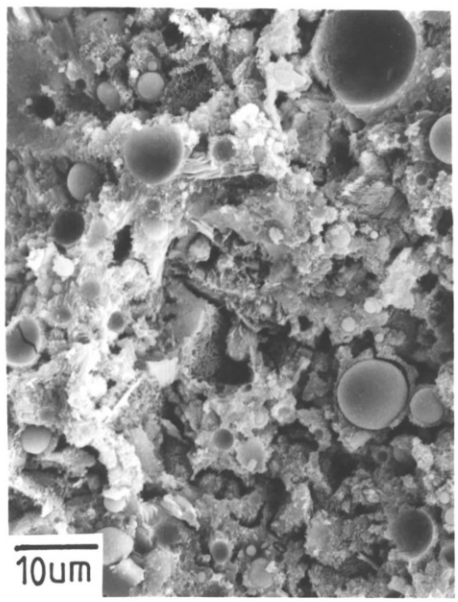

(a)

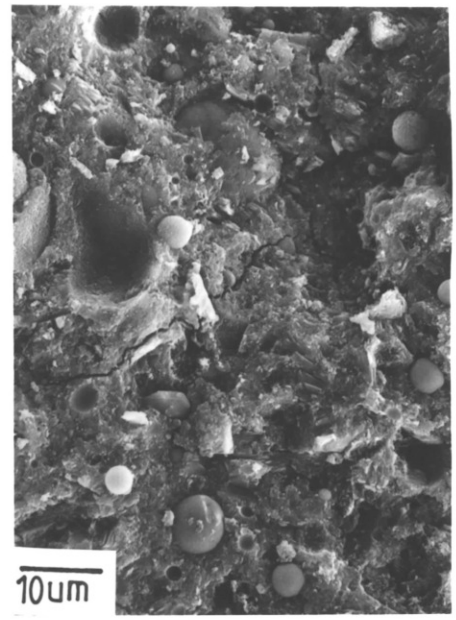

(b)

(c)

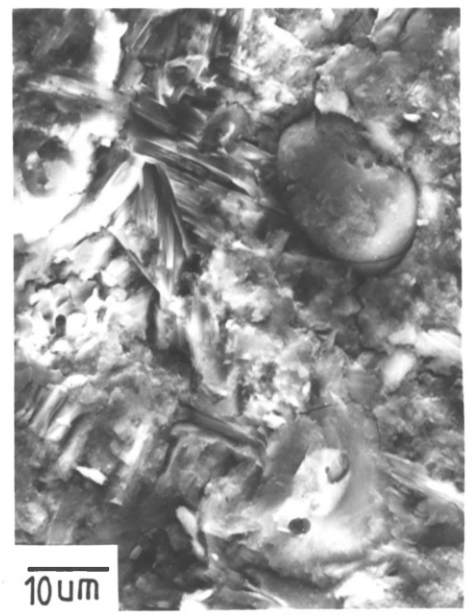

(d)

PLATE 5.2.22

Fracture surface of neat and blended cement (D/44)

(a) 7 days blended cement
(b) 90 days blended cement
(c) 7 days neat cement
(d) 90 days neat cement

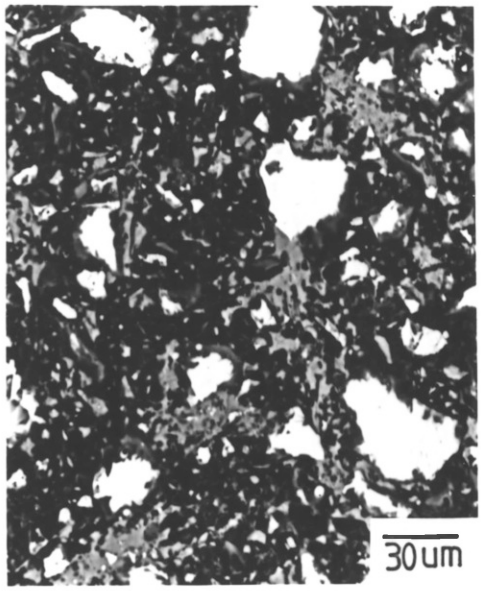

(a)

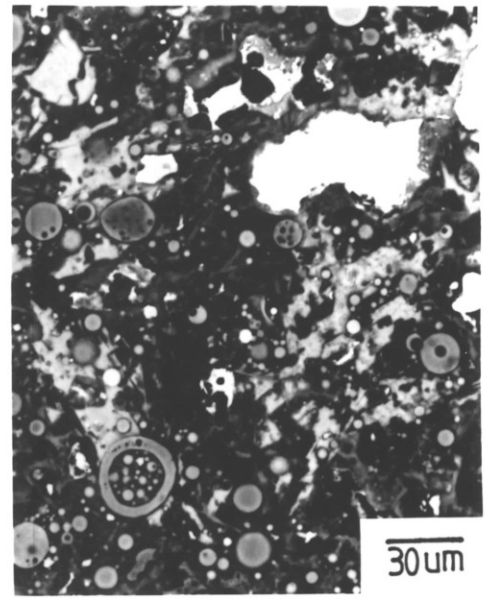

(b)

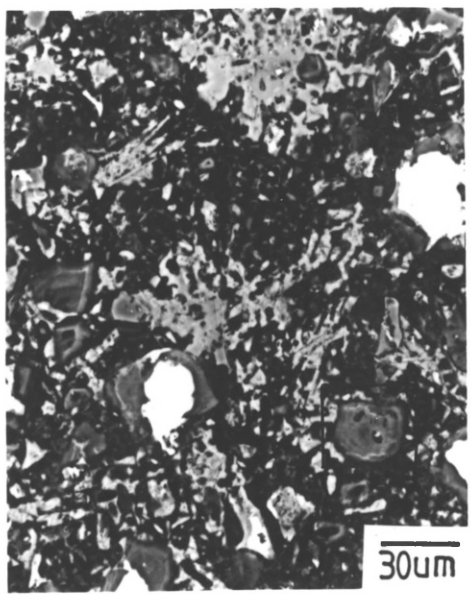

(c)

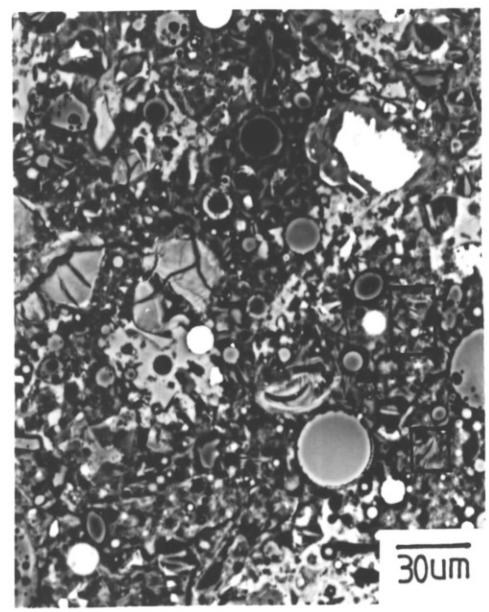

(d)

PLATE 5.2.23

BEIs of polished neat and blended cement (D/44)

(a) 7 days neat cement
(b) 7 days blended cement
(c) 90 days neat cement
(d) 90 days blended cement

at 90 days. The change in total area of the fly ash is also difficult to judge by direct observation. A quantitative image analysis should provide more information on these questions.

The radiating fibrous C-S-H rims, which form around the fly ashes through the pozzolanic reaction, are not easy to observe at the low magnification used for the 90 days old sample, since they are only about 1 μm thick, as indicated by the fracture surface [Section 5.2.I]. After 6 months [Plate 5.2.24(a)], these rims show up more clearly and in fact surround many of the fly ash particles, but not those of high iron content which still have a very sharp edge since they have little or no glassy phase to react with CH.

In the month old fly ash cements, a new microstructure was found, appearing in bands on the polished surface (e.g. some of them marked by the square in Plate 5.2.23(d) and 5.2.24(a)), suggesting that they may be lamellar. The microstructure may be the same as that on the left hand side of Plate 5.2.24(b), which shows a 90 day old blended cement fracture surface. The quantitative analysis by EDXA shows that this microstructure contains Al, S, Si and Ca, suggesting an AFm phase which is also a product of the reaction between fly ash and CH, as the Al and S from the p.f.a. diffuse through the low density C-S-H rim to react with CH in the matrix.

5.2.H *MICROSTRUCTURE DEVELOPMENT OF THE HYDRATES IN THE WHITE CEMENTS AND BLENDED CEMENTS*

AW neat and blended cement

Plate 5.2.25 shows the fracture surface of the neat and blended hydrated cement at different hydration times. In the 3 hour samples [Plate 5.2.25(a)) the amount of AFt rods on the particle surface is much less than that in OPC's, probably due to the low content of C_3A

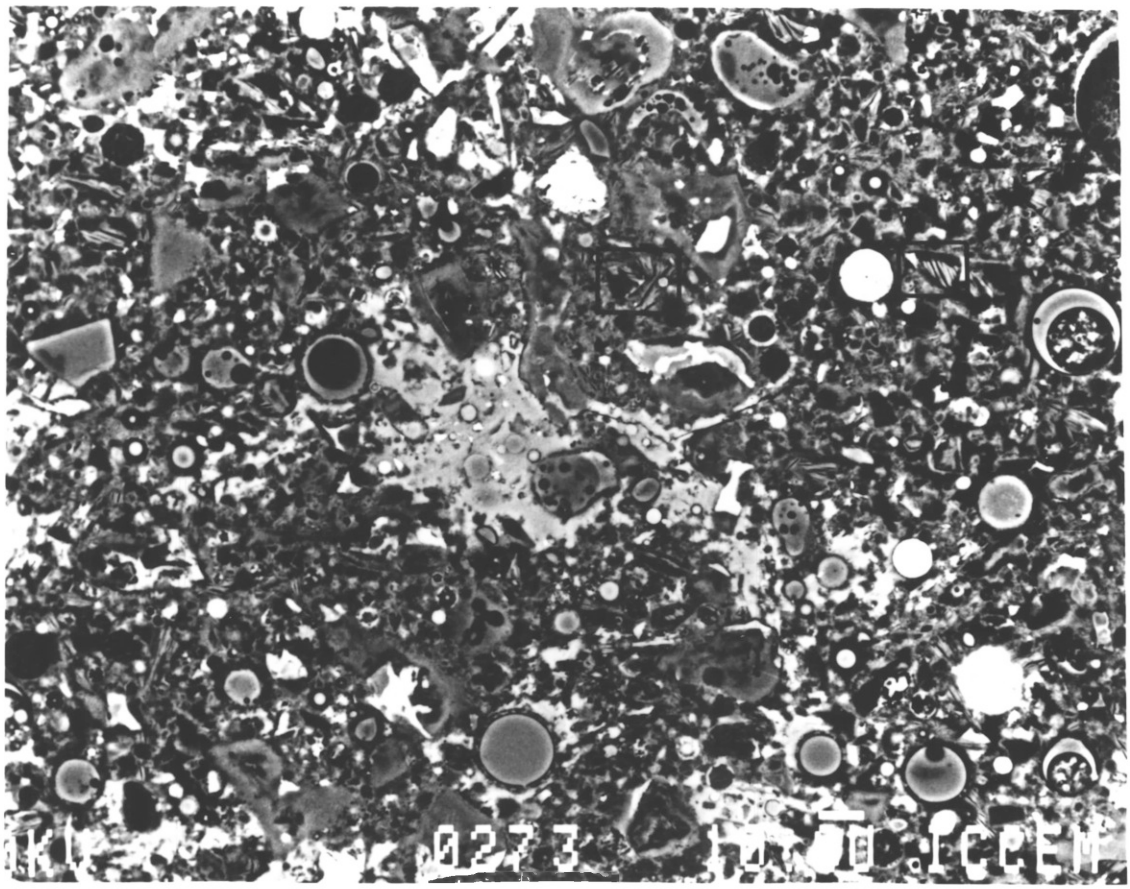

PLATE 5.2.24(a)

BEI of polished 6 months old D/44 blended cement

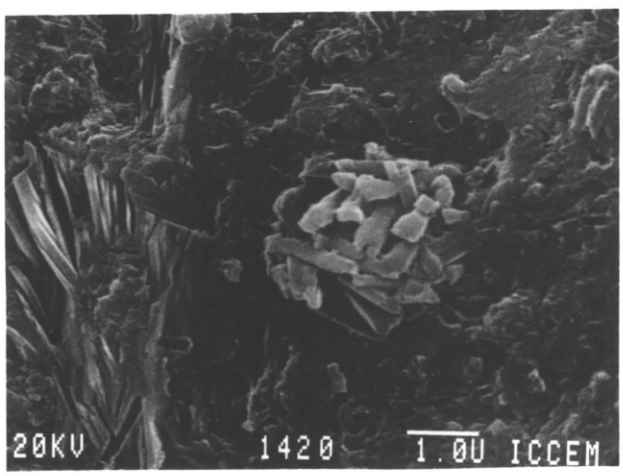

PLATE 5.2.24(b)

Fracture surface of 3 months old D/44 blended cement

in this cement. This may also be caused by a higher concentration of CH in the solution in the first few hours of hydration as there is much more C_3S present in AW cement. This can reduce the solubility of gypsum. There is no C-S-H on the particle surface in the fly ash cement because of the long delay in the initiation of C_3S hydration, as shown by the calorimetry curve [Fig.5]. A drastic change occurs in the microstructure of the neat cement at 6 hours [Plate 5.2.25(b)], when many large hexagonal plates appear, which have not been seen in any of the other cements. Both the X-ray analysis and DTA show no sign of AFm or calcium aluminate hydrates (e.g. C_3AH_8 or C_4AH_{19}), suggesting that these plates are more likely to be CH crystals. The environment in the solution may affect the growth of CH crystals. The amount of these thin CH plates starts to decrease after 12 hours, when they begin to grow into large blocks. However, this effect does not appear in the blended cement. By comparing the chemical compositions of this cement to the others [Table 3.1.1], the amount of alumina and total alkali oxide is lower in the former. The system which has less alkali oxide should have a relatively lower PH solution. This decreases the probability of AlO_2^{1-} in the solution forming $Al(OH)_3$ colloidal gel. Hence more AlO_2^{1-} is free and may be absorbed onto the $Ca(OH)_2$ (0001) plane by the cation Ca^{2+}, preventing the growth in this direction. At the later time, the aluminate ions may be removed to form calcium aluminate hydrate (AFt), allowing CH to grow freely again.

By adding the fly ash, the alkali, dissolving from the ash raises the PH value in the solution preventing the poisoning discussed above.

The secondary growth of AFt rods has been observed in the 12 hours neat cement, that is just after peak 3. By contrast, the corresponding fly ash cement, which is at the shoulder of peak 3, shows no sign of

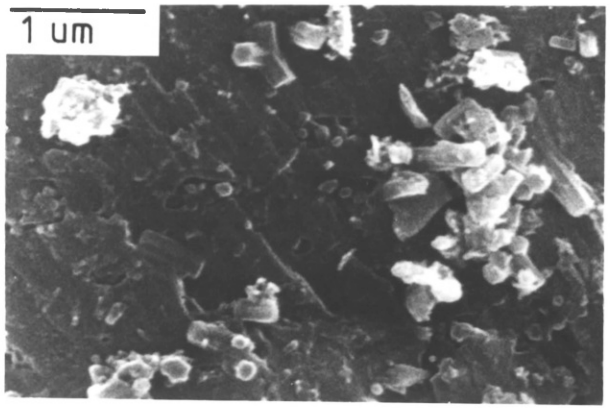

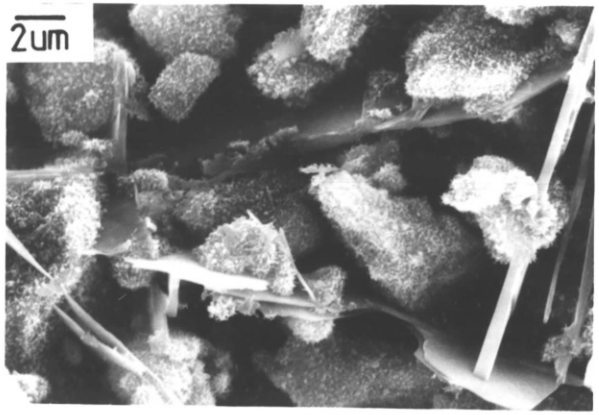

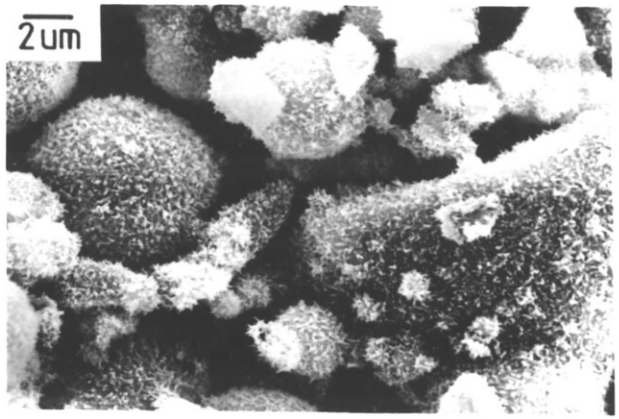

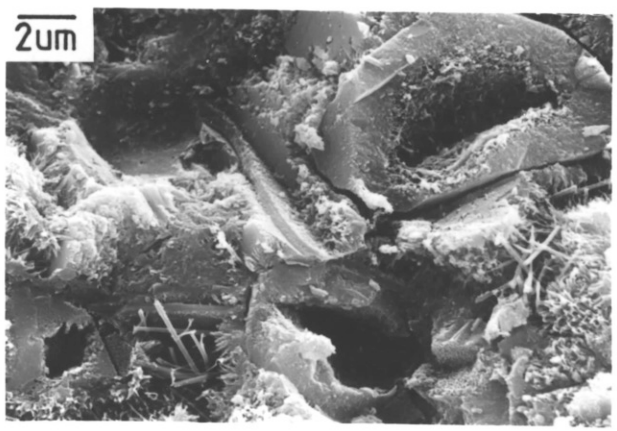

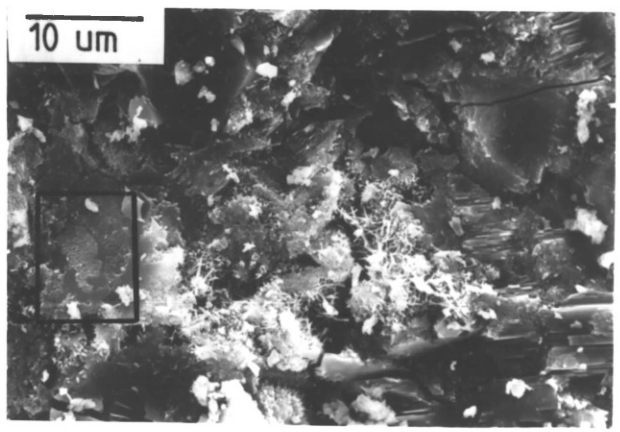

PLATE 5.2.25

Fracture surface of AW neat and blended cement

(a) Cement grain in 3 hr old neat cement paste

(b) 6 hr hydrated neat cement paste

(c) 12 hr hydrated blended cement paste

(d) AFt rods in 18 hr old blended cement

(e) Hollow shells in 2 day old neat cement

(f) 3 month old neat cement paste

the regrowth of AFt rods [Plate 5.2.25(c)]. Instead AFt starts to emerge through the hydrate layer by 18 hours [Plate 5.2.25(d)], after the peak 3, and grows significantly between 18 and 24 hours. This indicates that the addition of fly ash has retarded the secondary growth of AFt rods. However, no obvious explanation for the cause of the shoulder, just before peak 3, is suggested by the microstructure.

The X-ray results indicate that the gypsum in both mixtures is consumed between 6 and 12 hours, coinciding with the secondary growth of AFt rods in the neat cement. This seems to suggest that the reserved C_3A hydration in the fly ash cement may also occur within this period corresponding to the shoulder of peak 3. However, this does not necessarily mean that the shoulder is caused by the renewed C_3A hydration since peak 3 could start from 6 hours and gradually take up the gypsum to form short AFt rods which might be covered by the dense C-S-H. As the time goes on, the concentrations of sulphate and Ch in solution decrease and this induces the formation of long fibrillar AFt rods. The X-ray results also show that no AFm is present between 6 hours and 1 day; actually they have never been detected in all the examined samples. Unfortunately, there is no clear explanation for the formation of a shoulder before peak 3 in fly ash cement, and further work has been necessary such as using back scattered image to observe the distribution of C_3A phase or quantitative X-ray analysis in the consumption of C_3S and C_3A phases.

Coincident together with the growth of AFt rods is the appearance of Hadley grains most of which are still occupied by the hydrating cement grains. Inside some of the hollow shell walls, AFm platelets are observed, but the X-ray results show no evidence for the existence of AFm in any hydrated sample. This is probably due to the amount of AFm in the sample being below the threshold of the X-ray diffractometer

(3-4%). However, these results do not provide enough evidence for the broad shoulder of peak 3 in the neat cement to correspond to the formation of AFm. Another possibility is that the shoulder is caused by further change of chemistry in the solution, encouraging further growth of AFt.

In the 2 days sample [Plate 5.2.25(e)], there are many separated hollow shells, which have a thick shell wall, indicating that the core of these Hadley grains contained a large amount of C_3S. Their microstructure is not often seen in the OPC cements (and if so, only after 7 days hydration) since they contain less C_3S, and the C_3S hydration rate is slower than in AW as shown in the TG results. The boundary between the shell, consisting mostly of "inner" product, and the "outer" fibrous hydrates can be identified and indicates the original grain size. A gap is formed along this boundary as the "inner" products shrank much faster during the drying.

After 3 months hydration [Plate 5.2.25(f)] some cement grains are completely hydrated and replaced by the "inner" product which has created a pseudomorph of the original grains (for instance that marked by the square). This morphology has also been seen in well cured C_3S paste [Williamson, 1972]. Although the amount of AFt decreases with hydration time, there is still more present at 3 months than in the other cements, as expected, because only a very small fraction has been converted to monosulphate. There is enough sulphate to react with all the C_3A to form ettringite. Also the reaction probably is completed at early ages before the hydrate shell becomes sufficiently dense to prevent aluminate ions passing through. Therefore, less monosulphate forms inside the Hadley grains consistent with the finding discussed above.

BW neat and blended cement

Plate 5.2.26 shows the microstructure of the neat and blended cements at various stages of hydration. During the first few hours of hydration a very small number of AFt rods can be observed, and the size of the rods is very small [Fig. 5.2.26(a)]. In addition there are many large secondary gypsum crystals and this is rather unexpected for the C_3A content of 5.5% is similar to that in D/44 and BT OPCs. After 3 hours, the particles in both mixtures are gradually covered by type I C-S-H and become very similar to those of the OPCs.

There is no significant change in microstructure between 12 and 24 hours in the neat cement when the particles are fully covered by C-S-H. At 30 hours [Plate 5.2.26(b)], the secondary growth of AFt rods has started; this is much later than in any of the other cements examined, corresponding to the delay of peak 3 [Section 5.2.D]. In 2 day old neat cement [Plate 5.2.26(c)], after peak 4, large numbers of hexagonal plates have formed, and are very similar to those in Westbury blended cement. In the areas containing large amounts of these pastes, the number of AFt rods seems to be less, in fact sometimes none can be observed, agreeing with the observation of Scrivener [1984]. In other areas there are still plenty of long AFt rods.

In the fly ash cement, the secondary growth of AFt rods and the appearance of hexagonal plates occur after 1 day's hydration [Plate 5.2.26(d)], after peaks 3 and 4, which are very close to each other as shown in the calorimetry curve. The amount of the hexagonal plates increases with hydration time, and the number of AFt rods decreases [Plate 5.2.26(e)].

These observations confirm that peaks 3 and 4 in both cements are associated with the same two reactions, and that these are advanced by the addition of fly ash.

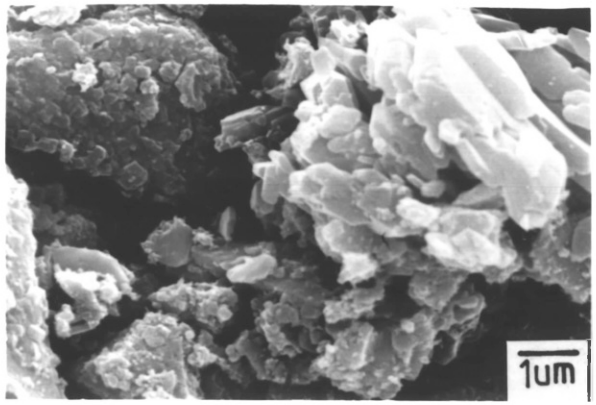

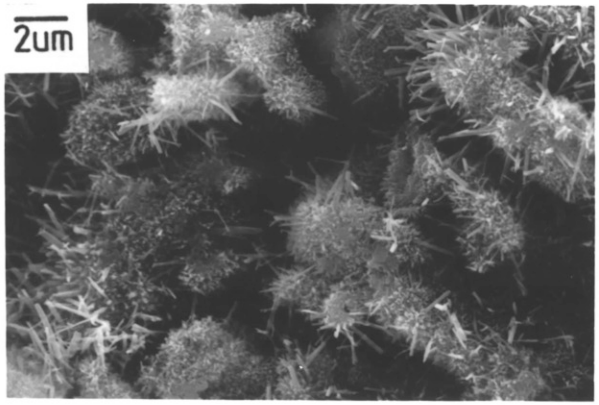

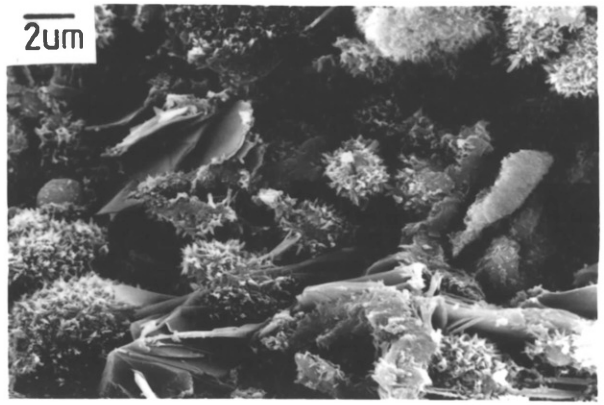

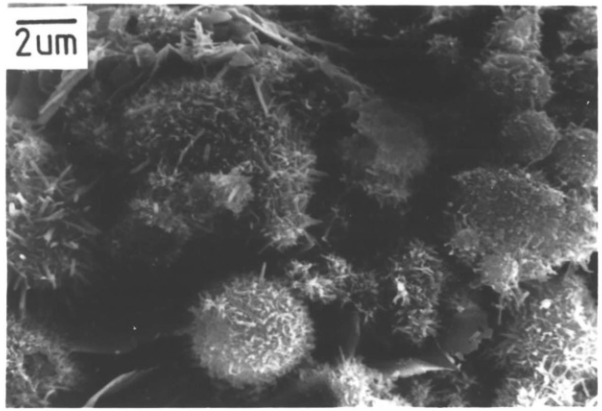

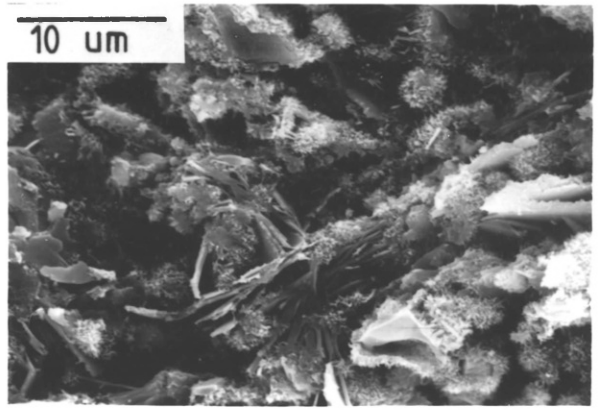

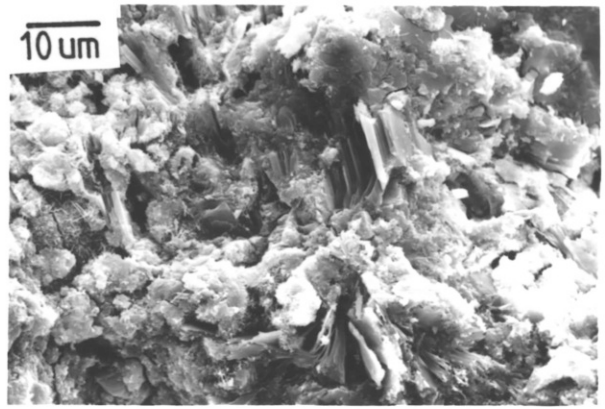

PLATE 5.2.26

Fracture surface of BW neat and blended cement

(a) 3 hr old neat cement paste

(b) AFt rods in 30 hr hydrated neat cement paste

(c) AFm plates in 2 day old cement

(d) AFt rods and AFm plates in 1 day old blended cement

(e) AFm plates in 36 hr hydrated blended cement paste

(f) 6 month old neat cement paste

The number of Hadley grains present in both these cements is much smaller than in the others, and there are no small AFm platelets to be seen inside the shells. In fact the platelets have never been found in these two cements.

The formation of the hexagonal plates is coincident with the appearance of the AFm peak in the X-ray analysis of both cements, indicating that the plates are AFm phase and that peak 4 corresponds to the formation of this phase in this cement.

In the later stages [Plate 5.2.26(f)], the structures become more compact as the large CH crystals infill the original water space, and the AFm plates grow parallel to each other, similar to the growth of CH, becoming blocks filling the porous area. On the other hand, the number of AFt rods can be observed to gradually decrease with hydration time and they have almost disappeared from both cements by 63 days. This is partially due to the transformation to AFm phase, and partially to the AFt rods being gradually covered by the growth of other hydrates as suggested by the observation that AFt can still be detected in the wet samples after 6 months by X-ray analysis.

5.2.I *THE MICROSTRUCTURE ON THE FLY ASH SURFACE AFTER ONE DAY HYDRATION*

The major change on the fly ash surface after 1 day is that the microstructure of the crystalline phase is revealed, following dissolution of the glass, caused mainly by the pozzolanic reaction between it and the calcium hydroxide in the bulk. The rate of glass dissolution varies from sphere to sphere. In all the examined fly ash samples, most of the crystalline phase has been revealed by 28 days hydration, the rate of dissolution seeming not to be affected by the choice of cement and fly ash.

At 2 days old [Plate 5.2.27], some of the hydrates on the fly ash surface are removed during fracture, leaving behind small fragments. In some cases, there is complete removal revealing a slightly etched surface. The removal of the hydrates is probably correlated to the dissolution of the glass phase of the fly ash which leads to voids forming between hydrates and the surface of the fly ash surface, as shown in the ion thinned sample [Plate 5.2.28]. At this stage voids only appear in some places, not completely around the ash. Ogawa et. al. [1980] suggested that the formation of these gaps has a close relation to the alkalies dissolving from fly ash. The incomplete removal is probably due to the lower dissolution in these regions so the hydrates are still fairly strongly bonded on the surface. On the other hand, the increase of bonding between the hydrates can lead the matrix to carry some of the surface hydrates with it during fracture.

After 5 days [Plate 5.2.29], the surfaces of most ash particles in the fracture surface are exposed, showing no trace of hydrates. Under high magnification it can be seen that most of the surface has been etched. The fly ash voids present are fairly smooth, indicating that the pozzolanic products have not been formed. This kind of microstructure has also been seen by Grutzeck et.al. [1981] in high lime fly ash blended cement pastes after 3 days hydration.

By 14 days [Plate 5.2.30] the crystalline phases in the fly ash can be clearly seen, and the voids are no longer smooth. Now most of the voids are filled with C-S-H honeycomb and some are covered with small hexagonal platelets, probably an AFm phase. Both of these are formed from the pozzolanic reaction between the silica and alumina in the glassy phase of the fly ash and the CH in the paste.

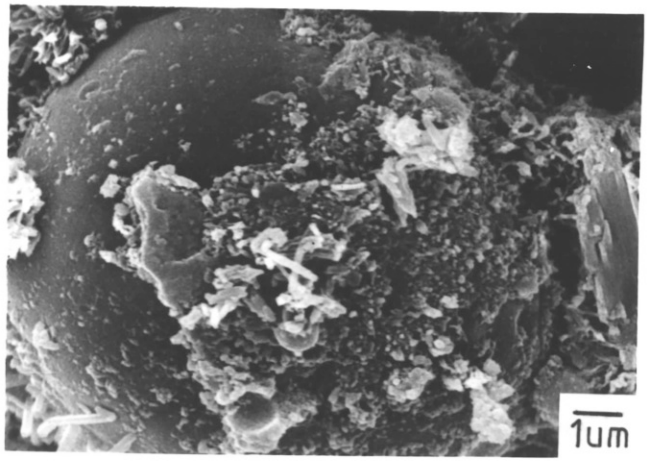

PLATE 5.2.27

Fly ash surface after 2 days hydration

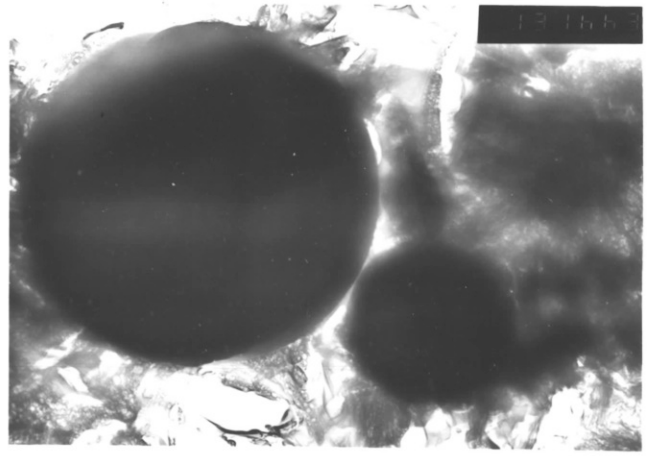

PLATE 5.2.28

Ion thinned 2 days old blended cement (D/44)
Mag. = x13k

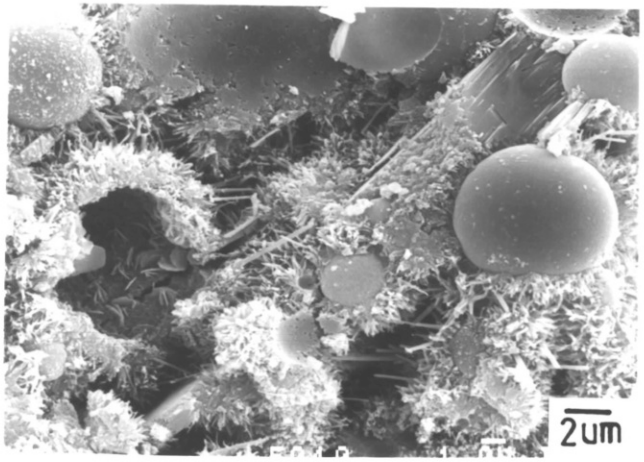

PLATE 5.2.29

Fly ashes after 5 days hydration (Westbury)

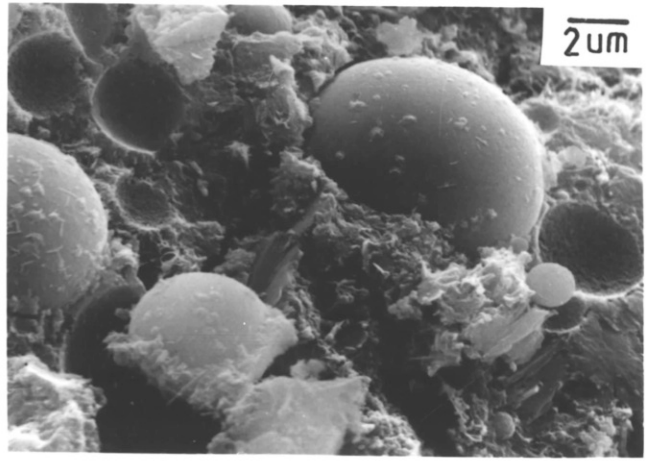

PLATE 5.2.30

Fly ash and void in 14 days old blended paste (D/44)

Plate 5.2.31 shows some crack paths in the hardened paste, which preferably go around the fly ash surface, separating it from the pozzolanic products. This indicates that the bonding between the fly ash surface and the products is weaker than that of the latter and the paste matrix at this time. Sometimes a space can be observed around the fly ash. This may be caused by dissolution of glass layer or an artifact breakage during drying.

After 28 days [Plate 5.2.32] the crystalline phases, such as mullite, protrude from the ash surface as more glass reacts. In many cases the glass is replaced by radiating bundles of fibrous C-S-H material, which in cross-section have a honeycomb morphology as the background structure in the hole at the top of the photograph. For example, the large sphere in the lower right hand corner has a rim of C-S-H which also indicates that this fly ash contains a higher proportion of glass phase than the others in the photograph. The C-S-H rim is strongly bonded to the surrounding cement matrix, and also to the fly ash surface as most of the time there is no gap between the rim and surface. Although parting occasionally does occur around the fly ash, this is possibly due to separation during the preparation of the specimen.

The voids are typically filled with honeycomb C-S-H as mentioned above, but sometimes there is another microstructure which has been seen inside the voids [Plate 5.2.33]. This is dominated by the doughnut shaped rings of material with small hexagonal platelets. The wall of C-S-H around the sphere is very thin, implying that this fly ash contains a high concentration of Al in the glass phase and not silica. Therefore the hexagonal platelet probably is AFm phase. However, the composition of these doughnut shaped materials is not known and neither is their formation.

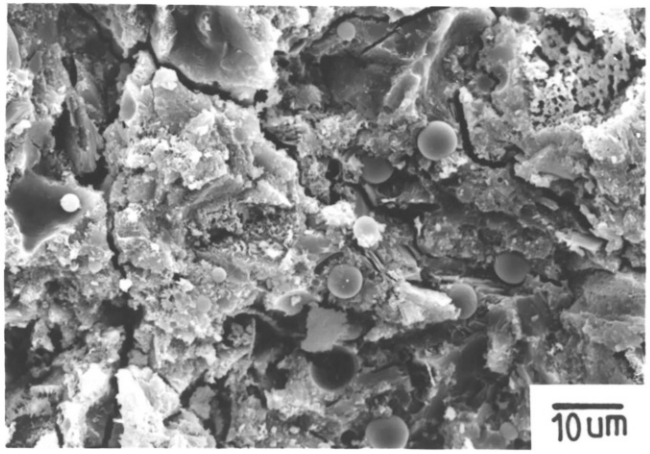

PLATE 5.2.31

Fracture surface after 28 days hydration (Westbury blended cement)

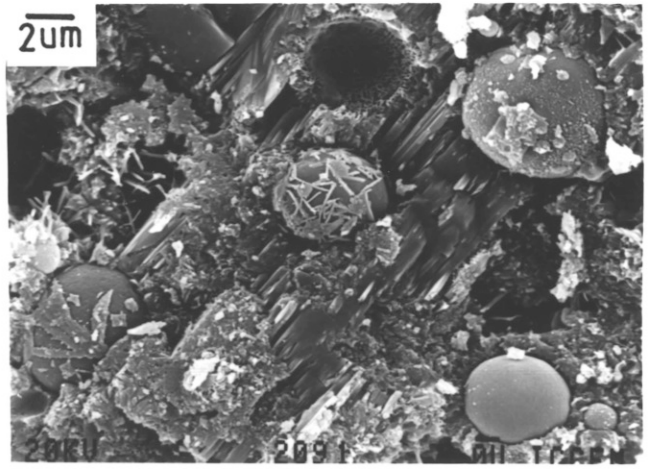

PLATE 5.2.32

Fly ash after 28 days hydration (AW)

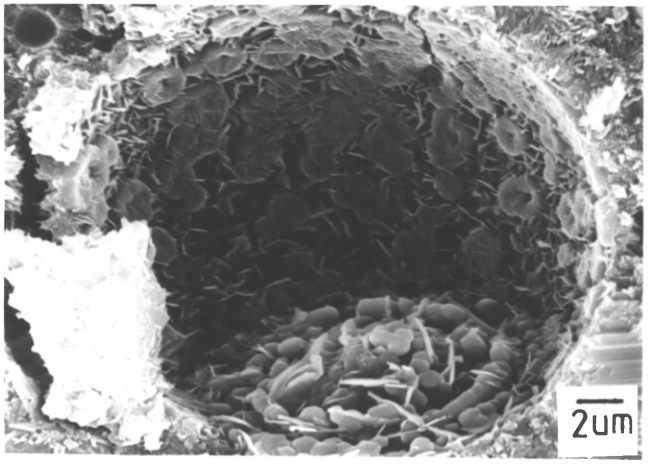

PLATE 5.2.33

Microstructure inside the void (D/44)

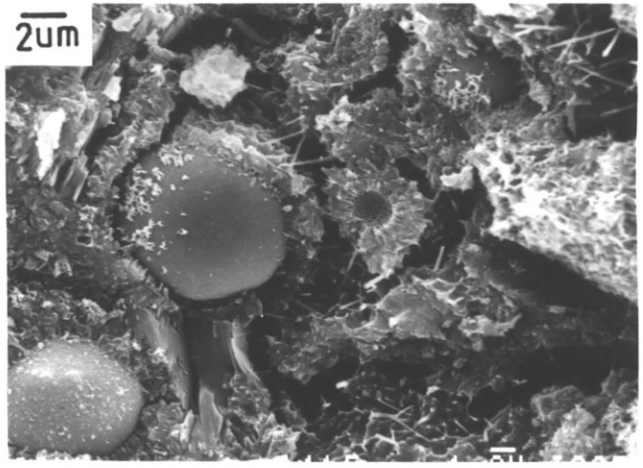

PLATE 5.2.34

Fly ash after 2 months hydration (D/44)

The C-S-H produced by the pozzolanic reaction has a higher permeability than that produced by the hydration of silicate phases in the cement [Grutzeck et.al., 1981 and Mehta, 1983] so ions can travel freely to and from the surface of the ash to continue the reaction. Therefore, in the month old samples [Plate 5.2.34], thicker rims of C-S-H are observed. The boundary between the fibrous C-S-H and the cement hydrates can be clearly recognised and indicates the size of the original fly ash. On the other hand, some spheres still do not have a rim of C-S-H, implying that they are probably composed entirely of crystalline phases.

CHAPTER 6

HYDRATION OF CEMENT AND FLY ASH CEMENT AT 40 °C

6.1 REVIEW OF PREVIOUS WORK

6.1.A *HYDRATION OF CEMENT*

An increase in the hydration temperature can cause the shortening of the induction period, whilst the second heat peak, corresponding to the hydration of C_3S, is sharper and more intense. The third peak, C_3A hydration, is also advanced and enhanced as shown in the claorimetry curve [Killoh, 1980]. Later, when the hydration becomes diffusion-controlled, the rate of hydration is diminished and probably arises from a dense layer of C-S-H surrounding the cement grains caused by accelerated ageing [Bentur et al., 1979].

There is no significant difference in the hydration products of Portland cement from room temperature up to 100 °C, though there are differences in morphology and microstructure [Taylor and Roy, 1980]. The size of CH crystlas is smaller at higher temperature because of the decrease of CH solubility with temperature [Boyer, 1976]. Odler and Skalny [1973] have found, in studying C_3S hydration at 25 - 100 °C, that the C/S ratio of C-S-H increases with temperature. However, Lach and Bures [1974] have reported that the formation of CH grew rapidly and the amount of C-S-H decreased above 80 °C. They assumed that at temperatures above 80 °C the C-S-H gel has a lower C/S ratio than those formed at lower temperatures. The maximum stability temperature of ettringite is between 100 - 110 °C, when it decomposes to monosulphate and hemihydrate at 690 - 1380 kPa pressure [Roy et al., 1977; Satava

and Veprek, 1975]. Although some workers [Barvinok et al., 1974; Lach and Bures, 1974] suggested a lower decomposition temperature, it could be that ettringite loses some water of a quasi-zeolitic type at lower temperatures whilst still retaining the basic lattice up to 110 °C [Bensted, 1983]. AFm is reported stable up to 190 °C [Satava and Veprek, 1975; Sanzhaasinen and Andreeva, 1978].

6.1.B *THE POZZOLANIC REACTION AND THE DEVELOPMENT OF STRENGTH*

The pozzolanic reaction is known to be very temperature sensitive. Takemoto and Uchikawa [1980] have studied the hydration of the pozzolana-$Ca(OH)_2$ system [40% of lime and 60% of pozzolana] at 20 °C, 40 °C and 60 °C. They found that there had not been any change in the products of the fly ash-CH system by increasing temperature, but the degree of the reaction is increased significantly from 20 °C to 40 °C, especially at early ages (before 28 days) and the decrease slows down between 40 °C and 60 °C (except in Kanto). Buttler and Walker [1982] have also found that the rate of the pozzolanic reaction increases with temperature from 30 °C to 70 °C in the fly ash-$Ca(OH)_2$ system.

In the fly ash cement, this effect is generally expressed by the changes of the compression strength at various temperatures. It has been found that the initial strength always increases with the temperature, but the long term strength is reversed, as the accelerated pozzolanic reaction contributes to strength development [Watt and Thorne, 1966; Owens and Buttler, 1980; Dalziel, 1980]. Dalziel [1980] has compared the strength of fly ash cement to that of neat cement and found that the contribution to strength made by the fly ash decreases with increasing temperature.

At temperatures above 65 °C the strength in neat and fly ash cements is almost the same.

Feldman [1981] has measured the change of porosity at various temperatures and the results are consistent with results for development of strength. The porosity of the high temperature sample is lower initially and remains constant after ∿60 days, but there is a continuous decrease in the 20 °C sample. This seems to indicate that the reactions are almost stopped at 60 days hydration, probably caused by the difficulty of the ions to diffuse through dense C-S-H layer which rapidly forms at early ages.

6.2 PRESENT WORK

Experimental Approach

D/44 cement and Fiddlers Ferry fly ash were used in this experiment. The neat and blended cement pastes were prepared in the same way as those examined at room temperature [Section 5.2]. The paste was cast in polypropylene cylindrical moulds, sealed and cured in a water bath at a temperature of 40 °C. The hydration was stopped at the appropriate times by freeze-drying. The hydrated samples were examined by SEM, X-ray analysis and thermal analysis.

For measuring the heat evolution during the hydration at 40 °C, the pastes were mixed outside the calorimeter, the same technique as used above, 10 g of neat or blended cement paste being weighed out in a polythene bag which was sealed and immediately placed inside the calorimeter in a water bath at 40 °C.

6.2.A *HEAT OF HYDRATION*

The heat output during the hydration of neat and blended cement at 40 °C is plotted against the hydration time in Fig. 6.2.1. The neat cement curve shows that there are two major exothermic reactions, peaks 2 and 3 at 3 and 4 hours respectively, followed by a rapid fall with a shoulder at about 10 hours. The effects of the fly ash on the hydration of cement are the retardation and enhancement of peaks 2 and 3. There is a small shoulder which appears before peak 3.

Comparing these curves to those obtained at 20 °C, [Fig. 5.2.2(b)], peaks 2 and 3 in both cases are advanced and enhanced by the increase of temperature, especially peak 3. Peaks 2 and 3 have been advanced by 5 and 7 hours respectively and their heights have been increased by 65% and 70%. The reaction which produces the shoulder peak in the neat cement at 40 °C should also be present at the lower temperature. However, it may occur much more slowly so producing a broad and low heat output peak which is not easily observed in the curve.

The total heat output of the neat cement after hydration time greater than 50 hours at 40 °C and 20 °C is very similar [Fig. 6.2.2(a)]. The energy evolved in the high temperature hydration increases rapidly in the first 10 hours corresponding to peaks 2 and 3 and reaches a constant value after 40 hours. In

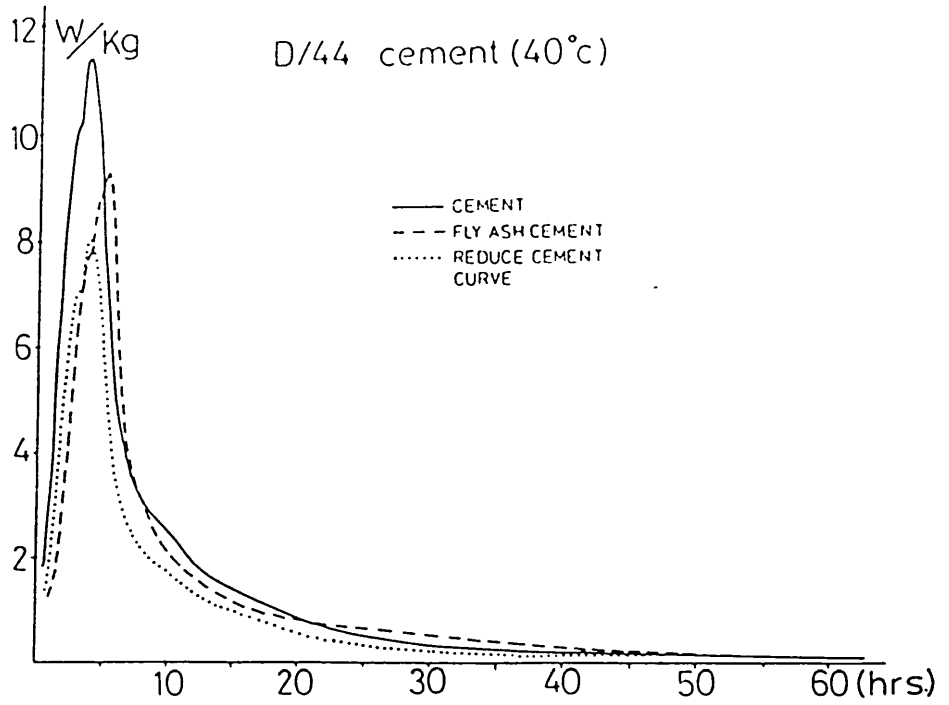

FIG. 6.2.1 Rate of heat evolution for D/44 and D/44 + Fiddlers Ferry fly ash at 40°c hydration.

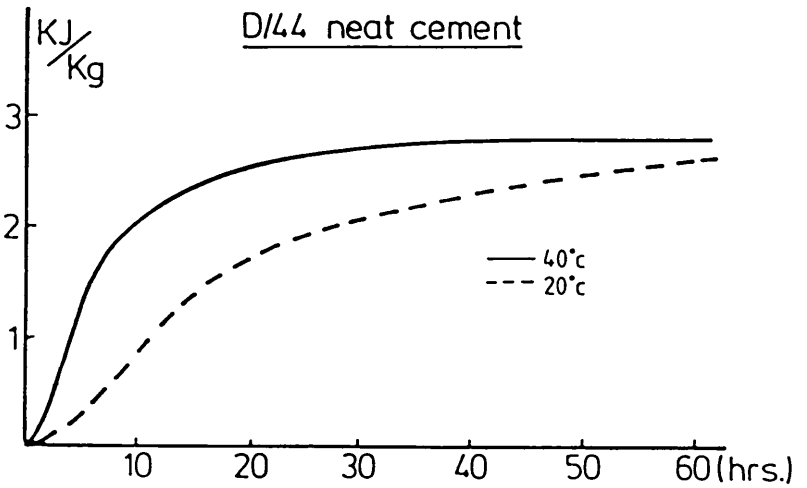

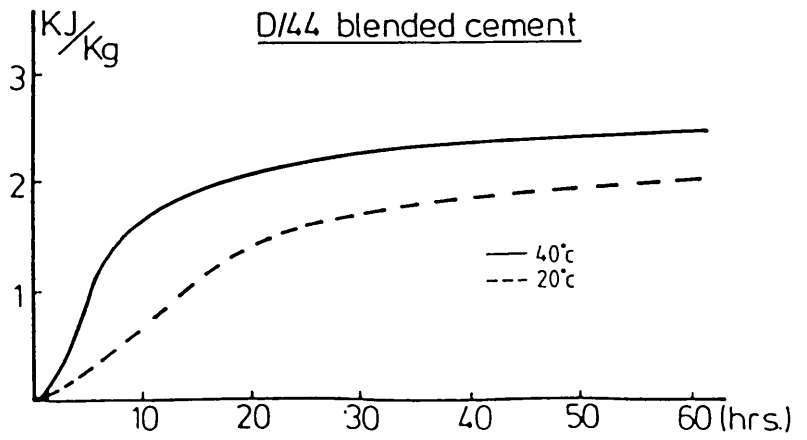

FIG. 6.2.2 Comparing the energy output of the hydration at 40°c and 20°c.

contrast, at 20 °C, the energy output of the hydration increases more slowly but continues rising, eventually reaching almost the same value. However, there is a significant difference between the total heat outputs of the blended cements at two different temperatures [Fig. 6.2.2(b)]. The higher heat output of the 40 °C sample is probably caused by the contribution from the pozzolanic reaction. Since the maximum CH content in the blend occurs at 2 days hydration [Section 6.2.B], this indicates that the reaction must takes place before this time which is well within the time of the heat measurement.

6.2.B *THE RATE OF FORMATION AND CONSUMPTION OF CH*

The hydrated samples were analysed using TG, allowing the amount of CH to be deduced [Appendix IV]. The weight of CH per ignited weight of cement at 800 °C is plotted against the hydration time in Fig. 6.2.3.

The rate of formation of CH in both neat and blended cements decreases with hydration time, and after 28 days the amount of CH in the former becomes almost constant. This is probably due to the thickness and density of the hydrate layer on the cement grain surfaces rapidly increasing at early ages, leading to a corresponding reduction in the ion duffusion rate, eventually almost stopping this process.

The amount of CH in the fly ash cement is less than that in the neat paste before 12 hours hydration as the initiation of C_3S hydration is retarded by the addition of fly ash. On the other hand, the rate of formation of CH is faster in the blend as the C_3S

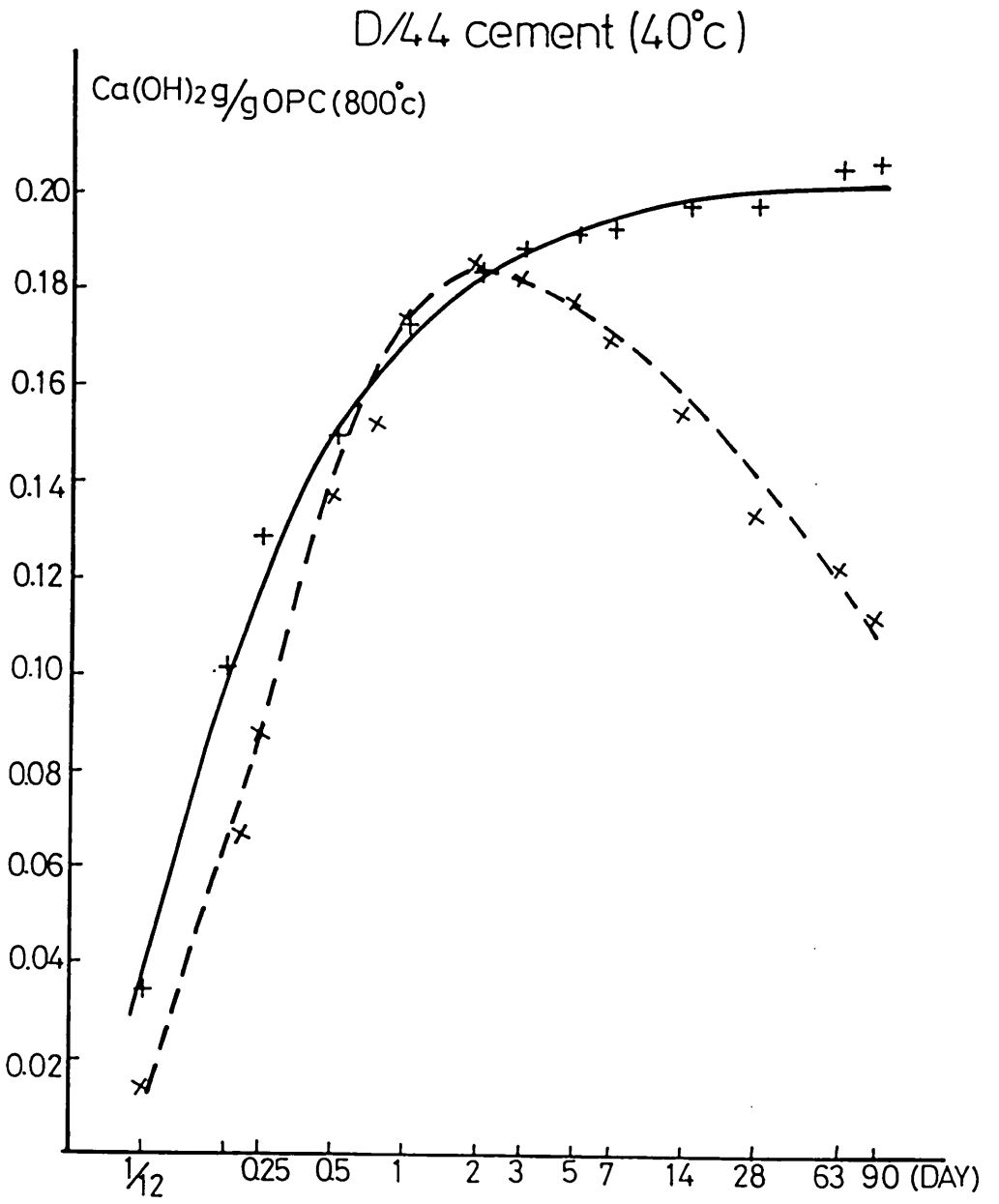

FIG. 6.2.3 Calcium hydroxide content in D/44 and D/44+Fiddlers Ferry fly ash at 40°c hydration.

hydration is accelerated. After half a day, the weight ratio is briefly enhanced by a small amount before reaching its maximum value as the consumption of CH by the pozzolanic reaction starts to exceed the production by hydration of the silicate phases.

Comparing the present results with those obtained at room temperature [Fig. 5.2.9(a)], the onset and rate of CH formation in both neat and blended cement is accelerated by the increase of temperature, as also indicated by the calorimetry results [Section 6.2.A]. However, this rate decreases much more rapidly in the neat high temperature sample due to the faster build up of the hydrate layer, as described above, and after 28 days the amount of CH in the low temperature sample becomes greater.

In the high temperature fly ash cement, the rate of CH formation is always faster than that of the low temperature cement until the maximum is reached. As the amount of CH enhancement in the high temperature sample is relatively small, it seems that the fly ash does not accelerate the hydration of C_3S as much as at low temperature. The concentration of CH reaches its maximum value at 2 days hydration, 12 days earlier than in the low temperature sample, implying that the rate of CH consumption by the pozzolanic reaction is made faster by increasing the temperature of hydration. By 90 days of hydration, 38.9% of CH has been reacted in the high temperature sample, but only 20% has been reacted in the low temperature sample.

6.2.C *COMPRESSIVE STRENGTH DEVELOPMENT*

The compressive strength of the neat and blended cement was determined using 0.5 inch cube specimens [Section 2.7]. The strength development as a function of hydration time is shown in Fig. 6.2.4.

In the neat cement paste, the rate of increase of strength decreases gradually with age until 14 days, when it starts to decrease more rapidly. Although the strength in the blended cement is initially below that of the neat cement paste, there being 30% less cement, the strength increases at a much faster rate because of the pozzolanic reaction and overtakes that of the neat cement at 90 days hydration.

Comparing these curves to those corresponding to the lower temperature, shown in Fig. 5.2.12, it is seen that the elevation of curing temperature increases the early age strength of the neat cement but reduces it at later times, the cross-over occurring at 28 days. The increase of temperature accelerates the development of strength in the fly ash cement up to 90 days when the cross-over occurs, earlier than those found by Dalziel [1980] and Kokubu et al. [1960], at about one year. This seems to indicate that raising the curing temperature increased the rate of gain of strength in the fly ash cement more than in the neat cement due to the ash pozzolanicity contributing effectively to the strength at earlier ages.

The ratio of the fly ash cement strength to the neat cement strength at the same age is shown as a function of curing age in Fig. 6.2.5. The curve increases monotonically with time even as

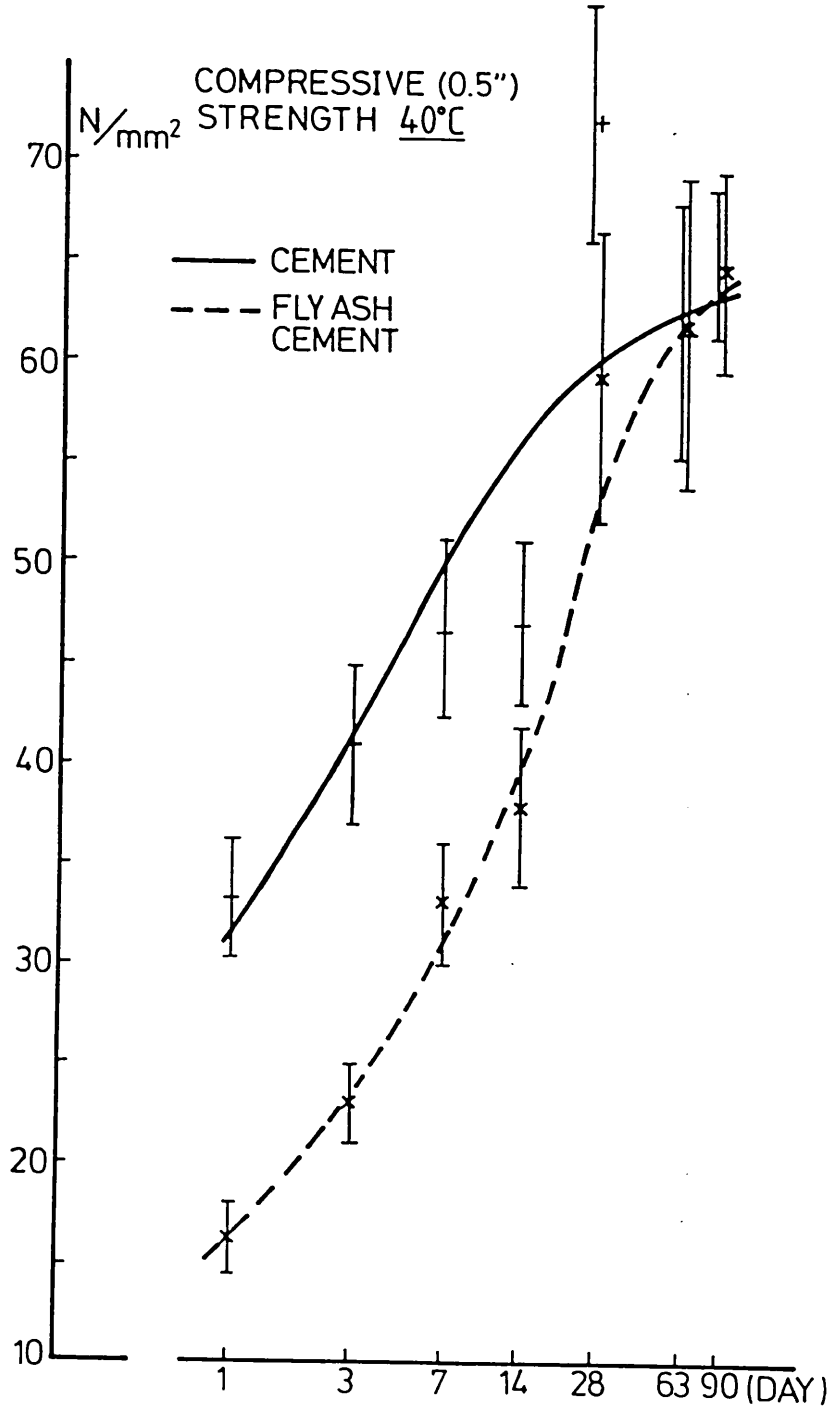

FIG. 6.2.4 Development of strength in cement and fly ash cement at 40°c hydration.

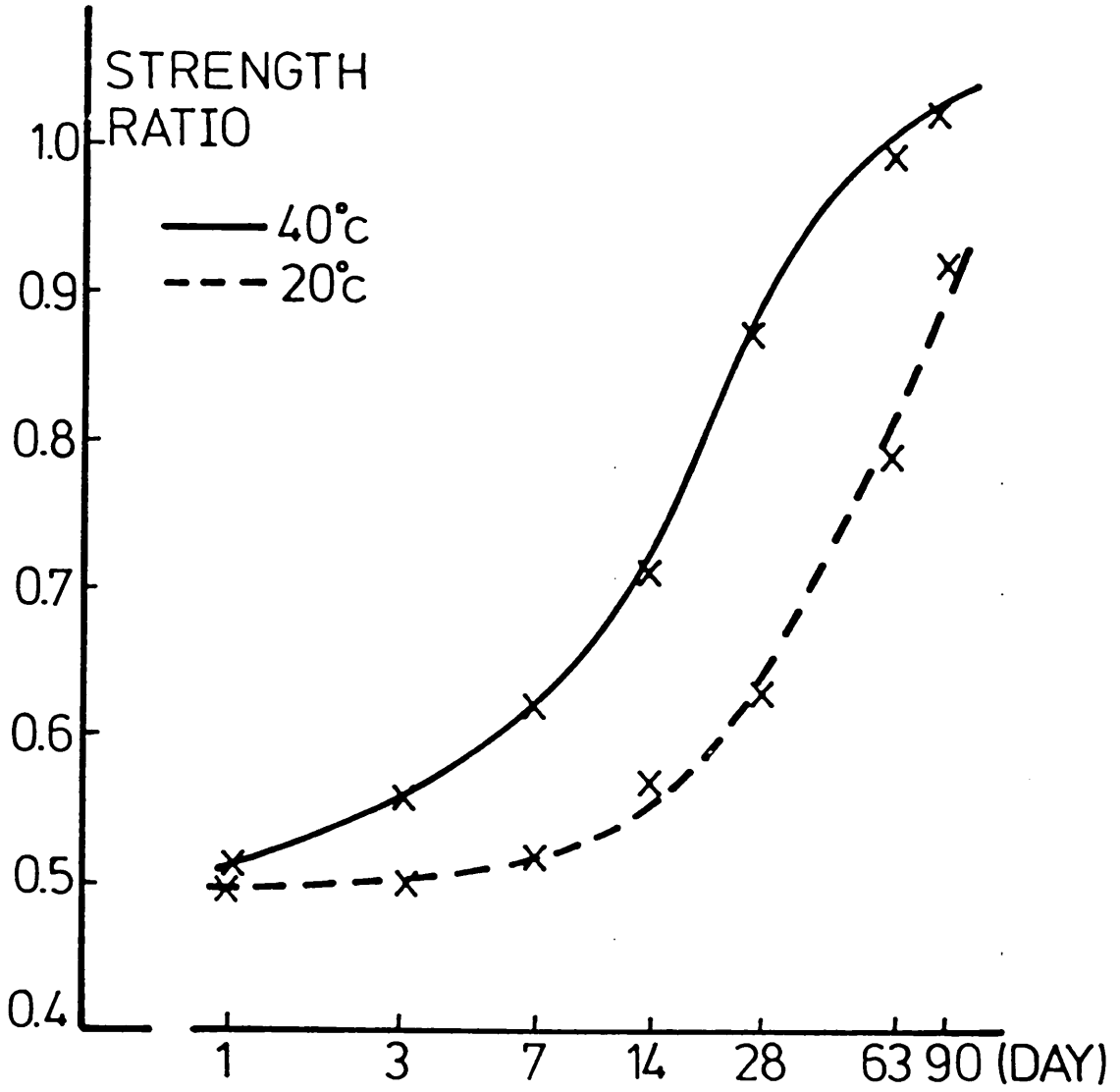

FIG. 6.2.5 Ratio of strength of the fly ash cement paste to the strength of the neat cement paste as a function of age.

early as one day, indicating that the contribution of the fly ash to the strength of the blend has already started. The gradient of the curve begins to decrease after 28 days, implying that the contribution of the fly ash to the strength is becoming less important and indicating that the pozzolanic reaction is slowing down. Nevertheless the ratio starts to exceed unity at about 63 days.

The strength ratio at 40 °C, discussed above, is higher than that at 20 °C throughout the examined range of 1 - 90 days. However, the gradient of the former decreases considerably towards the end of this period whereas that of the latter does not. This observation is consistent with the work of Dalziel [1980] who found the highest pozzolanic contribution at one year to be for the 20 °C cured sample. Thus raising the curing temperature advances the fly ash contribution to the strength (from 7 days to 1 day for 20 °C and 40 °C) so enhancing it at early hydration times, whereas later a reduction is found.

6.2.D *CALCIUM ALUMINATE HYDRATES*

X-ray analysis

The hydrated samples were analysed by X-ray diffractometry to investigate the hydrates of the aluminate phase. Some of the X-ray diffraction patterns of the neat cement and blended cement at various hydration times are displayed in Figs 6.2.6 and 6.2.7.

The calcium sulphate in both systems appears in the form of soluble anhydrite (5.9 Å) after 2 hours hydration, and has been completely consumed after 6 hours by the hydration of the aluminate phase.

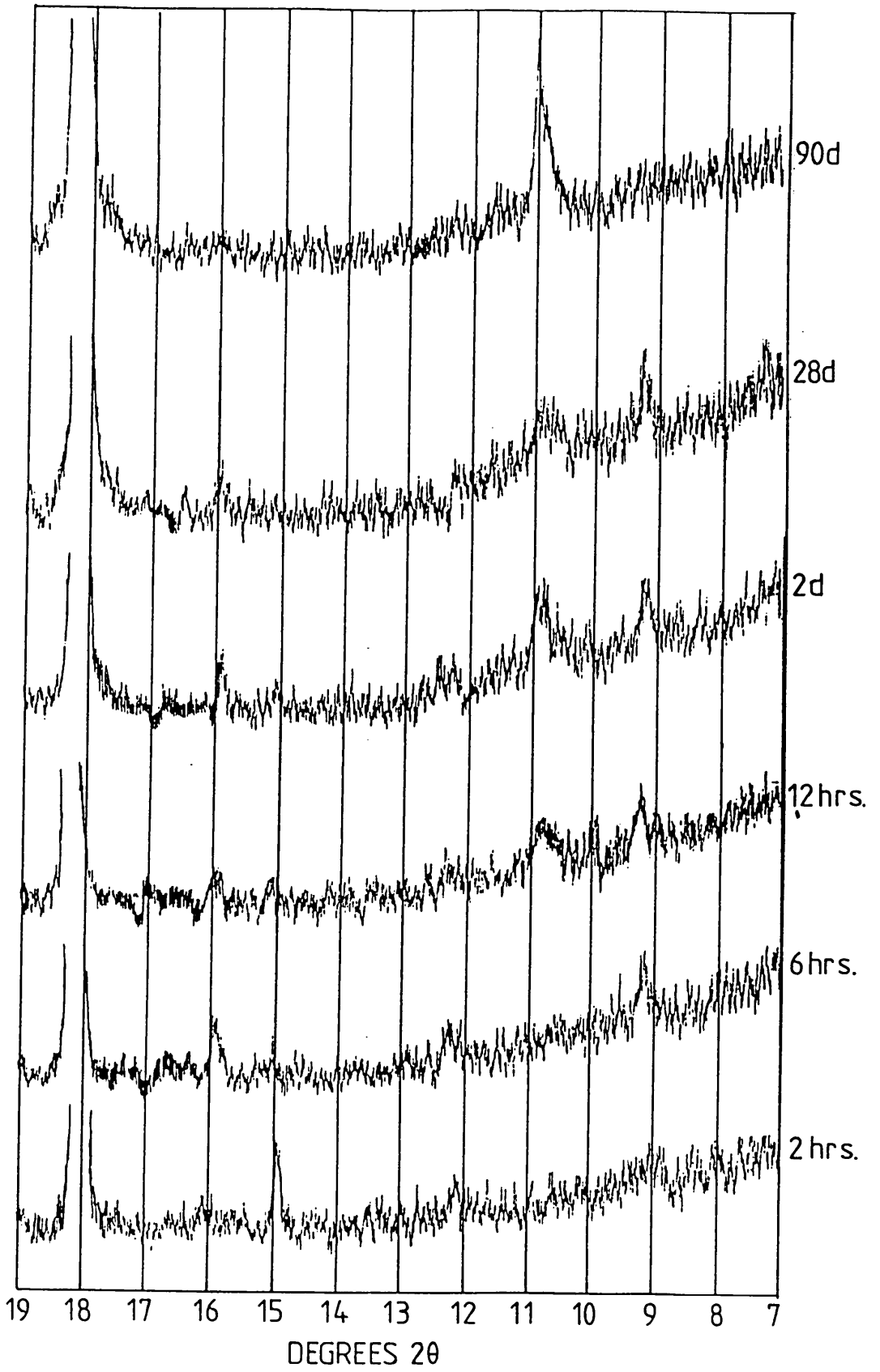

FIG. 6.2.6 XRD traces for D/44 neat cement paste at various ages.

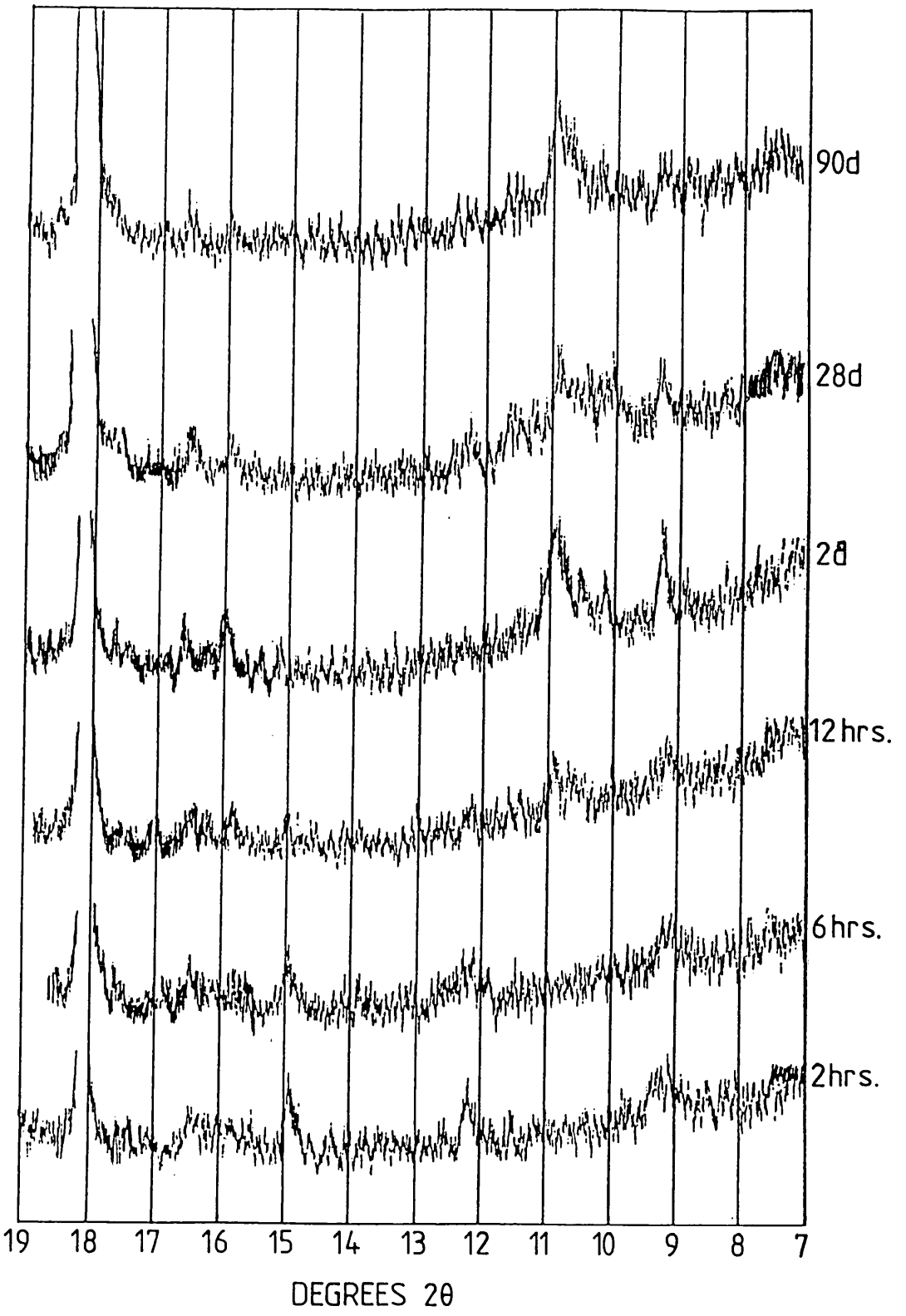

FIG. 6.2.7 XRD traces for D/44 blended cement paste at various ages.

Ettringite (9.7 Å) has been seen in all of the examined samples except at 90 days, in which the ettringite has probably been destroyed by the drying process because the wet six months old sample still shows a strong ettringite peak [Fig. 6.2.8(a)].

The AFm phases start to appear after 6 hours hydration. The most common AFm phase in the neat cement samples has a strong reflection at 8.2 Å and is accompanied by a small amount of what is probably an AFm solid solution (8.5 Å). In the fly ash cement, various types of AFm phases appear at different times; the strongest peaks are mainly at 8.9 Å and 8.2 Å.

An unexpected result is that no peak corresponding to the AFm phase (8.9 Å) has been found in the six months wet samples [Fig. 6.2.8(a)]. However, after the samples have been freeze dried, a strong AFm peak appears in both [Fig. 6.2.8(b)]. Such observations are not found in the room temperature cured wet samples, and this anomaly is not yet understood.

Differential thermal analysis

Fig. 6.2.9 shows the DTA results in the heating range between 25 - 300 °C at various periods of hydration. The peak at about 170°C, corresponding to the decomposition of AFm, appears at 12 hours in both cement pastes consistent with the X-ray results. Unfortunately, any advancing effect of the fly ash on the formation of AFm has not been found, probably because the time between experiments is too long, especially between 6 and 12 hours. Relating these results to the calorimetry curves [Fig. 6.2.1],

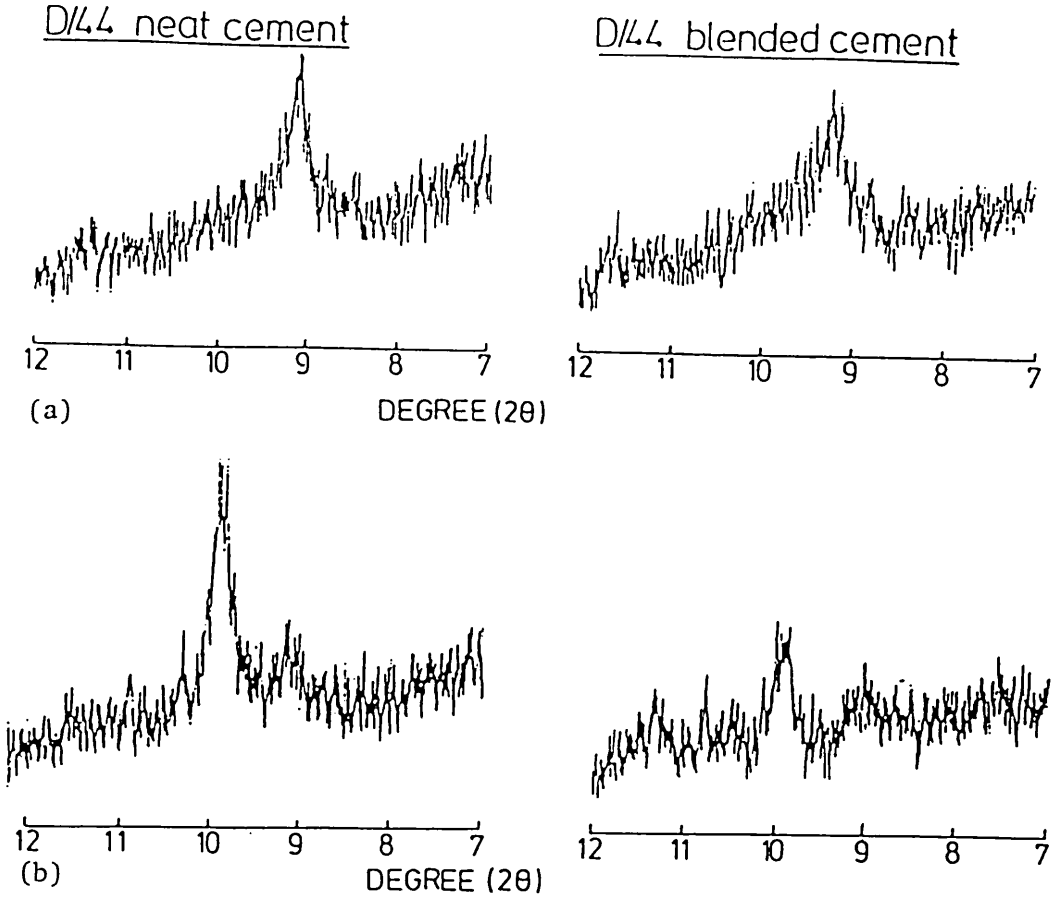

FIG. 6.2.8 XRD traces of a wet and dried six months old sample. (a) wet sample (b) dried sample

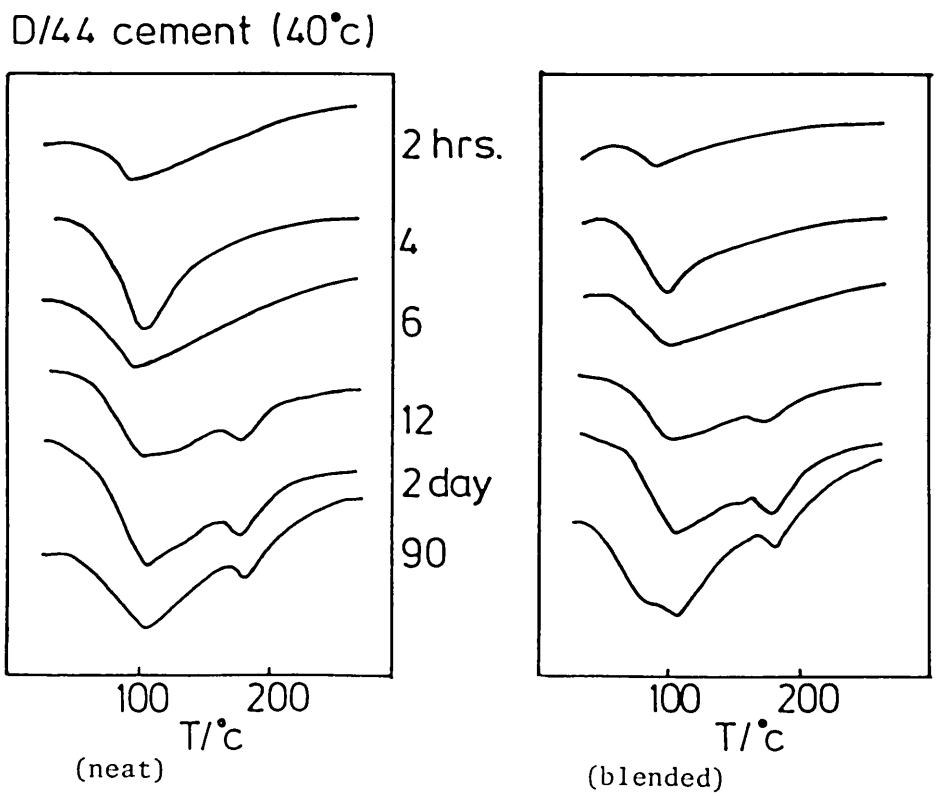

FIG. 6.2.9 DTA cures of the D/44 and D/44+Fiddlers Ferry fly ash cement pastes.

the appearance of the AFm phase coincides with that of the shoulder peak in the neat cement, but not with any peak in the fly ash cement suggesting that the formation of AFm is very slow.

Comparing these results with those obtained at low temperature, the appearance of AFm is advanced to a much earlier time by the increase of temperature because the hydration of C_3A is enhanced leading to earlier depletion of calcium sulphate in the system.

6.2.E *MICROSTRUCTURE OF HYDRATES IN BOTH NEAT AND BLENDED CEMENTS BETWEEN 2 HOURS AND 90 DAYS HYDRATION*

In the 2 hours cement sample [Plate 6.2.1], at the middle of the acceleratory period, many CH crystal platelets have been observed and the surfaces of the grains are fully covered by the growing Type I C-S-H together with some short ettringite rods, most of which are themselves covered by the C-S-H. The addition of fly ash has delayed the growth of C-S-H, as shown by the much less dense covering of smaller C-S-H on the particles' surfaces, and the still clearly observable short ettringite rods [Plate 6.2.2].

Between 2 and 5 hours hydration, the only changes in the microstructure are the increase in number and size of C-S-H on the particle surfaces and the appearance of some Hadley grains.

The secondary growth of the ettringite rods occurs after peak 3, at 6 hours, in both cements [Plate 6.2.3]. In the neat cement, monosulphate platelets have been observed on the cement grains and on the inner wall of the hollow shells. This suggests that the shoulder before peak 3 in the blended cement does not correspond to the secondary growth of ettringite.

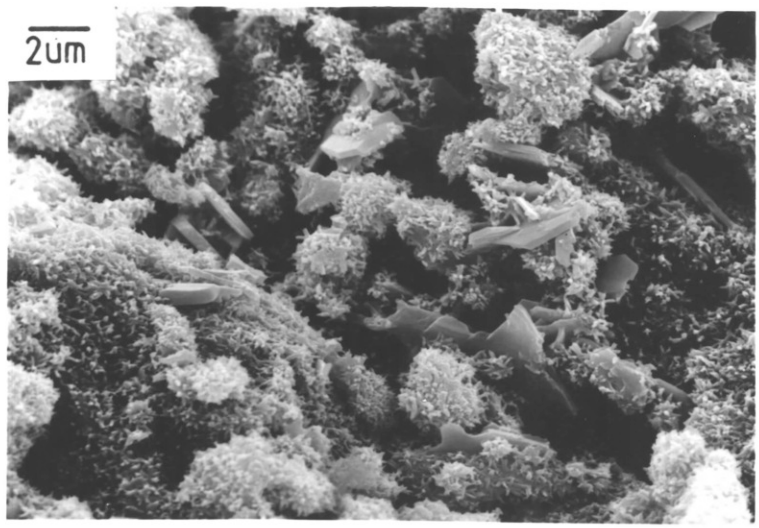

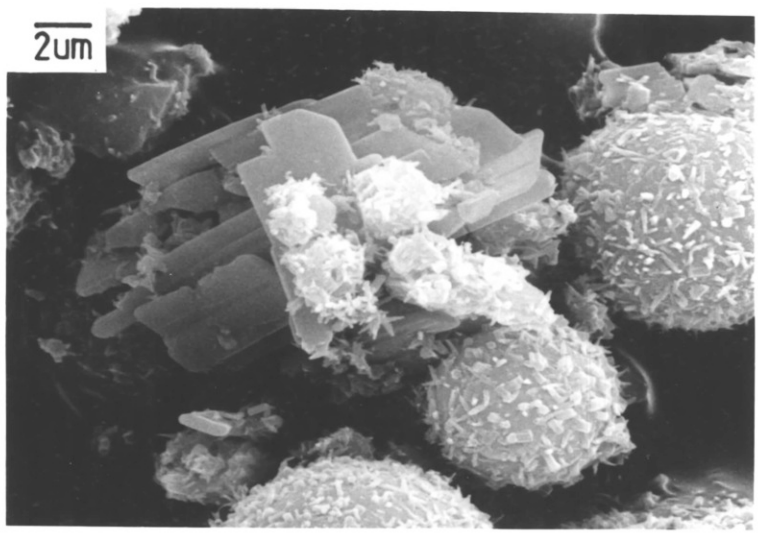

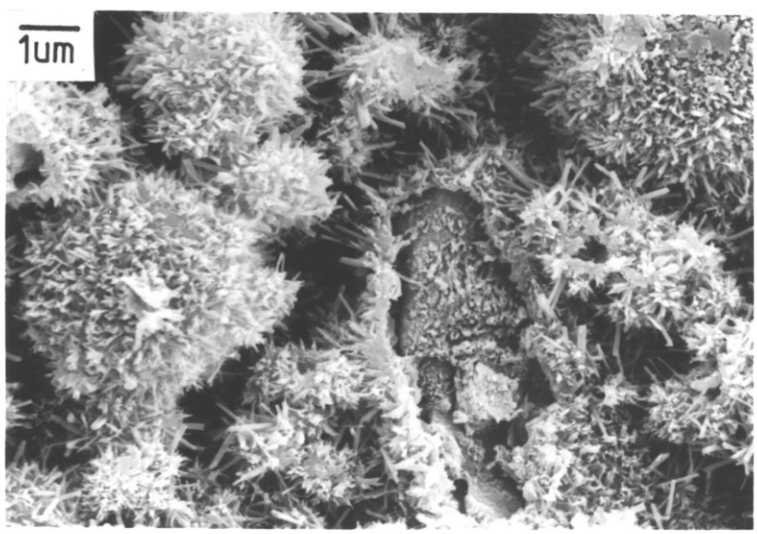

PLATE 6.2.1

2 hours old neat cement paste

PLATE 6.2.2

2 hours old blended cement paste

PLATE 6.2.3

AFt rods and Hadley grain in 6 hour old blended cement

In the 12 hour old samples, large hexagonal AFm plates have been seen and are much more plentiful in the fly ash cement where the sulphate concentration is lower and more AFt phase is formed [Plate 6.2.4]. There are also many monosulphate platelets, some of which are accompanied by small spherical particles. The appearance of the AFm plates is consistent with the results obtained in the X-ray diffraction and DTA. At this time, the C-S-H is converted to Type II and the hydrates in the fly ash surfaces begin to be peeled off during fracture.

The number of the monosulphate platelets and small spheres increases with the ages, but the amount of the large AFm plates does not increase with time. This indicates that the C_3A and C_4AF phases have been stopped to leach into solution and react with ettringite as the hydrate shells become denser. On the other hand, the amount of ettringite is decreasing. Some may be transformed to the monosulphate phase but most of it is buried by the other hydrates, as shown in Plate 6.2.5. Even at 90 days hydration, ettringite can still be seen in the porous area, and is sometimes accompanied by AFm platelets [Plate 6.2.6]. On the right hand side of the picture there are a few large AFm plates.

After one day's hydration, the blended cement [Plate 6.2.7] displays a clear fracture between the fly ash and the surrounding hydrates. The surfaces are exposed showing some signs of crystal phases and the voids are filled with C-S-H honeycomb or AFm platelets as the pozzolanic reaction is taking place. Further reaction of the glass phase leads to a much clearer observation of the crystal phase and the gradually thickening C-S-H layer. After

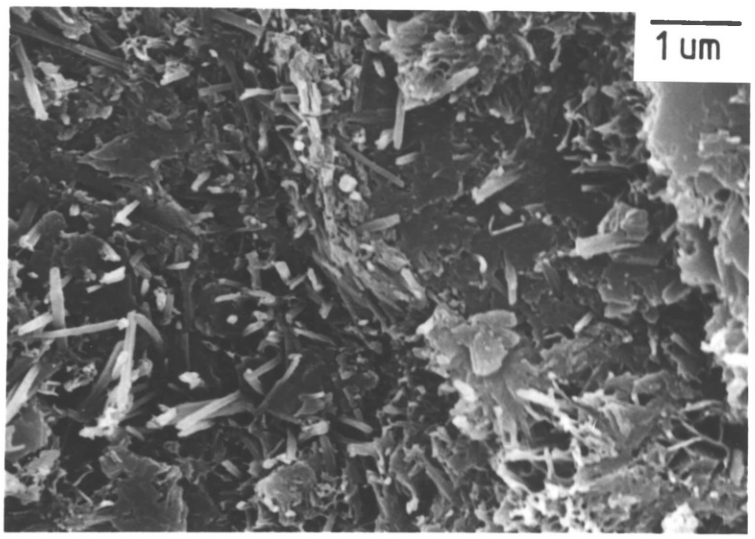

PLATE 6.2.4

AFm plates in 12 hour old blended cement

PLATE 6.2.5

AFt rods in 5 day old neat cement

PLATE 6.2.6

3 months old neat cement paste

5 days [Plate 6.2.8], rims of fibrous C-S-H can be seen around the voids, which are filled with C-S-H honeycomb (LHS), and the fly ashes. The thickness of the rims increases with time by refilling the space left by dissolution of the fly ash particles which are eventually completely replaced [Plate 6.2.10].

The progress of the reaction varies from sphere to sphere depending on the amount of glassy phase present. This can be observed in Plate 6.2.9 after 63 days, which shows that two 2 μm fly ash particles are almost converted into radiating C-S-H (as arrowed), whereas a large fly ash particle is still heavily covered by mullite crystals without any sign of a C-S-H rim. A void with a thin layer of C-S-H products can also be seen. This seems to indicate that the small fly ash particles contain a higher proportion of glass phase.

Plate 6.2.11 shows the back scattered image of polished neat and blended cement at 90 days hydration. Almost all the cement grains are surrounded by a thick layer of hydrate and some have even been completely replaced by hydrate, appearing as dark grey coloured grains. The amount of CH in the blended cement is much less than in the neat cement because of the pozzolanic reaction which also produces a rim of C-S-H around the iron-free fly ashes (dark grey circles). Many lamellae can be seen in the fly ash cement, and some are occupying the porous area similar to the situation in the 6 months old room temperature cured sample; there are many more than in the 90 days room temperature cured sample since the pozzolanic reaction is accelerated by the increase of temperature as shown by TG.

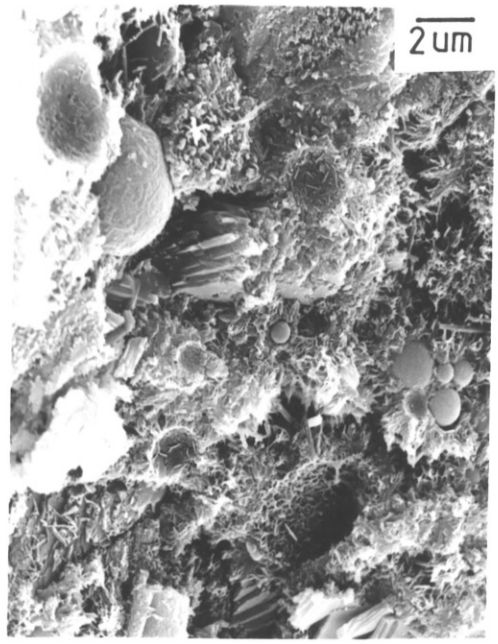

PLATE 6.2.7

Fracture surface of 1 day old hydrated blended cement paste

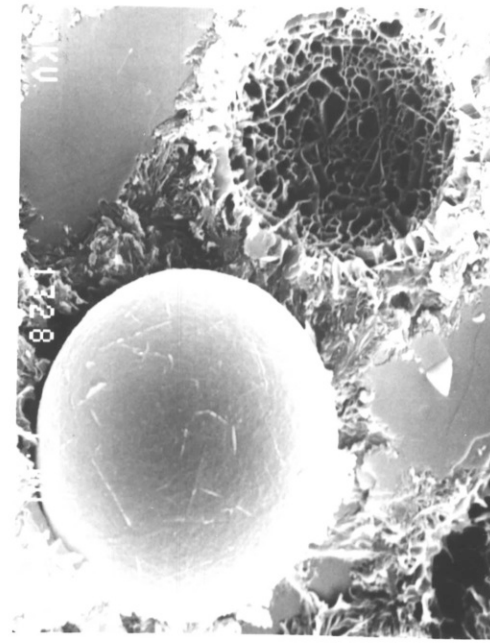

PLATE 6.2.8

Fly ash and void after 5 days hydration

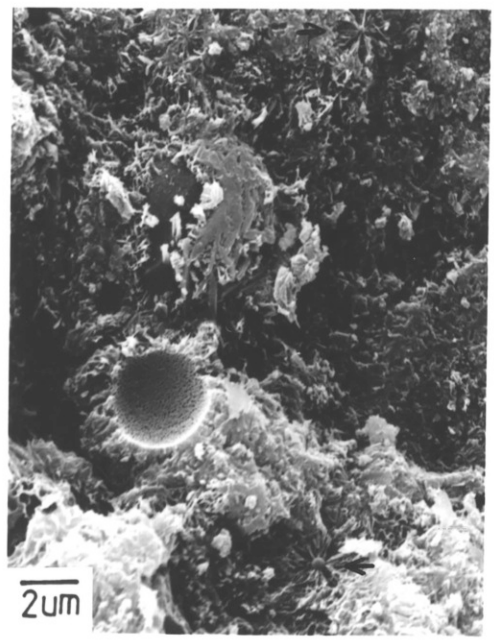

PLATE 6.2.9

A completely reacted fly ash in 90 days paste

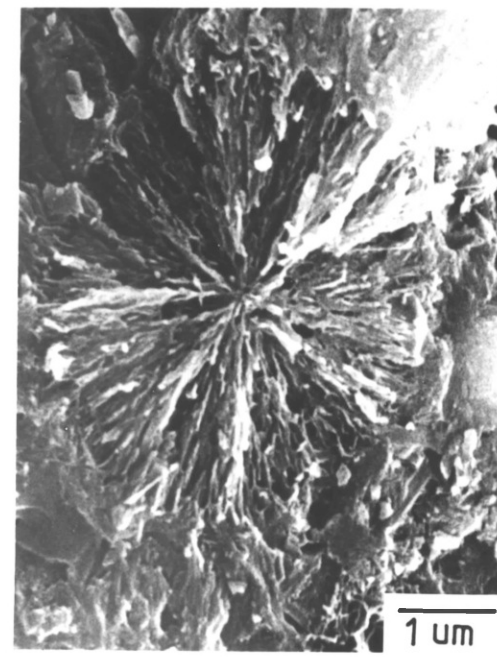

PLATE 6.2.10

Fly ashes in 63 days hydrated paste

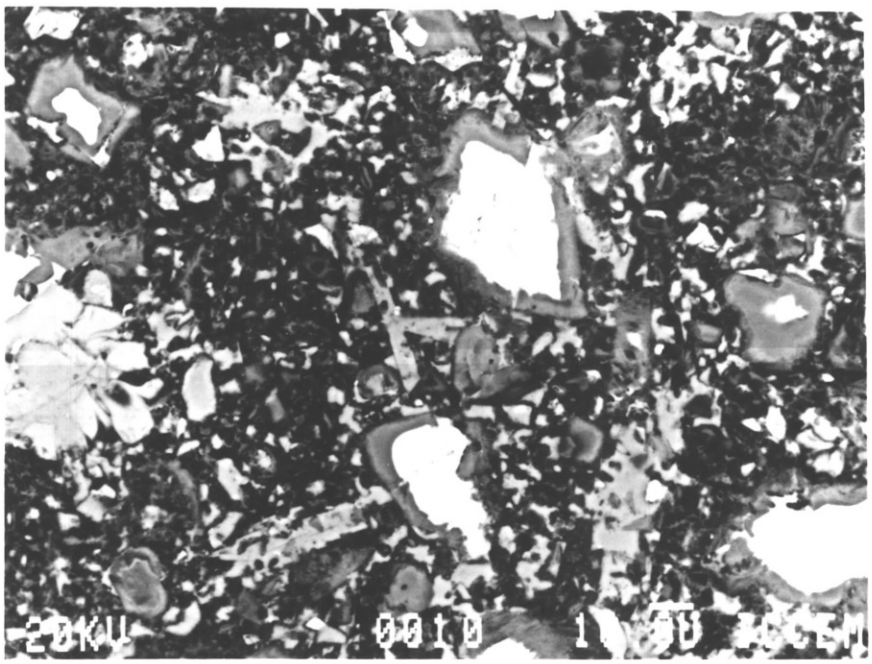

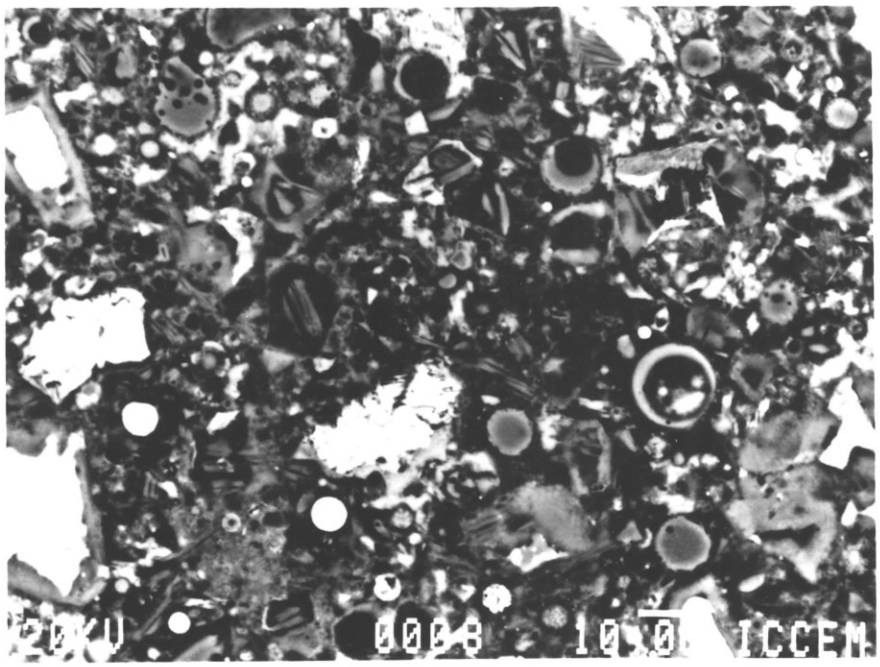

PLATE 6.2.11

BEIs of polished 90 days neat and blended cement

(a) neat cement
(b) blended cement

CHAPTER 7

DISCUSSION

7.1 HYDRATION OF CEMENTS AND THE INFLUENCE OF ADDING FLY ASH

The results of examining both neat and blended cements [Section 5.2] are now used to discuss the hydration of cement and the effects of adding fly ash.

7.1.A *THE FIRST HEAT EVOLUTION AND INDUCTION PERIODS*

After water is mixed with the cement, the dissolution of the cement phases and calcium sulphate evolves a large amount of heat. However, the dissolution of the cement phases is incongruous, leading to a much higher concentration of Ca^{2+} than Al^{3+} and Si^{4+} in the solution, hence the PH rises rapidly. The amount of dissolved Al^{3+} is proportionally higher than that of Si^{4+}, with respect to the relative abundance of C_3A and C_3S, as Locher [1980] has found that more C_3A has reacted in the first few minutes of hydration. This is probably due to the poisoning effect of aluminium on the solubility of silicate, as pointed out by Jennings [1983]. AFt rods form in the areas richer in aluminium, that is where large amounts of C_3A are exposed to contact with water. Such a circumstance is not necessarily related to the bulk content of C_3A, as pointed out by Scrivener [1984]. In fact, this is demonstrated by comparing Plates 5.2.26(a) and 5.2.27(a) which show that similar amounts of AFt have been observed in both AW (2% C_3A) and BW (5.5% C_3A) 1 hour old cement pastes, suggesting that in BW cement a smaller proportion of C_3A exists on the grain surfaces. Very little C-S-H has been observed in this period, presumably because only a small amount of Si^{4+} has dissolved.

There has been a suggestion that the induction period is caused by the formation of a membrane around the hydrating grains, preventing the leaching of Si^{4+} and Al^{3+} into solution [Double et al., 1978; Jennings and Pratt, 1979(a)]. Following an experiment in which the addition of aluminium was found to reduce the solubility of silicates, Jennings and Pratt [1979(a)] infer that this membrane is composed of alumino-silicates. However, such a structure has not been observed on the fracture surface, although Scrivener [1984] has seen a layer of amorphous product with AFt rods close to the grains, in a 2 hours ion thinned section. The negative result of the present work may be due to a similarity in appearance of the layer surface and the hydrating grain.

The influence of fly ash

Plowman and Cabrera [1982] have found that gypsum forms after mixing fly ash with water, due to the dissolution of alkali-sulphates and lime. Hence, it seems reasonable to suppose that fly ash blended paste contains more calcium sulphate per weight of cement than the corresponding neat paste. This more likely to affect the hydration rate of alite, and the renewed hydration of C_3A, than the initial formation of the small AFt rods, which is instead dependent on the available aluminium ions.

Although Jawed and Skalny [1981] have found no evidence for dissolution of Al and Si from fly ash into water, appreciable amounts can be detected if NaOH solution is used as solvent. In the absence of direct evidence, it may be supposed that this dissolution also occurs in CaOH solution, such as that which forms in the hydration of cement. Hence, more AFt should be formed,

although this is difficult to verify by observing the fracture surface. AFt rods have been found on both the cement and fly ash surfaces confirming that the fly ash provides precipitation sites for the hydrate.

The prolonging of the induction period, found in every fly ash cement examined [Section 5.2.A], is probably due to the Al and Si dissolved from the fly ash and/or the adsorption of Ca^{2+} onto the fly ash surface. Jennings and Pratt [1979(b)] have suggested that the failure of the (hypothetical) membrane, and hence the end of the induction period, is caused by the precipitation of CH on or near its outer surface, possibly via the build-up of osmotic pressure. Al and Si ions, which may be released into the solution by the fly ash, are known to poison this precipitation [Jawed and Skalny, 1981; Jennings and Pratt, 1979(b)], while the adsorption of Ca^{2+} ions onto the fly ash surfaces clearly reduces the concentration of $Ca(OH)_2$ in solution, again delaying its precipitation. Either or both of these mechanisms may contribute to the stability of the membrane. Alternatively, the Al and Si ions might also be directly incorporated into the membrane increasing its stability.

7.1.B *ACCELERATORY PERIOD*

Fine needles of C-S-H can be observed on the cement grain surfaces at the end of the induction period. Although C-S-H naturally forms in their foils, these roll up and form into needles during drying [Jennings and Pratt, 1979(b)]. The number and size of C-S-H needles increase rapidly during this period and a shell devleops around the grains. Scrivener [1984] observed that these shells are formed by C-S-H precipitated on the existing gel

layer which contains a framework of AFt rods. Gradually the C-S-H foils (or needles) interlock with each other to build up the bonding between the grains. After 12 hours hydration, the bonding is strong enough to cause some of the shells to rupture during fracture, revealing Hadley grains. Most of the unhydrated cores are separated from the shell due to the dissolution of the C_3A phase [Pratt and Ghose, 1983].

The number of Hadley grains is significantly less in BW pastes than in the others. This probably caused by less C_3A reacting due to the small amount exposed on the surface of the grains [discussed in 7.1.A]. Support for this can be found in the observation that gypsum still remains in the pastes after 12 hours hydration. In the AW pastes, which contain more calcium sulphate per gram of C_3A, gypsum has by then been completely consumed. Hence the hydrate shells are probably closely attached to the anhydrous core, making them more difficult to rupture during fracture.

Any changes in the AFt rods are difficult to observe because the growth of C-S-H rapidly overcomes them, although it can of course be concluded that their length does not exceed the thickness of the C-S-H layer.

The influence of the fly ash

As the addition of fly ash prolongs the induction period, the amount of C-S-H and CH in the blended cements is less than in the corresponding neat cements. This feature is indeed revealed by study of the microstructure [Plates 5.2.6 and 5.2.7] and the TG curves [Section 5.2.C]. On the other hand, the amount of CH in the blended cements increases more rapidly and, except in Westbury

pastes, overtakes that in the neat cement before 1 day's hydration. This indicates that the C_3S hydration in the blends is accelerated as has been confirmed by the enhancement of peak 2 in the calorimetry curves [Section 5.2.A]. The acceleration is caused by the fly ash providing extra precipitation sites for the C-S-H. This reduces the thickness of the hydrate layer, allowing the diffusion of ions to proceed faster. This effect may also be partially caused by the increase in the amount of gypsum dissolved from the fly ash. Copeland and Kantro [1968] have shown how the variation of gypsum affects the hydration of alite in Portland cement and found that the optimum value for the sulphate addition is 3% [Fig. 7.1.1]. Similarly Theisen [1983] has found that the C_3S hydration, peak 2, is retarded as the gypsum concentration is increased from 3 to 4%, thereafter remaining approximately constant [Fig. 7.1.2]. BW, AW and D/44 cements contain less than 3% of calcium sulphate (by QXRD), hence the additional gypsum should have a greater effect than in Westbury cement which contains 4.5%. This may be one of the reasons why the C_3S hydration in the latter is not enhanced as much as in the others. However, the major cause is probably the high C_3A content in this cement. More AFt can form after the induction period, increasing the number of AFt rods precipitated on the fly ash surface, and so reducing the space available for the precipitation of C-S-H.

The enhancing effect of fly ash on the C_3S hydration in BT is stronger than in the other cements as can be seen by observing the calorimetry curves [Fig. 5.2.1(a)]. The effect of extra gypsum from the fly ash is negligible since the total sulphate content of the cement is more than 3%. The BT cement used in this experiment had

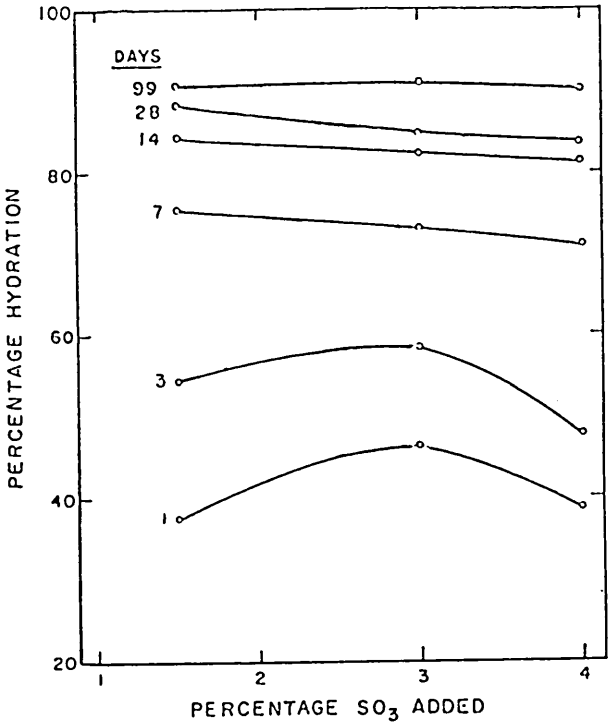

FIG. 7.1.1 HYDRATION OF CEMENT ALITE IN THE PRESENCE OF GYPSUM.
(from Copeland and Kantro, 1968)

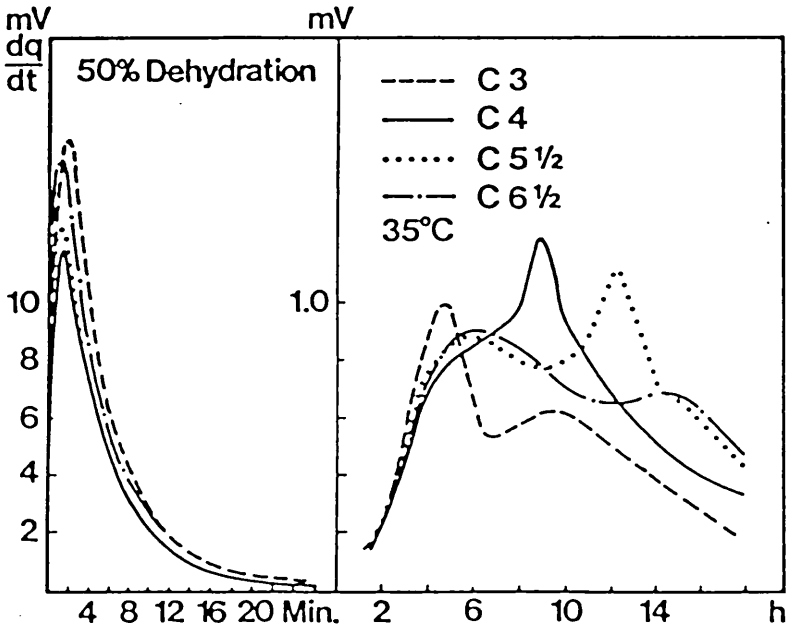

FIG. 7.1.2 RATE OF HEAT DEVELOPMENT AS A FUNCTION OF TIME AT : DIFFERENT LEVELS OF GYPSUM CONTENT.
(form Theisen, 1983)

been stored for at least 2 years and hence was subject to significant aeration, causing the powder to agglomerate (as indicated by particle size analysis this cement is much more coarse than the others used), and so reducing its reactivity. The addition of fly ash may help to disagglomerate the powder and to recover some of its reactivity.

7.1.C *SECONDARY GROWTH OF AFt*

The secondary growth of AFt rods occurs between 12 and 18 hours, except in BW cement where it occurs between 24 and 30 hours. This growth corresponds to the third peak in the calorimetry curves.

In hydration without the C_3S phase, this discontinuous reaction does not appear. Thus, although the mechanism of the renewed C_3A hydration is still not clear the strong influence of the C_3S hydration is indicated. Scrivener [1984] has suggested that the high Ca^{2+} concentration in the solution reduces the solubility of C_3A and gypsum (or calcium sulphate) at early ages. However, after the precipitation of C-S-H and CH, the Ca^{2+} concentration drops again. This would allow the solubility of C_3A and gypsum to recover, promoting the secondary formation of AFt. Alternatively, the formation of C-S-H could further the disintegration of the protective membrane, which consists primarily of silicate ions, allowing more aluminate to dissolve.

The new AFt rods, which form from the renewed hydration of C_3A, are longer than those formed during peak 1, indicating that the solution is in a lower degree of supersaturation with respect to AFt. These secondary AFt rods grow until the level of calcium sulphate is too low for the reaction to proceed.

Jennings and Pratt [1979(a)] have also observed a rapid growth of long AFt rods in pastes hydrated in a large volume of water. This could be due to the dilution lowering the concentration of Ca^{2+} and so encouraging the dissolution of Al^{3+} and gypsum.

The onset and rate of the reaction depends on the relative abundance of the various forms of calcium sulphate, distinguished by the amount of bonded water and having different dissolution rates, because this significantly affects the concentration of SO_4^{2-} in solution. If the calcium sulphate is predominantly of the more soluble forms (e.g. gypsum and hemihydrate), the SO_4^{2-} concentration rises rapidly, leading to a fast reaction (and hence a tall peak 3), as in D/44 and AW [Table 3.1.2]. In contrast, the anhydrite form produces only a gradually increasing SO_4^{2-} concentration, so that the reaction is slower. Indeed a lower and later peak is obtained with Westbury cement which contains only the anhydrite form. Note that BT cement contains the same amount of calcium sulphate as Westbury, but this is instead largely hemihydrate and the reaction is correspondingly faster and earlier [Fig. 5.2.1(a)]. Similar results have been obtained by Theisen [1983].

Of course, the amount of C_3A or, more precisely, the area of it exposed on the surface of the grains, also has a strong affect on this renewed C_3A hydration. An interesting feature is the late onset of peak 3 in BW cement, which contains approximately the same amount of C_3A as the other OPCs, and calcium sulphate as gypsum and hemihydrate. This may be caused by the C_3A existing largely in the interior of the grains, as has been noted in the previous two sub-sections, so that the reaction can only occur when the surrounding C_3S has reacted.

Influence of fly ash

In general, the addition of fly ash retards the renewed C_3A hydration, the exceptions being BW and Westbury cements, but enhances the rate of reaction in the cement. The retardation is probably due to the increase of the Ca^{2+} concentration. Although the initiation of the C_3S hydration is retarded by the addition of the fly ash, the rate of C_3S dissolution is generally accelerated so that the concentration of Ca^{2+} in solution can in fact be greater in the blended pastes. Verification of this is indeed found in the amounts of crystallised CH indicated by the TG curves [Section 5.2.C]. The increased concentration of Ca^{2+} in the solution can retard the dissolution of C_3A and calcium sulphate [as described above], hence peak 3 is delayed. The extra calcium sulphate from the fly ash may also contribute to this delay by providing more calcium ions, although its largest effect may be an increase in the rate of the reaction caused by the additional sulphate ions. Nevertheless the dominant effect of the addition of fly ash on this increase is probably due to the corresponding extra precipitation sites for the secondary AFt rods.

In Westbury blended cement, peak 3 appears at almost the same time as that in the neat cement. As described in Section 7.1.B, the addition of fly ash only accelerates the hydration of C_3S by a small amount. Therefore, the retardation of the renewed C_3A hydration is diminished.

The advanced appearance of peak 3 in BW blended cement is probably caused by the increased C_3S dissolution leading to an earlier exposure of the C_3A in the interior. When this finally occurs the low concentration of Ca^{2+} in solution allows

the C_3A hydration to proceed more quickly giving the sharp peak observed in the calorimetry curves.

7.1.D *FORMATION OF AFm*

When the concentration of sulphate in the solution drops, AFm starts to form through the reaction between the C_3A and C_4AF phases and AFt phases. This reaction takes place after one day's hydration in the neat cement pastes [Table 5.2.2] and corresponds to peak 4. The rate of this reaction generally is very slow, except in BW cement, giving a low and broad peak.

The microstructure has shown that small AFm platelets only appear inside the separated hydrate shells where the concentration of sulphate is significantly low. This is due to the continuous formation of "inner" C-S-H, thickening the shell which slows down the diffusion of the ions, especially for the aluminium and sulphate [Scrivener, 1984]. Hence, the solution outside the shell is deficient in aluminium ions and rich in sulphate ions so that the AFt phase can be maintained. AFt phase can still be detected after 6 months hydration by X-ray analysis.

In AW cement, the AFt phase remains as the stable alumino-sulphate phase in the microstructure, as shown by X-ray diffraction [Fig. 5.2.15]. Sufficient calcium sulphate is present to react with all the C_3A phase before the permeability of the shells is too low for Al^{3+} and SO_4^{2-} to pass through.

Large hexagonal plates have been observed in BW cement [Plate 5.2.26(c)], which correspond to the AFm phase as confirmed

by X-ray analysis. The reason for the difference in size of the AFm plates, compared to those formed inside the shells, may be due to the greater free space available. This indicates that aluminium ions are not isolated from the pore solution by the hydrate shell. A more prominent peak 4 was resolved when large AFm plates are formed [Fig. 5.2.3(a)].

Influence of fly ash

The DTA results [Table 5.2.2] showed that the addition of fly ash had advanced the conversion reaction from AFt to AFm, although this is not shown in the calorimetry curves of D/44 and Westbury cements. The advancement is probably caused by the secondary formation of AFt which is accelerated by the fly ash, leading to faster depletion in sulphate ions in the solution. The effect in the rate of this reaction is not very clear, except in BW blended cement in which the rate is enhanced significantly. This is probably due to the availability of greater amounts of ettringite and C_3A which form the large AFm plates [Plate 5.2.26(e)].

In Westbury blended cement, the AFm plates (similar to those in BW pastes) have been seen after 1 day's hydration, as well as the small AFm platelets inside the shells, indicating that some aluminium ions have diffused through the hydrate shells into solution. As described above [Section 7.1.B], the C_3S hydration has only been accelerated in very small amounts by the fly ash, hence the density of the shells is lower than that of other blended cements and Westbury neat cement. One unexpected result is that the appearance of the large AFm plates does not coincide with any of the heat evolution peaks.

7.2 THE POZZOLANIC REACTION

Several methods [Section 5.2.B, C and G] have been applied to investigate the pozzolanic reaction. The first section below, brings the results of these methods together, in order to assess when the pozzolanic reaction starts. The second section proposes a mechanism for the reaction of fly ash in the cement paste mainly based on the change in microstructure.

7.2.A *THE ONSET AND RATE OF THE POZZOLANIC REACTION*

The pozzolanic reaction is defined as a reaction between the fly ash (or more precisely its glassy component) and the calcium hydroxide phase, in the solution, to produce gelatinous hydrated calcium silicates and aluminates. Hence, the reaction results in a depletion of the amount of CH in the blended cement paste. Thermogravimetric (TG) analysis has been used to measure the amount of CH in the neat and blended cement, and the results show that the maximum CH content in the blends occurs at about 14 days hydration. However, the maximum only indicates the time when the CH consumed by the pozzolanic reaction starts to exceed that produced by the hydration of cement, and not the onset of the reaction. Therefore only considering the decrease of CH content in the blended cement, we are unable to investigate the early stages of this reaction. Extra CH is produced in the blended cement relative to a similar amount of neat cement (as the C_3S hydration is accelerated). Therefore simply subtracting the amount of CH in the blends from that in corresponding neat cement does not enable us to assess accurately the onset of the reaction either.

On the other hand, the dissolution of fly ash has started as early as a half day's hydration and this process continues with time [Fig. 5.2.4]. It is generally believed that the alkali ions are first liberated from the ash and exist in the liquid phase as K^+ and Na^+ ions, which probably contribute to the high PH in the solution. The glassy phase of the fly ash would be rapidly attacked by the highly alkaline solution, releasing silicate and aluminate ions.

Takemoto and Uchikawa [1980] have suggested that some of the SiO_4^{4-} and AlO_2^- ions combine with the surrounding Ca^{2+} forming a gel layer around the fly ash particle. This layer may prevent further SiO_4^{4-} and AlO_2^- ions going into solution. Due to the osmotic pressure generated by the difference of concentration of ions, a void is formed between the surface of grains and the layer. Finally, some regions of the layer are broken down when the osmotic pressure is high enough. The SiO_4^{4-} and AlO_2^- diffuse out into the solution and react with calcium and hydroxyl ions to produce C-S-H and Ca-Al hydrate. The place in which these reactions occur depends on the age of the hydration and the mobility of the ions (to be discussed in the next Section]. It is not certain when the gel layer starts to rupture; this time would be considered the onset of the pozzolanic reaction because the release of ions into solution is unrestricted. The decrease in the weight of fly ash from 12 hours suggests that any such rupture occurs before this time.

As described above, the CH content in the blended cements is the amount formed by hydration of the cement less the amount consumed in the pozzolanic reaction. All the curves [Fig. 5.2.8-9] show that the time after which the consumption exceeds the formation

(i.e. the maximum in CH content) occurs at the same time. As previously mentioned the rate of C_3S hydration is accelerated in the blended cement, however, it can be assumed that the relative rates of hydration between different cements will be the same in neat and blended cement. Fig. 5.2.10 displays the rate of CH formation in all the neat cements. AW shows the most rapidly increasing rate of formation, and Westbury the slowest. The other two have similar intermediate rates. For the maximum to occur at the same time in all cements, the consumption of CH in AW blended cement must proceed faster and, in contrast, that in Westbury proceeds slower. This indicates that the rate of pozzolanic reaction depends on the amount of CH present in the paste, which is proportional to the silicate phase content, and is accelerated by increasing the CH level. Takemoto and Uchikawa [1980] also found similar results in the pozzolana and $Ca(OH)_2$ system.

However, the variation of the rate of pozzolanic reaction does not show up significantly in the microstructure of the fracture surface.

7.2.B *THE MECHANISM OF FLY ASH HYDRATION IN THE CEMENT PASTE*

The present mechanism is based mainly on the model suggested for high lime fly ash by Grutzeck et al. [1981].

Before 1 day's hydration, the fly ash surfaces are fully covered by the cement hydrates (C-S-H and AFt) and the amount is very similar to those on the cement grains. This indicates that bonding between the hydrate layers and the underlying fly ash particles is stronger than that between layers on different particles at this stage. The pozzolanic reaction probably takes

place on both the surface of the fly ash and away from the surface, since there is not much restriction on the movement of ions in the fluid at these early ages.

After 1 days's hydration, the fly ash surface is gradually revealed as the hydrate layer is removed during fracture, indicating that the bonding between them is now weaker than that between hydrate layers on different particles. Generally the surfaces of both the voids and the spheres are smooth and no pozzolanic reaction products have been observed [Plate 5.2.29]. One possible explanation for this is the formation of a thin interfacial zone between the fly ash surface and the cement matrix suggested by Grutzeck et al. [1981]. The bonding of this interface and the hydrate matrix is very weak and thus provides a clear fracture. On the other hand, this may also be due to the increasing dissolution of the glassy phase in the ash. If the pozzolanic reaction takes place away from the fly ash,or the formation of products is much slower than the dissolution, this process will produce a gap between the fly ash surface and the product layer leading to a clear fracture.

With increasing hydration times, the paste becomes more dense and the mobility of the ions in the fluid decreases, especially for the silicate and aluminate ions which are larger than calcium and hydroxyl ions. Hence the pozzolanic reaction becomes more likely to occur on the surface or near the surface of the fly ash. The products of the reaction (honeycomb C-S-H and hexagonal plates of AFm) have been seen in the voids of the 14 day old samples [Plate 5.2.30] supporting this theory. As the reaction proceeds gradually with time, most of the ashes convert to a rim of radiating C-S-H fibres which contain many open channels to allow the ions

access to and exit from the glass surface, leading to a continuous inwards growth of the C-S-H. The majority of the aluminate ions in the glass are more likely to be carried away in the solution because they have a smaller electric charge and less oxygen atoms than silicate and form AFm plates near the fly ash or the porous area. This AFm phase probably incorporates significant amounts of silicate from the fly ash. However, only the C-S-H phase around the surface of the fly ash can be observed on fracture surfaces so it is impossible to assess the extent to which the silicate ions have reacted in the matrix.

7.3 THE EFFECT OF THE ADDITION OF FLY ASH ON THE STRENGTH OF THE CEMENT

A replacement of 30% of the cement by fly ash has reduces very greatly the initial strength development. Although the rate of strength increase after the first day is faster in the blended cement, up to 90 days of hydration the strength of the blend remains lower than that of the neat cement. For a range of cements, Dalziel [1982] has found that the 30% fly ash blend can improve the long term strength (>180 days) of the weakest cement more than that of the strongest cement. Plowman and Cabrera [1980] have shown that the detrimental effect on the early strength can be eliminated by reducing the amount of fly ash from 30% to 15% in most of their cases, but this does not give a long term strength as good as that of the former. Generally, it has been accepted that 20 to 30% replacement is the optimum amount to provide the highest long term strength.

Although the pozzolanic reaction probably starts well before 7 days of hydration, its contribution to the strength is only noticeable after 7 - 14 days and coincides with the onset of the decrease in the total amount of CH of the paste. Mehta [1983] has suggested that the improvement of the strength is partially due to the pore refinement or transformation of large pores into fine pores. Feldman [1981] has also found that there is 90% reduction in the large pores of the blended cement between 14 days and 6 months, compared with only 66% in the neat cement. The overall change in the microstructure is the conversion of high density phase (CH) and large pores to low density products (C-S-H and AFm) and small pores, as a result of the pozzolanic reaction. Feldman and Beaudoin [1976] studied the relationship between the development of strength and the microstructure of the reaction products of Portland cement. They indicated that the low density, amorphous materials (such as C-S-H) have the best bonding properties, and the dense, large crystals of CH the poorest at similar porosity contents.

On the other hand, the microstructure shows that the C-S-H rim around the fly ash particles is strongly bonded with the cement hydration products so it serves to strengthen the bond between the fly ash particles and the matrix.

7.4 THE EFFECT OF INCREASING THE CURING TEMPERATURE ON THE HYDRATION OF CEMENT, THE POZZOLANIC REACTION AND THE STRENGTH

The hydration of cement and the pozzolanic reaction have been discussed in the previous two Sections. The effect of increasing the curing temperature from room temperature (20 °C) to 40 °C on these reactions is discussed in this Section using the results in Section 6.2.

7.4.A *THE HYDRATION OF CEMENT AND THE INFLUENCE OF THE FLY ASH*

The mechanism of hydration of the cement is known to be the same as that at room temperature [Section 6.1], but the hydrations of C_3S and C_3A, corresponding to peaks 2 and 3, are accelerated significantly (the reaction is advanced in time and enhanced) when the curing temperature is increased to 40 °C [Fig. 6.2.1]. The amount of hydration which has occurred after 60 hours at 20 °C is reached after 35 hours at 40 °C hydration [Fig. 6.2.2(a)]. Therefore, a dense structure is formed at an earlier age and this may be one of the reasons that the hydration process slows down. Actually, hydration of the silicate phases seems to have almost stopped after 28 days hydration as is reflected by the rate of formation of CH in the paste [Fig. 6.2.3]. One possible explanation is that there is probably more C_3A phase hydrated at 40 °C because peak 3 is much higher than peak 2 compared to those at 20 °C hydration. This can lead to a negative influence on the degree of hydration of C_3S at later ages [Jons and Osbaeck, 1980]. They suggested that the hydration of C_3A competes with C_3S for available water in the paste and may cause a reduction in the free water near C_3S surface. Another possibility is that the C_2S phase is producing the majority of the CH at this late stage of hydration, but its hydration is significantly slowed down or even stopped at this stage by the effect of higher hydration temperature as shown by Kantro et al. [1962]. They proposed that the increase in the thickness of the gel coating around C_3S or C_2S grains is dependent on the amount of excess lime in the coating, the gel coating is disrupted more as lime excess increases, resulting in slower build up in thickness of the coating. For C_2S hydration

at 50 °C, the excess of lime in the gel coating was found to be less than that at lower temperature, so a faster build up in thickness was expected. Eventually the rate of diffusion of ions through the coating becomes negligible and the reaction stops. This is probably the main reason for the low long term strength in the 40 °C cured neat cement sample. Further quantitative X-ray analysis on the residue amount of the C_3S, C_2S and C_3A phases at various hydration times may provide more definite conclusions on both cases.

The effects of the addition of fly ash on the hydration of cement at 40 °C are similar to those at 20 °C, except that the enhancement of the C_3S hydration is not as much as that at lower temperature, as shown by the TG results [Fig. 6.2.3 and Fig. 5.2.9(a)]. This is probably due to the earlier onset on the pozzolanic reaction. The dissolution of aluminate and silicate ions from the fly ash surface reduces the amount of Ca^{2+} ions absorbed so that less C-S-H is precipitated on the surface of the fly ash.

7.4.B *THE POZZOLANIC REACTION AND THE DEVELOPMENT OF STRENGTH*

The pozzolanic reaction has been considerably accelerated by the increase of temperature. The time at which the CH consumed by the pozzolanic reaction starts to exceed that produced by the hydration of cement has been advanced from 14 days to 2 days hydration. The acceleration is probably caused by the enhanced dissolution of aluminate and silicate ions from the glassy component of the fly ash, and the formation of a large amount of CH at much earlier ages. Some of the fly ash particles (most of them

less than 2 μm in diameter) are completely reacted and replaced by radial fibrous C-S-H after 28 days hydration [Plate 6.2.9]. Such changes have not been observed even after 6 months hydration at 20 °C.

Due to the accelerated pozzolanic reaction, the fly ash contribution to strength development has also accelerated, especially at early ages (before 28 days) [Fig. 6.2.5]. However, the contribution is reduced at later ages resulting from the slowing down of the pozzolanic reaction. Most of the glassy component of the fly ash has probably been consumed after 90 days, when significant numbers of fly ash particles have become completely converted to C-S-H.

CHAPTER 8

CONCLUSIONS AND SUGGESTIONS FOR FURTHER WORK

8.1 CONCLUSION

This Section contains conclusions drawn from the work carried out during this project and is divided into three parts corresponding to those in the Discussion.

8.1.A *THE INFLUENCE OF FLY ASH ON CEMENT HYDRATION*

The effect of the addition of fly ash on the early hydration of cement can be explained in terms of its effect on the constituent phases. Compared to the neat cement, the induction period is prolonged and the C_3S hydration enhanced in all the blended cements. The use of a particular fly ash or the cement only affects the degree of these changes. The renewed C_3A hydration in peak 3 is enhanced by the fly ash, but the onset of this hydration is dependent on the type of cement or more precisely on the degree of enhancement of the C_3S hydration.

The exothermic reaction, peak 4, does not correspond to the hydration of C_4AF, but probably corresponds to the transformation of AFt to AFm which is advanced by the addition of fly ash.

In addition to these effects already mentioned, the physical arrangement of the constituent phases in the cement grains can significantly affect the cement hydration and the influence of the fly ash on the hydration.

8.1.B *POZZOLANIC REACTION*

Although the onset of the pozzolanic reaction cannot be deduced in the present work, the effects of the reaction can be noticed after 7 days hydration. These include the rapid decrease in the CH content, and the contribution of the fly ash to the compressive strength which continues to increase with age leading to the improvement in long term strength. The rate of reaction is increased with the amount of C_3S phase in the cement.

The microstructure shows that the hydration mechanism of this low-lime fly ash is generally similar to that of the high-lime fly ash suggested by Grutzeck [1981]. The fly ash spheres in the paste are consumed from the outer surface inwards, being replaced mainly by the radiating fibrous C-S-H. Occasionally AFm has formed in the interfacial region between the C-S-H rim and the fly ash surface, but most of the aluminate ions diffuse out to form AFm plates near the fly ash or in porous areas.

8.1.C *THE EFFECTS ON THE HYDRATION OF CEMENT AND THE POZZOLANIC REACTION BY RAISING THE CURING TEMPERATURE OF THE HYDRATION*

Raising the curing temperature accelerates the early hydration of the cement, hence increasing the early strength. However, the slowing down in the hydration of silicate phases leads to a lower long term strength in the high temperature cured paste.

The pozzolanic reaction is accelerated significantly by the increase in temperature, and reduces the loss in early strength in the blended cement. However, the acceleration leads to a decrease in the contribution to the strength from the pozzolanic reaction at later ages as most of the glassy component of the fly ash has been consumed.

8.2 SUGGESTIONS FOR FURTHER WORK

8.2.A *EARLY HYDRATION*

Some suggestions have been made in the course of the present work. Overall, there is a lack of knowledge about the early hydration of fly ash cement, especially with regard to the development of microstructure and solution chemistry. The following lists some possible research areas which may improve our understanding of this area:

Solution chemistry

It is very important to know the amount of aluminate, silicate and alkali ions released from the fly ash during the first few hours of mixing, since these are vital factors in determining the length of the induction period. In order to simulate the fluid conditions which exist in the cement paste, experiments should be carried out in $Ca(OH)_2$ solution rather than in water.

Environmental cell in HVEM (high voltage electron microscope)

The technique can provide valuable information about the hydration of fly ash cement during the first few hours, especially any changes near and on the surface of the fly ash particles such as the possible formation of a layer of gelatinous material (possibly Al-Si rich) on the fly ash surface and the presence of any C-S-H foils on the fly ash surface.

Ion beam thinning

Ion thinned sections of cement may provide information about the interfacial region between the hydrate layer (or the C-S-H rim) and the fly ash surface. The bonding of the C-S-H fibres (produced by pozzolanic reaction) and the hydrate matrix may also be studied by this technique.

8.2.B *LATER HYDRATION*

The cross-section of the fly ash particles is clearly observed in back scattered electron images of the polished surfaces. Therefore the percentage volume of the fly ash can be measured so that the percentage of fly ash reacted with hydration times may be deduced. By using the image analyser, the size distribution of the fly ash particles can be obtained, hence the reactivity of particles of different size ranges may be studied.

Although quantitative X-ray analysis is very difficult, it can provide much information about the hydration mechanism. Analysis of the ettringite and monosulphate phases should give more knowledge about their transformation. On the other hand, it is vital to discover the degree to which these two phases are damaged by the drying process and to carry out the X-ray analysis on the hydrating undried sample.

APPENDIX I

The setting up of the calorimetry system was performed by the cement group at Imperial College; the system is illustrated in Fig.2.1.2. The computer, through the interface, can switch the DVM between calorimeters via the relay box, and records the data from the DVM which has been converted into binary form by a BCD (binary coded decimal) card.

Computer programs

The programs, written by Dr C J Gillham, perform the following functions:

1) Data acquisition, CALPR - controls acquisition of data from calorimeters during the experiment with three options of timing:
   i) single time series of regular intervals;
   ii) two sequential time series, each of regular intervals;
   iii) logarithmic time intervals.

2) Calibration, CALIB - loaded by CALPR at the end of the run for calibration and can also be called independently if the calibration phase of CALPR has not been reached or completed. The object is to find K_1 and K_2 by solving the first order of differential equation,

$$W = \frac{dQ}{dt} = K_1 E + K_2 \frac{dE}{dt} \qquad \ldots\ldots (1)$$

where Q = total heat generated in calorimeter
W = the power production
E = the e.m.f. output from the calorimeter.

During the calibration the power is $W_H + W_S$, where W_H is the heater power, and W_S is the residual specimen power (assumed unchanged over the calibration period).

The solution of equation (1) is

$$E = \frac{W_S + W_H}{K_1} + Ae^{\frac{-K_1 t}{K_2}} \qquad \ldots\ldots (2)$$

K_1 and K_2 can be obtained from the steady state e.m.f. ($E_{plateau}$) reached during the calibration and time ($t_{1/e}$) taken to reach 0.632 $E_{plateau}$.

Before the calibration is started, $W_H = 0$, steady state ($t \to \infty$),

$$E_{background} = \frac{W_S}{K_1}$$

Taking $t = 0$ when heater is switched on, $E = E_b$

$$0 = \frac{W_H}{K_1} + A\,e^{\circ} \rightarrow A = -\frac{W_H}{K_1}$$

$$E - E_b = \frac{W_H}{K}\left(1 - e^{-K_1/K_2 t}\right)$$

As $t \to \infty$, $E \to E_{plateau}$.

$$K_1 = \frac{W_H}{E_p - E_b}$$

$$K_2 = K\, t_{1/e}$$

where $t_{1/e}$ is the time taken to reach 0.632 $E_{plateau}$.

3) Processing, POWER - once K_1 and K_2 are known, the power W corresponding to the measured e.m.f. E can be deduced (1). The resulting values can be plotted or tabulated; in addition W may be integrated yielding the total heat output.

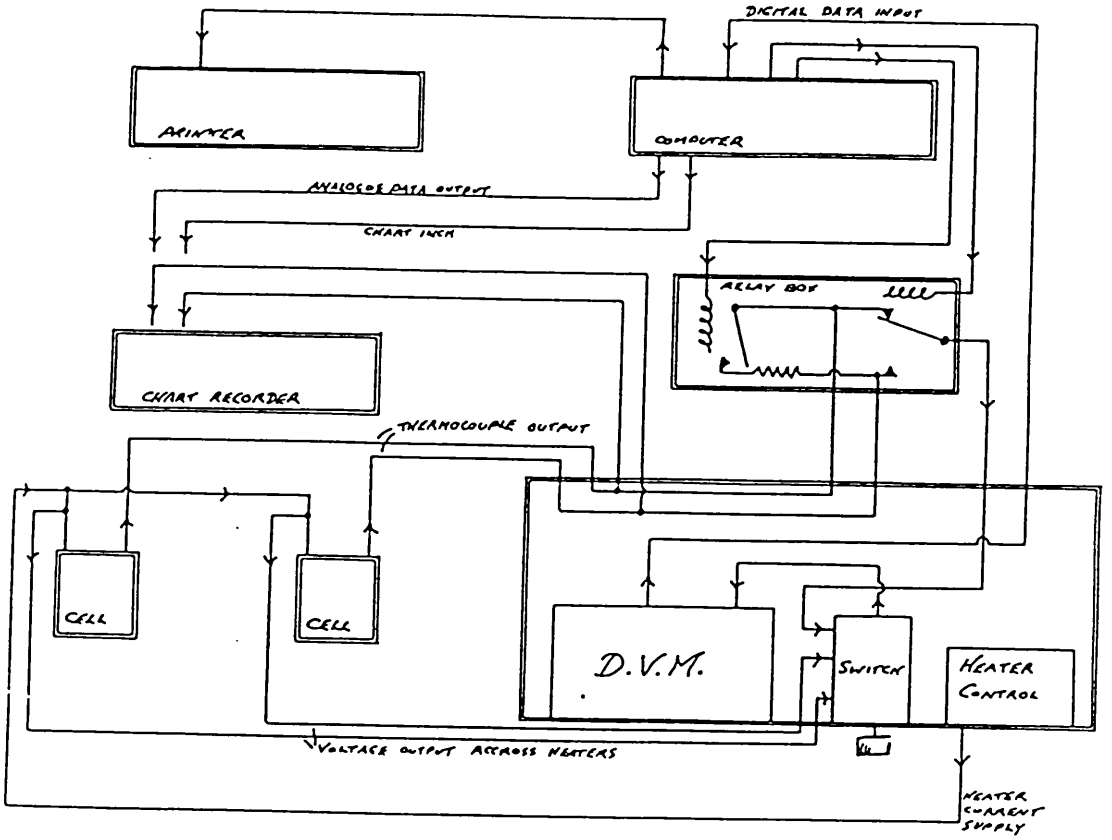

FIG.2.1.2 BASIC CALORIMETRY SYSTEM — IMPERIAL COLLEGE SET UP

APPENDIX II

Malvern 3600 particle size analyser

This instrument can measure the size distribution by weight of solids in liquid suspension. It consists of a laser source, sample cell and an array of concentric diodes to detect diffracted light, the system is illustrated in Fig.2.2.1. The particles in suspension diffract the incident light, which is a parallel and monochromatic beam, to give a stationary diffraction pattern which is received by a multi-element photo-diode detector and produces an analogue signal proportional to the received light intensity. The signal is analysed by a PET computer using a "model independent" programme. The programme sets up 15 weight bands dictated by the receiver lens used in the measurement. By a heuristic technique it obtains a good guess at the proportion of weight in each of the size bands from which it constructs the corresponding diffraction pattern using Fraunhofer Diffraction Theory. This "calculated" energy is compared with that "measured" in a least squares sense to obtain an error coefficient. The system then iteratively refines the weight in the bands to minimise this error coefficient, thereby improving the size distribution estimate. If the error coefficient is less than 3.5 a satisfactory fit has been found.

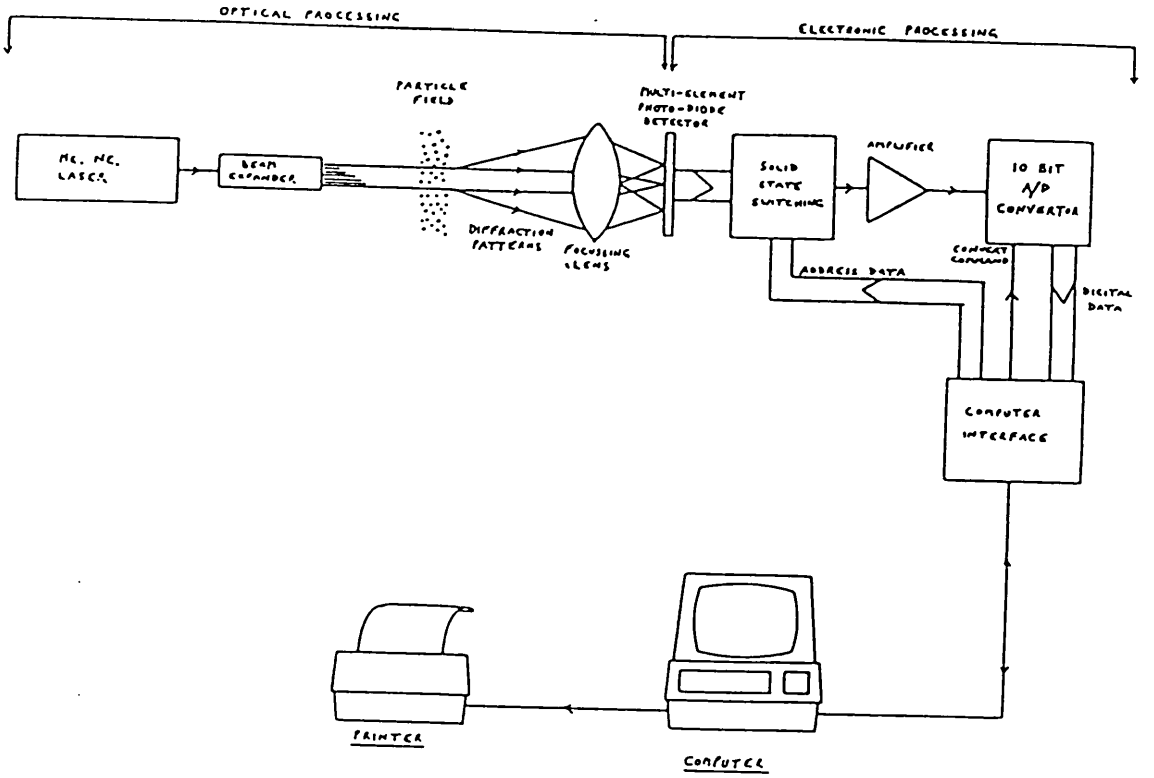

FIG. 2.2.1 BASIC OPTO-ELECTRONIC SYSTEM TO OBTAIN PARTICLE SIZE AND DISTRIBUTION.

APPENDIX III

Experimental procedure of QXDA

The method was developed by Mr W A Gutteridge of the Cement and Concrete Association.

To all the samples is added an internal standard, TiO_2, by weight in the ratio of 1:5. The mixtures are ground to a particle size of less than 5 micrometers by milling in an agate ball mill for 40 minutes with cyclohexane as a grinding aid. The samples for the diffractometer are made by loading a sample holder from the back so as to reduce the effects induced by preferred orientation. Intensity data were collected by step counting at each interval of 0.05 degrees 2θ for 20 seconds over the range 25° to 38° (261 points).

There are 50 primary standards collected from a set of some 30 chemically synthesised cement minerals. The intensity data is collected by step counting as for the cement, but the count time for each interval is 100 seconds. Hence each set of primary standard data contains 261 values. The first value in the set is the normalised intensity N_1 at 25°, 2θ; the second value is the normalised intensity N_2 at 25.05°, 2θ. Thus 261 equations can be obtained using the selected M primary standards.

$$N_{(p)\,\text{cement}} = \sum_{x=1}^{x=M} (N_p)x \cdot W_x + B_p.$$

W_x is the weight fraction of the x^{th} primary standard and B_p represents the background contribution to the cement data at each point. Values for W_x are obtained from the 261 equations by the method of least squares. A reliability factor R is calculated using the following relation which gives an assessment of the fit to the

experimental data:

$$R = \frac{\sum_{p=1}^{p=261} [(N_p)_{cement} - \sum_{x=1}^{x=M} ((N_p)_x \cdot W_x) + B_p]^2}{\sum_{p=1}^{p=261} [(N_p)_{cement}]^2}$$

Finally the weight fraction of each component in the cement is expressed as a weight percentage and a total W_T obtained. Both R and W_T are used to assess the reliability of the analysis. It has been found that the analysis of anhydrated cement appears to be reliable when R is less than 0.01 and W_T is 100 ± 2 percent. Fig.2.5.1 is one of a typical unhydrated cement analysis. The analyses obtained from QXDA can be checked against those obtained from the "KOSH" and "SAM" extractions.

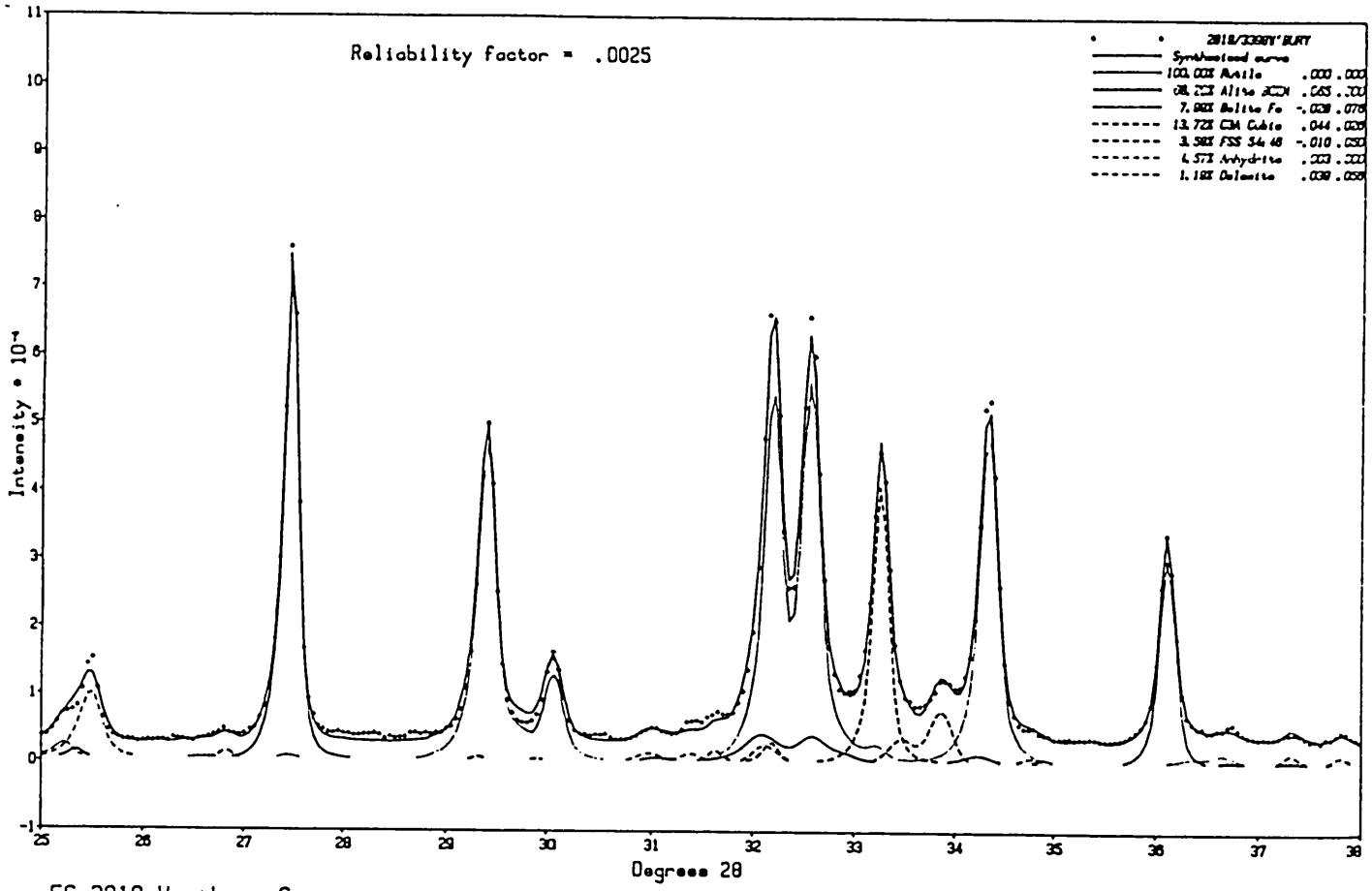

ES 2819 Westbury Cement

C&CA WED, DEC 21, 1983, 4:31 PM

FIG.2.5.1 QXRD FOR AN ORDINARY PORTLAND CEMENT.

APPENDIX IV

The weight loss during heating of the hydrated neat and blended cement between 25 °C and 900 °C is plotted in graphs such as that shown in Fig.5.2.6. There is a large weight loss at approximately 450 °C - 550 °C which is mainly due to the water bonded to CH, although there are contributions from other phases [Taylor, 1984]. It is usual to use an extrapolation procedure to correct such effects as shown in Fig.5.2.7. Hence the amount of water in the CH can be measured, and the amount of CH calculated as follows:

$$Ca(OH)_2 \xrightarrow{\text{heat}} CaO + H_2O\uparrow$$

	$Ca(OH)_2$		CaO		$H_2O\uparrow$
molecular weight	74		56		18

If x(g) of H_2O has been evaporated, the amount of $Ca(OH)_2$ will be A(g), where

$$A(g) = \frac{x \times 74}{18} = \underline{4.1156 \times x}$$

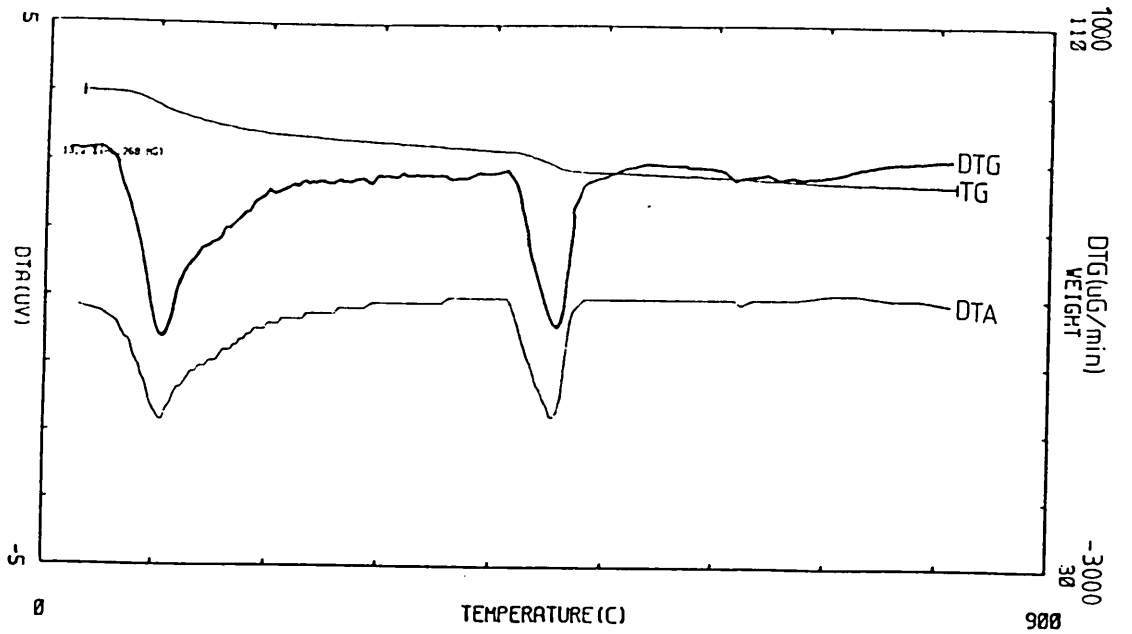

FIG. 5.2.6 AN OUT-PUT OF A THERMAL ANALYSIS

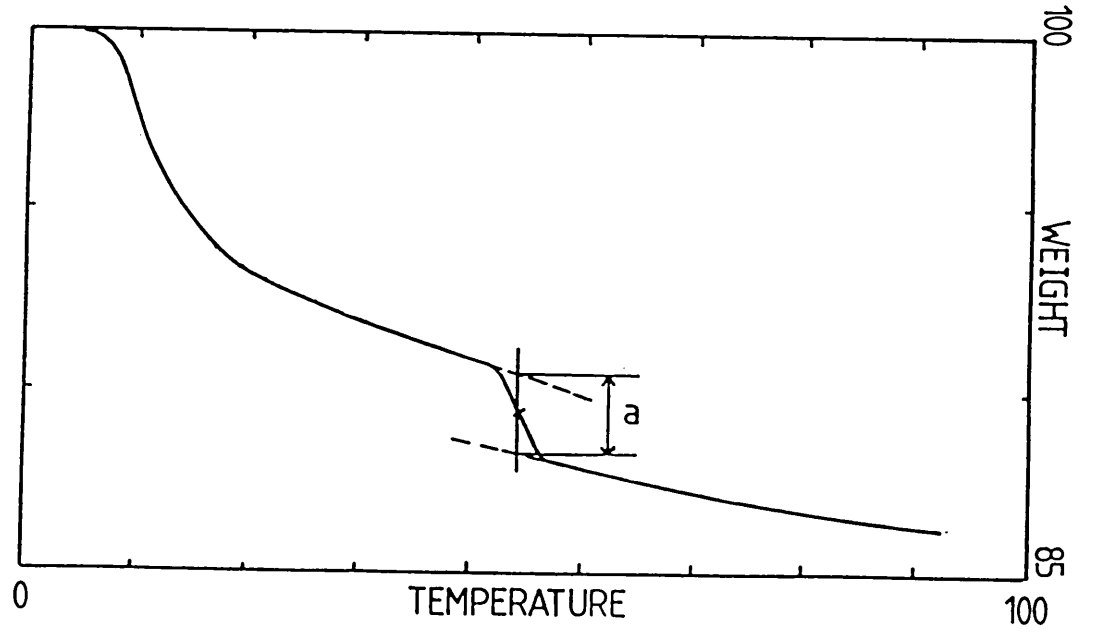

FIG. 5.2.7 USING AN EXTRAPOLATION PROCEDURE TO OBTAIN THE PERCENTAGE OF THE WEIGHT OF THE WATER (a) IN CH PHASE.

APPENDIX V

(a) The general formula to calculate the amount of C_4AF in the neat cements

$$\frac{Mi}{Ms} = k \frac{Ii}{Is} \quad \ldots\ldots\ldots (1)$$

$$Mi = Ms\ k \frac{Ii}{Is} \quad \ldots\ldots\ldots (2)$$

$$Ms = \frac{1}{5} M_{residue} \quad \ldots\ldots\ldots (3)$$

[as Ms, the mass of TiO_2, is added in the ratio of 1 to 5 parts of mass of residual from "SAM" solvent.]

$$M_{residue} = x\ Mc \quad \ldots\ldots\ldots (4)$$

where x = the ratio of the weights after and before the wash and Mc = the weight of hydrated cement before washed.

Substituting (3) and (4) into (2)

$$Mi = \frac{1}{5} k * x\ Mc \frac{Ii}{Is} \quad \ldots\ldots\ldots (5)$$

So the amount of C_4AF per weight of cement is

$$\frac{Mi}{Mc} = \frac{1}{5} k \times \frac{Ii}{Is} \quad \ldots\ldots\ldots (6)$$

(b) The general formula to calculate the amount of C_4AF in the fly ash cement.

Now the formula (4) is changed to

$$M_{residue} = x\ (Mc + Mf) \qquad \ldots\ldots\ldots\ (7)$$

where Mf is the mass of fly ash in the original hydrated cement and is 30% of total weight.

So $$M_{residue} = x\ (Mc + \tfrac{3}{7}\ Mc) \qquad \ldots\ldots\ldots\ (8)$$

Substituting (8) and (3) into (2)

$$Mi = \tfrac{1}{5}\ k\ x\ (\tfrac{10}{7})\ Mc\ \frac{Ii}{Is}$$

$$Mi = \tfrac{2}{7}\ k\ x\ Mc\ \frac{Ii}{Is} \qquad \ldots\ldots\ldots\ (9)$$

So the amount of C_4AF per weight of cement is

$$\frac{Mi}{Mc} = \tfrac{2}{7}\ k\ x\ \frac{Ii}{Is} \qquad \ldots\ldots\ldots\ (10)$$

(c) To calculate the value of k.

Using formula (6) and Mi/Mc = 0.035

$x = 0.2255$ $\qquad \frac{Ii}{Is} = 0.4987$

$\therefore$ $k = 1.5562$

REFERENCES

Abdul-Maula, S. and Odler, I. (1981) 'Hydration reactions in fly ash-portland cements' in Proc. Symp. 'Effects of fly ash incorporation in cement and concrete' Mat. Res. Soc. Boston 82-91

Alexander, L. and Klug, H.P. (1948) 'Basic aspects of x-ray absorption' Analytical chemistry, 20 No.10 886

Barnes, B.D., Diamond, S. and Dolch, W.L. (1978) 'Hollow shell hydration of cement particles in bulk cement pastes' Cem. Concr. Res. 8 263-272

Barnes, B.D., Diamond, S. and Dolch, W.L. (1979) 'Micromorphology of the interfacial zone around aggregates in portland cement mortar' J. Am. Ceram. Soc. 62 21-24

Barvinok, M.S.,Komokhov, P.G. and Bondareva, N.F. (1974) 6th. Int. Congr. on Chem. Cem., Moscow,II (2) 151

Ben-Dor, L. (1983) 'Thermal methods' in 'Advances in cement technology' ed. S.N.Ghosh (Pergamon Press) 673-711

Bensted, J. (1978) 'γ-dicalcium silicate and its hydraulicity' Cem. Concr. Res. 8 73-76

Bensted, J. (1983) 'Hydration of portland cement' in 'Advances in cement technology' ed. S.N.Ghosh (Pergamon Press) 307-347

Bensted, J. and Varma, S.P. (1974) 'Some applications of infra-red and Raman spectroscopy in cement chemistry -part I: Examination of dicalcium silicate' Cem. Tech. 5 256-261

Bentur, A., Berger, R.L., Kung, J.H.,Milestone, N.B. and Young, J.F. (1979) 'Structural properties of calcium silicate pastes :II, Effect of curing temperatures' J. Amer. Ceram. Soc. 62 362-366

Berger, R.L., Bentur, A., Milestone, N.B. and Kung, J.H. (1979) 'Structural properties of calcium silicate pastes : I, Effect of the hydrating compound' J. Amer. Ceram. Soc. 62 358-362

Berger, R.L., Frohnsdorff, G.J.C., Harris, P.H. and Johnson, P.D. (1966) 'Application of x-ray diffraction to routine mineralogical analysis of portland cement' in Highways Research Board SR90, 'Structure of portland cement paste and concrete' 234-253

Bertaut, E.F., Blum, P. and Sagniéres, A. (1959) Acta. Cryst. 12 149

Birchall, J.D., Howard, A.J. and Bailey, J.E. (1978) 'On the hydration of portland cement' Proc. Roy. Soc. London, A 360 445-453

Birchall, J.D., Howard, A.J. and Double, D.D. (1980) 'Some general considerations of a Membrane/Osmosis Model for portland cement hydration' Cem. Concr. Res. 10 145-155

Boikova, A. (1980) 'Cement minerals of complicated composition' Proc. 7th. Int. Congr. Chem. Cem. Pares II, I.6-I.11

Boikova, A., Domansky, A.I., Parnyonova, V.A., Stavitskaja, G.P. and Nikushchenko, V.M. (1977) 'The influence of Na_2O on the structure and properties of $3CaO.Al_2O_3$' Cem. Concr. Res. 7 483-492

Boyer, J.P. (1976) 'Influence of temperature increases during the induction period of C_3S hydration on the microsturcture and strength of C_3S motars' M.S.Theses, Unversity of Illinois, Urbana

Breval, E. (1976) 'C_3A hydration' Cem. Concr. Res. 6 129-138

Brown, P.W., Franz, E., Frohnsdorff, G. and Taylor, H.F.W. (1984) 'Analyses of the aqueous phase during early C_3S hydration' Cem. Concr. Res. 14 257-262

Brunauer, S. and Kantro, D.L. (1964) 'Hydration of calcium silicates' in 'The chemistry of cements' ed. H.F.W. Taylor (Academic Press) 287-312

Buttler, F.G. and Walker, E.J. (1982) 'The rate and extent of reaction between calcium hydroxide and pulverized fuel ash' in Int. Symp. 'The use of PFA in concrete' 1 71-82

Bye, G. (1983) 'Portland cement composition, production and properties' (Institute of Ceramics, Pergamon Press, Oxford)

Chatterjee, A.K. (1979) World Cem. Technol. 10 124 and165

Collepardi, M., Baldini, G., Pauri, M. and Corradi, M. (1978) 'Tricalcium aluminate hydrate hydration in the presence of lime, gypsum or sodium sulphate' Cem. Concr. Res. 8 571-580

Collepardi,M., Baldini, G., Pauri, M. and Corradi, M. (1979 a) 'Retardation of Tricalcium aluminate hydration by calcium sulphate' J. Amer. Ceram. Soc. 69 33-35

Collepardi, M.,Monosi, S., Moriconi, G. and Corradi, M. (1979 b) 'Tetracalcium alumino-ferrite hydration in the presence of lime and gypsum' Cem. Concr. Res. 9 431-438

Copeland, L.E. and Kantro, D.L. (1964) 'Chemistry of hydration of portland cement at ordinary temperature' in 'The chemistry of cements' ed. H.F.W.Taylor (Academic Press) Part I 313-370

Copeland, L.E. and Kantro, D.L. (1968) 'Hydration of portland cement' Principal paper. Proc. 5th. Int. Symp. Chem. Cem. Takyo Session II-5 387-421

Corstanje, W.A., Stein, H.N. and Stevels, J.M. (1973 and 1974) 'Hydration reactions in pastes C_3S + C_3A +$CaSO_4.2_{aq.}$ + water at 25°c I, II, and III' Cem. Concr. Res. 3 791; 4 193 and 4 417

Cottin, B. and Vibert, C. (1976) Cem.-Wapno-Gips 30 193

Dalgliesh, B.J. and Ibe, K. (1981) 'Thin foil studies of hydrated portland cement' Cem. Concr. Res. 11 729-739

Dalgliesh, B.J., Pratt, P.L. and Moss, R.I. (1980) 'Preparation techniques and the microscopical examination of portland cement paste and C_3S' Cem. Concr. Res. 10 665-676

Dalgliesh, B.J., Pratt, P.L. and Toulson, E. (1982 a) "Fractographic studies of early hydration products in cement paste' J. Mat. Sci. 17 2199-2207

Dalgliesh, B.J., Ghose, A., Jennings, H.M. and Pratt, P.L. (1982 b) 'The correlation of microstructure with setting and hardening in cement paste' Int. Conf. Concr. at early ages, Paris 1 137-143

Dalziel, J.A. (1980) 'The effect of curing temperature on the development of strength of mortar containing fly ash' 7th. Int. Congr. on Chem. Cem. III, IV-93, Paris

Dalziel, J.A. (1982) 'The behaviour of pulverised fuel ash with different portland cement' in 'The use of PFA in concrete' Int. Symp. I 191-199

Davis, R.E. (1949) 'A review of pozzolanic materials and their use in concrete' Symp. on use of pozzolanic materials in mortars and concretes, special technical publication No. 99, ASTM,3-15

Diamond, S. (1976) 'Cement paste microstructure - an overview at several levels' in 'Hydraulic cement pastes : their structure and properties' (Cement and Concrete Association) 2-30

Diamond, S. (1980) 'Hydration reactions of C_3A contained in an unusual fly ash' 7th. Int. Congr. on Chem. Cem. Paris III, IV-19

Diamond, S. (1981) 'The characterization of fly ashes' in 'Effects of fly ash incorporation in cement and concrete' Mat. Res. Soc. Boston 12-24

Diamond, S. (1982) Int. Symp. 'The use of PFA in concrete' Theme II hydration mechanisms - Discussion, 70

Double, D.D. (1978) 'An examination of the hydration of portland cement by electron microscopy' Silicates Ind. 11 233-246

Double, D.D. (1983) 'New developments in understanding the chemistry of cement hydration' Phil. Trans. Roy. Soc. London A310 52-56

Double, D.D., Hellawell, A. and Perry, S.J. (1978) 'The hydration of portland cement' Proc. Roy. Soc. London A359 435-451

Feldman, R.F. (1981) 'Pore structure formation during hydration of fly ash and slag cement blends' in Proc. Symp. 'Effects of fly ash incorporation in cement and concrete' Mat. Res. Soc. 124-133

Feldman, R.F. and Beaudoin, J.J. (1976) 'Microstructure and strength of hydrated cement' Cem. Concr. Res. 6 389-400

Feldman, R.F. and Ramachandran,V.S. (1966) 'The influence of $CaSO_4.2H_2O$ upon the hydration character of $3CaO.Al_2O_3$' Mag. Concr. Res. 18 185-196

Fierens, P. and Verhaegen, J.P. (1976) 'Induction period of hydration of C_3S' Cem. Concr. Res. 6 337-342

Forrester, J.A. (1970) 'A conduction calorimeter for the study of cement hydration' Cem. Tech. 1 95-99

Forrester, J.A. (1980) 'Shear mixed cement pastes' Poster, 7th. Int. Congr. Chem. Cem. Paris

Fujii, K. and Kondo, W. (1979) 'Rate and mechanism of hydration of β-C_2S' J. Amer. Ceram. Soc. 62 161-167

Fukuhara, M., Gota, S., Asaga, K., Daimon, M. and Kondo, R. (1981) 'Mechanisms and kinetics of C_4AF hydration with gypsum' Cem. Concr. Res. 11 407-414

Funk, H. (1960) 'Two different ways of hydration in the reaction of βC_2S with water at 25-120°c' Proc. 4th. Int. Symp. Chem. Cem. Washington paper III-S7, I, 291-295

Ghosh, S.N. (1983) 'Portland cement phases : Polymorphism,solid solution, defect structure and hydraulicity' in 'Advances in cement technology' ed. S.N.Ghosh (Pergamon Press) 289-305

Ghose, A. and Pratt, P.L. (1981) 'Studies of the hydration reactions and microstructure of cement - fly ash pastes' in 'Effects of fly ash incorporation in cement and concrete' Mat. Res. Soc. Boston 82-91

Glasser, F.P. (1979) in 'Cement production and use' ed. J.Skalny, (Engineering Foundation) 31

Groves, G.W. (1981) 'Portland cement clinker viewed by transmission electron microscopy' J. Mat. Sci. 16 1063-1070

Grutzeck, M.W., Roy, D.M. and Schectz, B.E. (1981) 'Hydration mechanisms in high-lime fly ash in porland cement composites' in 'Effect of fly ash incorporation in cement and concrete' Mat. Res. Soc. Boston 92-101

Gupta, P., Chatterji, S. and Jeffery, J.W. (1973) 'Studies of the effects of various additives on the hydration reactions of tricalcium aluminate, Part 5' Cem. Tech. 4 146-149

Gutt, W. and Osborne, G.J. (1970) 'The effect of potassium on the hydraulicity of dicalcium silicate' Cem. Tech. 1 121-125

Gutteridge, W.A. (1984) 'Quantitative x-ray powder diffraction in the study of some cementive materials' Proc. Brit. Ceram. Soc. 'Chemistry and chemically-related properties of cement', (London, 12-13 April)

Halse, Y., Pratt, P.L., Dalziel, J.A. and Gutteridge, W.A. (1984) 'Development of microstructure and other properties in fly ash OPC systems' Cem. Concr. Res. 14 491-498

Han, K.S., Gard, J.A. and Glasser, F.P. (1981) 'Compositions of stable and metastable C_3A solid solutions crystallized from simulated clinker melts' Cem. Concr. Res. 11 79-84

Harada, T., Ohta, M. and Takagi,S. (1978) 'Effect of polymorphism of tricalcium silicate on hydration and structure characteristics of hardened paste' Yogo Kyokai Shi 86, 7 (quoted in Skalny and Young 1980)

Herath Banda, R.M. and Glasser, F.G. (1978) 'Crystallization of the molten phase in portland cement clinker' Cem. Concr. Res. 8 665-670

Holten, C.L.M. and Stein, H.N. (1977) 'Influence of quartz surfaces on the reaction $C_3A + CaSO_4.2H_2O$ + water' Cem. Concr. Res. 7 291-296

Javelas, R., Maso, J.C., Ollivier, J.P. and Thenoz, B. (1975) 'Observation directe au microscope electronique par transmission de la liason de ciment- graulats dans des mortiers de calcite et de quartz' Cem. Concr. Res. 5 285-294

Jawed, I., Goto, S. and Kondo, R. (1976) 'Hydration of tetracalcium aluminoferrite in the presence of lime and sulphates' Cem. Concr. Res. 6 441-454

Jawed, I. and Skalny, J. (1981) 'Hydration of tricalcium silicate in the presence of fly ash' in 'Effects of fly ash incorporation in cement and concrete' Mat. Res. Soc. Boston 60-71

Jeffery, J.W. (1952) Acta. Cryst. 5 26

Jeffery, J.W. (1964) 'The crystal structure of the anhydrous compounds' in 'The chemistry of cements' ed. H.F.W.Taylor (Academic Press) 131-162

Jennings, H.M. (1983) 'The developing microstructure in portland cement' in 'Advances in cement technology' ed. S.N.Ghosh (Pergamon Press) 349-396

Jennings, H.M., Dalgliesh, B.J. and Pratt, P.L. (1981) 'Morphological development of hydrating tricalcium silicate as examined by electron microscopy techniques' J. Amer. Ceram. Soc. 64 567-572

Jennings, H.M. and Pratt, P.L. (1979 a) 'An experimental argument for the existence of a protective membrane surrounding portland cement during the induction period' Cem. Concr. Res. 9 501-506

Jennings, H.M. and Pratt, P.L. (1979 b) 'On the hydration of portland cement' Proc. Brit. Ceram. Soc. 'Mineralogy of ceramics' 28 179-193

Jones, F.E. (1944 a) 'The quinary system $CaO.Al_2O_3.CaSO_4.K_2O.H_2O$ (1% KOH) at 25°c' J. Phys. Chem. 48 356-378

Jones. F.E. (1944 b) 'The quinary system $CaO.Al_2O_3.CaSO_4.Na_2O.H_2O$ (1% NaOH) at 25°c' J. Phys. Chem. 48 379-394

Jons , E.S. and Osbaeck, B. (1980) 'The influence of the content and distribution of Al_2O_3 on the hydration properties of portland cement' Proc. 7th. Int. Congr. Chem. Cem. Paris, IV, 514-519

Jons, E.S. and Osbaeck,b. (1982) 'The effect of cement composition on strength described by a strength-porosity model' Cem. Concr. Res. 12 167-178

de Jong, J.G.M., Stein, H.N. and Stevels, J. (1967) 'Hydration of C_3S' J. Appl. Chem. 17 246-250

de Jong, J., Stein, H. and Stevels, J. (1968 a) 'The influence of aluminium hydroxide and lime on the hydration of C_3S' J. Appl. Chem. 18 9-17

de Jong, J., Stein, H. and Stevels, J. (1968 b) 'Mutual interaction of C_3A and C_3S during hydration' Proc, 5th. Int. Symp. Chem. Cem. Tokyo, Supplementary paper, II-35, II,311-320

Kantro, W.L. (1975) 'Tricalcium silicate hydration in the presence of various salts' J. Test. Eval. 3 312

Kantro, D.L., Brunauer, S. and Weise, C.H. (1962) 'Development of surface in the hydration of calcium silicates. II. Extension of investigations to earlier and later stages of hydration' J. Phys. Chem. 66 1804

Kawada, N. and Nemoto, A. (1967) 'Calcium silicate in the earlier stages of hydration' Zement Kalk-Gips 56 65-71

Kawada, N. and Nemoto, A. (1968) Sement Gijutsu Nempo 22 124

Killoh, D.C. (1980) 'The heats of hydration of cement blended with pulverised fuel ash' Initial Report, Cem. and Concr. Assoc.

Kiss, L.T., Lloyd, B. and Raask, E. (1972) 'The use of copper oxychloride to alleviate boiler slagging' J. of the Inst. of fuel April 213-223

Klemm, W.A. and Skalny, J. (1977) 'Selective dissoltion of clinker minerals and its application' Martin Marietta Laboratories, Technical Report 77-132

Kokubu, M. (1968) 'Principal paper - fly ash and fly ash cement' 5th. Int. Symp. Chem. Cem. Tokyo IV 75-113

Kokubu, M., Miura, I.,Takano, S. and Sugiki, R. (1960) 'Effect of temperature and humidity during curing on the strength of concrete containing fly ash' Trans. Japan. Soc. of Civil Eng. No. 71 Extra aper (4-3)

Kondo, R. and Ueda, S. (1968) 'Kinetics of mechanisms of the hydration of cements' Proc. 5th. Int. Symp. Chem. Cem. Tokyo, Principal paper II-4, II,203-255

Kovacs, R. (1975) 'Effect of the hydration products on the properties of fly ash cement' Cem. Concr. Res. 5 73-82

Kurczyk, H.G. and Schwiete, H.E. (1960) 'Concerning the hydration products of C_3S and β-C_2S' Proc. 4th. Int. Symp. Chem. Cem. Washington paper III-S13, L 349-358

Neville, A.M. (1981) 'Portland cement' in 'Properties of concrete' ed. A.M.Neville (Pitman)

Nishi, F. and Takiuchi, Y. (1975) Acta. Cryst. B,31 1169

Nurse, R.W. (1952) 'The dicalcium silicate phase' Proc. 3rd. Int. Symp. Chem. Cem. London 56-77

Nurse, R.W., Midgleym H.G., Gutt, W. and Fletcher, K. (1966) 'Effect of polymorphism of tricalcium silicate on its reactivity' in Highways Research Board SR90, 'Structure of cement and concrete' 258-268

Mackenzie, R.C. (1964) 'Differential thermal analysis' in 'The chemistry of cements' ed. H.F.W.Taylor (Academic Press) II 271-289

Maki, I. and Chromy, S. (1978 a) 'Microscopic study on the polymorphism of Ca_3SiO_5' Cem. Concr. Res. 8 407-414

Maki, I. and Chromy, S. (1978 b) Il Cement, 3 247

Manmohan, D. and Mehta, P.K. (1981) 'Influence of pozzolanic, slag and chemical admixtures on pore size distribution and permeability of hardened cement paste' Cement,Concrete and Aggregates, v.3, No.1 63-67

Marinho, M.B. and Glasser, F.P. (1984) 'The early stages of the hydration of tricalcium aluminate and its sodium-containing solid solutions' Proc. Brit. Ceram. Soc. 'Chemistry and chemically-Related Properties of Cement' (London, 12-13, April)

Mascolo, G. Marchese, B., Frigione, G. and Sersale, R. (1973) 'Influence of polymorphism and stabilising ions on the strength of alite' J. Amer. Ceram. Soc. 56 222-223

Mather, K. (1976) 'Examination of cement pastes, hydrated phases, and synthetic products by x-ray diffraction' in Transportation Research Circular No.176, June, 'Evaluation of Methods of Identifying phases of cement paste', 9-30

Mehta, P.K. (1983) 'Pozzolanic and cementitious by products as mineral admixtures for concrete - A critical review' Proc. of the CANMET/ACI, first Int. Conf. on the use of fly ash. silica fume, slag and other mineral by-products in concrete, Canada 1-47

Midgley, H.G. (1964) 'The formation and phase composition of portland cement clinker' in 'The chemistry of cements' ed. H.F.W.Taylor (Acadmic Press) 89-130

Midgley, H.G. (1974) 6th. Int. Congr. Chem. Cem. Moscow, Suppl. Paper Section I

Mohan, K. and Taylor, H.F.W. (1981) 'Pastes of tricalcium silicate with fly ash - analytical eletron microscopy, trimethylsilylation and other studies' Proc. Symp. 'Effects of fly ash incorporation in cement and concrete' Mat. Res. Soc. Boston 54-59

Mondal, P. and Jeffery, J.W. (1975) Acta. Cryst. B31 689

Lach, V. and Bures, J. (1974) 6th. Int. Congr. on Chem. Cem. Moscow II, 73

Lachowski, E.E., Mohan, K., Taylor, H.F.W. and Moore, A.E. (1980) 'Analytical electron microscopy of cement paste part,II : Pastes of portland cements and clinkers' J. Amer. Ceram. Soc. 63 447-452

Lauf, R.J. (1981) 'Cenospheres in fly ash and conditions favouring their formation' Fuel, 60 1177-1179

Lauf, R.J. (1982) 'Microstructures of coal fly ash particles' Ceramic Bulletin 61 No.4 487-490

Lea, F.M. (1970) 'The chemistry of cement and concrete' 3rd. (Edward Arnold Ltd.)

Lerch, W. (1946) 'The influence of gypsum on the hydration reactions of portland cement' Proc. ASTM 46 1252

Locher, F.W., Richartz, W. and Sprung, S. (1976) 'Setting of cement I. Reaction and development of stucture' Zem-Kalk-Gips 29 435

Odler, I. and Abdul-Maula, S. (1984) 'Possibilities of quantitative determination of the AFt - (Ettringite) and AFm - (Monsulphate) phases in hydrated cement pastes' Cem. Concr. Res. 14 133

Odler , I. and Dörr, H. (1979) 'Early hydration of C_3S, II, The induction period' Cem. Concr. Res. 12 13-20

Odler, I. and Schüppstuhl, J.(1981) 'Early hydration tricalcium silicate, III, Control of the induction period' Cem. Concr. Res. 11 765-774

Odler, I. and Skalny, J. (1973) 'Hydration of tricalcium silicate at elevated temperatures' J. Appl. Chem. Biotechnol 23 661-667

Ogawa, K., Uchikawa, H., Takemoto, K. and Yasui, I. (1980) 'The mechanism of the hydration in the system C_3S-pozzolana' Cem. Concr. Res. 10 683-696

Ono, Y., Kawamura, S. and Soda, Y. (1968) 'Microscopic observations of alite and belite and hydraulic strength of cement' Proc. 5th. Int. Symp. Chem. Cem. Takyo, I,275-284

Ono, Y., Uno, T. and Kanai, Y. (1965) 'Synthesis of five polymorphic modifications of C_3S' Semento Gijutsu Nempo English synopses 19 37-41

Owens, P.L. and Buttler, F.G. (1980) 'The reactions of fly ash and portland cement with relation to the strength of concrete as function of time and temperature' 7th. Int. Congr. on Chem. Cem. III IV,60-65

Parrott, L.J. (1984) 'An examination of two methods for studying diffusion kinetics in hydrated cements' Materiaux et Constructions 17 No.98 131

Plowman, C. and Cabrera, J.G. (1980) 'The influence of pulverized fuel ash on the early and long term strength of concrete' 7th. Int. Congr. Che. Cem. Paris, III, IV-84

Plowman, C. and Cabrera, J.G. (1981) 'The influence of pulverised fuel ash on the hydration reactions of calcium aluminates' in 'Effects of fly ash incorporation in cement and concrete' Mat. Res. Soc. 71-81

Plowman, C. and Cabrera, J.G. (1982) 'Hydration mechanisms, mineralogy and morphology of the C_3A-PFA system' in Int. Symp. 'The use of PFA in concrete' 1 111-120

Pollitt, H.W.W. (1964) 'Raw materials and processes for portland cement manufacture' in 'Chemistry of cements' ed. H.F.W.Taylor 27-49

Pratt, P.L. (1982) 'Mechanisms of hydration of portland cement' in 'Characterisation and performance prediction of cement and concrete' (Engineering Foundation) 51-68

Pratt, P.L. and Ghose, A. (1983) 'Electron microscope studies of portland cement microstructure during setting and hardening' Phil. Trans. Roy. Soc. London, A310 93-103

Pritts, J.M. and Daugherty, K.E. (1976) 'The effect of stabilising agents on the hydration of β-C_2S' Cem. Concr. Res. 6 783-796

Raask, E. (1968) 'Cenospheres in pulverized fuel ash' J. of the Inst. of fuel Sept., 339-344

Raask, E. (1969) 'Fusion of silicate particle in coal flames' J. of fuel 40 366-374

Raask, E. (1970) 'A light weight material' British Chemical Eng. 15 No.9 1165-1167

Raask, E. (1980) 'Quartz, sulphates and traces elements in PFA' J. of the Inst. of Energy June, 70-75

Raask, E. (1982) 'Flame imprinted characteristics of ash relevant to boiler slagging corrision and erosion' Transactions of the ASME 104 858-866

Raask, E. and Goetz, J. (1981) J. Inst. energy 54 163

Raask, E. (1982) 'PFA constituents and surface characteristics in concrete applications' in Int. Symp. 'the use of PFA in concrete' 1 5-16

Raccanelli, A. (1969) 'Effects of additions of alkali sulphates and calcium sulphate on the early reactions of portland cement hydration' Ind. Ital Cemento 34 (1) 3-14 (quoted from Copeland and Kantro,1969)

Ramchandran, V.S. and Beaudoin, J.J. (1976) 'Significance of water/solid ratio and termperature on the physico-mechanical characteristics of hydrating $4CaO.Al_2O_3.Fe_2O_3$' J. Mat. Sci. 11 1893-1910

Rayment, P.L. (1982) 'The effect of pulverized-fuel ash on the c/s molar ratio and alkali content of calcium silicate hydrates in cement' Cem. Concr. Res. 12 133-140

Regourd, M. (1979 a) Cement Production and Use ed. J.Skalny, (Engineering Foundation) New York 41

Regourd, M. (1979 b) 'Fundamentals of cement production : The crystal chemistry of portland cement minerals, New data' in 'Cement production and Use' ed. J.Skalny (Engineering Foundation)

Regourd, M. (1979 c) I1, Cemento, 75 323

Regourd, M. and Guinier, A. (1974) Principal Paper, Proc. 6th. Int. Congr. on Chem. Cem. Moscow

Roy, D.M., Oyefesobi, S. and Sarkar, A.K. (1977) 'Ettringite stability and related hydration studies' Am. Ceram. Soc. Bull. 56 305 (Abstr.)

Sanzhaasuren, R. and Andreeva, E.P. (1978) 'Study of structure formation processes in aqueous suspensions of tetracalcium aluminoferrite in presence of gypsum and calcium hydroxide' (Russ.) Vestn. Mosk. Univ., Ser. 2: Khim(2) 160-4 (quoted from Taylor and Roy, 1980)

Satava, V. and Veprek, O. (1975) 'Thermal decomposition of ettringite under hydrothermal conditions' J. Am. Ceram. Soc. 58 357-9

Schwiete, H.E., Ludwig, U. and Jager, P. (1966) 'Investigations in the system $3CaO.Al_2O_3$-$CaSO_4$-CaO-H_2O' in Highways Research Board SR90, 'Structure of portland cement paste and concrete' 353-367

Scrivener, K.L. (1984) 'The development of microstructure during the hydration of portland cement' Thesis for PhD. Imperial College

Seligmann, P. and Greening, N.R. (1960) Proc. 4th. Int. Symp. Chem. Cem. Washington 408

Seligmann, P. and Greening, N.R. (1964) 'Studies of early hydration reaction of portland cement by x-ray diffraction' Highway Research Record 62 80-105 PCA Res. Bull. 185

Shin, G.Y. and Glasser, F.G. (1983) 'Chemistry of cement pore fluids :I. Suspension reactions of $Ca_{3-x}Na_{2x}Al_2O_6$ Solid solution with and without gypsum additions' Cem. Concr, Res. 13 366-376

Simons, H.S. and Jeffery, J.W. (1960) 'An x-ray study of pulverised fuel ash' J. Appl. Chem. 10 328-336

Skalny, J. and Young. J.F. (1980) 'Mechanisms of portland cement hydration' Proc. 7th. Int. Congr. Chem. Cem. Paris II, II-113 II-1145

Skoblinskaya, N.N. and Krasiluikow, K.G. (1975 a) 'Changes in crystal structure of ettringite on dehydration,1' Cem. Concr. Res. 5 381-394

Skoblinskaya, N.N., Krasilnikov, K.G., Nikitina, L.V. and Varlanrov, V.P. (1975 b) 'Changes in crystal structure of ettringite on dehydration, 2' Cem. Concr. Res. 5 419-432

Spierings, G.A.C.M. and Stein, H.N. (1976) 'The influence of Na_2O on the hydration of C_3A I. Paste hydration and II. Suspension hydration' Cem. Concr. Res. 6 265 and 6 487

Sprung, S. (1980) 'Effect of the burning process on the formation and properties of the clinker' Proc. 7th. Int. Congr. on Chem. Cem. I, I-2/1

Stein, H.N. (1961) 'Influence of some additives on the hydration reactions of portland cement I. Non-ionic organic additives' J. Appl. Chem. 11 474-482

Stein, H.N. (1963) 'Some characteristics of the hydration of $3CaO.Al_2O_3$ in the presence of $CaSO_4.2H_2O$' Silc. Ind. 28 141-145

Stein, H.N. (1977) 'The initial stages of the hydration of C_3S' II Cemento, 74 3

Stein, H.N. (1980) 'The colloid chemistry of calcium aluminate hydrates' Proc. 7th. Int. Congr. Chem. Cem. Paris IV ,449-454

Stein, H.N. and Stevels, J.M. (1964) J. Appl. Chem. 14 335

Stevula, L. and Petrovic, J. (1981) 'Hydration of polymorphic modifications of C_3S' Cem. Concr. Res. 11 183-190

Suzuki, K., Nichikawa, T., Kato,K. Javashi, H. and Ito, S. (1981) 'Approach by zeta potential measurement on the surface change of hydrating C_3S' Cem. Comcr. Res. 11 759-764

Tadors, M.E., Skalny, J. and Kalyoncu, R.S. (1976 a) 'Early hydration of C_3S' J. Am. Ceram. Soc. 59 344-347

Tadros, M.E., Jackson, W.Y. and Skalny, J. (1976 b) 'Study of the dissolution and electrokinetic behavour of tricalcium aluminate' in 'Colloid and interface science' ed. M.Kerker, IV,211

Tadros, M.E. and Skalny, J. (1977) 'Retardation of tricalcium aluminate hydrate by sulphates' J. Am. Ceram. Soc. 60 174

Takemoto, K. and Uchikawa, H. (1980) 'Hydration pozzolanic cement' Proc. 7th. Int. Congr. Chem. Cem. Paris IV-2/1

Tarte, P. (1968) 'Recherches structurales sur les constituents des ciments II. les phenomenes de replacement isomorph dans L'aluminate tricalcique' Silc. Ind. 33 333-339

Taylor, H.F.W. (1964) 'Tabulated crystallographic data' in 'The chemstry of cements.' ed. H.F.W.Taylor (Academic Press) II 347-405

Taylor, H.F.W. (1979) 'Cement reactions : The silicate phases' in 'Cement production and use' (Engineering Foundation) 107-115

Taylor, H.F.W. (1984) 'Studies on the chemistry and microstructrue of cement paste' Proc. Brit. Ceram. Soc. 'Chemistry and chemically-related properties of cement' London 12-13 April

Taylor, H.F.W. et al (1984) Report of Rilem committee 68-MMH Task group 3, Chairman H.F.W.Taylor

Taylor, H.F.W. and Roy, D.M. (1980) 'Structure and composition of hydrates' Proc. 7th. Int. Congr. Chem. Cem. I, II-2/1

Theisen,K. (1983) 'Relationship between gypsum dehydration and strength development in portland cement' Zement-Kalk-Gips, 10 571

Thomas, N.L. and Birchall, J.D. (1983) 'The retarding action of sugars on cement hydration' Cem. Concr. Res. 13 830-842

Thorpe, A.N., Senftle, F.E., Alexander, C.C. and Dulong, F.T. (1984) 'Oxidation of pyrite in coal to magnetite' Fuel 63 662-668

Tong, H.S. and Young J.F. (1977) 'Composition of solutions in contact with hydrating β-dicalcium silicate' J. Am. Ceram. 60 321-328

Uchikawa, U. and Uchida, S. (1980) 'Influence of pozzolana on the hydration of C_3A' Proc. 7th. Int. Congr. Chem. Cem. Paris IV, 24-29

Watt, J.D. (1969) 'The physical and chemical behaviour of the mineral matter in coal under the conditions met in combustion plant PartII' BCURA Industrial Report Aug.

Watt, J.D. and Thorne, D.J. (1966) 'The composition and pozzolanic properties of pulverized fuel ash' J. of Appl. Chem. 15 585-604 16 33-39

Williamson, R.B. (1972) 'Solidification of portland cement' Prog. Mater. Sci. 15 189-286

Yamaguchi, G., Ono, Y., Kawamure, S. and Soda, Y. (1963) 'Strength of motars made from the modifications of C_2S' Semento Gijuster Nempo 17 64-66

Yamaguchi, G., Shirasuka, K. and Ota, T. (1966) 'Comparison of hydration properties between monoclinic and inverted triclinic alite' in Highways Research Board, SR90 'Structure and portland cement paste and comcrete' 263-268

Young, J.F. (1972) 'A review of the mechanisms of set-retardation in portland cement pastes containing organic admixtures' Cem. Concr. Res. 2 415-433

Young, J.F. (1978) 'A discussion of the interactions between hydrating calcium silicates and set-modifying admixtures' Silic. Ind. 43 209

Young, J.F. (L(81) 'Hydration of portland cement' J. of Educat. Modules for Mat. Sci. and Eng. 3 No.3 409-427

Young, J.F. and Tong. H.S. (1977) 'Microstructure and strength development of β-C_2S paste with and without admixtures' Cem. Concr. Res. 7 627

Young, J.F., Tong, H.S. and Berger, R.L. (1977) 'Compositions of solutions in contact with hydrating tricalcium silicate pastes' J. Am. Ceram. Soc. 60 193-198